MODELLING SURFACE TOPOGRAPHY FROM REFLECTED LIGHT

A thesis submitted to Middlesex University

by

Neda Sotoudeh

in partial fulfilment of the requirements for the degree of

Doctor of Philosophy

April 1997

School of Electronic Engineering, Middlesex University

INDEX

ACKNOWLEDGEMENTS

I would like to express my gratitude to the following people at Middlesex University and University of Teesside.

Professor George Goldspink, my director of studies, for his valuable guidance and support throughout this research programme and for proof reading the draft version of thesis. I would also like to thank him for raising the funds for the many international visits I had to make in connection with the presentation of my publications.

Mr. Graham Greatrix head of the Physics group at Teesside University who is also my second supervisor, for his thorough support and encouragement as well as valuable technical input into the investigation. His much needed comments and constructive criticisms on the draft of the thesis is also greatly appreciated.

Dr. Ramon Prasad for help with the mathematical aspects of the work in particular that of Hilbert transformation.

Professor John Butcher for his interest in the project and for assisting towards the funds for one of my presentations in the United States.

Dr. Andrew Campbell of the Physics group at the University of Teesside for his help and technical advice on various aspects of the project.

Miss Marva Ghabidian of the computer centre, for constantly upgrading the memory space on the mainframe for the processing routines to be completed.

My colleague, Mr. Papu Rao, with whom I have had many useful discussions on the various aspects of this project and for his assistance in the preparations of many of the diagrams presented in the thesis.

ABSTRACT

This thesis is concerned with the use of the modulus of the Fourier spectrum to characterise object features and also to reconstruct object surfaces in the complete absence of phase information. In general, a phaseless synthesis is completely meaningless and many characteristic features of the object are obliterated when the modulus of the spectral components is inverse Fourier transformed with zero phase. However, the outcome is different when the object possesses some form of regularity and repetition in its characteristics. In such circumstances, the utilisation of both the modulus and the intensity of the spatial spectrum can reveal information regarding the characteristic features of the object surface.

The first part of this research has utilised the intensity of the spectral components as a means of surface feature characterisation in the study of a machined surface. Two separate approaches were adopted for assessing the zero-phase images. Both the optically recorded Fourier spectrum and the computer simulated Fourier spectrum were used to extract surface related parameters in the zero-phase synthesis. Although merely a characterisation, the zero-phase synthesis of the spectral components revealed periodic behaviour very similar to that present in the original surface. The presence of such cyclic components was confirmed by their presence in travelling microscope images and in scanning electron microscope images of the surface.

Additionally, a novel approach has been adopted to recover finer periodicities on the surface. The scale sensitivity of the frequency domain fosters an exceptional means through which digital magnification can be performed with the added advantage that it is accompanied by enhanced resolution. Magnification realised through spatial frequency data is by far superior to any spatial domain magnification. However, there are limitations to this approach.

The second part of this research has been centred around the possible use of a non-iteratively based approach for extracting the unknown phases from the modulus of the Fourier spectrum and thus retrieving the 3-D geometrical structure of the unknown object surface as opposed to characterising its profile. The logarithmic Hilbert transform is one such approach which allows a non-iterative means of extracting unknown phases from the modulus of the Fourier spectrum. However, the technique is only successful for object surfaces which are well-behaved and display well-behaved spectral characteristics governed by continuity. For real object surfaces where structure, definition and repetition governs the characteristics, the spectrum is not well behaved. The spectrum is populated by maxima, minima and many isolated regions which are occupied by colonies of zeros disrupting the continuity.

A new and unique approach has been devised by the author to reform the spectral behaviour of real object surfaces without affecting the fidelity that it conveys. The resultant information enables phase extraction to be achieved through the logarithmic Hilbert transform. It is possible to reform the spread of spectral behaviour to cultivate better continuity amongst its spectral components through an object scale change. The combination of the logarithmic Hilbert transform and the Fourier scaling principle has led to a new approach for extracting the unknown phases for real object structures which would otherwise have been impossible to perform through the use of Hilbert transformation alone. The validity of the technique has been demonstrated in a series of simulations conducted on one-dimensional objects as well as the two-dimensional object specimens. The limitations of the approach, improvements and the feasibility for practical implementation are all issues which have been addressed.

GLOSSARY

$h(x,y)$	height description function in the spatial domain
F	Fourier transformation operator
F^{-1}	inverse Fourier transformation operator
$H(u,v)$	frequency description function in the frequency domain
$h_e(x)$	even part of the height description function
$h_o(x)$	odd part of the height description function
$H_e(u)$	even part of the Fourier transform of the object
$H_o(u)$	odd part of the Fourier transform of the object
R	real variable
I	imaginary variable
$\phi(u,v)$	two-dimensional phase function
$\phi'(u,v)$	arbitrary phase function
$H'(u,v)$	arbitrary frequency domain modulus
$h_{mod}(x,y)$	reconstructed object function with original modulus and arbitrary phase
$h_{pha}(x,y)$	reconstructed object with original phase and arbitrary modulus
$h_{int}(x,y)$	reconstructed object function with original intensity and zero phase
$R(x')$	autocorrelation function
$R(u)$	Fourier transform of the autocorrelation function
$S(u)$	energy spectrum
$h(n)$	sampled version of the object function
$R_s(k)$	sampled version of the autocorrelation function
$Sinc(x)$	the sinc function sin x/x
$Sgn(x)$	the signum function
$h_{hil}(x)$	Hilbert retrieved signal
$\sum E_{total}$	total squared error parameter
Λ	average spatial wavelength (m)
λ	wavelength of incident illumination (m)
$\|\rho\|$	scattering coefficient
F_1	obliquity factor for scattering coefficient
V_x	phase variation parallel to the surface
V_z	phase variation perpendicular to the surface

β_0	mean slope (deg)
σ	root mean square roughness of the surface(m)
θ_i	angle of incidence (deg)
θ_r	angle of scattering (deg)
D	diameter of the Fourier transforming lens
f	focal length of the Fourier transforming lens
q_c	cutoff spatial frequency of the lens (cycles/m)
M	magnification factor
v'	distance of the image from the lens (m)
u'	distance of the object from the lens(m)
N	number of raster scans or lines of video
N_s	number of suppressed raster scans
N_{hor}	number of horizontal elements
C_{pv}	vertical cyclic pitch (m)
C_{ph}	horizontal cyclic pitch (m)
$<\delta>$	average size of speckle (m)
α	angle subtended by the aperture of the imaging lens (deg)
L	distance of the scattering surface from the observing screen (m)
s	distance between the DC point and the fundamental frequency (m)
f_{TV}	focal length of the TV camera lens (m)
q	spatial frequency of the object (cycles/m)
O_s	size of the object (m)
$O_{grooves}$	cyclic pitch of the grooves (m)
$q_{grooves}$	spatial frequency of the grooves (cycles/m)
$s_{grooves}$	distance between the DC and the fundamental for the grooves
C_{po}	cyclic pitch in the diffraction plane (m)

CHAPTER 1

INTRODUCTION

1.1 General Overview

The pace at which surface characterisation technology advances depends upon the new and improved methods of assessing surface profiles. Today the techniques for examination and analysis of surfaces are many and varied (G.C. Allen and I.T. Brown, 1989). A convenient starting point for assessing their development is contact profilimetry. Since the advent of the commercially available contact profiling instruments in the 1930's, (T.R.Thomas, 1988), industry and research has been unified towards standardising the parameters generated by stylus type measuring instruments.

Whilst contact profilimetry is undoubtedly still the basis for generating the surface quantitative parameters, never the less its potential limitations due to sequential scanning, mechanical loading of the tip, geometrical dimensions and the shape of the probe, have inherently favoured alternative routes. Contact methods are not always feasible and not necessarily favoured because surfaces interact in three-dimensions and not just in two (P.J. Sullivan, 1989), (K.J. Stout, 1981). For very many manufacturing industries, such as integrated circuitry and magnetic and optical storage media, conventional contact profilimetry would be detrimental to the surface itself, and any other means of serial assessment such as microscopic examination would be far to cumbersome, to be of any significance in the evaluation of such surfaces for quality control. Even the lightest loading on the stylus tip, would leave ploughed tracks on the surface, with severity of the tracks depending upon the loading of the tip, as well as the nature of the material characteristics of the surface itself.

In this context, studies conducted on a typical copper surface, which is usually machined for precision optical surfaces, showed obvious track marks in a scanning electron micrograph of the surface, despite the fact that the loading of the tip was gradually reduced from 3.3mN to 1.1 mN (D.W. Chetwynd, *et al.*, 1992).

A promising alternative which is non-contact, non-destructive, allows for three-dimensional sampling of the surface topography, and is most suitable for mass inspection of manufactured surfaces, is the use of optical techniques based on spatial frequency methods. The use of spatial frequency techniques for surface feature reconstruction, however, necessitates having access to both the "modulus" and the "phase" of the optically diffracted data in a typically recorded spectrum. A complete topographical map can then be generated from the synthesis of the spectral data through an inverse Fourier transformation algorithm.

The difficulty is that one does not have access to both the modulus and the phase of the optically diffracted data to enable the synthesis process to take place. In fact the main drawback, which has inhibited the full development of the spatial frequency approaches for routine analysis and study of surface topography, in the manner that stylus profilimetry has been utilised and accepted worldwide, is the inability to measure phase at optical frequencies. At oscillations of 10^{15} hertz and above, there are no detectors that can perceive individual fluctuations of the light waves (C. Outwater and V. Hammersvald, 1974). Detectors respond to the time-average of the square of the field known as the intensity, and in doing so, there would be no trace of phase variation in a typically recorded optical spectrum (N. Sotoudeh, *et al.*, 1989). With the phase of the optical data completely obliterated, most researchers focus their attention on the available source of knowledge i.e the intensity of the diffracted field and how useful it can be in revealing surface topographical details.

Many of these researchers (J.L. Mundy and G. Porter, 1980), (R. Brodmann, 1986), (D. Jordan, *et al.*, 1988), have not used a frequency synthesis approach., i.e they have not used the intensity information in the absence of phase information to activate the inverse Fourier transformation in an attempt to observe what can be revealed. Instead, they have tried to relate the intensity of the diffracted spectrum to the available mathematical models which predict diffraction for a particular surface. With the surface deterministic parameters encoded in these mathematical models, it is then possible to ascertain surface statistical parameters from the measured intensity spectrum.

The problem is that these models are very general. Unless the object surface height description conforms to the available statistical model used in light scattering predictions, it is not possible to extract surface related data from the measured intensity information. Only a limited range of engineering surfaces give rise to topographical behaviour whose optically extracted parameters based on the models, shows good correlation with that of stylus profilimetry (N. Sotoudeh, *et al.*, 1989), (E. Marx, *et al.*, 1994). Even so, for many cases, the optical value of the surface roughness obtained from light scattering, has to be multiplied by a factor to obtain agreement with the roughness value from stylus profilimetry (E. Marx, *et al.*, 1994).

A second approach would be the incorporation of the intensity or the modulus of the diffracted spectrum in object synthesis using the frequency synthesis approach. However, mountable evidence from past (L.B. Lesem, *et al.*, 1969) and recent (D. Cochran, 1994) investigations, in support of lack of intelligibility of the modulus data as compared to the phase information, has clouded the judgement of many in attempting to utilise intensity-only information in object characterisation. This has further nurtured the need for a means of extracting the unknown phase, particularly, where there are many other areas where lack of such knowledge has presented itself as a great problem.

Apart from optical profilimetry, lack of phase has long manifested itself in areas such as X-ray crystallography (G.N. Ramachandran and R. Srinivasan, 1970), electron microscopy (R.W. Gerchberg and W.O. Saxton, 1972) and optical astronomy for space object imaging (J.R. Feinup, 1979). It was however in electron microscopy that lack of phase prompted the urge for initiating phase restoration algorithms somewhat twenty four years ago. As pioneers, lack of fidelity together with poor resolution in the object domain, inspired (R.W. Gerchberg and W.O. Saxton, 1972) to initiate the first phase restoration algorithm to improve upon the defocused and impaired micrographs often encountered in electron microscopy. By utilising the data related to the imperfect images alongside their corresponding diffraction patterns, they devised an iterative algorithm that developed phase information which was consistent with both the measured intensity in the diffracted plane and an improved reconstruction of the object in the object plane.

This was also the starting point for the development of a number of phase restoration algorithms, mainly hybrids, of the original version, by various researchers (J.R. Feinup,1978), (J.R. Feinup, 1982), (J.R. Feinup, 1984) (R. Bates and R. Fright, 1983) who were also confronted with a similar challenge in other fields.

Although inevitably a phase retrieval problem, restoration of phase in electron microscopy is regarded as a partial phase problem. This is due to the availability of a "prior knowledge" regarding the object which places the microscopical phase problem in a more privileged position than the majority of phase retrieval cases encountered in practice. In more general cases of signal reconstruction one may not be fortunate enough to have access to prior knowledge regarding the object in the manner that is available in electron microscopy. For instance the object may be unaccessible or an image of the object cannot be formed through physical means, such as in X-ray crystallography (R.P. Millane, 1990).

Under such circumstances one has to make preliminary assumptions regarding the nature of the object and its transform, i.e. non-negativity, limited extent, non-factorable, finite energy, and utilise these as prior knowledge in the phase restoration algorithm (J.R. Fienup, 1983). It is highly unlikely that such prior constraints lead to a straightforward closed form calculation of the desired signal in the absence of additional information.

At the present time there is no fully embracing theory that can be systematically applied for solving the phase problem as a whole. Workers and researchers tend to invent their own approaches and theories in response to a particular problem with which they are confronted. Many approaches lead to methods which are interesting but not practical. For instance, evidence has it (J.R. Fienup, 1990) that in many iteratively based approaches, prior phase knowledge is **"indeed"** crucial in reaching a solution. In the context of this research and many similar cases, it is not physically possible to measure the phase of the optically diffracted data, even if it were to be with very limited accuracy. It thus appears that in the absence of a more reliable phase retrieval technique, there seems to be limited scope for restoring topographical behaviour from the diffracted intensity information using the classical iterative approach.

Ideally, any proposed alternative should be non-iterative in nature, well suited for a whole group of object surfaces, and independent of preliminary assumptions regarding the nature of the object. The Logarithmic Hilbert transform fulfils such criteria in certain respects, i.e. it is non-iterative and it need not incorporate prior knowledge regarding the object. However, its usefulness is fairly limited in terms of applicability to object surfaces in general. As phase data is extracted from the Ln (modulus), i.e. the natural logarithm of the modulus of the frequency components, the continuity of the logarithm is essential along the path which phase data is evaluated.

Real object surfaces do not respond in this particular manner, i.e. their frequency characteristics portray a whole group of discontinuities. The task of improving continuity, reducing zeros in number whilst maintaining the integrity of the object, has been the main challenge in this research programme. These changes which are invoked via a unique concept, complement a traditional Hilbert transform operation. Although, this complementary approach will not be the answer to a fully embracing theory, never the less it would widen the scope of signal restoration and retrieval beyond what can be offered by the existing techniques when they are in isolation. Although a most fundamental part of this research study, this investigation is not totally centred around retrieving the unknown phase. A major part of this study is devoted to the characterisation and extraction of surface related features in the absence of phase information.

Whilst supportive literature belittles any significance that a modulus only reconstruction can have in the absence of phase (D. Cochran, 1994), (A. Oppenheim and J. Lim, 1981), (J. Behar, *et al.*, 1988), this study proves that there are very many structural configurations in the engineering regime whose particulars can be adequately revealed through a phase-less reconstruction.

Thus, before focusing on means for extracting the unknown phase, it is also important to identify the class of object surfaces which can be "characterised" through the support of the diffracted intensity information or modulus information alone. After all, not all classes of object surfaces need be chaperoned by phase information in order to be characterised or even fully restored! For instance, loss of phase is not detrimental to cosinusoidal, sinusoidal and triangular variations, whose spatial details are well preserved by the modulus data in the absence of phase information.

Figure 1.1 shows a simulated reconstruction by the author, whereby a triangularly shaped object has been successfully retrieved from the modulus of its spectral components in the complete absence of the phase information. Apart from a lateral shift (* part of the three-fold phase ambiguities) the two images are completely identical.

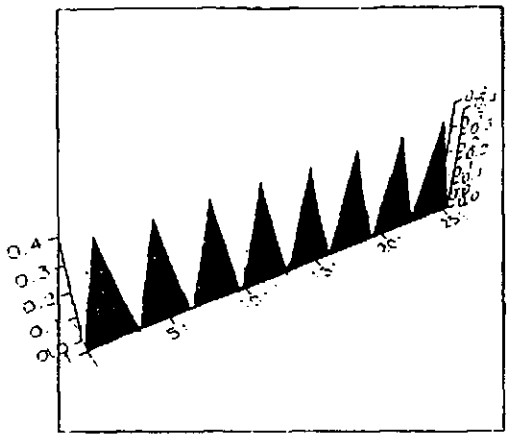

Figure 1.1a: Original triangular corrugations.

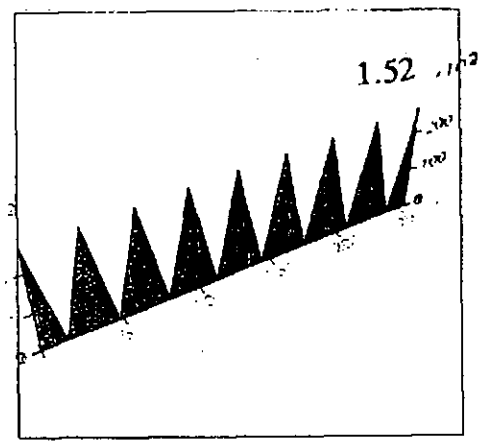

Figure 1.1b: zero-phase reconstructed image of the triangular variations using the modulus of the spectral components.

A phase-less synthesis, need not be an exact clone of the original topographical behaviour. It might merely serve to reveal dominant characteristic behaviour as part of the geometrical structure of the object. The phrase "phase-less" only ministers the characteristic representation of the object. "Characterisation" therefore, does not refer to full reconstruction. Thus, although the object may not be restored in all faithfulness in the absence of phase, certain aspects of it would be in a recognisable format. The question is what aspects of an object surface would survive in a phase-less synthesis which could be significant in the characterisation of such surfaces?

An example of a typical surface topography is an archaeological record of the machining characteristics at any point in time. It contains information about the machine, the tool and the process. None of what has been said about the modulus information in the past, does justice to the abundance of information that it can reveal in connection with the machining trends.

*see chapter 4

Well-defined patterns and regularities left by the tool mark and instrumental vibrations known as tool-chatter, are all parameters which can well be identified through a modulus-only / intensity-only synthesis and are important in the identification and classification of different engineering surfaces. This has been the main motivation behind zero-phase characterisation of object surfaces which has also formed a significant part of the investigation in this research study.

In summary, the study conducted in this research is two fold. It is aimed at " characterisation " as well as " full reconstruction" of real type object surfaces by utilising spatial frequency techniques based on the sole use of the intensity as well as the modulus of the frequency components. In the investigations conducted in this study, intensity/modulus information acts as the only precursor to the identity of the unknown object surface and the findings of this study reveal topographical details based only on the use of this information and no other auxiliary data.

Earlier on, this introduction started by putting emphasis over the importance of phase retrieval in the context of electron microscopy, mainly to improve upon the degraded spatial resolution which is often encountered in an electron micrograph. For instance, in electron microscopy, instrumental limitations such as stray magnetic fields (R. Bates and D. Mnyama, 1986), often impairs the quality of the perceived data in the final image. This frequently results in the resolution of the image plane being poorer in quality than that in the diffraction plane. Indeed in this context, studies conducted on a particular biological sample, purple membrane by Misell (D.L. Misell, 1978), have shown that the resolution in the image plane is of the order of 0.6nm as compared with 0.3nm in the diffraction plane. The message is that spatial frequency domain harbours much enhanced resolution as compared with the spatial domain, a fact which is much cherished where resolution is an important issue, such as in surface topographical studies.

Apart from the much enhanced resolution offered in the frequency space, there are other advantages attached to a frequency related operation that prove most valuable in surface related studies. Indeed two of the most significant findings in this research study, owe their usefulness to one unique concept which exists between the object and the scale of its transform in the frequency domain. In view of their significance in topographical studies, these other aspects of a frequency related operation have been discussed in the following section.

1.2 The Significance of the Frequency Domain in Mapping Topographical Behaviour

In connection with surface analysis and characterisation, spatial frequency techniques have significant advantages over spatial domain techniques in several respects:

(i) **The merging of various topographical characteristics**

The frequency map automatically combines various topological characteristics. This operation merely denotes the additive property associated with a frequency transformation, leading to the frequency distribution of any individual feature to be co-central with all other frequency distributions, irrespective of the location of the feature on the object specimen.

This has great implications for optical surface analysis based on spatial frequency methods. Assuming that the object specimen has dimensions comparable with the wavelength of the incident illumination, upon interaction of a coherent stream of radiation with the object surface, it's overall topographical information merges into one single diffraction pattern. Thus an aggregation of fine as well as coarse structural variations concurrently contribute to the overall mapping of the frequency characteristics.

On the other hand, microscopic examination of the same surface would require cumbersome inspection through different magnification scales, to account for the whole range of spatial structures present on the surface. Furthermore, it would be highly unlikely for a visual examination of this nature to bring together such diverse range of structural asperities into one single photograph. Even so, the presence of certain topographical features may never be acknowledged simply because such features are located on a different part of the surface other than the region which is being studied.

(ii) Enhancing the presence of fine spatial features

The inverse dimensional property that operates between the object and its frequency transform renders the space-frequency transition scale sensitive. That is, the frequency map expands or contracts in response to the scale of the object.

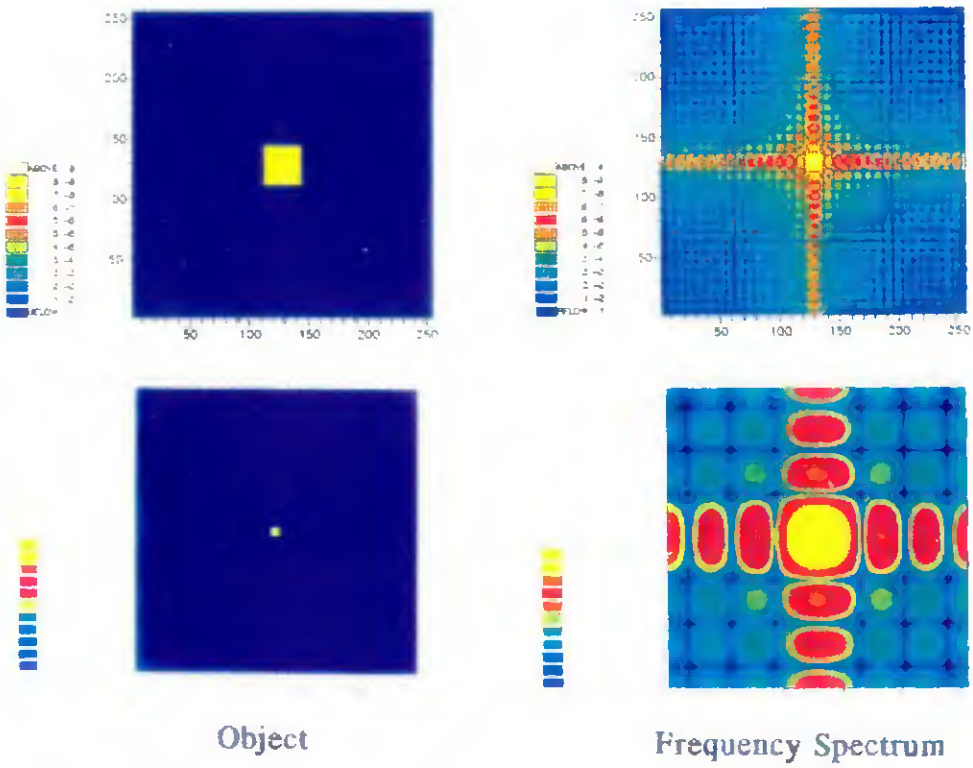

Figure 1.2: Relationship between the size of the object and the distribution of its frequency components.

Such scale sensitivity associated with the frequency domain enhances the presence of the small features in the frequency map by enlarging their corresponding signature. As the dimensional size of a defect is usually on a much smaller scale compared to the rest of the surface micro-geometry, this property enables one to alienate the signature of a defect from the rest of the surface characteristics in the frequency map. In particular, when the surface micro-geometry exhibits some form of regularity in its structure. In fact, so distinct is the signature of a defect in a frequency map against some form of regularity (H.G. Lipson and H. Lipson, 1981), that frequency domain techniques have found their way into the inspection of very large scale integrated circuits

to identify flaws or unwanted blemishes where microscopic examination would be far too time consuming (D.B. Holt, *et al.*, 1991).

The scaling principle has been fundamental to the findings of this research. Just as the scale of the object affects the scale of its transform, any change in the scale of the transform will also bring on a change in the size of the object. Thus the scale of the transform can be deliberately altered, to vary the size of the restored object in the object domain. In Chapter 5, this philosophy has been adopted to retrieve spatial structures whose presence can only be accounted for when realised on a larger scale (N. Sotoudeh, *et al.*, 1992).

An equally important attribute, which is also unique to the scaling operation, is the rearrangement of the spectral components in favour of enhanced continuity as the size of the object is reduced. That is many of the discontinuities of the spectra are phased out and the spectrum displays a more continuous trend in the amplitude variations amongst the spectral components (N. Sotoudeh, *et al.*, 1994), (N. Sotoudeh, *et al.*, 1993). The series sum of the whole host of spectral components more readily converges to a reconstruction of an object if there is enhanced continuity amongst its spectral components.

For example, by virtue of its continuity and gradual decrease in the amplitude of spectral components, a Gaussian profile can be restored through utilisation of fewer terms than the number of frequency components that need be incorporated to restore an object with sharp transitions. As has been hinted previously, this trend, namely continuity amongst spectral components is exactly what is favoured by the Logarithmic Hilbert transformation. Chapter 6 conjures this aspect of the scaling principle to facilitate the full restoration of a real object surface from the modulus of its frequency characteristics, which would have

otherwise been impossible to retrieve had the discontinuities remained as part of the spectral characteristics.

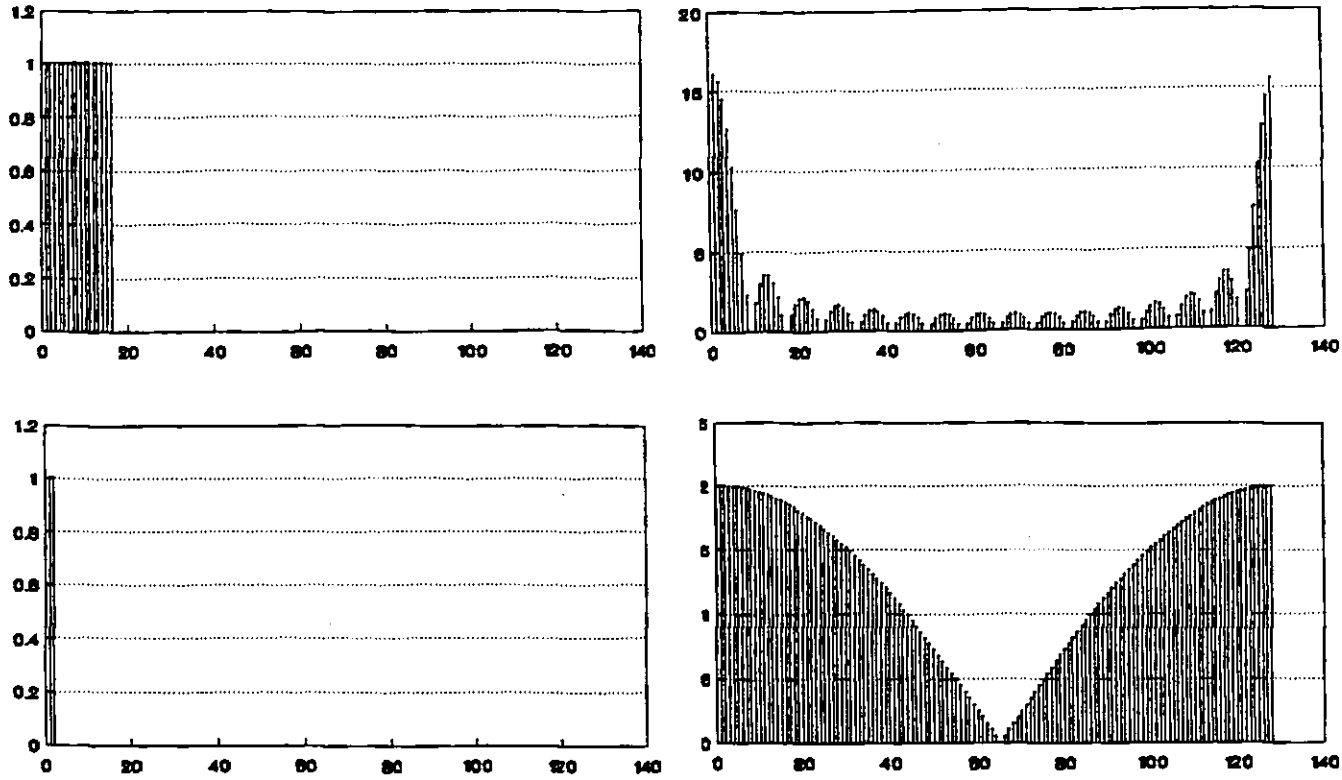

Object **Frequency Spectrum**

Figure 1.3: A novel means of enhancing continuity amongst spectral components via compressing the scale of the object.

(iii) <u>The averaging of various topological characteristics</u>

Previously, the term "merging" has been used to denote the additive property associated with a frequency transformation, leading to the frequency characteristics of various spatial structures to be added together with respect to a centre of symmetry. However, there is also an <u>average</u> value emerging out of such an operation and that is located at the centre of symmetry of a frequency map and is often referred to as the DC component.

This is the average signal reflected by the object surface and it controls the "contrast" of the object with respect to its background. This contrast in turn can

influence the quality of the perceived information in an object image, particularly when the structure of the surface is deduced from shading variations across its image. For instance, depending upon the angle of illumination, different aspects of an object surface such as edges and borders give rise to a different shading variation as compared to the other regions. It may well be that the average signal reflected from the object surface is of such magnitude that it obscures the changes in the shading variations associated with these features.

Put in another form, the shape of the object is questionable whenever the average background contribution is near to or of similar magnitude to the delicate signal associated with the low intensity level of such shading variations. Figure 1.4 shows one such situation, typical of reflective objects whereby the shading variation associated with the depth feature is almost obscured by the surrounding background signal. Examination of the frequency spectrum confirms the presence of a domineering background signal by projecting a highly intense DC point.

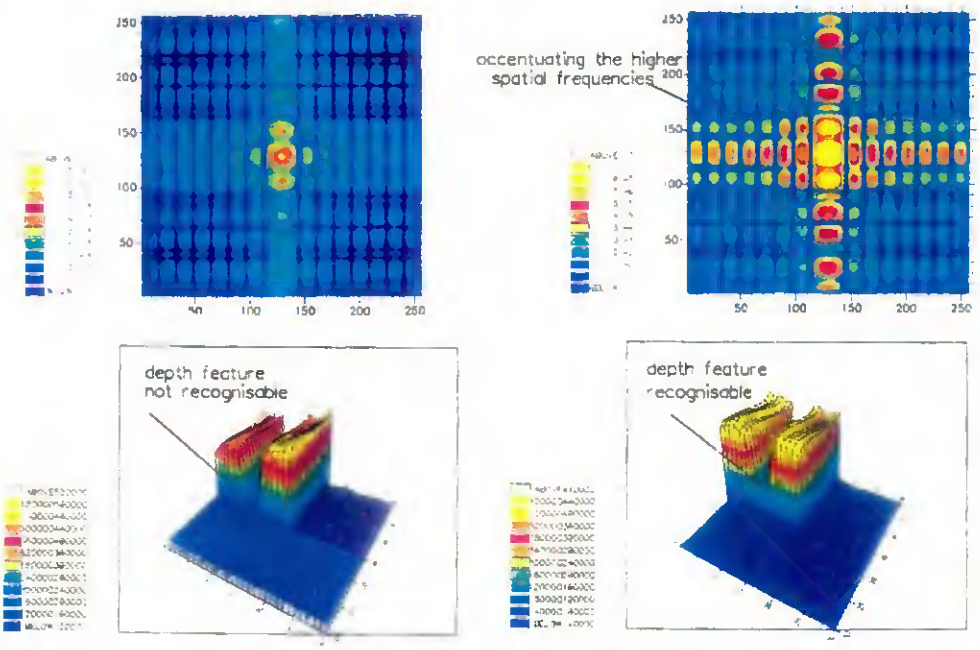

Figure 1.4: Lack of contrast between the object and the surrounding background can obscure true structural variations, this fact can easily be picked up in a frequency map and most conveniently rectified; (a)-typical spectrum of an object with poor contrast leading to a poor reconstruction of the object. (b)-rectified spectrum which shows good contrast between the object and the surrounding background leading to a faithful reconstruction of the object (N.Sotoudeh, *et al*, 1993).

If one were to improve the perception of such information through thresholding in the spatial domain, it would be difficult to specify a threshold level which maintains the fidelity of the object characteristics. However, it is far easier to rectify the problem in the spatial frequency domain, through attenuation of the DC signal and selective enhancement of the desired features.

(iv) The conciseness with which spatial data can be represented

It has long been recognised that objects can be fully reconstructed from only a fraction of their sampled information in the frequency domain (R. Raja and V. Radhakrishnan, 1977). This idea has already been exploited in surface analysis and classification based on utilising Fourier models of surface topography as concise topographical archives (I. Sherrington and E.H. Smith, 1988). For instance, typical studies conducted by Sherrington and Smith, revealed that surfaces which map the simplest spectra, i.e. those which contain the fewest and most clearly defined frequency components, such as ones produced by shaping and horizontal milling, can be adequately restored through utilisation of fewer than 300 coefficients out of the original number of 512x512 data points. This is less than 0.1% of the original number of frequency samples.

The fact that spectral data can be considerably compressed and still be representative of the structural details, has also been put to use in this study for an entirely different purpose. Indeed, compactness of spectral characteristics is another way of fostering a change of scale. Compression of spectral data, leads to expansion of spatial details. A larger sized reconstruction in the spatial domain, implies enhanced resolution in terms of more pixels being available to map topographical details. This is a necessity when a whole range of spatial details have to be resolved. This philosophy, has been fully exploited in chapter 5, to reveal a whole range of topographical undulations in a typically machined surface, in a very novel way.

Can there be a more concise means of restoring spatial behaviour, other than leaving out a range of spectral coefficients? Generally speaking, in signal transmission and coding (M. Hayes, *et al.*, 1980), based on spatial frequency techniques, the subject of compactness can be carried even further. That is, to dispose of the modulus or the phase information and to retrieve the unknown structure from the knowledge of either the modulus or the phase but not both. Frequency data would appear more compact, in the sense that only one set of information is transmitted and processed. Since evidence has it that the phase of the frequency components is a more intelligible entity as compared with the modulus information (L.B. Lesem, *et al.*, 1969), (J. Powers, *et al.*, 1970) and (O.K. Marwadi, 1972), related research in image coding and signal transmission usually focuses on the use of phase information in its own capacity to represent the unknown signal or image.

In the context of this research and in majority of signal restoration problems, the information available is that of modulus data and not phase data. It would be a breakthrough in many respects, if the modulus information were the only information from which phase data could be accurately extracted. This is one more instance where the findings in this research would be beneficial to image coding and signal transmission enthusiasts at large. The complementary combination of Hilbert transformation and the scaling philosophy, introduced in chapter 6, has lent itself to a most profound and unique means of retrieving unknown object structures with impeccable quality from only the modulus of the spectral characteristics. It should be noted however, that there are limitations beyond which this approach would cease to be effective, and these have been fully investigated in chapter 6.

1.3 Contact Techniques for Mapping Surface Topography

Contact techniques rely upon stylus type measuring instruments for generating the parameters which are used to characterise surface topography. A stylus is a pyramid or conical diamond with a flat or rounded tip resting lightly on a surface and traversing slowly across it. The up and down movements of the stylus relative to a datum are converted by a transducer into an electrical signal from which a map representing the surface profile is obtained. Due to the shape of the stylus probe, the scanned profile is a convolution of the tip geometry and the surface spatial features. Convolution has in general a smearing out or a smoothing effect and can be interpreted as the evaluation of one variable, i.e. the surface spatial parameters, over the narrow range of another variable, i.e. the finite size of the stylus sensing tip. This implies that the measured surface profile is a smoothed out version of the true surface contours in particular when the surface undulations are in the form of bumps and pits. As the finite width of the stylus tip often denies access to the regions of the surface such as the depth of the valleys and the peak heights (R.F. Babus'haq, *et al.*, 1992) the sensed spatial information from which various characteristic parameters are to be extracted, can be a misrepresented picture of the true surface behaviour.

Conical styli usually have a radius of $< 10\mu m$ whereas pyramidal styli have a width of $2\mu m$. The finite size of the stylus determines the accuracy with which the profile can be traced. This requires a knowledge of the dimensions of the shortest structures that arise in surfaces so that the size required by the type of the stylus is defined in advance (I. Sherrington and E.H. Smith, 1987). Although stylus radii as fine as $0.1\mu m$ have been reported (J. Jungles, *et al.*, 1970), (T.V. Vorburger, *et al.*, 1979), surface irregularities as small as atomic dimensions $\approx$ 1nm are believed to exist. Contact techniques are limited at the low dimensional end by the stylus radius and at the high dimensional end by the length of trace (I. Sherrington and E.H. Smith, 1986).

The main drawback, apart from the limitations that the geometrical structure of the stylus imposes on its surface wavelength sensing capabilities, is the force exerted by the probe tip on the specimen whilst recording the profile (R.F. Babus'haq, *et al.*, 1992). Plastic damage is expected to occur in many materials during the traverse under standard loading of the tip. For instance a standard 0.7mN contact force on a stylus tip of nominally 2μm square provides an average pressure of ~200 MPa (D.G. Chetwynd, *et al.*, 1992). Whilst profiles on harder materials such as steel are almost intact and not affected by such pressure, evident trace marks can be seen on softer materials and on highly smooth surfaces.

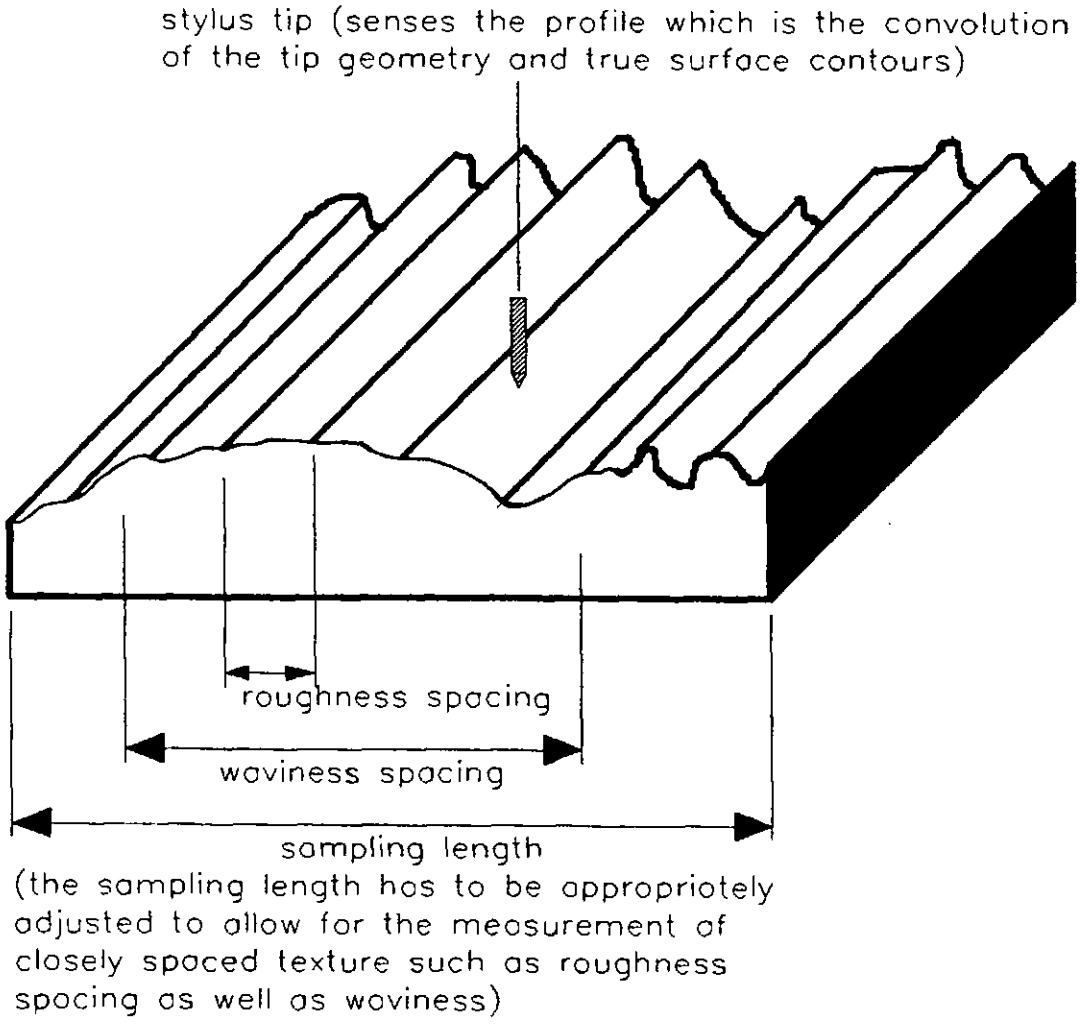

Figure 1.5: Conventional means of assessing surface topography via stylus profilimetry.

In addition, contact profiling techniques are inherently much slower than the non-contact methods since they gather data sequentially, one element at a time. Depending on the set-up time, a one-dimensional scan of the surface profile can take from one to ten minutes; not a very attractive feature for on-line assessment of surface parameters (T.V. Vorburger and E.C. Teague, 1981).

1.4 Non-Contact Techniques for Mapping Surface Topography

1.4.1 The Scanning Tunnelling Microscopy

Scanning tunnelling microscopy has emerged as the most impressive technique for imaging metallic and semi-metallic object specimens at atomic resolutions where the conventional contact profiling instrument ceases to be useful. The sensitivity of the device to surface height variations of the order of magnitude of 1nm and less makes scanning tunnelling microscopy renowned for mapping surface crystallography as opposed to surface topography. Surface protrusions and bumps on nano-scale may indeed be due to the position of the individual atoms on the surface, thus enabling surface crystallography to be sensed.

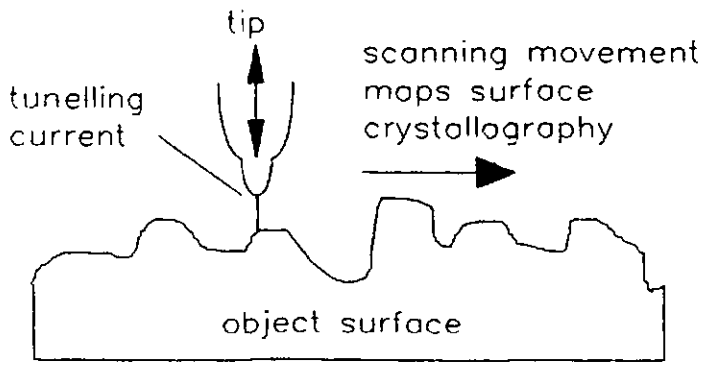

Figure 1.6: Schematic of scanning tunnelling microscopy.

The principle of the technique introduced by (G. Benning and H. Rohrer, 1983) for which they won a Nobel prize, relies on the effect known as quantum mechanical tunnelling to map structural asperities (P.J. Goodhews and F.J. Humpries, 1988). The electron distribution of a solid conductor, extends into the free space within the close proximity of the surface of the object specimen. If two surfaces, namely the sensing

probe and the object specimen, are brought close enough for their electron distributions to overlap. A tunnelling current can flow if a potential difference is applied between them. The magnitude of the tunnelling current varies most sensitively with respect to the spacing between the probe and the object specimen. Typically, the current may change by three orders of magnitude for a change in spacing of one atomic diameter.

A pre-set tunnelling current without the presence of the object specimen would act as a datum or reference current. When the probe encounters an object, the electrical resistance at the interface increases as compared with the previous situation when no object was present. A feedback system aimed at maintaining the tunnelling current constant, i.e. at its pre-set value, would reduce the distance between the probe and the object specimen until the pre-set tunnelling current is restored (R. Garcia, 1991).

In an attempt to maintain a constant tunnelling current, as the probe scans the surface it undergoes a series of vertical displacements thereby producing a map of the surface topography. The probe movement is achieved by mounting it on piezoelectric crystals. Small voltage changes causes these crystals to expand or contract. The STM image is formed by the variation in voltage that is needed to drive the probe tip up and down.

However, such map would only be a true image of the object surface provided the probe does not press against the object specimen in order to reduce the resistance (whilst adjusting the gap). This would result in an unwanted deformation in both the object and its image.

Although the current state of the art in mapping the surface topography in the sense that it outperforms the resolution offered by the stylus by four orders of magnitude, i.e. the sensing tip is $\approx 10^{4}$ finer than that of stylus, like stylus profilimetry,

it is still a sequential technique which is also susceptible to making occasional contact with the object surface. This leaves room for further research into optical techniques which are non-contact, area sampling and inherently much faster than any serial means of surface assessment.

1.4.2 Optical Techniques As An Alternative Approach

In section 1.1, the difficulty in utilising optical techniques for mapping surface topography was put down to the difficulty in measuring the phase of the diffracted information. The ability to measure phase depends upon the frequency of a particular wave motion (W.O. Saxton, 1978), (R.P. Millane, 1990). The limit for the current measurement of phase is 110GHz with a device known as reflectometer by Hewlett Packard (Hewllet Packard Manual, 1994). At much lower frequencies in the context of radio astronomy, phase has been successfully measured throughout the radio spectrum in the range of 0.03-3.0 MHz (R. Bates and R. Fright, 1984). However, measurement of phase is reported to be more difficult and often less accurate than measurement of intensity. For instance in many circumstances, the phase of a propagating wavefront is more prone to distortion than the amplitude. As an example, in radio astronomical imaging, phase is unavoidably perturbed often quite severely by the propagation of radiation through the turbulent atmosphere (R.P. Millane, 1990). In these circumstances, phase is indirectly inferred from a series of phase distorted images of the astronomical objects, known as speckle images (R. Bates, 1982), (J.C. Dainty and J.R. Fienup, 1987).

At very high frequencies, namely that of optical frequencies i.e 10^{15} Hertz and above, the measurement of phase with electronic detectors is not currently possible. In the optical range, phase can be measured indirectly, by coding it into amplitude variations in a typical interference pattern.

Two of the most common techniques based on this approach, for recording the optical phase are (i)-holography and (ii) interferometry. Both these techniques have certain drawbacks so far as their suitability in topographical studies is concerned.

(i) **holography**

At optical frequencies, holography has provided a partial solution by using a reference beam to record phase as amplitude variations. However, practical difficulties imposed by holography are far from attractive in a particular object feature reconstruction. To record the holographic interference pattern, photographic emulsions are used with very high resolution. By way of example a normal photographic film such as Kodak PanX has a resolution of 90 lines/mm whereas holographic emulsions offer a resolution of 3000 lines/mm (C. Outwater and V. Hammersvald, 1974). This by no means can be rivalled by electronic detectors such as CCD imagers which typically offer a resolution of 17μm for a 403H x 512V element device, which is equivalent to ≈50 lines/mm; or at best 7.6μm for a 1920H x 1036V element device by Toshiba, which allows for a resolution of 100 lines/mm (J. Stewart, 1988). Secondly, object isolation is vital for recording the holographic interference pattern. On average the exposure time for a hologram would be anything between 1 sec to a minute. During the exposure interval, any movement of the object, the optics, or the film, by acoustic or other vibration will obliterate the interference pattern. Unless there is access to a pulsed ruby laser to allow for very quick exposures, around ≈1/billionth of a second (R.J. Collier, 1971), object isolation is crucial. In a typical holographic setup, all elements should be stationary to less than ≈λ/10, or one tenth of the wavelength of the incident illumination λ.

(ii) **interferometry**

Optical interferometry also allows for phase to be indirectly deduced from the measurement of detected intensity across the interference pattern. The technique has been proposed by various authors for mapping the structural asperities of surfaces, though with very limited scope, used mainly for the restoration of very smooth and highly polished optical surfaces (T.V. Vorberger and E.C. Teague, 1981). Interferometric techniques, extract surface topographical data from an interference pattern of light and dark fringes. The undulation of each fringe reveals the peaks and valleys of the surface similar to the type of the roughness profile mapped by the stylus. However, added instrumentation and data processing are required to convert the optical fringes into profile data (J.C. Wyatt and K. Creath, 1992). Furthermore, if the surface roughness is greater than $\lambda/2$, the interference fringes tend to merge into one another, making it impossible for conventional interferometry to track one fringe at a time. Interferometry is also highly sensitive to surface vibrations, and in addition it requires surfaces which have high reflectivity so that the contrast of the fringes is high.

For some surfaces, which have very steep slopes, the interferometric measurements often recover a profile which does not resemble the original corrugations. In this context, work done by (C. Wyatt and K. Creath, 1992) shows marked discrepancies between the recovered structure and the original variations as shown in figure 1.7. Improvements can be made when measuring steep slopes by using multiple wavelengths instead of a single wavelength, however, the precision would be degraded and often single wavelength measurements have to be accompanied by multiple wavelength measurements to regain

the precision. This increases the labour both in terms of making extra measurements and extra processing of the measured data.

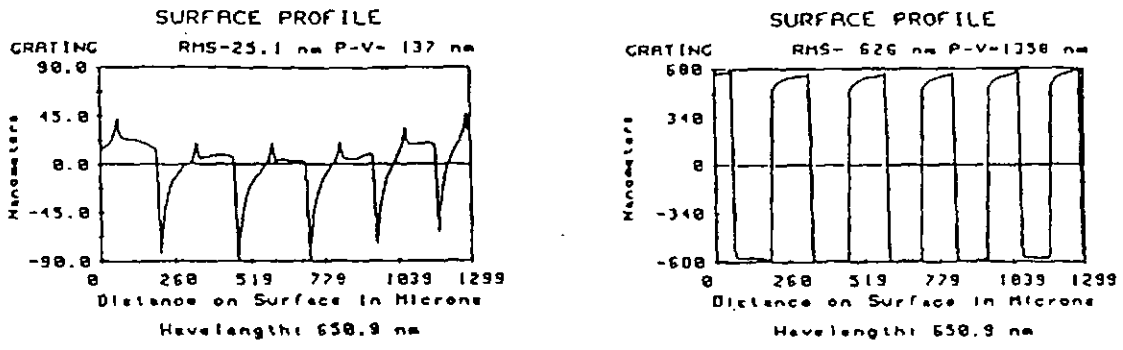

Figure 1.7: (a)-Typical profile obtained from interferometric measurements with a surface with very steep slopes; as seen the square wave corrugations are highly distorted; (b)-corrected profile obtained with the use of multiple wavelength measurements from (C. Wyatt and K. Creath, 1992).

Like holography, interferometry also requires precise and delicate adjustments, which are not really suitable in on-line assessment of topographical details. It also has a limited dynamic range in terms of the different surface roughnesses which can be mapped successfully through this technique (K. Creath and J. Wyatt, 1990). For instance, interferometric techniques which use a reference surface, yield a measurement for surface roughness which is the difference between the test and the reference surface. This can result in large errors when the rms roughness of the test surface is the same as or close to the rms roughness of the reference surface. A typical quote is that there will be a 42% error in the measured value of the rms roughness when the test surface has similar roughness to that of reference surface (K. Creath and J. Wyatt, 1990). With many difficulties attached to measuring the optical phase, the notion of restoring part of the topographical behaviour in the absence of such information becomes more intriguing. The next section, examines the circumstances under which a phase-less recovery can reveal useful characteristic information.

1.5 The Feasibility of a Phase-less Synthesis in Object Feature Characterisation

This section highlights the credibility of a modulus-only synthesis/ intensity -only synthesis when the object surface exhibits some form of regularity and thus puts forward the idea of a "zero-phase characterisation" and consequently its significance in surface characterisation. The subject of reviving the lost phase information from the modulus of the Fourier spectrum is discussed in section 1.6.

Various attempts have been made to reconstruct objects from either the magnitude or the phase information (A.A. Pakhomov, 1996), (M.H. Hayes, 1982) at the Fourier domain. In fact it has been shown through theoretical simulations that the phase of the object signal often captures more intelligibility of the object as compared with the amplitude of the object signal (J.S. Lim, 1990). The term "object intelligibility", which has been used on several occasions, refers to any recognisable feature or aspect of the object of interest. To facilitate comparison between the original object, its modulus only reconstruction and its phase only reconstruction, the aforementioned terms have been expressed in symbolic notation.

If h(x,y) represents the amplitude distribution of the object in the spatial domain and H(u,v) and ϕ(u,v) represent the amplitude and phase distribution of its frequency components in the Fourier domain, then having access to both H(u,v) and ϕ(u,v), the spatial domain distribution of the original object h(x,y) can be obtained from (1.1):

$$h(x,y) = F^{-1} |H(u,v)| e^{i\phi(u,v)} \qquad (1.1)$$

where F^{-1} is the inverse Fourier transformation operator and a Fourier transform relationship is assumed to exist between the object domain and the frequency domain.

The modulus-only reconstruction $h_{mod}(x,y)$ is when equation (1.1) is inverse Fourier transformed with the original moduli $|H(u,v)|$ and arbitrary phase $\phi'(u,v)$, where $\phi'(u,v)$ can be any constant phase including zero phase, i.e. :

$$h_{mod}(x,y) = |H(u,v)|\ e^{i\phi'(u,v)} \tag{1.2}$$

The phase-only reconstruction $h_{pha}(x,y)$ is when equation (1.1) is inverse Fourier transformed with the original phase $\phi(u,v)$ and arbitrary amplitude $H'(u,v)$, including unity amplitude, i.e. :

$$h_{pha}(x,y) = F^{-1}\ |H'(u,v)|\ e^{i\phi(u,v)} \tag{1.3}$$

The key to intelligibility of phase-only synthesis over magnitude-only synthesis lies in the inherent nature of a phase-only synthesis (1.3) which can effectively be identified as a high pass filtering of the spectral characteristics. Research carried out by Oppenheim *et al.*, (A.V. Oppenheim, *et al.*, 1979) unravelled that inverse Fourier transformation of the frequency data with the right phase and unity magnitude is similar to a spectral whitening process with the qualities of a high pass filtering, thus emphasising high frequency components such as edges, corners and borders namely distinguishable aspects in an object. This can be seen by rewriting equation (1.3) using value of unity for the modulus of the spectral components i.e. $|H'(u,v)| = 1$ or expressing $|H'(u,v)|$ as:

$$|H'(u,v)| = |H'(u,v)| \cdot \frac{1}{|H'(u,v)|} \tag{1.4}$$

$$h_{pha}(x,y) = F^{-1}\left[\ |H'(u,v)|\ e^{i\phi(u,v)} \cdot \frac{1}{|H'(u,v)|}\ \right] \tag{1.5}$$

Equation (1.5) can only restore the predominantly distinct features of an object provided that the spectral characteristics of the object is continuous and that there is a gradual decrease in the amplitude of the frequency components towards the extremities of the spectrum. This seems to be the usual behaviour for the majority of the signals encountered in the context of image processing and inevitably the reason behind the success of a phase-only synthesis. Typical results by Cochran, (D. Cochran, 1994) which confirm the high pass filtering of a phase-only reconstruction have been shown in figure 1.8, in the reconstruction of a normalized image using phase-only synthesis and modulus-only synthesis. The phase-only synthesis, has preserved the edge definition and the fine contours of the original image, i.e the main characteristic features in an image which undoubtedly aid in the recognition of the object. However, the modulus-only synthesis, has resulted in a complete loss of the object information. There should be some information in the centre of the display, but in this case it is too weak to be recognisable.

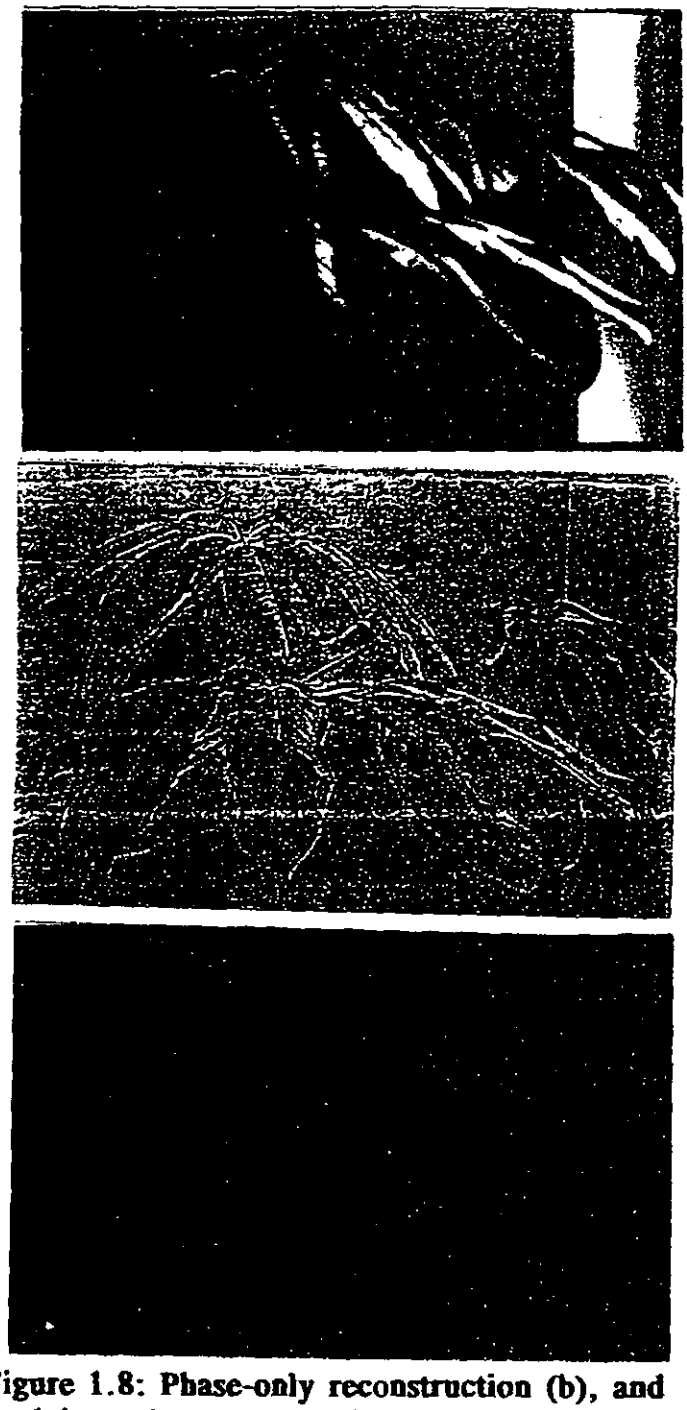

Figure 1.8: Phase-only reconstruction (b), and modulus-only reconstruction (c), of a typical normalised image (a), from (D.Cochran, 1994).

Though phase $\phi(u,v)$ tends to dominate modulus $|H(u,v)|$ in terms of preserving much of the object's intrinsic characteristics and hence much of its intelligence, the available experimental data is restricted to the intensity of the Fourier components i.e. $|H(u,v)|^2$, and it is intensity which has to be employed for retrieving information regarding the object. In addition existing evidence (R. Bates and D. Mynyama, 1984), (G. Ramachandran and R. Srinivasan, 1970), (M. Perry, 1994), (A.V. Oppenheim, *et al.*, 1979) which identifies $h_{pha}(x,y)$, as a more intelligible version of the object characteristics as compared to $h_{mod}(x,y)$, has been gathered from the study of object signals in general. If such a general class of object signals is streamlined to include only objects which possess structural regularity, then a modulus only reconstruction $h_{mod}(x,y)$, can be as informative as a phase only reconstruction $h_{pha}(x,y)$.

Thus, it can be argued that much of the object's perceivable intelligence in a modulus only reconstruction is dependent upon the shape or the geometrical structure of the original object. For instance, when the object or the scene of interest does not have any dominant structural characteristics the distribution of the frequency components is in turn vague and does not display nor inform one of any governing structural configuration possessed by the object. In such cases the inverse Fourier transformation of the modulus spectrum $|H(u,v)|$ with zero phase would lead to a reconstructed version of the object $h_{mod}(x,y)$, which bears no resemblance to the original object.

Closely related to modulus-only synthesis i.e. inverse Fourier transformation of $|H(u,v)|$ with zero phase $\phi(u,v)=0$, is the intensity-only synthesis $h_{int}(x,y)$ or the inverse Fourier transformation of $|H(u,v)|^2$ with zero phase $\phi(u,v)=0$ which is also known as the autocorrelation of $h(x,y)$ as expressed by equation (1.6). This function will also fail to disclose any recognisable aspects of the object in the absence of any form of regularity. Under such circumstances, both $h_{mod}(x,y)$ and $h_{int}(x,y)$ respond to zero-phase characterisation by appearing as a "bright blob" in the centre of display. This is

because a zero-phase characterisation is basically equivalent to a cosine only synthesis whereby all spectral components are regarded as cosinusiodals with no lateral shifting i.e. zero-phase enforces all the cyclic components to have a common alignment. This inevitably results in the concentration of energy in the central region whicb can be characterised as the "blob like" appearance.

$$h_{intensity}(x,y) = F^{-1} |H(u,v)|^2 e^{i\phi'(u,v)} \qquad (1.6)$$

where $\phi'(u,v)=0$.

However, any form of regularity, repetition and collection of similar patterns (J.J. Lee, *et al.*, 1995), changes the score in favour of zero-phase characterisation by making the modulus spectrum $|H(u,v)|$, as well as the intensity spectrum, a more intelligible entity in itself. This is because information regarding regularity is always coded in a reciprocal manner into the spatial frequency domain and if any other object related information such as the actual shape of repetitive features or their region of existence is obliterated under a modulus sign, this particular aspect of the object i.e. its regularity, survives such an ordeal.

In this context, typical studies conducted on the analysis of smoked foil patterns (J.J. Lee, *et al.*, 1995) has also based the intensity only synthesis, $h_{int}(x,y)$, as a characterisation parameter for quantifying the regularity in smoked coil patterns in gaseous detonations. Such quantification forms the basis for correlating the dynamic detonation parameters, with the extent of regularity picked up in a reconstructed version of the intensity only image $h_{int}(x,y)$ of the smoked foil pattern. Some extracts from this published work by Lee, *et al.*, in figures 1.9 and 1.10, show the sensitivity of $h_{int}(x,y)$ to tracking regularity and revealing the degree of correlation in a number of different coil patterns.

As seen, well-defined, and regularly spaced definition, leads to excellent correlation between the retrieved $h_{int}(x,y)$ image and the original pattern. This correlation is lost when the pattern loses definition and appears random. The vagueness in $h_{int}(x,y)$ is characterised by the concentration of energy in the central region of the intensity only image.

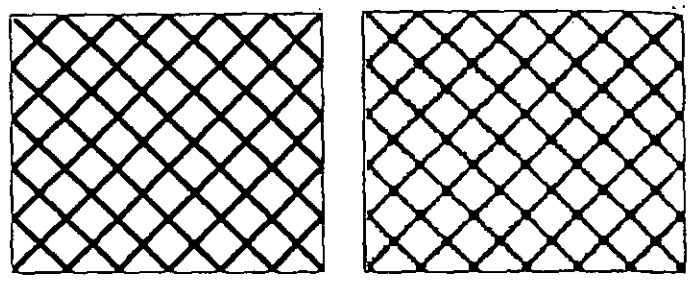

Figure 1.9: Illustration of sensitivity of $h_{int}(x,y)$ to picking up regularity in an object; (a)- original perfect image of a smoked foil pattern, (b)-intensity only retrieved image, $h_{int}(x,y)$ of the pattern from (J.J.Lee, *et al*, 1995).

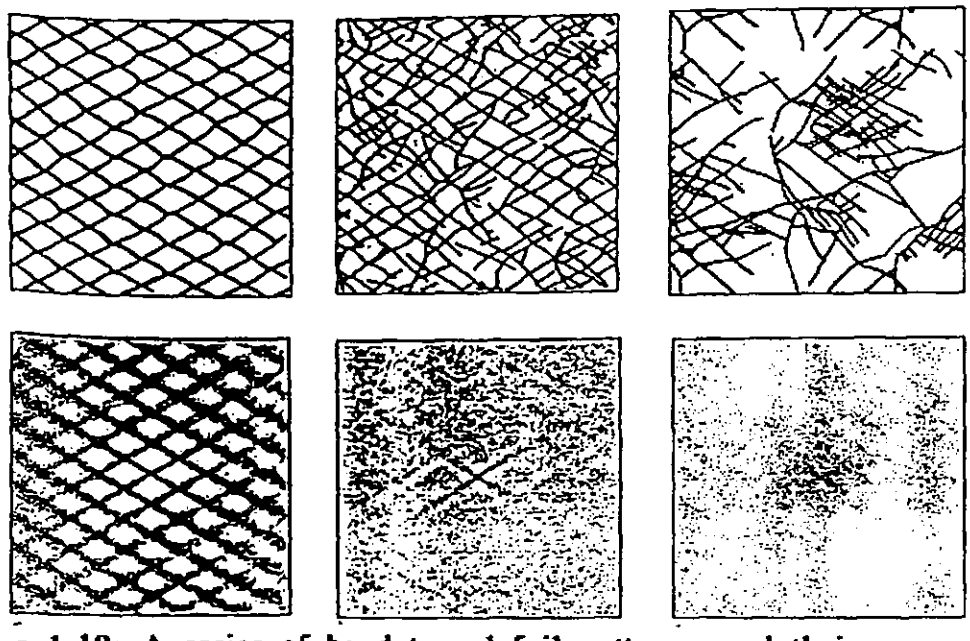

Figure 1.10: A series of hand traced foil patterns, and their corresponding reconstructions of the intensity only images, h_{int} (x,y), showing the trend in correlation between $h_{int}(x,y)$ and the original image with a change in regular behaviour from (J.J. Lee *et al*, 1995).

1.5.1 Application of Zero-phase Characterisation to Surface Analysis

In surface manufacturing industry exact recovery of the surface spatial structure is less important than the establishment of surface quantitative parameters such as the dimensional range of the various spatial features. These are the circumstances under which phase information loses its importance and an intensity based synthesis $h_{int}(x,y)$, can be used to characterise the object without regard to its shape and position. Not all surfaces can be characterised in this way; only those whose frequency behaviour is supportive of some form of regularity that is present in the original topography.

Surface finishing processes such as shot blasting, grit blasting and spark erosion, leave far too vague and random a pattern on the surface (I. Sherrington and E.H. Smith, 1988), to be of any consequence in a zero-phase characterisation study. A typical clue as to the inappropriateness of a particular frequency map in a zero-phase synthesis lies in how irregular the frequency map appears to be in itself. Frequency data which are sparse, usually denote very random behaviour in the parent object. There would be little point in attempting to characterise them through a zero-phase synthesis. The outcome is very likely to be a blob like appearance in the spatial domain as already discussed in section 1.5. Figure 1.11 shows the typical spectra of a grit blasted surface, illustrating how diffuse the spectral coefficients are. A less diffuse spectrum, showing some indication of a particular alignment present in the surface can be seen for a shaped surface.

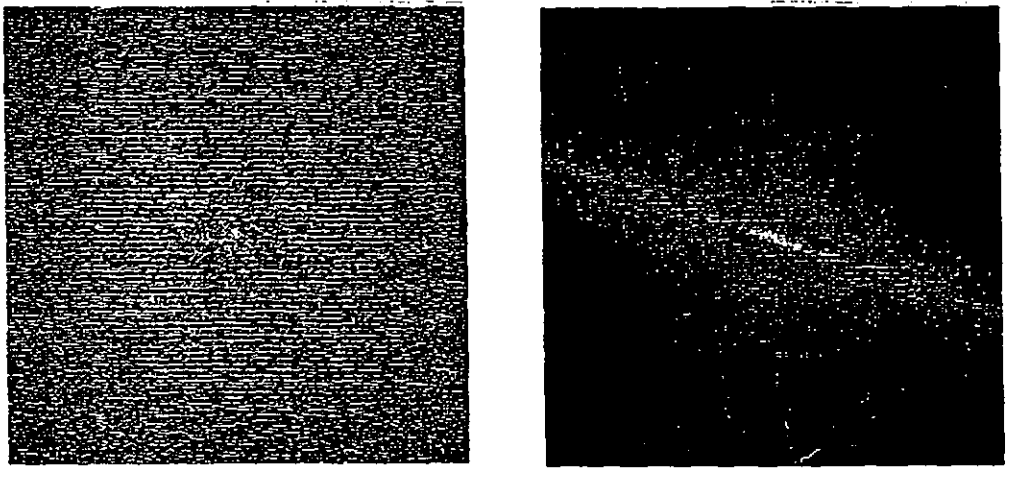

Figure 1.11: Frequency spectra of two kinds of engineering surface showing the distribution of the frequency components, (a)- the spectrum of a grit blasted surface, very diffuse in nature, and (b)-the spectrum of a shaped surface containing few discrete components; from (I.Sherrington and E.H. Smith, 1988).

It is possible to retrieve the particular regularity, which is denoted by the presence of a few discrete components in the frequency spectrum, through a zero-phase synthesis. Ground surfaces, also have a predominant direction of lay to their structure and their frequency characteristics have a random distribution of spectral components superimposed upon a number of discrete frequency components (I.Sherrington and E.H.Smith, 1988). Their spectrum looks very similar to that shown in figure 1.11b. However, more predominant regularity in the frequency domain can be seen for a different class of finishing processes.

Turned, polished and super polished surfaces (J M. Guerra, 1993), possess profiled contours with a strong indication of some form of regularity. Their mapped spatial characteristics are also betoken of such behaviour. These are the type of finishing processes which are most amenable to zero-phase characterisation. A typical spectrum associated with the frequency behaviour of a turned surface, and used in characterisation studies in this thesis is shown below in figure 1.12. The abundance of well-defined spatial regularity can be seen through the presence of whole series of spectral lines in the frequency spectrum.

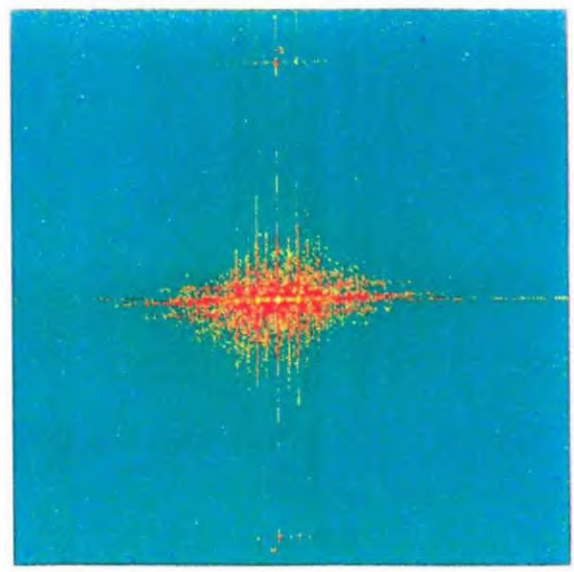

Figure 1.12: Typical spectrum of a turned surface showing the presence of pronounced regularity in the object specimen, from the results in chapter 5.

When structure and regularity prevail, zero-phase characterisation latches on this information, in a typical characterised profile. On the basis of past evidence, and in view of the vagueness of a typical modulus or intensity spectrum researchers have hesitated to acknowledge any standing that a phase-less object synthesis may have. This has deterred the possible application that phase-less synthesis of spectral data may have in very many situations. Another set back, is the difficulty in interpreting the nature of the retrieved characteristics or accounting for any spurious behaviour which cannot be linked to the object surface in any way. It would be very useful if some guidelines were constructed as to how different information associated with the object were to be effected in the absence of phase, thus making the interpretation of the characterised images more meaningful. The feasibility of the zero-phase characterisation as a means of surface feature assessment, as well as the interpretation of characterised surfaces, forms the initial part of the investigation conducted in this research study and is occupying chapters 4 and 5 of the thesis.

1.6 Retrieval of the Phase Information

In the introductory part of this chapter, it was noted that the retrieval of phase in the context of image enhancement and restoration was prompted through iterative techniques. These techniques rely on some initial knowledge, such as the distorted image of the object, or some speculative guess as to what the image might look like, or an assumption regarding the lost phase which is close to the solution phase, in order attempt to initiate the iterations with a reasonable chance of success.

Often, such prior knowledge is unavailable, leaving the plight of the iterations entirely in the hands of a pseudo-random phase as an initial guess. The difficulty is that there is no guarantee that the looped iterations converge to a solution of the object solely on the basis of a pseudo-random phase assumption. This has proved to be the case on many occasions and iterations in excess of several hundred loops (A. Ahn and A. Yagle, 1994), have been reported to be unsuccessful.

These iterations require many inverse and forward Fourier transformations. Considering the fact that a typical Fourier transformation of an NxN image array requires $2N^2\log_2 N$ multiplications and $N^2\log_2 N/2$ additions (R.J. Collier, 1971), (H.Baher, 1990) the number of mathematical operations involved for several hundred iterations would be excessively large.

Further, still many such iterative techniques rely on an interpolated version of the spectral data associated with a given size of an image to facilitate the convergence of the reconstructions with an acceptable level of error (M. Hayes, *et al.*, 1983). For instance an NxN image is usually interpolated to a size of 2Nx2N or 4Nx4N which again prolongs the computational routines.

The Ln Hilbert transform is a direct phase retrieval technique, which extracts phase from the logarithm of frequency components through an integral relationship. This relationship can be implemented digitally on a computer whereby a set of phase data can be associated with a given modulus function. The problem with Hilbert is the zeros of the complex frequency function and its effect on the extracted phases. As far as extraction of phase is concerned, continuity amongst spectral components is vital. Any discontinuities or zeros in the path of integration render the logarithm of the modulus of the frequency components infinite. Real object surfaces whose spectral behaviour runs into many discontinuities violate this basic requirement many times.

Further still, for real object surfaces which show a collection of similar patterns, the spectral characteristics becomes more complex. The spectrum is further populated by maxima, minima and a whole colony of zeros. The spectrum also appears impulsive, with many subsidiary lobes setting in as the number of features increases. Apart from the numerous minima, the colony of zeros results in parts of the spectrum being buried in total darkness thus leaving many regions of the frequency map in total isolation from one another.

This further violates the continuity that is demanded in a Hilbert transform operation. From a restoration point of view, a reconstruction can be more confidently relied upon if it were synthesised from frequency components whose amplitude can be detected with reasonable accuracy. Zeros and minima are potential sources of ambiguity and error. If these were to contribute to the identity of the object, invariably the faithfulness of the retrieved object would be questionable in a whole population of such details. The second part of this research study adopts a very novel way of manipulating the spectral data to promote the characteristics which are favoured by a Hilbert related operation without altering the information that the spectrum is meant to convey. That is to reduce and remove discontinuities, smooth out spectral behaviour, and cultivate better continuity amongst spectral components. Figure 1.13 shows what is meant by such an improvement.

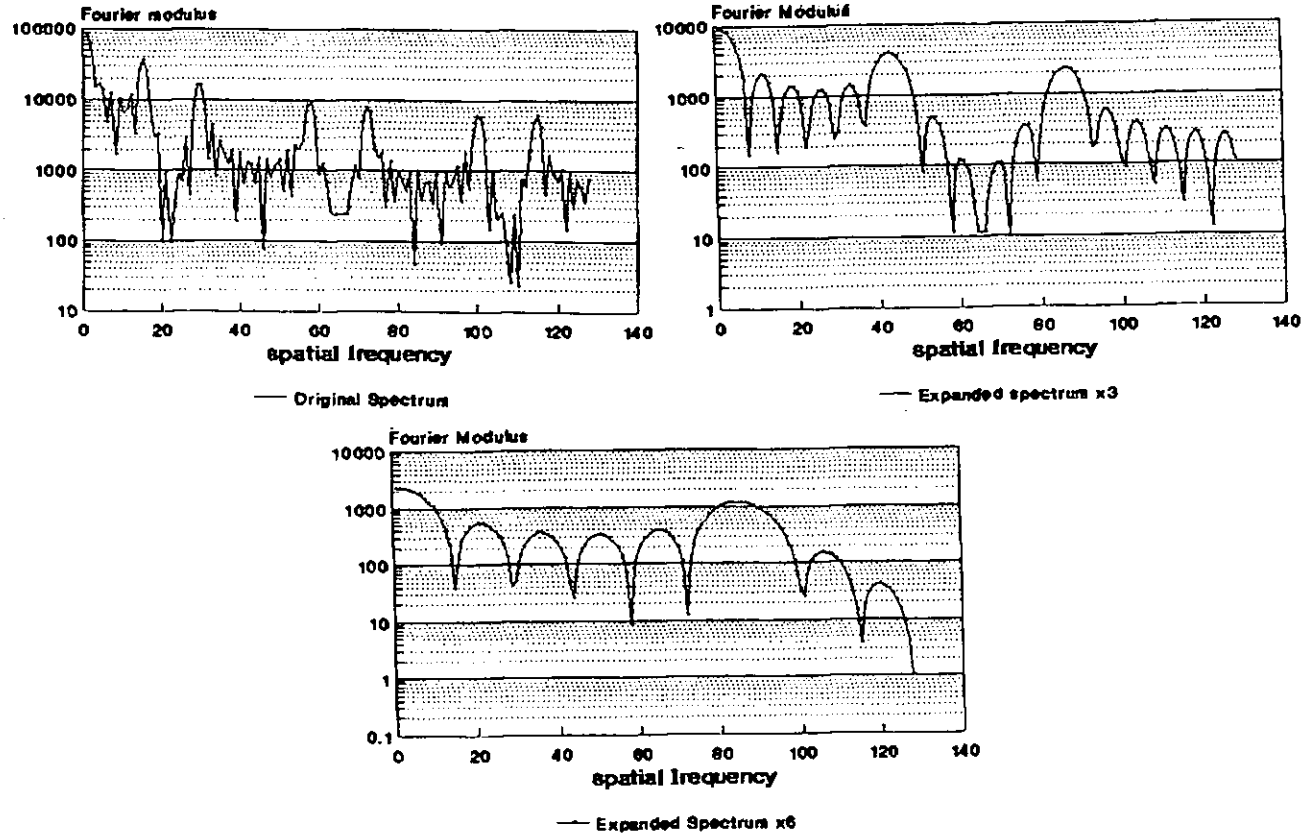

Figure 1.13: Illustration of the rearrangement of spectral components when the frequency behaviour is smoothed out; figures (a), (b) and (c) are three type of spectral behaviour belonging to the same object signal.

The displayed spectral characteristics all belong to the same object specimen studied in this research exercise. However, note how the spectral characteristics in figure 1.14 (c) possess an exceptionally smooth transition between spectral components with much of the oscillatory behaviour phased out.

A smoother transition between spectral data fosters better convergence of spectral components, serves as a better arrangement for extraction of the unknown phases, and by virtue of a more rapid convergence, can be represented more compactly from a selected number of spectral components.

Although not evident from the one-dimensional spectra, there is also an awesome reduction in the population of zeros in the two-dimensional version of the spectral characteristics of figure 1.13(c) as compared with 1.13(a). Not only were the number of zeros dramatically reduced, but the remaining number only occupied the outer extremities of the spectral characteristics. Being in the position they are, these could then be conveniently excluded from the path of integration leaving the spectral data free from any trace of zeros!

1.7 The Scope of the Thesis

This thesis is devoted to two different kind of study performed on real object surfaces. Both studies have been based upon the utilisation of the modulus of the spectral characteristics to retrieve object related information which is valuable in the assessment of topographical behaviour. This evaluation has been conducted under two different set of circumstances:

i) when the intensity data are devoid of phase and

ii) when the unknown phases are extracted from the modulus characteristics and used to reveal the full structural topography of the object surface.

When intensity data are devoid of phase, intensity-only synthesis has been used to reveal characterisation parameters for a machined surface which is governed by predominant regularity as a direct result of the type of the finishing process used. This study has been carefully labelled as a "characterisation study", because it merely retrieves the characteristic behaviour of the surface and is therefore not a true reconstruction of the topography, although, depending upon the original shape of the features, the nature of the recovered undulations can be very similar to it. This study has further identified, through a very novel approach, the techniques for finer spatial variations present on the surface and which can easily be implemented through practical means. This novel approach will be beneficial to any surface imaging technique which needs to resolve finer spatial data but is beset by a lack of pixel resolution in the object domain.

Extraction of the unknown phases has formed the second part of the major investigation carried out in this research programme. To exploit the non-iterative qualities of a Hilbert transformation, a novel complementary approach has been suggested based on the combined used of the Fourier scaling principle and the logarithmic Hilbert transformation to extend the scope of phase retrieval to that of real type object surfaces.

The study has taken a step by step approach to reveal the profound impact that a scaling operation can have upon the retrieval of unknown phases starting from full reconstruction of both repetitive and non-repetitive one-dimensional signals, to ultimately, the three-dimensional reconstruction of a real object specimen. Repetition provokes a most difficult type of spectral behaviour so far as non-iterative algorithms based on Hilbert transformation are concerned.

To achieve these goals, the chronological structure of the work arranged in this thesis has been set out in the following manner. For background information, chapter 2 brings an insight into the frequency domain behaviour of engineering surfaces by examining the scattering profiles of both randomly rough surfaces and periodically rough surfaces and reviewing their suitability for phase-less characterisations. Chapter 3 explains the experimental arrangements for recording the optical diffraction patterns which are to be utilised in zero-phase studies as well as discussing the main features of the purpose written software by the author which has been utilised for processing the data, characterising and fully reconstructing the object surfaces used in this study.

Chapter 4 is concerned with the application of zero-phase characterisation to the study of a known object structure, namely a transmittance profile. Chapter 5 contains the main bulk of zero-phase characterisation in the study of a machined surface. Chapter 6 is the pivoting point of this research and is dedicated to the retrieval of unknown phases, the recovery of which leads to the full restoration of a real object specimen. Finally, chapter 7 summarises the findings of this work, together with further suggestions for future investigations.

CHAPTER 2

FREQUENCY DOMAIN CHARACTERISTICS OF ENGINEERING SURFACES

2.1 Introduction

This chapter examines the frequency domain characteristics of typical engineering surfaces and identifies the type of spectral behaviour which is most amenable to Fourier analysis in the absence of phase information. In this respect two of the most important types of engineering surfaces encountered in practice have been examined in connection with their associated spatial frequency characteristics. Namely, the one-dimensional cross spectrum of "random" surfaces has been compared with that of "regular" profiles and their suitability in zero-phase synthesis has been discussed.

Further to this the author has taken a brief look at the most popular mathematical model which is usually utilised to map scattering from such surfaces and has noted its shortcomings and inherent drawbacks to date. Finally, the chapter comes to an end by proving the sensitivity of zero-phase synthesis to the type of regularity portrayed by a typical machined surface. This sensitivity has been shown for a repetitive object whereby the most salient features of the object have been proved to be recoverable through a zero-phase synthesis of the spectral components.

CHAPTER 2

2.2 Scattering from Random Surfaces

For random topographical patterns, the height variations of the surface has to be defined statistically. Statistical models for surfaces are described in terms of two parameters: i) an amplitude distribution function, depicting the variations of the surface height with respect to the mean level of the surface, and ii) a lateral separation parameter specified by a correlation length, depicting the minimum distance for which correlation exists between random features; the correlation length is analogous to the spatial period for a periodic profile.

The height variations above and below the mean level of the surface, are defined by a suitable height description function. The most common height descriptive function for surfaces is a Gaussian or normal distribution. A good deal of surfaces in the engineering sector and in the optical regime, have irregularities which are symmetric about the mean level of the surface and can be described by a Gaussian type height distribution function (I.Sherrington and E.H.Smith, 1987), (D.Whitehouse and J.Archard, 1970). The surface profile and the height distribution function shown by the histogram are illustrated for a Gaussian type roughness distribution in figure 2.1. The length of each bar in the histogram, represents the fraction out of the total number of the surface features which have heights equal to the values given on the abscissa, measured relative to the mean level of the surface. Note that a symmetrical random distribution of the surface roughness implies that the positive slopes of the surface are equally compensated by negative slopes, giving rise

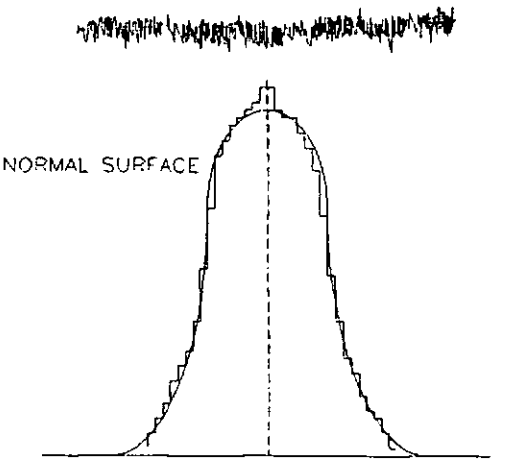

Figure 2.1 : A random profile and its height distribution function modelled by a Gaussian curve.

to a symmetrical distribution of the histogram about the mean level. As shown, the histogram showing the height distributions, can be modelled by a smooth Gaussian curve which encloses the same total area, and whose half width is related to the root mean square (rms) roughness of the surface. What will be mapped into the frequency domain, is very much a function of the height distribution of the surface or consequently its reflectance profile. That is, the far-field diffraction pattern is the Fourier transform of the surface reflectance profile. It therefore follows that if the distribution of the height variations are Gaussian in nature, the distribution of the diffracted or the scattered intensity variations would also be Gaussian in nature.

A purely Gaussian variation in the frequency domain would be very vague in the sense that it would not have any distinct features embedded in the scattered spectrum. Thus, based on the argument presented in chapter 1, section 1.5, there would be little gained by characterising such behaviour through a zero-phase approach in which case both the modulus-only synthesis and intensity-only synthesis would be vague in terms of revealing any surface characteristic information. However, because the bell-shaped behaviour has been observed in the scattering profile of a wide range of engineering surfaces, mathematical models were sought which produced scattering envelopes typical of such behaviour. With the surface statistics incorporated in the models, it is then possible to extract surface related parameters from the measurements of the scattered spectrum predicted by the model. Two of the parameters which are usually extracted from light scattering measurements, based on the use of mathematical models are the rms roughness σ, and the mean slope of the surface β_0. Before reviewing these models however, it is important to explore the characteristic scattering of randomly rough surfaces in general. To assess the typical scattering profiles of the most common engineering surfaces, some preliminary measurements were taken using a He-Ne laser with a wavelength of $0.632\mu m$ and a photodiode/ amplifier to detect the scattered

intensity. A 2mW laser beam directed at an angle of 45° illuminated a circular region of 2mm diameter on the surface. The scattered intensity which had its peak at an angle of 45°, was then traced with a photodiode along an arc, for different angles of detection. Using the responsivity of the photodiode in A/W and the transimpedance 1/resistance(ohm)$^{-1}$ of the amplifier, the scattered intensities were scaled and normalised with respect to the strongest reflector. The detected scattered potential at each angle was then plotted on a logarithmic scale to accommodate the wide dynamic range of the detected potential for various samples. For clarity in the graphs, the angle of 45° which peak reflection resides, has been changed to 0° to clearly reveal the extent in scattering from specular direction. Figure 2.2 shows the scattering envelopes for a handful of different machined surfaces, having different reflectivities, rms roughnesses and spatial periods.

For comparison with the strongest reflector amongst the set of samples i.e the polished brass specimen, the scattering profiles have been normalised with respect to this reflector. The dominating aspect of the characteristics is that they all exhibit the bell shaped behaviour depicted by a Gaussian curve, though the spread of the curve varies with the extent of scattering from the specular direction. The samples include polished brass with $\sigma = 0.21\mu$m and average spatial period of $\Lambda = 263.3\mu$m; Dural Aluminium with $\sigma = 1.04\mu$m and average spatial period of $\Lambda = 199.91\mu$m; surface ground steel which has different characteristics when aligned in different directions i.e an rms roughness of $\sigma = 0.13\mu$m, average spatial period of $\Lambda 145.15\mu$m and rms roughness of $\sigma = 0.35\mu$m , average spatial period of $\Lambda = 51.15\mu$m; unpolished brass with rms roughness of $\sigma = 0.65\mu$m, average spatial period of $\Lambda = 83.13\mu$m; and finally stainless steel with rms roughness of $\sigma = 1.43\mu$m and average spatial period of $\Lambda = 103.2\mu$m. Both the rms roughness and the average spatial period parameters have been quoted, to allow means for comparison of the degree of diffuseness for each curve. The effect of these two parameters on the scattering properties of the machined surfaces were shown

by E.C.Teague (E.C.Teague, *et al.*, 1982) Through comparing the properties of the light patterns produced by scattering a 1mm He-Ne laser beam from sinusoidal profile precision roughness specimens. In their studies, with fixed lateral spacing, namely a groove wavelength of $\Lambda = 100\mu m$, the angular spacing of the diffracted beams remained fixed, but the number of intense beams from specular directions increased as the roughness amplitude increased from $0.3\mu m$, to $1\mu m$ and $3\mu m$. However, with a specimen of fixed roughness, i.e average roughness of $1\mu m$, and different spatial periods of $\Lambda = 40\mu m$, $\Lambda = 100\mu m$, $\Lambda = 800\mu m$, the angular spacing of the scattered beam decreased as the period of the groove spacing increased. The rms roughness also influences the amount of light reflected into specular beam. Evidence has it (E.C.Teague *et al.*, 1982), that when the rms roughness is greater than 0.1λ i.e, $\sigma > 0.1\lambda$ almost 90% of the radiation is scattered into off specular direction. In this respect the amount of light reflected into specular direction should be considerably reduced as the roughness of the surface increases. This is due to the fact that most of the energy is redistributed else where in the form of scattering.

The impact of these two parameters on the scattering envelope can be seen in figure 2.2. The degree of roughness affects the peak intensity reflected into specular direction and the diffuseness of the characteristics is controlled by the spatial period parameter as well as the corresponding roughness amplitude for each specimen. All samples behave as expected apart from the relative intensities of stainless steel and unpolished brass. Stainless steel has the highest roughness therefore, therefore most of the scattering should be in the off-specular direction leaving a low intensity beam in the specular direction. Consequently the peak intensity should be well below that of unpolished brass which has a lower roughness. However, what should not be forgotten, is the effect of reflectivity on the level of detected intensity. As it happens

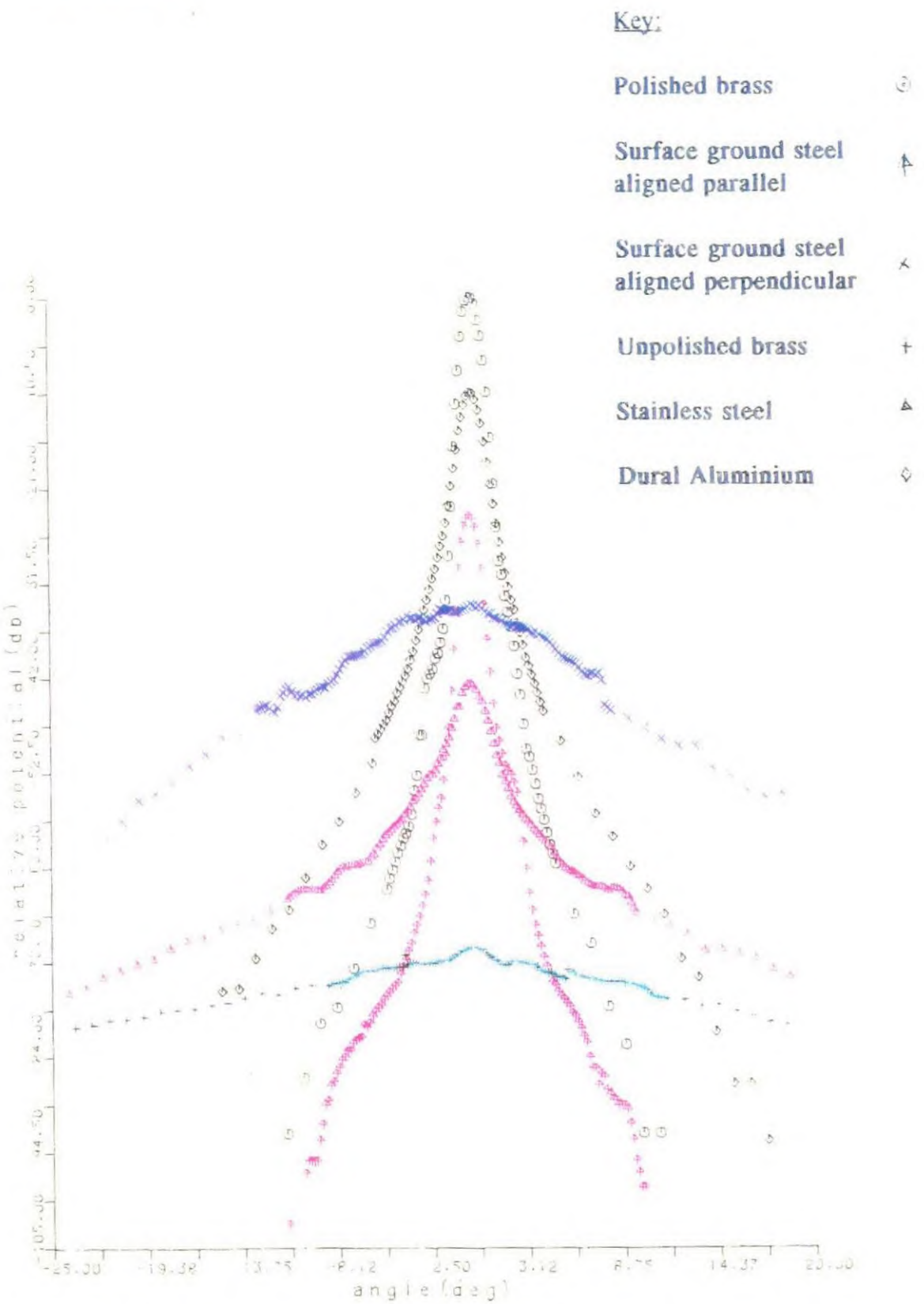

Figure 2.2: Reltaive scattering profiles, showing the drop in the peak of the scattering as well as the extent of the diffuseness with respect to the strongest reflector amongst the set, namely polished brass.

in this case, stainless steel has a higher reflectivity as compared with that of unpolished Brass whose surface was oxidised; therefore its relative scattered intensity falls above that of unpolished brass. The fact that for a given roughness amplitude, average spatial period governs the degree of diffuseness has been shown in the next set of graphs. For instance, amongst the measurements, polished and unpolished copper appeared to have the same

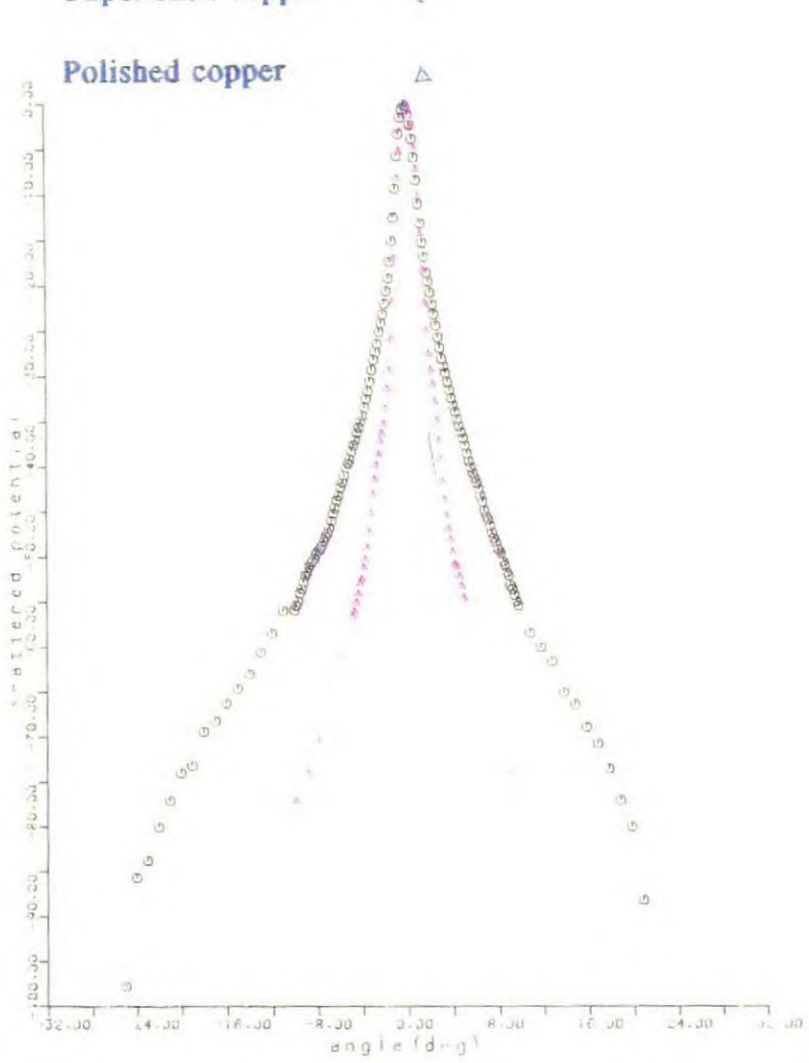

Figure 2.3: Showing the effect of mean slope on the extent of scattering for polished and unpolished copper surface.

rms roughness but different spatial periods. i.e polished copper had an rms roughness of $\sigma = 0.1\mu m$, spatial period of $\Lambda = 120.57\mu m$ where as unpolished copper had rms roughness of $\sigma = 0.1\mu m$, average spatial period of $\Lambda = 50.538\mu m$. The unpolished copper diffracts light diffusely into angles of + 22° and -22° from the specular direction, whereas, the polished copper diffracts light into angles of +10° and -10° degrees only depicting less diffuse characteristics. The effect of surface roughness and its lateral distribution on the observed scattering for randomly rough surfaces was then incorporated into mathematical models to allow for quantitative means of predicting the

scattering envelope. In this context, the main contribution to date, which forms the basis of many light scattering predictions (J.Jungles, 1992), (E.Lorincz *et al.*, 1986), (M.Younes *et al.*, 1984), (G.Porter and J.Mundy, 1980),(L.H.Tanner, 1979), (L.H.Tanner, 1976), (C.Chandley, 1976) was initiated by Beckmann and Spizicchino back in 1963. In their extensive monograph, Beckmann and Spizicchino developed a rigorous treatment of the way light is scattered from the surfaces which can be statistically defined by a Gaussian distribution of the height amplitude and a Gaussian distribution of their autocorrelation function. In their derivations, surfaces possessing Gaussian distribution of their roughness amplitude, also give rise to Gaussian shape scattering envelopes, for which the scattering envelope can be predicted by the measure of the mean slope of the surface obtained experimentally by a Talysurf type instrument. Because the complete aspects of the background theory can be found in Beckmann's manuscript, the full theory will not be given here, only the main formulation, leading to the evaluation of the scattered intensity has been addressed. The scattering envelope can be traced, through the evaluation of the scattering coefficient $|\rho|$. This is the ratio of the field reflected in any direction, to that reflected into the specular direction by a perfectly smooth conducting surface of similar dimensions. Through appropriate substitution for surface statistical descriptions, namely its height distribution function and its autocorrelation function, an expression for this coefficient is evaluated which can be identified in (2.1) as:

$$|\rho| = \sqrt{\frac{2F_1^2 \cos\theta_i}{(\cos\theta_i+\cos\theta_r)}} \cdot e^{-\frac{V_x^2}{2V_z^2 \tan\beta_0^2}} \qquad (2.1)$$

where

$$F_1 = \sec\theta_i \frac{1+\cos(\theta_i+\theta_r)}{\cos\theta_i+\cos\theta_r} \qquad (2.2)$$

and

$$V_x = \frac{2\pi}{\lambda}(\sin\theta_i-\sin\theta_r) \qquad (2.3)$$

and

$$V_z = \frac{2\pi}{\lambda} (\cos\theta_i + \cos\theta_r) \qquad (2.4)$$

where θ_i is the angle of incidence, θ_r is the angle of scattering, F_i is the obliquity factor, β_0 mean slope of the surface, V_x and V_z are the summation of the variation of the phase, among waves scattered parallel to and perpendicular to the surface as defined above.

Evaluation of the scattering coefficient for known angles of incidence and observation, together with appropriate substitution for the mean slope, allows for the scattering pattern to be predicted through this formulation. A polar plot of the variation of the scattering coefficient (proportional to the scattered potential) at different viewing angles by the detector would reveal scattering characteristics as depicted in figure 2.4. A linear plot of such scattering variations with the angle of observation, would be an exponential intensity distribution, as shown in figure 2.5. The scattering envelope in this figure has been defined with respect to the mean normal to the surface and angles of incidence and scattering have been specified with respect to this normal.

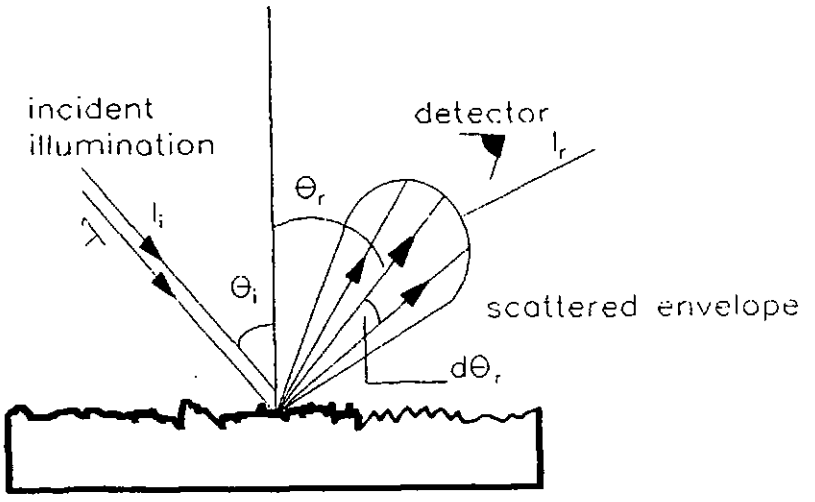

Figure 2.4: Typical scattering profile of a randomly rough surface.

As part of the preliminary investigation, this predictive pattern for the scattering behaviour, was tested by the author for two different ground specimens one of which was a standard specimen from Rubert. Ground surfaces have directional characteristics and this sample had an rms roughness of $\sigma=0.2\mu m$, $\beta_0 = 0.3^\circ$, average spatial period of $\Lambda=160.2\mu m$ along the lay and $\sigma=0.2\mu m$, $\beta_0 = 1.4^\circ$ and average spatial period of $\Lambda=54.03\mu m$ across the lay. By selecting an appropriate value for mean slope, via using the figures measured by the talysurf profiler, a suitable scattering profile was calculated using formulae (2.1), which most closely resembled the experimental scattering envelopes. The actual and predicted scattering envelopes for the Rubert specimen have been shown in figures 2.6a and 2.6b. The results for the other non standard ground surface have also been plotted in figure 2.7a and 2.7b. This other ground specimen had an rms roughness of $\sigma=0.35\mu m$, mean slope of $\beta_0 = 1.89^\circ$, and an average spatial period parameter of $51.15\mu m$ when aligned perpendicular to the direction of illumination and a roughness of $\sigma=0.14\mu m$, $\beta_0=0.32^\circ$ and average spatial period of $145.18\mu m$ when aligned parallel to the direction of incident illumination.

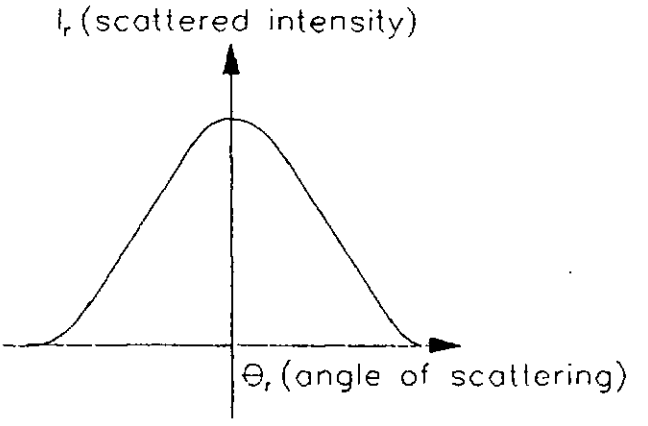

Figure 2.5: The distribution of the scattered intensity with the angle of observation shown on a linear scale.

Because ground surfaces, have directional characteristics, the scattering pattern would be quite different depending upon the orientation of the specimen with respect to the angle of incident illumination. The results shown in figure 2.6a and 2.6b once again show the dependency of the scattering behaviour on the average wavelength parameter. As expected, for a given roughness, large spatial wavelengths along the

8 ° from the specular direction. However, when the surface is rotated so that the illumination samples the topographical behaviour across the predominant lay of the surface, the scattering envelope extends into angles of + 45° and - 45° degrees from the specular direction depicting the presence of roughness features with very small lateral spacing.

Although this formulation has been utilised to trace the scattering behaviour of a selected group of randomly rough surfaces, the main drawback attached to the use of this approach is that it is not capable of predicting scattering behaviour for non-isotropic surfaces. That is surfaces whose roughness is not evenly distributed and they exhibit different roughness characteristics for different directions of alignment. For instance the type of characteristics exhibited by ground and turned surfaces. It should be mentioned however that the only reason it has been possible to model the scattering profiles of ground surfaces in figures 2.7 and 2.8, is because different surface statistics namely mean slopes have been substituted in the formulation to trace the different type of scattering in each direction. A single mean slope substitution would not have revealed the overall scattering geometry which clearly shows the directional characteristics of the surface.

The argument is that it would be misleading to try and extract surface statistics from a single trace of scattering behaviour along an arc or line measurement. It would be far more informative if different traces were to be utilised for revealing surface topographical parameters as true surface behaviour may not be reflected by the one single scattering measurement. As most surfaces, with pronounced lay have non-isotropic characteristics, utilisation of the two-dimensional scattering profile would be a better precursor to the overall surface variations.

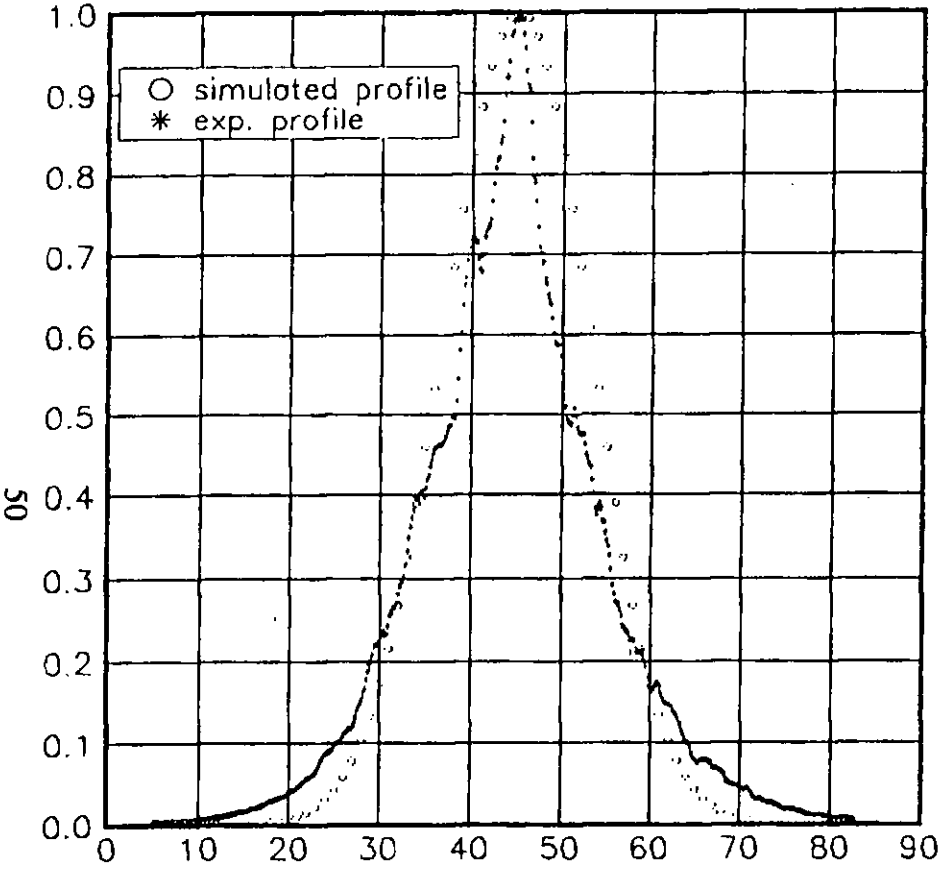

Figure 2.7a: Experimental and theoretical optical scattering profiles for a ground surface of rms roughness σ=0.2um with the plane of the dominant lay perpendicular to the plane of incidence.

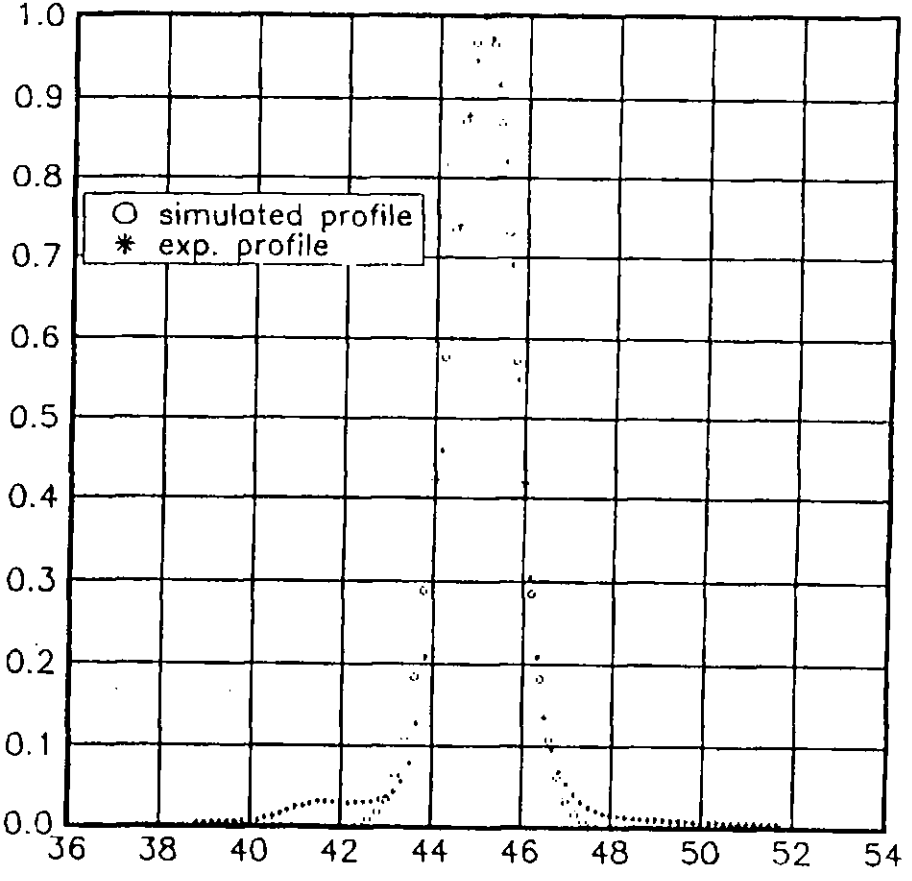

Figure 2.7b: Experimental and theoretical optical scattering profiles for a ground surface of rms roughness σ=0.2um with the plane of dominant lay parallel to the plane of incidence.

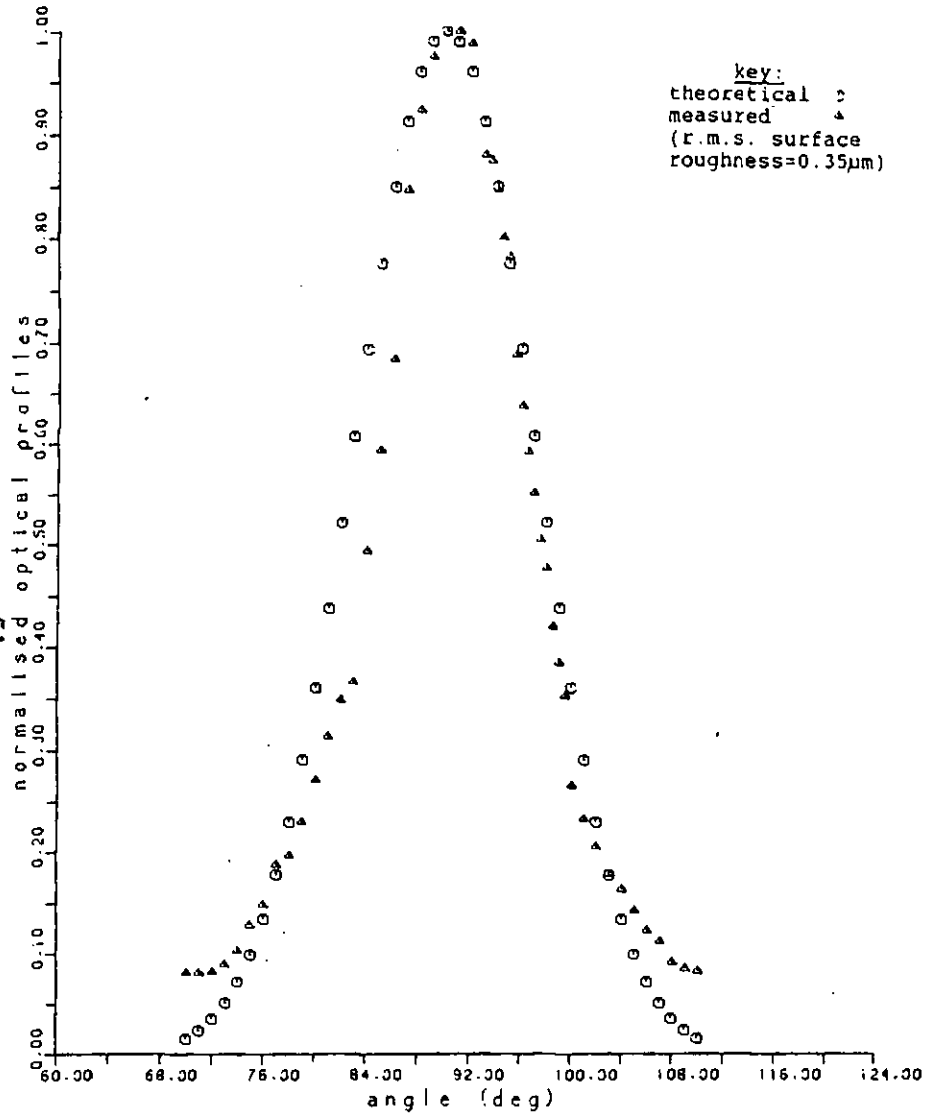

Figure 2.8a: Experimental and theoretical optical scattering profiles for a ground surface of rms roughness σ=0.35um with the plane of the dominant lay perpendicular to the plane of incidence.

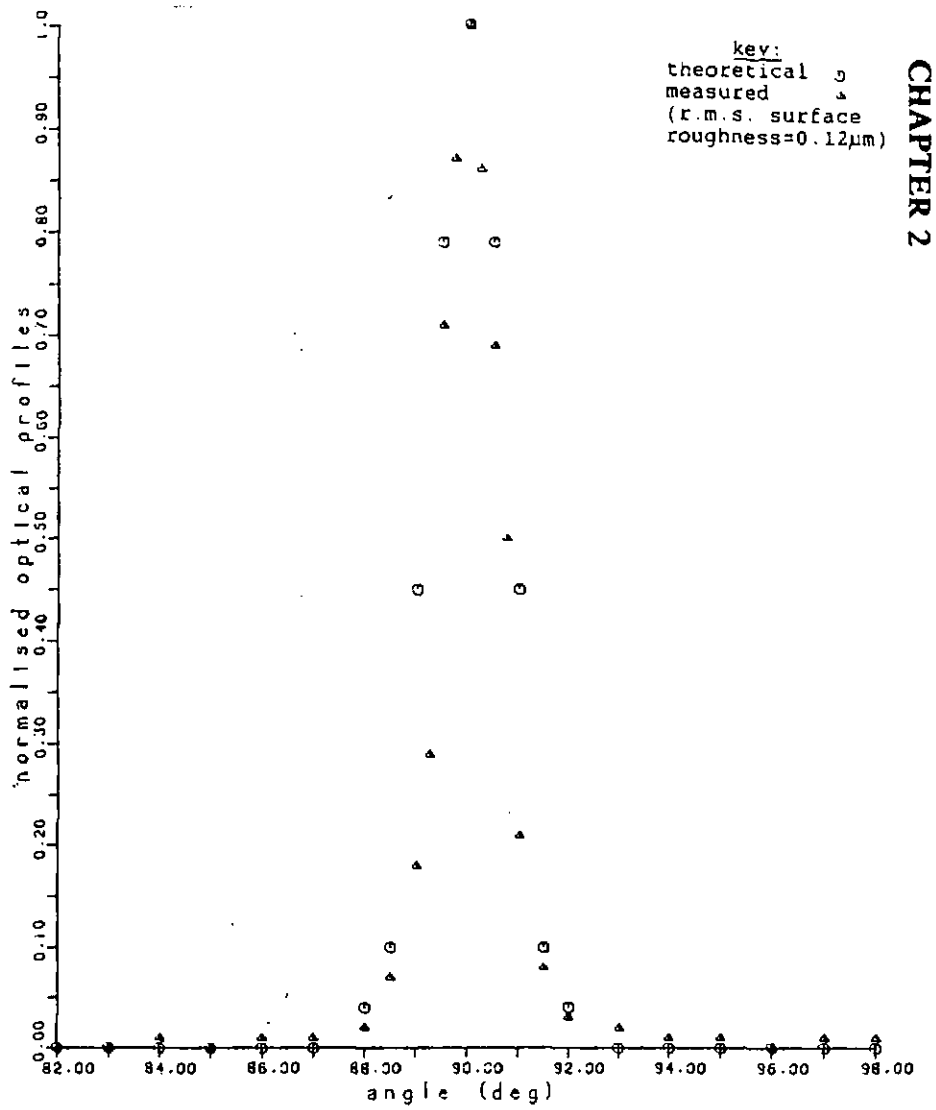

Figure 2.8b: Experimental and theoretical optical scattering profiles for a ground surface of rms roughness σ=0.12um with the plane of the dominant lay parallel to the plane of incidence.

As far as the predictive patterns for the ground specimens are concerned, all four profiles have been reasonably traced through Beckmann's formulation (2.1) with appropriate substitution for mean slope parameters in each case. However, apart from the aforementioned drawbacks, two other important issues need to be raised in connection with the modelling of the two optical profiles. Firstly, the famous formulation by Beckmann as stated in equation (2.1) has been strictly derived for very rough surfaces with a Gaussian height distribution and a Gaussian autocorrelation function. The only precursor to the degree of the roughness being as stated by Beckmann, is the value of the parameter $V_z^2\ \sigma^2$ for specular reflection. That is if this parameter is much larger than 1 then this formulation applies. Based on this definition, Obray (C.Obray, 1983) has stated that the roughness range for which this model should be applicable is for $\sigma > 2\mu$m. However, investigations conducted in this study, reveal that this model can still be used for predicting scattering behaviour for surfaces as smooth as $\sigma = 0.2\mu$m; i.e the standard Rubert specimens used. There seems to be no decisive means of clearly identifying a roughness range for which the model can effectively predict scattering. Further more, an issue which has been raised by many researchers, using this approach, is the lack of fidelity between optically extracted parameters, and that revealed by stylus profilimetry. This fact is again evident from the measurements on the Rubert specimen. The actual mean slopes are 0.38° figure 2.7a, and 1.4° figure 2.7b, whereas the optical predications require 0.3° and 4° to successfully track the envelope. For the second case, the mean slopes are 1.89° figure 2.8a, and 0.32° figure 2.8b, but the predictive profiles were generated for values of 3° and 0.28° respectively.

Although without exception, all the measured scattering profiles shown in figure 2.2, are governed by the bell shaped behaviour, similar to that of a Gaussian curve, it does not necessarily mean that the form of the height description is Gaussian in nature. In fact it has not been possible to trace most of these profiles using Beckmann's formulation apart from the ground surfaces.

Although polished surfaces, have an rms roughness which does not qualify them for having their profile traced through this formulation, according to the categorisation by Beckmann, never the less the examination of their height distribution histogram also reveals non-Gaussian characteristics in the first place. That is there is significant asymmetry in the histogram, denoting skewness, which should not be present for a typical Gaussian distribution. In this context, other researchers (C.Obray, 1983) have also cited surfaces with non-Gaussian height distributions. For instance Plateau horned surfaces have profile peaks which are shorn flat. This type of behaviour gives rise to highly skewed negative exponential height distribution as opposed to a Gaussian.
Other effects would also alter the height distribution histogram, significantly. For instance bumps on the surface commonly seen on softer materials, distorts the histogram of the height variations. Similarly an etched or pitted surface which is nominally smooth but has deep holes in it shifts the peaks of the histogram in other directions. This has been shown in figure 2.8 below referenced from (J.M. Elson, *et al.*, 1979).

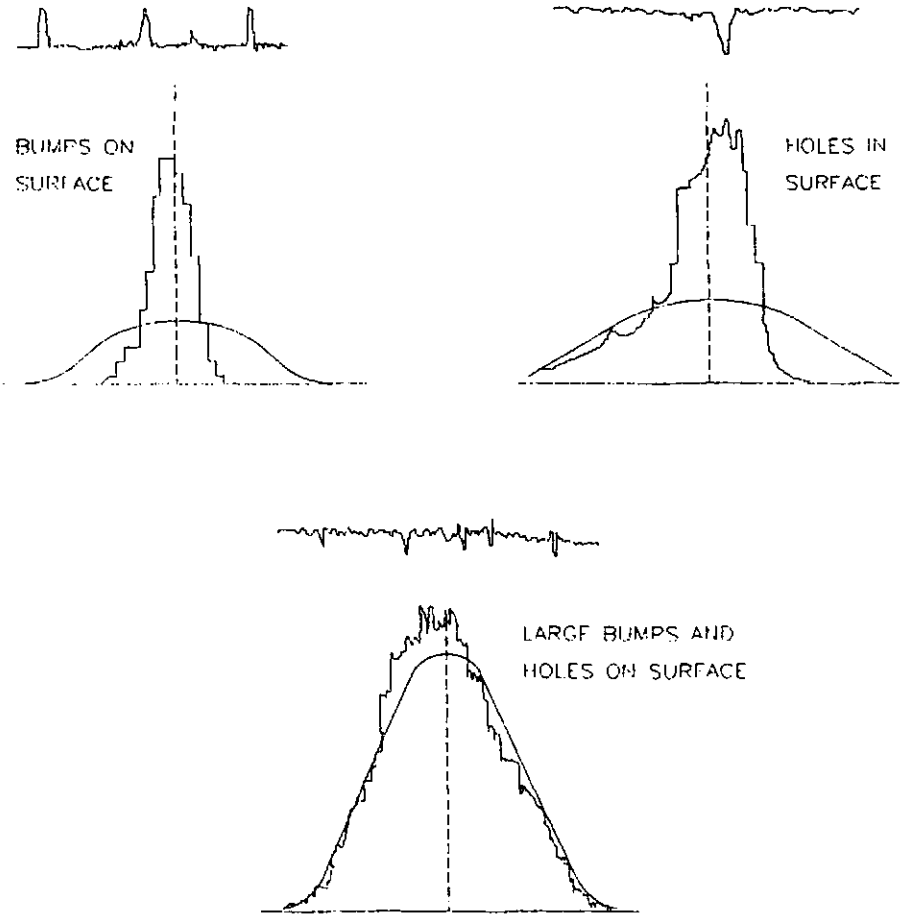

Figure 2.8: The effect of surface characteristics on the height distribution histogram.

Two other important parameters which need to be observed are the skewness and kurtosis properties of different samples. For Gaussian surfaces, there should be zero skewness and a kurtosis value of 3. As already addressed many surfaces do not give rise to the symmetrical distribution of height in the histogram of height variations. Even if deformations on the surface are not the cause, surface variations such as profiles dominated by peaks (+ve skewness) or profiles dominated by valleys(-ve skewness) can lead to asymmetry in the histogram. A kurtosis on the other hand is a measure of the peakedness of the surface. A kurtosis less than 3 shows a highly peaked surface whereas a kurtosis of greater than three shows non peaky behaviour with the roughness variations more rounded as opposed to being peaked (1.Sherrington and E.H.Smith, 1987). Apart from the aforementioned ground surfaces, other samples illustrated profound asymmetry and varying kurtosis coefficients other than 3.

2.3 Scattering from Structured Surfaces

Contrary to random surfaces which give rise to scattering envelopes governed by an exponential behaviour, structure and regularity in a surface redefines the scattering envelope allowing for such characteristics to be observed directly. For example, surface finishes with highly polished backgrounds for which the effect of tool-mark has left a definite pattern or periodicity on the surface, such as diamond turned surfaces, or face turned surfaces with grating like structures, exhibit scattering peaks caused by the periodic component of surface roughness superimposed on a Gaussian like pattern (Church *et al.*, 1979), (J.M.Elson, *et al.*, 1979) Which is the random component of the surface. This has been shown in figure 2.9. This assumption is based on the fact that the surface roughness can be regarded as an additive composition of periodic and random components. This definition is based on the gained knowledge concerning the physical process of surface generation. Periodicity is produced by copying the tool on the work piece or by vibration of the tool, which gives rise to tool-chatter components alongside the main periodic component.

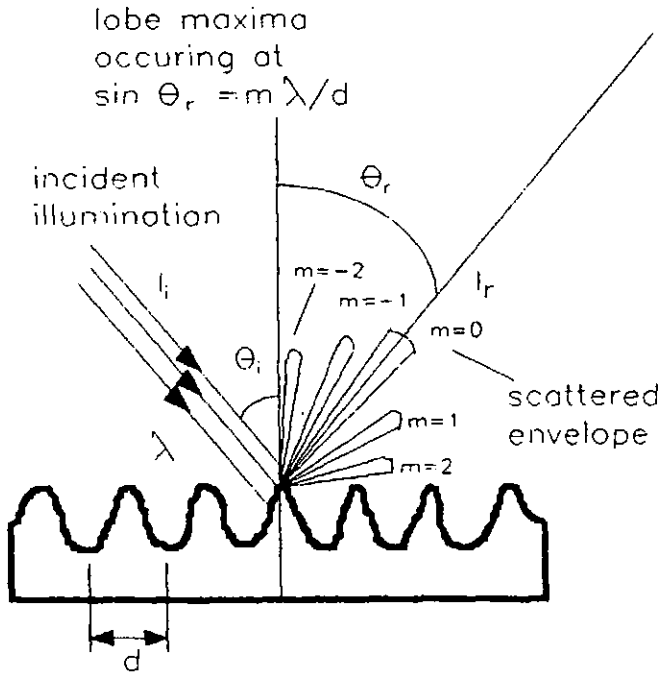

Figure 2.9: Typical scattering profile of a rough surface with predominant regularity.

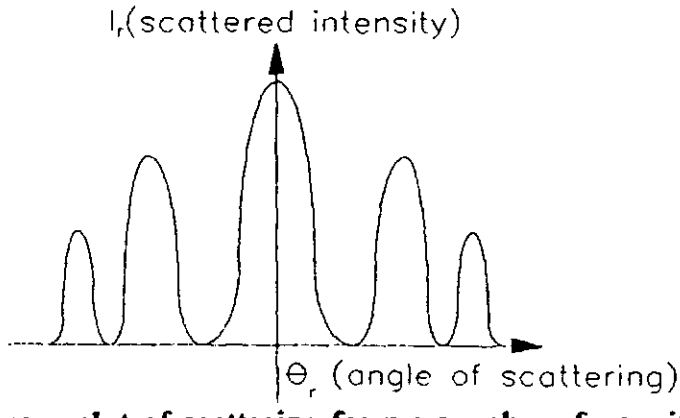

Figure 2.10: Linear plot of scattering from a rough surface with regularity

Randomness however, is produced by the detachment of the material (G.Staufert, 1979). Assuming that both processes are independent of one another, then the surface roughness can be assumed to be an additive superposition of periodic and random components. Therefore the far-field diffracted spectrum will be a superposition of the amplitude spectrum of the random component as well as the periodic component. Consequently the diffracted intensity has this additive effect incorporated in it.

Yet again, Beckmann and other authors (C.Obray, 1983) have made an attempt to predict scattering from periodically rough surfaces, however such prediction also necessitates a knowledge of the shape of the periodic corrugations in advance.

Therefore different models are needed to account for scattering behaviour from differently shaped periodic features. Most engineering surfaces with regularity do not usually possess one form of regularity. There is usually a whole series of definite marks or patterns left by the machine tool. It is very difficult to cater for complex structures as such through predictive mathematical models. In this respect this approach has neither been popular nor practical for extracting surface related parameters.

Another issue of concern is the range of validity of the formulations postulated by Beckmann. The theory upon which the scattering geometry can be predicted for randomly rough surfaces or periodic surfaces of definite sbape, makes certain assumptions in order for the predictions to be valid. The derivation of the formulae presented in equation (2.1) is based on the fact that the lateral size of the regularities is large compared to the wavelength of incident illumination. The calculation of the scattering geometry is based upon the definition of a mean angle of incidence which is the inclination of the incident radiation with respect to the normal to the mean level of the surface as shown in figure 2.4. When the lateral dimensions of the roughness features or regularities becomes small or comparable to the wavelength of incident illumination, i.e when the radius of curvature of irregularities is small compared to the wavelength of incident illumination, the predictions by this formulation are no longer valid. This is because in this case the local angle of incidence to the small feature would be significantly different from the mean angle of incidence, and the local slope will also be different from the mean slope to the surface and predictions of the scattered field which are based on the mean level of the surface geometry no longer apply.

Figure 2.11 shows the typical scattering cross section for a face-turned specimen with predominant regularity which has been used extensively in zero-phase

characterisation studies in this research investigation (N.Sotoudeh, *et al.*, 1989). As already explained, this envelope is a superposition of the spectral behaviour of the random component of the surface roughness as well as the spectral behaviour of the periodic component of the surface roughness. The distinct periodic behaviour present in the object surface is readily observable in the frequency map in the form of impulsive lobes. Turned surfaces, are a class of engineering surfaces which incorporate a wide range of different spatial structures with highly non-isotropic behaviour. Contrary to the ground surfaces, which are dominated by one particular wavelength parameter, depending upon their alignment, turned surfaces, are governed by a multiplicity of different spatial periods. This range could be from a few hundred micrometers, down to a few microns in which case the size of the features becomes comparable to the wavelength of incident illumination. For this particular surface, two types of different undulations present at right angles to one another have been observed. Namely, the coarse variations known as grooves with spatial period of $\approx 200\mu m$, followed by much finer variations known as the tool-chatter which run at right angles to the variations of the grooves ranging from $\approx 100\mu m$ to $5\mu m$. Both these characteristics result in well-defined and structured behaviour displayed distinctively in a two-dimensional frequency map.

When periodic characteristic set in the frequency spectrum, the characteristics are most amenable to zero-phase synthesis of the frequency map. Due to the sensitivity of both modulus $H(u,v)$ and intensity data $H(u,v)^2$, to the coded periodicity information, both these entities can be used to reveal the key characteristics of topographical behaviour, namely the cyclic pitch of the repetition and their corresponding variations. However, before proving this fact, it is also important to revise the zero-phase behaviour in response to the roughness distribution of the surface.

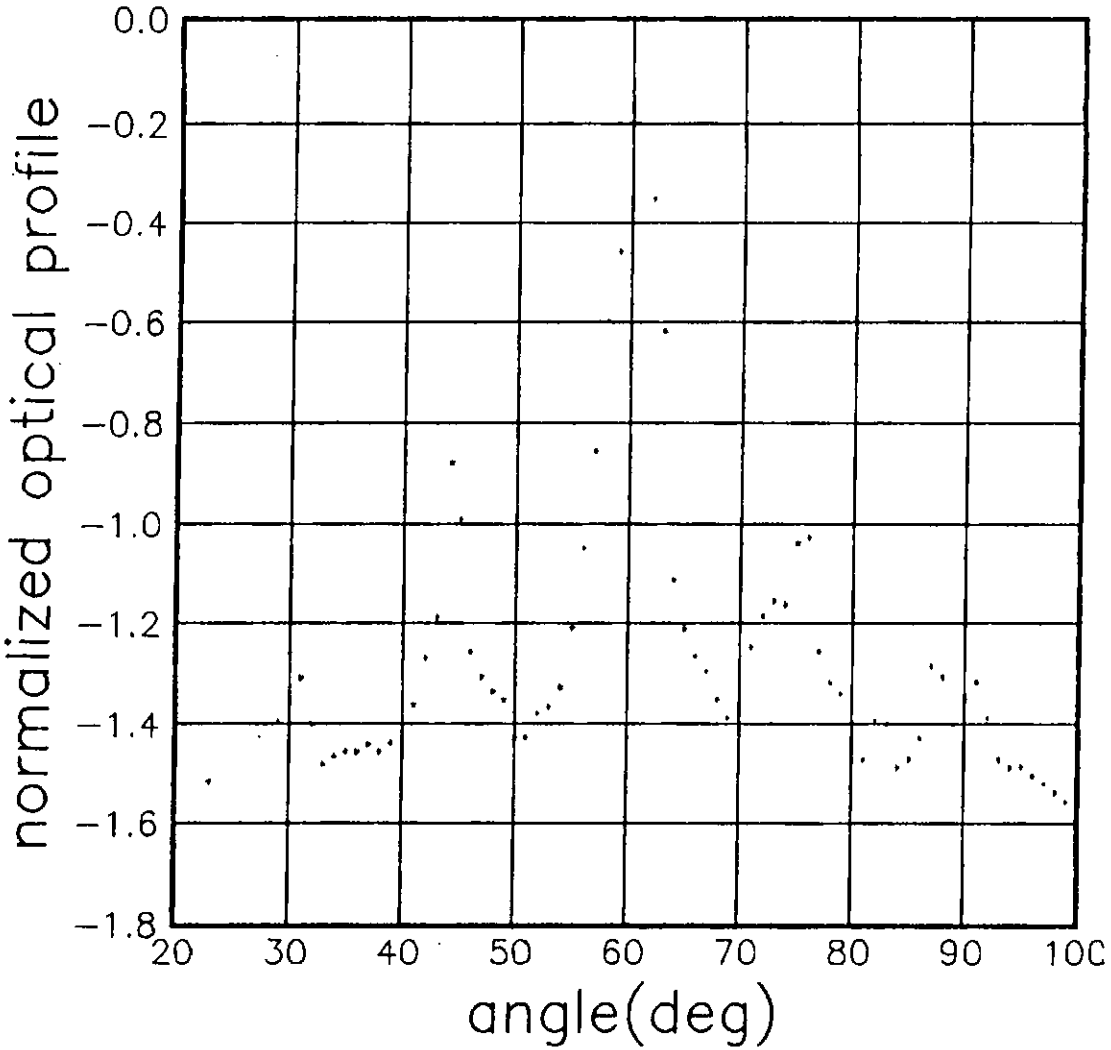

Figure 2.11: Scattering profile of a turned specimen with periodically rough characteristics from (N.Sotoudeh *et. al*, 1989)

The main purpose behind comparing the optical spectra of randomly rough surfaces and that of periodically rough surfaces was to unveil the typical behaviour of periodically rough surfaces, as opposed to random surfaces. That is, for periodic rough surfaces, periodicity has its signature engraved in the spectral characteristics of the object which is clearly identifiable not only in the scattering envelope of the object but also in its zero-phase synthesis (D.C. Champeney, 1973). In this context the observation noted by Church *et al.*, (Church, *et al.*, 1979) clearly reveals the relationship between the marked periodicity in an object profile, its spectral behaviour and its corresponding zero-phase characteristics. The scattering profile together with the zero-phase synthesis has been summarised into three main themes with only that of a highly periodic surface giving rise to distinct spectral characteristics and a most pronounced zero-phase response.

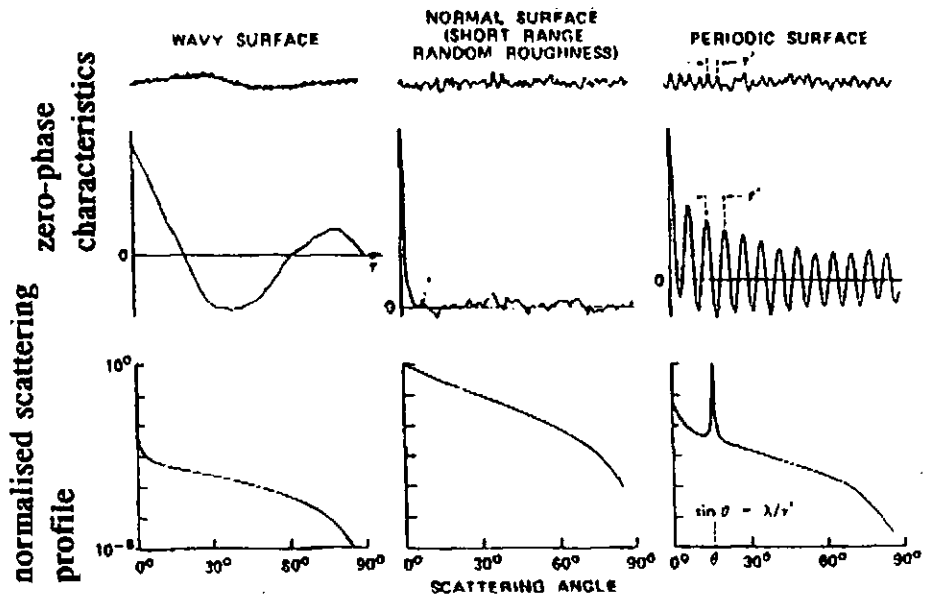

Figure 2.12: Normalised scattering behaviour for different types of rough surfaces with their corresponding zero-phase response.

With reference to figure 2.12, an undulated surface which has long range waviness is governed by lateral features of large dimensions. The scattering profile consequently gives rise to a very dominant sharp peak very close to the centre of the scattering. However the short range random roughness, have features of small lateral spacing and they result in scattering into very large angles as seen in figure 2.12a. The corresponding zero-phase characteristics are oscillatory in nature, having a slow trend,

bearing evidence that a slowly varying periodic component is present as part of the surface characteristics. In figure 2.12b, with no sign of periodic behaviour, the scattering envelope is governed by an exponential characteristics as already discussed. Due to the presence of short range random roughness, the scattering behaviour once again shows scattering into large angles from the specular direction. The zero-phase behaviour in this case shows no significant characteristics which serve to be informative.

Finally for a periodically rough surface, the scattering envelope is dominated by scattering peaks, depicted by the periodic component of the surface as shown in figure 2.12c. The zero-phase behaviour confirm the presence of dominant periodicity in both the scattering envelope and the surface by being highly oscillatory with a pitch that maintains the periodicity of the features. It is the circumstances as depicted in figures 2.12c and 2.10 that a phase-less synthesis of the object leads to meaningful results.

Although it has been attempted to use the phase less synthesis of spectral data as a tool for surface characterisation, earlier attempts were faced by disappointment. This is because it was expected to reveal information which it quite evidently could not. For instance very early application of the technique by King and Stout (T.J. King and K.J. Stout 1977), tried relating the zero-phase synthesis of the surface at various stages during a wear process to the deformations endured by the surface. However, they found out that the shape of the function did not alter significantly even though the shape of the surface was modified considerably. Zero-phase synthesis latches on the periodicity information present on the surface. Unless this periodicity is severely obliterated or modified, through wear and contact, the form of the synthesized characteristics would show no major changes particularly when the pattern is only governed by random behaviour.

However, although already stated and supported by way of evidence (J.J.Lee *et al.*, 1995) in the previous chapter, the actual proof as to why regularity is preserved in a zero-phase synthesis has not been revealed. This fact has been proved in the following section through a pictorial representation.

2.4 Latching on to the Periodicity Information

Figure 2.13 shows the proof pictorially for a repetitive profile, whereby a zero-phase synthesis is shown to be able to retrieve its characteristic behaviour namely the regularity and the geometrical arrangement of such regularity without due concern for the shape of the regular features. The diagram should be interpreted as follows. A regular arrangement of object features of any shape can be broken down into convolution of one single object with an infinite array of impulses which has been limited in size by an aperture which confines the array. In the frequency domain, shown with the symbol of FT in front of the brackets, the frequency behaviour can be seen to be equivalent to the Fourier transform of a single object multiplied by the fourier transform the array. The transform of this array of spacing d, is another infinite array with reciprocal spacing of 1/d. At this stage some simplifications can be made which will lead to easier interpretation of the results. In a phase-less synthesis, one is not actually concerned with the individual shape of the object features, it is however their lateral spacing and their regularity which are important issues. Based on this assumption, the shape of the object feature has been allowed to diminish to a point. The Fourier transform of a point is a continuum and thus the new frequency portfolio would be the multiplication of the constant value of the continuum by the infinite array with reciprocal spacing of 1/d. There is absolutely nothing that can happen to an infinite array of impulses when it is inverse Fourier transformed with zero-phase. It simply transforms into another array of reciprocal spacing, only at the expense of loosing its true boundaries and initial positioning.

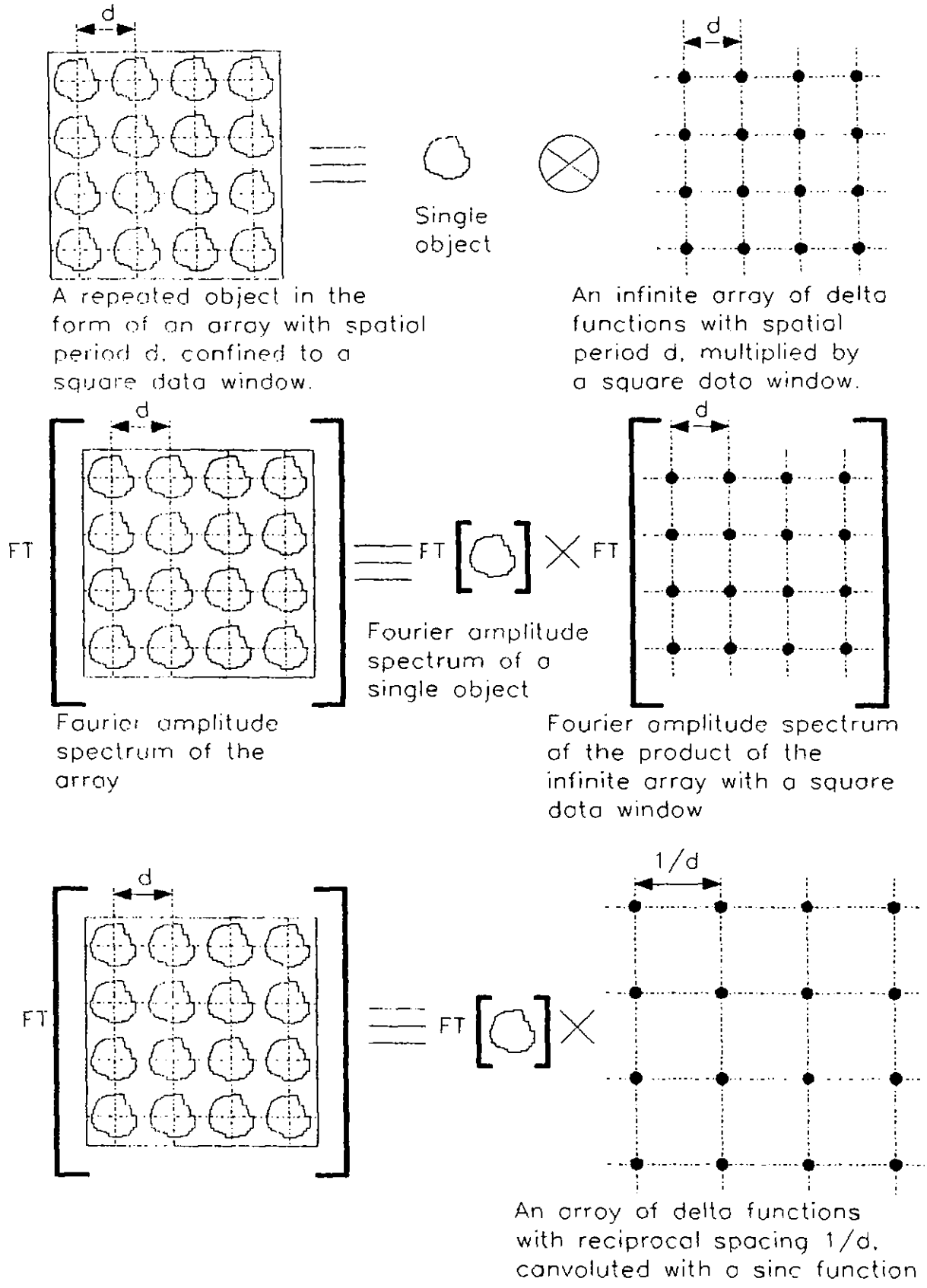

Figure 2.13: Illustration of how the object periodicity remains as part of the object characteristics in a zero-phase image of the object when either the modulus or intensity data is inverse Fourier transformed with zero-phase (pages 62 & 63).

Consider the object's geometrical structure is irrelevant and let the object diminish to a point, i.e. :

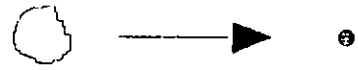

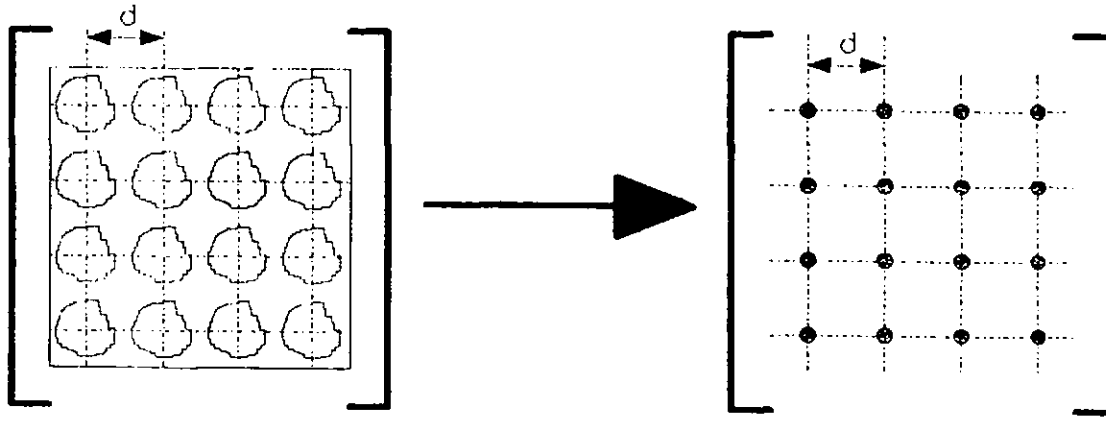

Hence the object array diminishes to an array of delta functions with arbitrary amplitudes (shown in grey).

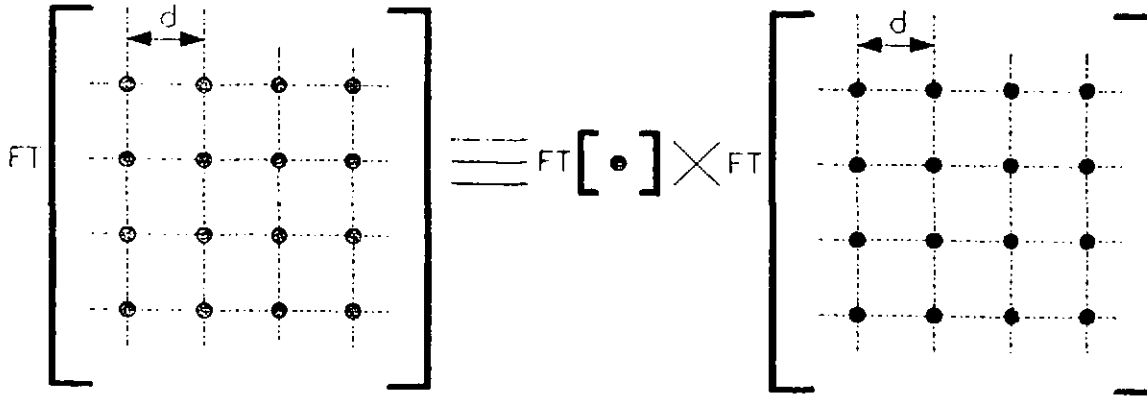

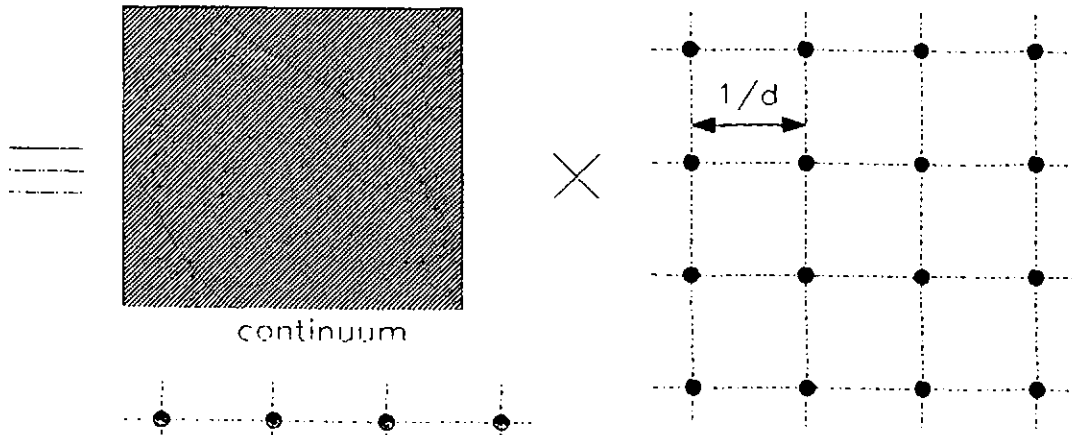

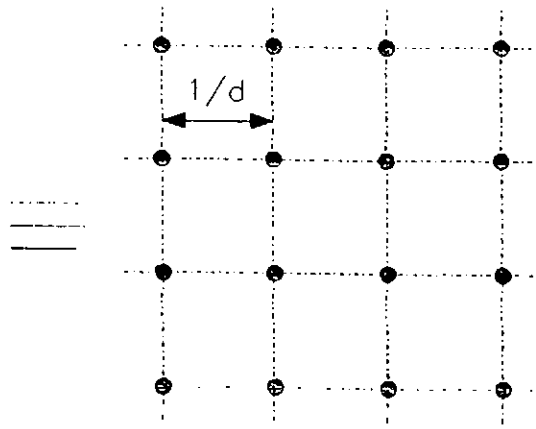

Hence a zero-phase IFT of this information always restores the periodicity of the object feature irrespective of its geometrical structure.

Thus in the very extreme cases where one overlooks the structural information of the object itself, both the modulus and the intensity synthesis of spectral data are still capable of preserving the periodicity information; a knowledge that could be utilised in the characterisation study of many engineering surfaces.

2.5 Discussion on what has been achieved

The study conducted on the observation and modelling of the one-dimensional cross section of scattering from randomly rough surfaces is not new. Many researchers, have utilised Beckmann's formulations, to extract surface related parameters such as rms roughness, or mean slope, as an alternative way for characterising the surface through optical scattering measurements. Incidently, many researchers have also come to realise that not all surfaces can be characterised through this technique, simply because, surface fluctuations, do not necessarily follow a Gaussian model (D.L. Jordan, *et al.*, 1988), (J.Eastman and P.Baumiester, 1974). That is the surface is not usually a smoothly varying surface, containing amplitude fluctuations of roughly the same characteristic size, such as that dictated by a Gaussian curve.

Even data extracted from the mathematical models based on Beckmann's approach, have reported evident anomalies between the optically extracted parameters, and those obtained from stylus profilimetry. In this context, studies conducted by (E.Marx, *et al.*, 1993) revealed that the rms roughness obtained from stylus profilimetry for handlapped stainless steel had to be multiplied by a factor of 0.79, to obtain agreement with the value obtained from light scattering. Though a little dated, this fact has also been reported by (C.Obray, 1983) and (Thwaite, 1982) where it was noted that an adjustment factor of x2 is required to obtain agreement between optically extracted roughness and that of stylus profilimetry.

CHAPTER 2

For a great many surfaces to be able to relate the observed diffracted intensity to the topology of the surface, one has to cater for new mathematical models which have utilised other descriptions for surface height statistics. For instance, the surface height distribution might be negative exponential instead of Gaussian and the autocorrelation function might be non-Gaussian.

Assessment and characterisation of repetitive and regular profiles seems to be even model difficult than those with merely random characteristics. This is because most surface finishing processes which give rise to regularity in the object, generate a whole range of regular characteristics alongside the dominant pattern observed on the surface. It is extremely difficult to cater for complex surface structures as such through mathematical models. Consequently this method has neither been practical nor feasible for characterisation purposes of such surfaces, especially when the surface has non-isotropic characteristics and endures features whose dimensions are comparable to the wavelength of the incident illumination.

When structure and regularity prevail, it has been shown that a frequency synthesis approach can be adopted to reveal surface characterisation parameters without any recourse to the phase of the optically diffracted data. The sensitivity of this approach to object feature regularity has been proved in section 2.5 for the most simplest form of regularity. It has been shown that typical regularity in the object is by no means prone to obliteration in a synthesised profile in the absence of phase information. This particular concept has led to the utilisation of zero-phase synthesis in object characterisation studies for an object with known geometrical structure in chapter 4 and a machined surface of unknown geometry in chapter 5.

CHAPTER 3

EXPERIMENTAL METHODS

3.1. Introduction

This chapter contains the experimental aspects of recording the optical diffraction pattern and highlights the main practical limitations imposed on the captured optical spectrum. It also addresses the purpose written software from the stage of capturing the diffraction pattern to the zero-phase characterisation of the object specimen in chapters 4 and 5. This software, is further elaborated through the implementation of the logarithmic Hilbert transform integral for the extraction of the object phase from its Fourier modulus spectrum, which is utilised in chapter 6.

Sections 3.2 provides the preliminary calculations as regards the approximate positioning of the relevant optics for capturing the overall diffraction pattern, as well as estimating the cutoff frequency of the Fourier transforming lens for assessing the highest spatial frequency of the object signal which is allowed through by the lens.

Section 3.3 discusses the camera and the digitiser used and identifies the overall resolution of this recording system in terms of the cyclic pitch of the imaging pixels available in the digitised information. Sections 3.4 and 3.5, portrays the speckle effect and the aliasing phenomenon. This section also provides the necessary calculations for estimating the maximum size of the spatial structures whose corresponding frequency information would give rise to aliasing when their frequency map is digitised.

As it will become evident in the body of this chapter, this information is of considerable importance in two respects:

i) Firstly, to ensure that the information associated with the largest spatial structures in the object specimen is not obliterated through aliasing and;

ii) Secondly to ascertain whether the cyclic pitch of the imaging pixels in the digitised image is such that it allows for "frequency compression" to take place without any loss of information; such scaling of the frequency spectrum has been identified as a novel means of restoring finer structures in chapter 5.

Section 3.6 provides a schematic diagram of the video micro-scaler arrangement for recording magnified images of the object specimens which have been used in chapters 4 and 5. Finally, section 3.7 lays out the main computational procedures which were used for processing the digitised information.

CHAPTER 3

3.2 Capturing the Diffraction Pattern

The experimental diffraction pattern was obtained via the set up of figure 3.1 on the next page. In this arrangement, the focal length of the Fourier transforming lens plays an important role in transmitting the diffracted stream of light waves on to the imaging screen at its back focal plane. The focal length of this lens is 20 cm. Very short focal length lens have many abberations whilst a larger focal length lens will collect insufficient light. The maximum spatial frequency transmitted by this Fourier transforming lens will be dependant on the lens aperture diameter as well as its focal length. Referring to figure 3.2a below, the cut off spatial frequency q_c of the lens can be formulated as :

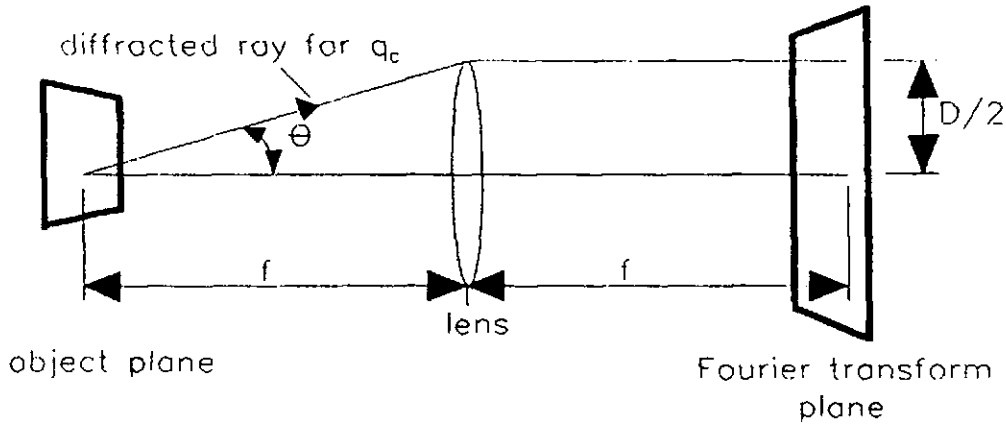

Figure 3.2a: Schematic diagram for the estimation of the cut off frequency of the Fourier transforming lens.

$$\sin\theta = \lambda q_c \qquad (3.1)$$

$$\tan\theta = \frac{D/2}{f} \qquad (3.2)$$

where f is the focal length of the Fourier transforming lens, for small θ, $\sin\theta = \tan\theta$ therefore:

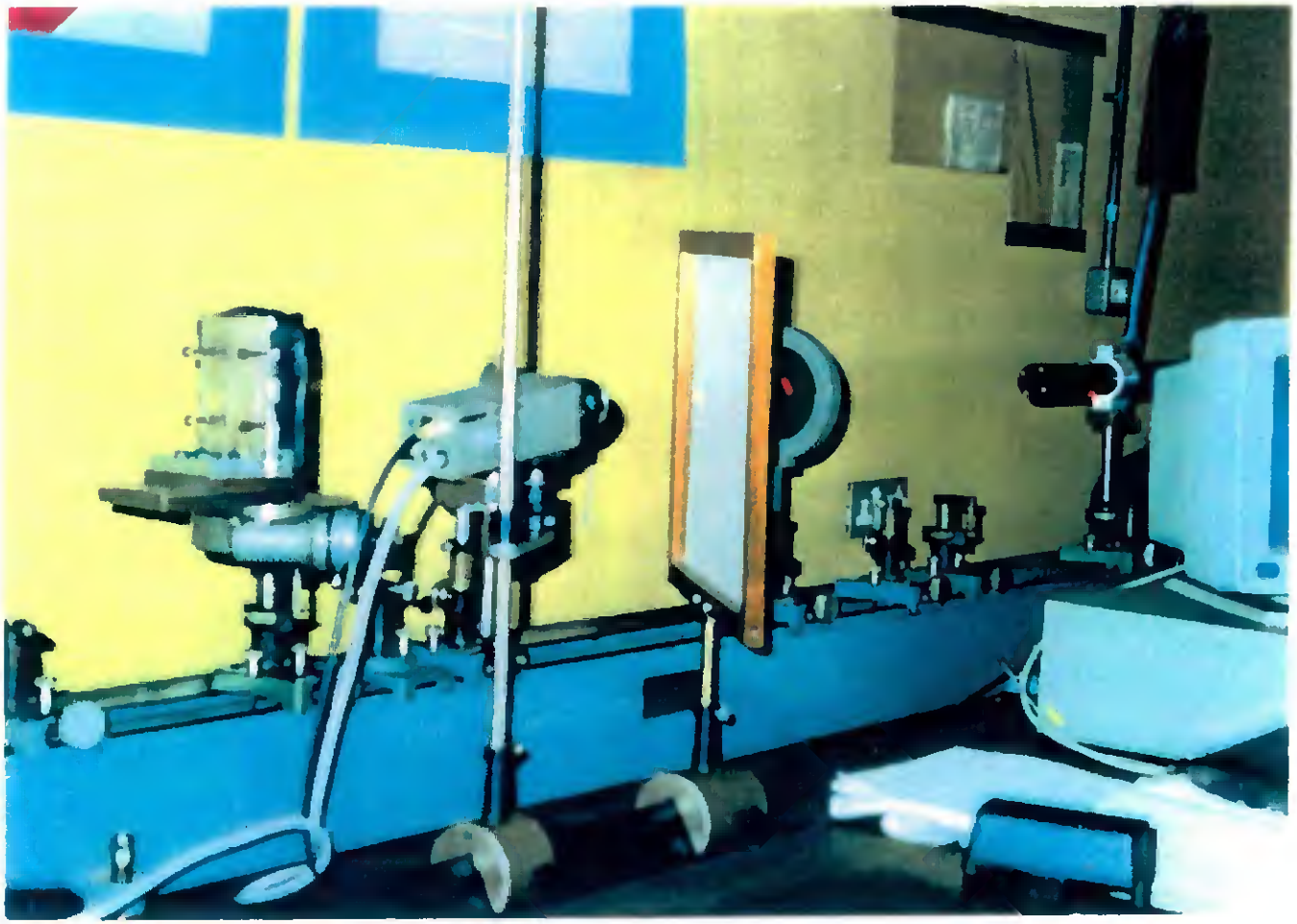

Figure 3.1: The experimental setup for capturing the diffraction pattern.

$$\lambda q_c = \frac{D/2}{f}$$

$$\therefore \quad q_c = \frac{D}{2\lambda f} \qquad (3.3)$$

the aperture diameter of the Fourier transforming lens is D=70mm, inserting numerical values into the above equation, the cut off spatial frequency of the lens would be:

$$q_c = \frac{70x10^{-3}}{2x0.632x10^{-6}x20x10^{-2}}$$

$$\therefore q_c = 277 \quad cycles/mm$$

This corresponds to a spatial period of $1/q_c$ or features with spatial period of approximately 3.6μm. The finest measured spatial features for the machined surface obtained via the alpha stepper, indicates cyclic components with a spatial periodicity of 5μm. Thus as far as the cut off spatial frequency of the lens is concerned, the frequency information of the 5μm features, would be admitted by the Fourier transforming lens into its back focal plane.

Two types of cameras were used to record the diffraction pattern and the magnified images of the object surfaces. i) Vidicon camera, ii) CCD camera. It is important that either camera must be placed far enough away from the screen on which the Fourier transform pattern is projected to ensure that the whole of the Fourier transform is imaged on to the Vidicon area of 11mmx11mm or CCD array of 8mmx6mm. The camera lens itself has a typical focal length f_{TV} of 16mm. The distance D/2 must be imaged to 5.5mm in the case of the vidicon camera.

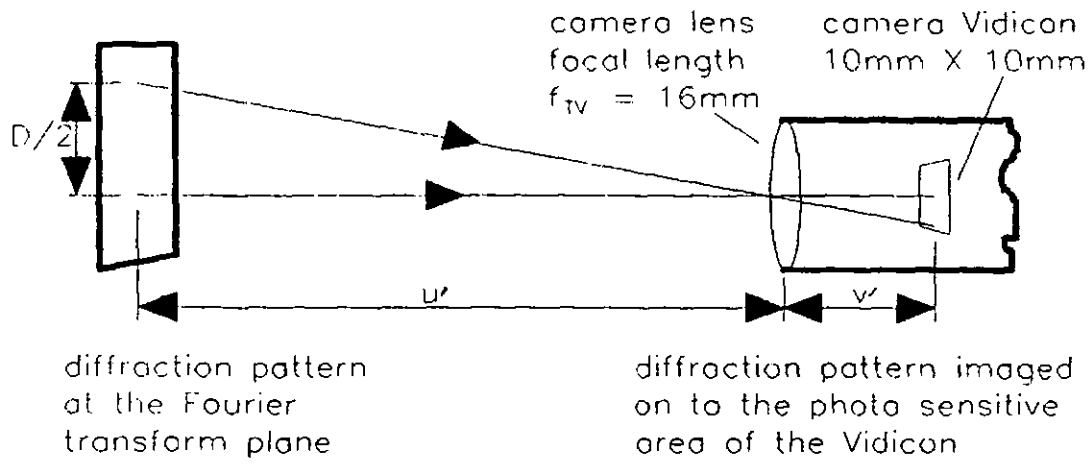

Figure 3.2b:Schematic diagram for the estimation of the approximate positioning of the camera for recording the whole of the diffraction pattern on to its photosensitive surface.

From figure 3.2b, in terms of the distance of the diffraction pattern from the camera i.e u' and the image of this pattern at the back focal plane of the camera lens i.e v', the ratio of the size of the image seen on the photosensitive surface to the size of the image at the diffraction plane M (the magnification factor) is :

$$M = \frac{v'}{u'} = \frac{5.5}{D/2} \qquad (3.4)$$

$$\frac{D/2}{u'} = \frac{5.5}{v'}$$

from the standard lens equation:

$$\frac{1}{u'} + \frac{1}{v'} = \frac{1}{f_{TV}} \qquad (3.5)$$

$$\frac{1}{u'} + \frac{1}{v'} = \frac{1}{16}$$

also from (3.4) v' would be

$$\frac{v'}{u'} = \frac{5.5}{D/2} \quad i.e \quad v' = \frac{11u'}{D} \tag{3.6}$$

allowing for $v' = 11u'/D$ in equation (3.5), u' would be obtained as:

$$u' = \frac{16\,(11+D)}{11}$$

substituting for the aperture diameter of the Fourier transforming lens, i.e 70mm then the distance of the camera from the Fourier transform spectrum is:

$$u' = 1.454\,(11+70) \quad i.e \quad u' = 117.8\,mm \tag{3.7}$$

hence the normal focusing of the camera lens at the above distance or more would adequately capture the whole of the diffraction pattern onto its photosensitive screen. Although, at this distance the whole of the diffraction pattern would be registered by the camera onto its photosensitive surface, the camera was moved closer to the screen for two reasons.

Firstly, the very high spatial frequency components were almost invisible to the camera. Whilst eye has a logarithmic response and is thus capable of viewing a large dynamic range, the camera characteristics is almost linear,and the range of intensities that it can accommodate is thus limited. Consequently, the spectral lines which were discernable with the naked eye, in the diffraction pattern were not picked up by the camera. Therefore, instead of capturing an image whose outer regions were missing, the camera was moved closer to the screen to capture a more magnified image of the diffraction pattern, focusing on the low to medium frequency information. The camera had to be moved fairly close to the observation screen and both the camera aperture and the polaroid film had to be adjusted to prevent excess light entering the lens. The magnified image was captured at an approximate distance of $u' \approx 70$mm.

Secondly, a closer positioning of the camera, would cause the viewed image of the diffraction pattern to appear larger, with more imaging pixels across the digitised scene. More imaging pixels, allows for a greater degree of freedom in manipulating the scale of the frequency data; an operation which in turn controls the scale of the events in the object domain. The significance of such scaling would become evident in chapter 5.

To avoid the effects that the luminance of the screen may have on the diffraction pattern, the camera should ideally be focused on the Fourier transform plane, without the inclusion of the imaging screen. However, if the screen is not present, the outer edges of the Fourier transform may well miss the camera lens aperture. With the screen present, the whole diffraction pattern can be captured by the camera but the luminance may be small. It was found that focusing the camera on the Fourier plane without the presence of the screen resulted in excess light of the direct reflective component entering the camera and the whole pattern was obliterated.

CHAPTER 3

3.3 The Camera and the Digitiser

Two types of cameras and digitisers were used for recording the diffraction pattern as well as the magnified images of the object surfaces used in the zero-phase characterisation studies of chapters 4 and 5.

The diffraction pattern for the machined surface was captured via the Vidicon camera. Although originally this was the recording device available, it offers a wider dynamic range in terms of the variations in the intensity of the light level as compared to a CCD and thus is less susceptible to blooming effects (R.Tienwen Chien and W.E.Snyder, 1975).

In order to estimate the spatial resolution of the type of images captured by the Vidicon camera, it's principle of operation would be discussed briefly. The target in a Vidicon consists of a photoconductive mosaic (usually lead oxide) deposited onto a transparent metal film known as the signal plate. Light through the signal plate and strikes the photoconductive mosaic changing its resistivity. This change in resistivity persists over the entire surface simultaneously for a period of time equal to one frame of scan (approximately 30 ms for U.S. standard televisions).

The image is formed by a scanning electron beam which strikes the mosaic plate. When the scanning electron beam strikes a particular piece of the mosaic plate, because the resistivity of that particular piece of the mosaic has already changed in proportion to the intensity of light which has struck that piece, the current passing from the beam to the mosaic to the signal plate would vary. Since the location of the electron beam is known for each instant in time, the current variations for each instant in time are directly related to the input intensity verses position.

The scanning of the mosaic plate by the electron beam generates pictures similar to the raster scan images formed in a standard Television. European television breaks a picture into 625 lines of video or raster scans from top to bottom. Out of these 625 lines, 48 lines are suppressed and the number of effective video lines available for imaging are (R.Coolen, 1981):

$$\begin{aligned} No.\ of\ effective\ lines &= (\ N-N_s\ ) \\ &= 625-48 \\ &= 577 \end{aligned} \qquad (3.8)$$

In order to estimate the pixel resolution of the raster type images generated by the Vidicon, one has to estimate:

i) the number of samples per line of video or per raster scan;

ii) the cyclic pitch or the separation of the raster scans which forms the entire image.

A photosensitive area of approximately 11mmx11mm is available for imaging on the photosensitive surface of the vidicon camera. The digitised scanned image produced by the camera will have a cyclic pitch which can be determined from the number of horizontal and vertical lines of video available for imaging.

For one image frame which consists of 577 lines of video or raster scans, the cyclic pitch or the separation of the raster scans in the vertical direction C_{pv} is:

$$\begin{aligned} C_{pv} &= \frac{11\,mm}{577} \\ &= 19\ \mu m \end{aligned} \qquad (3.9)$$

The number of horizontal elements per line of video or per raster scan (R.Coolen, 1981) is:

$$N_{hor} = aspect\ ratio\ x\ (N-N_s)$$
$$= \frac{4}{3}\ x\ 577 \qquad (3.10)$$
$$= 769\ pixels$$

Since each line of video is approximately 11mm long in the horizontal direction, the cyclic pitch of the elements in the horizontal direction C_{ph}, would be:

$$C_{ph} = \frac{11\,mm}{769} \qquad (3.11)$$
$$= 14\ \mu m$$

The digitisation of this analogue image is carried out via Microeye camera interface which passes the image to the microcomputer via a standard 8 bit port. The Microeye is not a frame grabber and does not store the image itself but stores it in a section of the microcomputer's RAM while image processing is carried out. Whilst each line of video is scanned in 64 μs (european TV system) by the camera, it takes 64 μs by the Microeye digitiser to write each pixel into the microcomputer's RAM. More so, each line of video is divided into 256 pixels by the digitiser, with a complete image corresponding to 256 of such lines.

Though, at the standard european rate of 625 lines, the captured image by the camera, offers a resolution of 769 x 577 pixels, this definition is somewhat degraded in spatial resolution by the digitising device to that of 256 x 256 pixels. Thus, the output image by the camera which is confined to a rectangular region of 11mm x 11mm , when digitised to 256 x 256 pixels would have a cyclic pitch of 11mm/256 horizontally, and a cyclic pitch of 11mm/256 vertically. The coarser cyclic pitch of the imaging pixels as set by the digitiser are thus, 42μm horizontally and vertically.

This cyclic pitch is important in two respects:

i) firstly, to ensure that there are no spatial frequency components in the diffraction pattern whose frequency matches that of the repetition intervals or the cyclic pitch of the imaging pixels, as this leads to aliasing;

ii) secondly, the recorded diffraction pattern by the camera does not have a localised granular pattern known as speckle incorporated in it. For this, one has to estimate the average size of the speckle granules in the diffraction pattern and note whether such fluctuations are picked up by the recording device and the digitiser.

The next section provides an estimate of the average size of this speckle as imaged by the camera on to its photosensitive surface and whether this effect can be neglected.

3.4 Speckle due to Coherent Illumination

The coherent illumination of the screen via using the laser source is accompanied by speckle. Speckle is the granular structure that seems to pervade any patch of laser illumination. The size of the speckle granules is dependant on the screen surface characteristics, numerical aperture of the imaging system and the screen distance. For a circular patch of illumination, of diameter P and wavelength λ , the average size of the speckle $<\delta>$ is given by :

$$<\delta> = \frac{1.2\lambda L}{P} \qquad (3.12)$$

where L is the distance of the scattering surface from the observing screen (T.V.Vorburger and E.C.Teague 1981). When observing the laser generated diffraction patterns, the observer nearest to the screen would have no difficulty in seeing the details of the pattern because the speckle noise is small, i.e the size of the speckle granules is small compared with the patch of laser illumination. The observer further from the screen would find that the size of the speckle is so large that it completely dominates the diffraction features and prevents them from being seen, i.e at a great distance the speckle granules may become bigger than the laser patch itself. Since the diffraction pattern is recorded via the camera, the camera image plane will see a different pattern from what the observer's eyes sees. Hence the camera location and its aperture should be selected such that speckle noise is minimised. It should be noted that making the camera lens aperture small will aggravate the problem. For the optical arrangement of figure 3.3 via using the lens the speckle size can be found from:

$$\langle\delta\rangle = \frac{1.2\lambda}{\alpha} \qquad (3.13)$$

where α is the angle subtended by the aperture of the imaging system at the image plane. In terms of the distances to the screen, the speckle can be reformulated as:

$$\langle\delta\rangle = \frac{1.2\lambda L}{D} \qquad (3.14)$$

where D in this case is the aperture diameter of the imaging lens. For the arrangement of capturing the diffraction patterns, where L equal the focal length of the Fourier transforming lens f_L=20cm, D is the aperture diameter of this lens i.e 70mm and λ=0.632 μm the speckle size at the Fourier plane is:

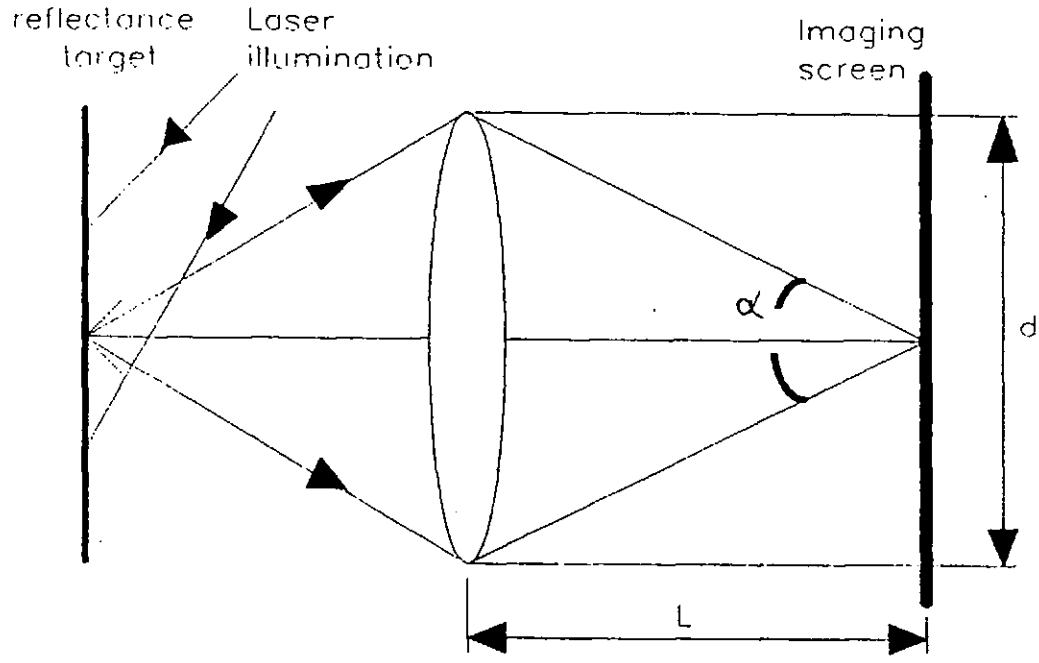

Figure 3.3: Estimation of the average size of the speckle at the Fourier transform plane.

$$\langle\delta\rangle = \frac{1.2 \times 0.632 \times 10^{-6} \times 20 \times 10^{-2}}{70 \times 10^{-3}} \qquad (3.15)$$

$$\therefore \langle\delta\rangle = 2.1\,\mu m$$

But from the point of view of the camera, this feature further experiences the magnification factor introduces by the camera of the order of 0.3 for the arrangement of figure 3.2b. Hence the speckle size captured onto the camera image plane is :

$$\langle\delta\rangle = 0.3 \times 2.1 \times 10^{-6}\ m \qquad (3.16)$$

$$\langle\delta\rangle = 0.63\mu m$$

$$\therefore \langle\delta\rangle \approx 0.6\ \mu m$$

This is the average size of the speckle granules as seen by the camera on its photosensitive surface. The size of 0.6 μm is far too small to pervade any patch of intensity variations in the diffraction pattern as seen by the camera from the location at which it is positioned.

3.5 Calculating the aliasing zone

Of prime importance is the problem of aliasing and the awareness of its zone within the limitations of the experimental set up. Aliasing arises when the cyclic pitch of the imaging elements of the detecting device matches the cyclic pitch of the information which is to be recorded. For object surfaces with regularity which is the type of objects studied in this research, the periodicity information must be intercepted at a sufficient sampling rate (minimum being half the cyclic pitch of the periodic features) so that the characteristics of the feature of interest can be restored from the sampled information.

What must be emphasized is that, since it is the frequency information which is being recorded, it is the frequency data associated with large regularities in the object which are at risk of being insufficiently sampled by the detector as opposed to fine regularities. The aliasing zone thus refers to the size the of largest features of interest in the object whose related frequency information is sampled at a sufficient rate by the detecting device.

The size of the largest feature of interest whose associated frequency information is adequately sampled by the detector/digitiser combination is then estimated from the optical arrangement of figure 3.4 as follows:

The output image from the Vidicon camera consists of 577 lines of video with a cyclic pitch of 19μm vertically and 769 elements along each line, whose cyclic pitch is 14μm. However, as mentioned, the 256x256 digitised image of degrades this resolution, to 42μm horizontally and 42μm vertically. The perception of the optical scene at a sufficient sampling rate, is thus checked at two stages: i) firstly from the point of view of the camera and ii) secondly from the point of view of the digitisation

of the camera scene. Firstly, the cyclic pitch of the smallest repetition interval in the frequency domain, as seen by the camera is estimated. It can then be commented whether the cyclic pitch of the camera imaging elements intercepts this information at a sufficient sampling rate.

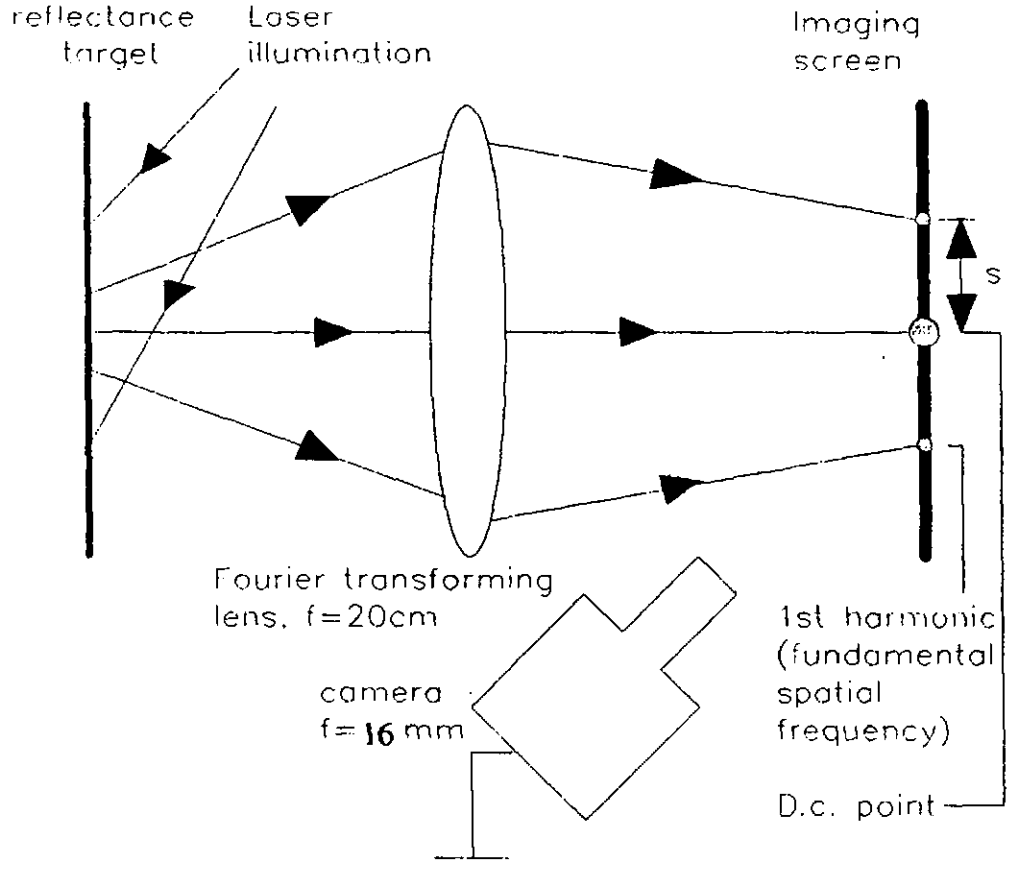

Figure 3.4: Schematic arrangement for the calculation of the aliasing zone.

With reference to figure 3.4, the image of the object's periodicity interval in the diffraction pattern, would be seen to have a cyclic pitch of C_{po}:

$$C_{po} = M.s \qquad (3.17)$$

where M is the magnification factor obtained from the distance of the camera from the screen and the focal length of its imaging lens; and s is the distance between the DC point and the fundamental frequency point in the diffraction pattern; i.e s is the cyclic pitch of the periodicity at the diffraction plane.

But, the Nyquist criterion, requires the cyclic pitch of the camera imaging elements to be smaller than or equal to the cyclic pitch of the periodicity in the diffraction pattern by a factor of 0.5 i.e :

$$C_{ph} \leq \frac{1}{2} . C_{po} \qquad (3.18)$$

assuming that the cyclic pitch of the imaging regions on the Vidicon, i.e C_{ph} is 19μm, this sets a minimum size for the image of the diffraction spots on the camera plane of 38μm i.e, using equation (3.17), Where the magnification factor M, as previously expressed is :

$$M = \frac{u'}{v'}$$

where u' is the distance of the diffraction pattern from the camera lens and v' is the distance of the image of this diffraction pattern in the back focal plane of the camera lens. Alternatively, using the standard lens equation, the magnification formulae can be expressed in terms of the focal length of the camera lens f_{TV} and the distance of the diffraction pattern from the camera, using equation(3.5), i.e:

$$\frac{1}{f_{TV}} = \frac{1}{u'} + \frac{1}{v'}$$

from rearranging equation (3.5) 1/v' would be:

$$\frac{1}{v'} = \frac{u'-f_{TV}}{u' \cdot f_{TV}}$$

substituting for 1/v' from (3.4), 1/M would be:

$$\frac{1}{M} = \frac{u'(u'-f_{TV})}{u' \cdot f_{TV}} \qquad (3.19)$$

hence

$$M = \frac{f_{TV}}{u'-f_{TV}} \qquad (3.20)$$

inserting numerical values into (3.19), for u′=70mm and f_{TV}=16mm, M would be:

$$M = \frac{f_{TV}}{u'-f_{TV}} = \frac{16x10^{-3}}{(70x10^{-3}-16x10^{-3})} = \frac{16x10^{-3}}{54x10^{-3}} \qquad (3.21)$$

$$\therefore M = 0.3$$

Substituting for M in (3.17), the distance s can be calculated as:

$$s = \frac{38x10^{-6}}{M} = \frac{38x10^{-6}}{0.3} = 126.66x10^{-6} \qquad (3.22)$$

This is the minimum separation that the cyclic pitch of the periodicity in the diffraction pattern can have so that the image of it as seen by the camera can be sampled at the minimum Nyquist rate.

The distance s, which is the distance between the DC point and the first or the fundamental harmonic component on the screen, is also the smallest distance between the Fourier elements for the periodic objects. This distance s, can be obtained as:

$$s = f \lambda q \qquad (3.23)$$

where λ is the wavelength of the incident laser beam i.e, $\lambda \approx 0.632\mu m$, f is the focal length of the Fourier transforming lens i.e f=20cm, and q is the spatial frequency of the object in cycles per m.

To calculate what size object it corresponds to, from s, the spatial frequency of the object, q, is obtained via rearranging (3.23), i.e:

$$q = \frac{s}{f.\lambda}$$
$$= \frac{126.66x10^{-6}}{20x10^{-2} \; x \; 0.632x10^{-6}} \qquad (3.24)$$
$$\therefore \; q = 1002.11 \; cycles/m$$

Since the object dimensions and its spatial frequency are reciprocally related, thus O_s, the object size would be:

$$O_s = \frac{1}{q}$$
$$= \frac{1}{1002.11} \; m \qquad (3.25)$$
$$\therefore \; O_s = 998 \; \mu m$$

Thus, 998μm is the largest object size, or the largest periodicity for a periodic object, for which, its associated frequency spectrum can be sampled at Nyquist rate by the camera. The grooves on the surface of the machined surface, which are the object characteristics with the largest spatial period, have a cyclic pitch of approximately 200μm i.e $O_{grooves}$ ≈200μm. The grooves are smaller in size than the largest estimated structure in equation (3.25) by approximately a factor of 5, i.e $O_{grooves} = 1/5 \; O_s$. This implies that their corresponding frequency information would be 5 times further apart than that of the 998μm features i.e:

$$O_{grooves} = 200\mu m$$
$$\therefore \; q_{grooves} = \frac{1}{200x10^{-6}} \qquad (3.26)$$
$$q_{grooves} = 5000 \; cycles/m$$

Thus their corresponding separation in the diffraction pattern would be $S_{grooves}$:

$$S_{grooves} = 20x10^{-3} \; x \; 0.632x10^{-6} \; x \; 5000$$
$$\therefore \; S_{grooves} = 632\mu m \qquad (3.27)$$

The image of this periodicity, on the photosensitive surface of the camera would have a cyclic pitch of:

$$C_{grooves} = 0.3 \; x \; 632x10^{-6}$$
$$\therefore \; C_{grooves} = 189.6\mu m \qquad (3.28)$$

This characteristic would be sampled at a sufficient rate both by the camera and the two resolutions offered by the digitiser. As already addressed in section 3.2, the camera had to be moved much closer to the diffraction screen, than the distance that was originally anticipated i.e 117mm or more. Moving the camera closer to the screen would obviously lessen its field of view, as far as the higher frequency components are concerned. But, there is little point in positioning the camera far away from the screen to capture the whole of the diffraction, when all that it is capable of registering, is the medium to lower frequency regions. This included the frequency information associated with the grooves, as well as the higher harmonic of the tool-chatter mainly in the range of 30μm-100μm. Thus, any lower harmonics of the tool-chatter components mainly the spatial features below 30μm, would not have their frequency information acknowledged by the camera.

3.6 The travelling optical microscope

The travelling optical microscope was used for two purposes: i) firstly to provide magnified images of the object surfaces to be used in computer simulated studies; and ii) secondly, for measuring the dimensional range of the features as well as obtaining enlarged photo-micrographs of the object specimen. Magnified images of the circular transmittance object and the machined surface, the two specimens used in zero-phase characterisation studies were obtained, by mounting the CCD camera onto the microscope, whose magnified image was then digitised via the Electric Studio digitiser. The final digitised image had a resolution of 768x576 pixels, from which the region of interest was extracted as a 512x512 matrix. Figure 3.5 shows the schematic diagram of the arrangement.

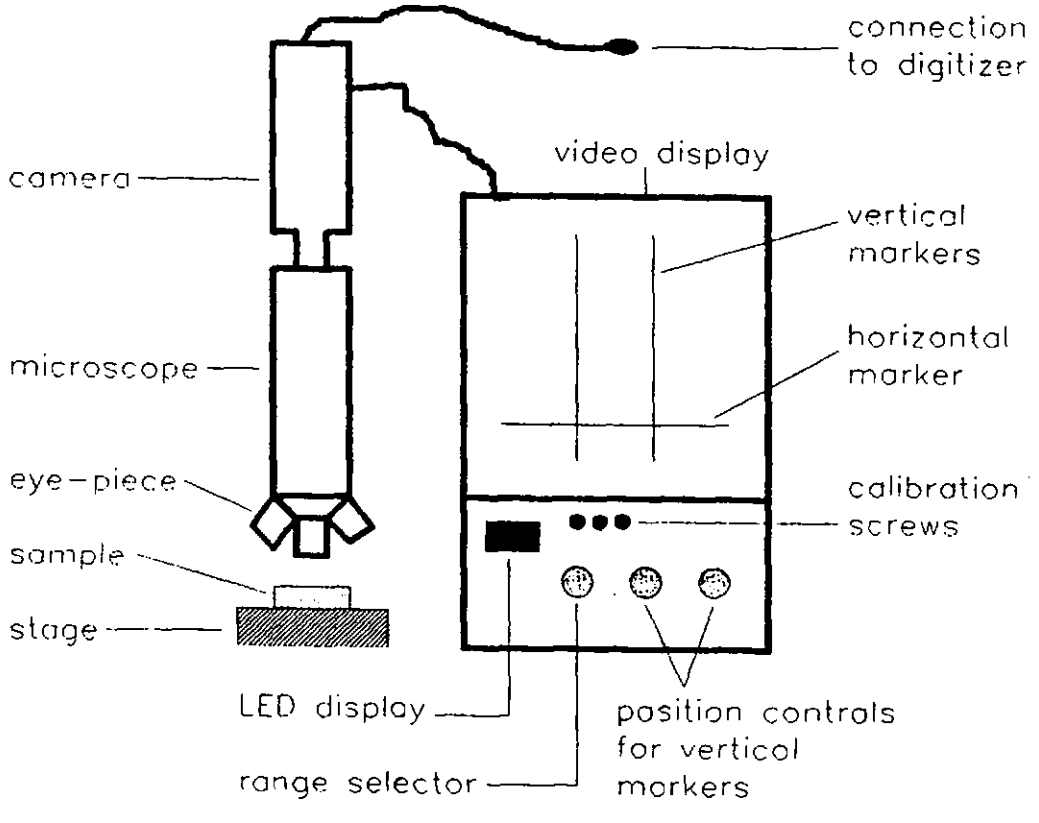

Figure 3.5: Schematic of the travelling optical microscope.

Figure 3.6 is the photomicrograph of the machined surface obtained via a polaroid camera imaging the monitor display of the travelling optical microscope. The cross hair displays surface features of ≈75μm spatial period, the darker broken lines above this feature having a length of ≈38μm-33μm; the next set of lines , i e fainter lines having a length of ≈22μm.

3.7 The Purpose Written Software

The digitised images captured by the digitiser were assigned numerical values for conventional processing of the images. A program was written to convert the ASCII images into hex and decimal values for transfer to mainframe and further processing on the Vax system. In circumstances where the odd and even frames had to be captured separately, a further routine combined these two into one single image of 769x577 lines. Further preprocessing involved averaging two to three frames of images for low pass filtering the captured images. The main programs for processing the data were written in pascal and consisted of "zero-phase" algorithms for inverse Fourier transformation studies with zero-phase in chapters 4 and 5, "Block changing" for conventional viewing of FFT data, which is part of any major FFT algorithm Figure 3.7, and finally the Hilbert transformation routine based on the digital

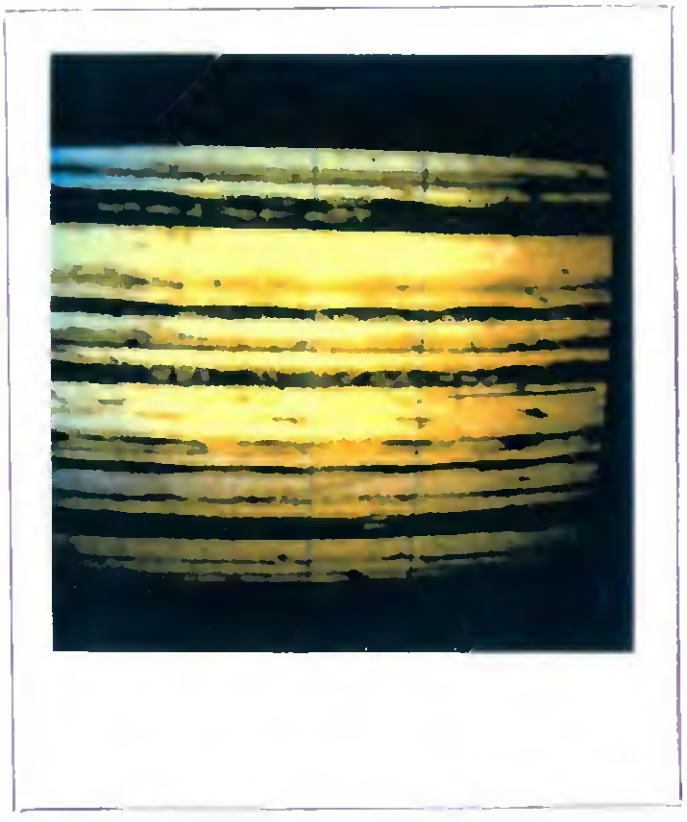

Figure 3.6:Photomicrograph of the machined surface showing a range of different spatial wavelengths present on the surface.

implementation of the algorithm presented in chapter 6, for the major object reconstructions displayed in chapter 6. Apart from the displayed colour graphics which is part of the Uniras graphics facility available on the mainframe, all the necessary software for processing and presenting the data in this thesis has been purpose written by the author.

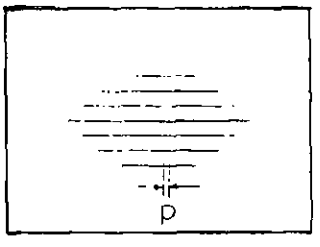

Original image

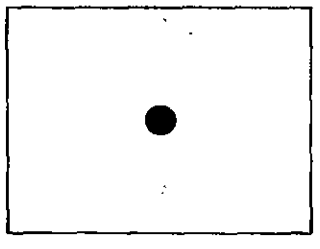

Optical Fourier transform pattern

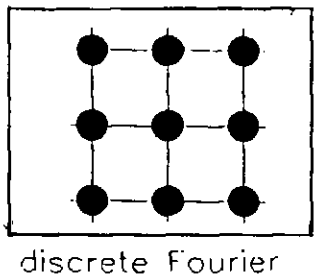

discrete Fourier transform pattern

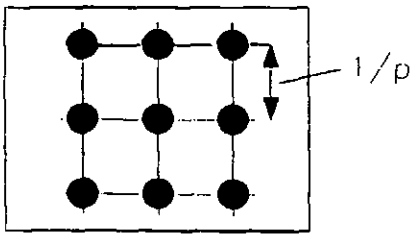

characteristics of the discrete FT repetition of the image

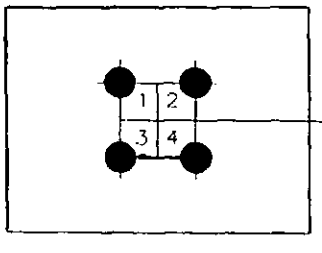

Fast Fourier transform display

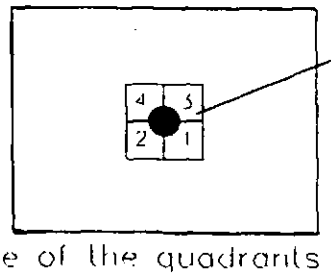

Exchange of the quadrants for the conventional display of the FFT

CHAPTER 4

STRUCTURAL CHARACTERISATION OF SURFACES USING ZERO PHASE

4.1 Introduction

The route towards the object image reconstruction from the modulus of its Fourier spectrum, is through the inverse Fourier transformation of such entity. Many object surfaces possess no dominant spatial characteristics which render the inverse Fourier transformation of the spectrum meaningless in the absence of phase. However, certain object surfaces possess structural information which in turn leads to a more meaningful interpretation of their recovered behaviour.

Dominant structural information is considered as any geometrical configuration which is well defined and repetitive and in turn transfers such characteristics to the frequency domain. The aim of this chapter is to show that structural characterisation of such object surfaces is not beset by the lack of phase of the Fourier spectrum. Furthermore, selective windowing of the Fourier map would allow a "closing in" technique whereby such structural characterisation would be a more realistic representation of the object reflectance profile in terms of its region of support.

The zero-phase characterisation study is split into two chapters, 4 and 5. This chapter deals with the characterisation study conducted on a transmittance target for which both the shape and the dimensions of the features were known and were digitally recorded.

The motivation behind such study is two fold:

i) Firstly, to investigate the nature of the recovered characteristics for a specimen with a known geometrical configuration. This study would provide an awareness of:

— the circumstances under which a zero-phase assumption would arrive back at a close reconstruction of the object behaviour when either the modulus or the intensity of the spectral characteristics is utilised;

— the general traits of a zero-phase recovery realised through the FFT operation, i.e consequential effect of sampling and digitisation in both domains on the recovered object characteristics;

This would set the scene for interpreting the zero-phase characterisation of a machined surface whose structural arrangement is a complex collection of many repetitive features with varying dimensions.

ii) Secondly, to explore whether certain object geometries can be made in favour of zero-phase characterisation through selective windowing of their frequency characteristics; this of course being feasible if the geometrical arrangement of the object gives rise to the type of frequency characteristics where the predominant region of the spectrum i.e the lower frequency region, is likely to possess zero-phase coefficients.

The rest of this chapter is set out in the following order: section 4.2 introduces the general traits of a phaseless object recovery. The term 'phaseless' is used to define object recovery from a Fourier modulus/ intensity spectrum for which the original absolute phase is not available and the modulus/intensity spectrum is inverse Fourier

transformed with zero phase. Although this term has been generalised to include both modulus and intensity data in the zero-phase synthesis of the object, the actual characterisation studies relate to the inverse Fourier transformation of the intensity of the spectral characteristics with zero-phase assumption. The reason for also pursuing the characterisation of the modulus data in the absence of phase is that there are many commonalties in the zero phase characterised images of both the modulus and the intensity of the spectral characteristics. Consequently, much of the typical behaviour in the inverse Fourier transformation of the intensity data can be more easily inferred by considering the characteristics in the zero-phase image of the modulus data.

Section 4.3 is an insight into performing zero-phase characterisation with the definition of such operation in both space and frequency domains. This section also defines the consequential effect of the data window aperture on the zero-phase characteristics, gearing awareness towards the window effect artifacts in a zero-phase recovery scheme. Section 4.4 is the analysis of the zero phase characterisation for a circular lattice used as the transmittance target. In the same section selective windowing of the Fourier spectrum is then explored as a possible means of 'closing in ' to the true extent of the object characteristics or its region of support. Lastly, to bring to light what other attributes in an object is secured through zero-phase characterisation, the circular symmetry of the transmittance object has been altered to elliptic, and the zero-phase characterisation study conducted on a lattice of repetitive features bearing an elliptic symmetry. Although already presented diagrammatically in chapter 2 page 61, in section 4.5, the author has provided the analytical proof as to how zero-phase characterisation latches on to the regularity in the object and is thus capable of preserving such intelligence despite the absence of phase information. Finally, section 4.6 summarises what emerges out of such study to be utilised in later chapters.

CHAPTER 4

4.2 General Traits of a Phase Less Object Recovery

In order to arrive at a true reconstruction of the object profile, one has to incorporate phase values alongside the Fourier modulus data. Absolute recovery of the phase is irrelevant (R. Bates and W.R. Fright, 1984), (R. Bates, 1984) and in general the form of the object that can be recovered from modulus information alone (J.S. Lim, 1990), could be the reconstruction from:

i) any arbitrary phase shift added to the true phase values;

ii) the mirror image of the actual object;

iii) the shifted version of the object

Within the above context object characteristics can be recovered from the modulus of the Fourier spectrum. The third aspect of the ambiguity, namely the insensitivity of the modulus data to the lateral movement has been shown below in figure 4.1 for the modulus spectrum of the shifted and unshifted versions of an object function. As seen, the distribution of the energy in the diffracted spectrum of the object does not depend on where it is positioned. An analogy can be made with a time-dependent signal, whereby the amount of energy distributed in a typical spectrum of the signal does not depend on when the signal occurs (D. Champeney, 1973).

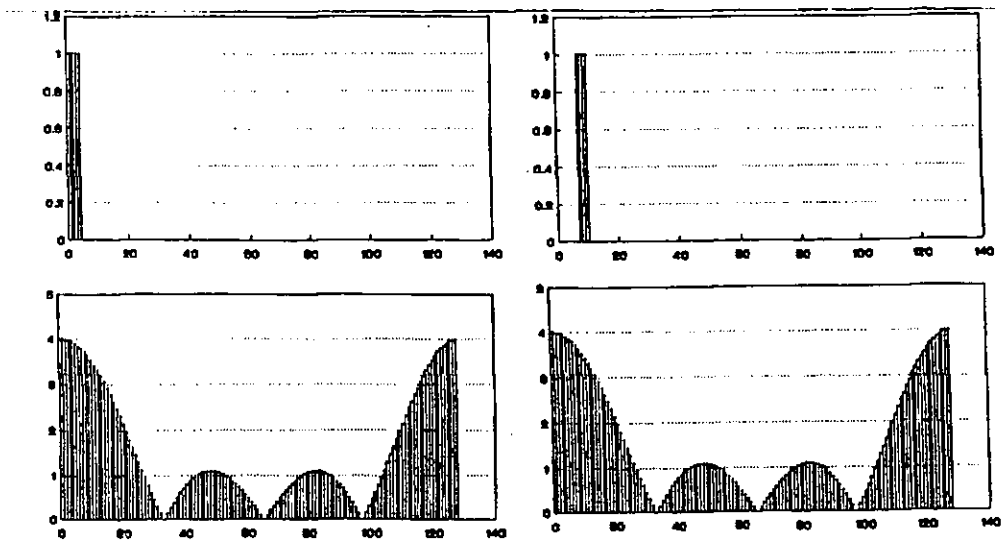

Figure 4.1: The inseositivity of the Fourier modulus spectrum to the lateral movement of the object.

It should be mentioned that these ambiguities also known as the three-fold phase ambiguities (J.S. Lim, 1990), are inherently present even though one may extract an appropriate phase function which will allow the object to be reconstructed. Indeed, the lateral movement of the reconstructed object from its original position is the most commonly observed effect in object reconstruction from the modulus of the Fourier spectrum. This effect has already been shown in figure 1.1 on page 7 of chapter 1 where a triangularly shaped object was reconstructed from the modulus of the spectral characteristics. Although the three-fold phase ambiguities describe the type of information which would be lost in a software generated reconstructed version of the object there could be more ambiguities surrounding the recovered characteristics of the object when it is synthesized through a zero-phase assumption. When the characterisation is realised through the inverse Fourier transformation of the "modulus" data with zero phase, it could lead to the following additional uncertainties in the nature of the recovered characteristics:

i) ambiguous intensity profile: the recovered reflectance or transmittance profile, would only be similar to the image of the actual object if the object shape can be synthesised from purely cosinusoidal components. Any sinusoidal component needed for the object synthesis, would not be activated in a zero phase operation.

ii) Spill over of the Object Characteristics: If the zero-phase characterisation is not the correct solution, the retrieved characteristics of the object would be extended well beyond its original bounds or region of support; for the case of repetitive objects, this appears as a spill over of repetitive features beyond their original existence.

Because the focus is on the inverse Fourier transformation of the "intensity" data with zero-phase one has to see how the faith of the characterisations is affected in the absence of phase in this case:

i) **Spill over of the object characteristics** the use of the intensity data will also result in the spillage of repetitive characteristics beyond their true region of existence.

ii) **Ambiguous intensity profile** the inverse Fourier transformation of the intensity spectrum is equivalent to the self convolution of the image of the object with its complex conjugate. Therefore, the intensity profile is ambiguous because it will take the shape of the result of such self convolution. However, evidence has it by way of investigation in this research study that if the zero-phase image of the modulus data is closely related to the actual shape of the object, then the zero-phase image of the intensity data will also bear close resemblance to the original object.

There is no doubt that there are many object geometries whose amplitude profile would be completely obliterated if their frequency characteristics were to be inverse Fourier transformed with a zero-phase assumption. However, there are also certain geometries whose structure can be synthesized from frequency components which bear no such knowledge of phase. To identify with such geometries, the requirements for a zero-phase recovery has been reviewed by the author in the next section in a typical modulus-only synthesis. Further to this, the reasons as to how an intensity-only synthesis could also lead to a reconstruction closely related to the original object has been discussed.

4.2.1 General Requirements for a Zero-Phase Object Recovery

This section identifies the necessary conditions which validate a zero-phase object recovery from the modulus of the spectral characteristics. A zero-phase assumption would only arrive back at the true object characteristics if the object has:

i) an even symmetry;

ii) a complex modulus spectrum with no amplitude negations.

Any object represented in functional form h(x) can be broken down into an even component $h_e(x)$ and an odd component $h_o(x)$ expressed in the following format:

$$h(x) = h_e(x) + h_o(x) \tag{4.5}$$

In the Fourier domain, the even part of the function $h_e(x)$, can be synthesized from purely cosine components and the odd part of the function $h_o(x)$ can be synthesised from purely sine components. This is because the even part has an even symmetry like a cosine and the odd part has an odd symmetry like a sine. In Fourier space the transform of the object function h(x) can be written as:

$$H(u) = H_e(u) + H_o(u) \tag{4.6}$$

expressed in terms of the real and the imaginary components, (4.6) can be written as:

$$H(u) = R + iI \tag{4.7}$$

$$\therefore \quad H_e(u) = \mathcal{F}\{h_e(x)\} = R \tag{4.8}$$

and

$$H_o(u) = \mathcal{F}\{h_o(x)\} = I \tag{4.9}$$

the modulus of the Fourier transform of the object function h(x) is:

$$| H(u) | = |\sqrt{H_e(u)^2+H_o(u)^2}| \tag{4.10}$$

If the object function has even symmetry, then $h_o(x)=0$ in (4.5). Similarly, the odd part of the transform in the Fourier space i.e $H_o(u)$ would also diminish. As a result the modulus of the Fourier spectrum H(u) would now be solely determined by the modulus of the even part of the spectrum $H_e(u)$, therefore:

$$|H(u)| = |H_e(u)| \tag{4.11}$$

Hence, the inverse Fourier transformation of $|H_e(u)|$ would only arrive back at the object function h(x), if $|H_e(u)|$ restores all the information of the complex Fourier spectrum without the modulus sign i.e if:

$$|H_e(u)| = H_e(u) \tag{4.12}$$

i.e the complex Fourier spectrum $H(u)=H_e(u)$ does not experience amplitude negations when expressed in modulus format.

To rephrase the above requirements in terms of the modulus and phase of the Fourier spectrum, equation (4.10) can be expressed as:

$$H(u) = |H(u)| e^{i\theta} \tag{4.13}$$

and $\theta=\tan^{-1} I/R$

where the real and imaginary parts can be written as:

$$R = H_e(u) = |H(u)| \cos\theta \tag{4.14}$$

$$I = H_o(u) = |H(u)| \sin\theta \tag{4.15}$$

For a zero-phase reconstruction to be valid, $H_o(u)=0$ i.e θ equals zero for which $\sin\theta=0$. The only prior knowledge about the object that makes the imaginary part of its Fourier spectrum zero is even symmetry in the geometrical configuration of the object. Insertion of a similar value for θ in equation (4.14) would make $\cos\theta=0$ thereby causing:

$$R = H_e(u) = |H(u)| \tag{4.16}$$

i.e the even part of the complex spectrum should not possess negative amplitude excursions so that the true sign of Fourier components does not alter under a modulus sign. In conclusion, every frequency spectrum under a modulus sign would dispose of the phase information and all the spectral components would have a zero-phase or a common alignment. Thus, zero-phase characterisation would only arrive back at a reconstruction of the object, if the object can still be synthesized from spectral components which have been displaced, or shifted with respect to one another from their original positions.

Whilst this reasoning has been centred around the use of the modulus of the spectral components for object synthesis, it is also reasonable to assume that if the modulus-only synthesis appears to bear a close resemblance to the original object, then an intensity-only synthesis is also likely to reveal such resemblance. There are a number of explanations as to why this is likely to happen. Firstly, a zero-phase inverse Fourier transformation of either the modulus or the intensity of the spectral components is a cosine-only synthesis. Therefore, the zero-phase images realised through either the utilisation of the modulus or intensity of the spectral characteristics should bear many similarities. Concentration of energy in the central region of zero-phase images is one such commonality. This issue has already been raised in chapter 1, section 1.5. Secondly, so far as the region of support or existence of the object is concerned, they both fail to disclose the true object boundaries because this information is equally destroyed in both the modulus and the intensity spectrum. However, if there happens to be a selected region of the spectrum for which the phase of the spectral components are truly zero, then not only the modulus-only synthesis of this selected region is likely to converge to a reconstruction that maintains the region of existence of the object features, an intensity-only synthesis is also likely to maintain a good approximation to the true boundaries of the object. This behaviour of intensity-only synthesis is best proved in section 4.4.5 where for a particular object, selective windowing of the

spectral characteristics restores the true region of existence of the object upon inverse Fourier transformation.

4.2.2 Definition of Object Characteristics

At this stage it is relevant to define the two terms object characterisation and object reconstruction in the context of this research. In reconstruction, the retrieved image of the object should be identical to the image of the object as seen in a photograph. Object characterisation would also arrive back at an intensity profile which may or may not be similar the true object. In characterisation recoveries however, the aim is to map the salient features of repetitive and structured profiles. These salient features are identified as:

i) the **cyclic pitch** of the periodic components;

ii) **similar structural regularity**;

iii) **spatial extent** or the most likely region of existence of repetitive behaviour.

It is the intent of this chapter to investigate whether such attributes in an object would survive a zero-phase operation. In performing an inverse Fourier transformation of the intensity spectrum with zero-phase, one would arrive at the autocorrelation function of the original object. Autocorrelation can also be realised directly from the spatial domain data, by integrating the product of the object and its shifted version within the object interval. This, of course, necessitates a knowledge of the object in image form.

Two separate sections have been assigned for the realisation of the auto-correlation function. Firstly, i) from the spatial domain data in section 4.3 and secondly, ii) from spatial frequency data in section 4.3.1. It was anticipated that the nature of the recovered characteristics could be more clarified if the zero-phase reconstruction were identified with the help of a spatial domain portrayal of such operation, complementing a frequency domain characterisation. The next section unfolds the mechanisms by which the autocorrelation operation can be realised in the object domain.

4.3 Spatial Domain Realisation of the Autocorrelation Function

The interpretation of the autocorrelation function is that it provides a degree of similarity between the signal and the shifted version of the signal by x' units (K.Wolf, 1979), (A.Barret and A.Mackay, 1987), (J.Proakis and D.Manolakis, 1988). The type of object chosen for characterisation are object exhibiting periodicity within a finite interval of the measurement. Periodic objects by definition show periodicity within the interval of $-\infty \rightarrow +\infty$, but being within a finite interval of measurement from -1/2 to 1/2 beyond which they do not exist, allows such objects to be classed as objects having a finite energy. i.e

$$\int_{-\infty}^{+\infty} h(x)^2 dx < \infty \tag{4.17}$$

where the infinite interval can be assumed by h(x) values existing between -1/2 to 1/2 and h(x) values being 0 on either side of this extremities (R.Bracewell, 1986). The autocorrelation can be written as:

$$R(x') = \int_{-\infty}^{\infty} h(x) \cdot h(x'+x)\, dx \tag{4.18}$$

the interpretation of which is displace $h(x)$ by shift x', *i.e.* $h(x+x')$ multiply by $h(x)$ and integrate the product. The lateral displacement x' can be regarded as a scanning parameter used to reveal the similarity between the signal and its shifted version. At this stage it is relevant to give an inlinking of how the measured energy spectrum and the autocorrelation function $R(x')$ are inter-related. The Fourier transform of (4.18) is:

$$R(u) = \int_{-\infty}^{\infty} R(x')\, e^{(-2\pi jfx')}\, dx' \tag{4.19}$$

But from Wiener-Khinchin theorem (J.G.Proakis, 1988), the Fourier transform of the autocorrelation function $R(x')$, is the energy spectrum $S(u)$, the entity which is recorded experimentally :

$$\mathcal{F}\,[R(x')] = S(u) \tag{4.20}$$

To relate the square modulus of the Fourier spectrum $|H(u)|^2$, to the autocorrelation R(x), the energy spectrum S(u) is now evaluated from the Fourier transform of the object function h(x). If the surface reflectance profile $h(x)$ is a finite energy signal, that is:

$$\int_{-\infty}^{\infty} h(x)^2\, dx < \infty$$

then it has a Fourier transform $H(u)$, given by

$$H(u) = \int_{-\infty}^{\infty} h(x)\; e^{-i2\pi ux} dx \tag{4.21}$$

where the Fourier transform can be written as:

$$H(u) = R(u) + jI(u) = |H(u)|\, e^{j\theta(u)} \tag{4.22}$$

$$H(u) = |H(u)|\,(\cos\theta_{(u)} + j\,\sin\theta_{(u)}) \tag{4.23}$$

which has a modulus $|H(u)|$ and a phase $\theta(u)$ where the square of the above equation would result in a loss of phase. i.e:

$$\begin{aligned} H(u)^2 &= |H(u)|^2(\cos\theta_u + j\sin\theta_u)^2 \\ H(u)^2 &= |H(u)|^2 \end{aligned} \tag{4.24}$$

Since in recording the energy spectrum $H(u)^2$, the phase component is lost, the autocorrelation function can be envisaged as a zero-phase reconstruction of the object characteristics in the spatial domain. From Parseval's theorem the energy computed in both domains is:

$$\int_{-\infty}^{\infty} h(x)^2 \, dx = \int_{-\infty}^{\infty} H(u)^2 du \tag{4.25}$$

i.e the total energy computed in the spatial domain and the spatial frequency domain are equivalent therefore:

$$S(u) = H(u)^2 \tag{4.26}$$

But from (4.20), the autocorrelation $R(x')$ and the energy spectrum $S(u)$ are a Fourier transform pair. Also, from the above identity (4.26), the energy spectrum S(u) is equivalent to the square modulus of the Fourier transform $|H(u)|^2$. Hence, the square modulus of the Fourier transform and the autocorrelation function form a transform pair. This implies that the inverse Fourier transformation of $|H(u)|^2$ arrives back at the autocorrelation function R(x´) i.e:

$$\mathcal{F}^{-1} \, |H(u)|^2 = R(x') \tag{4.27}$$

4.3.1 Frequency Domain Realisation of the autocorrelation function

The previous section outlined the interpretation of the autocorrelation function from the integral equation of (4.18) by realising such operation in the spatial domain. The purpose of this section is to provide an insight as to how the same operation can be realised from the spatial frequency map of the object using the FFT algorithm (W.H.Press, *et. al*, 1986).

4.3.2 The Effect of the Finite Window aperture on the Zero-Phase Characteristics

Since the object is restored through digital means using the FFT algorithm, operations such as sampling, digitisation and processing a finite length of data could have their toll on the restored characteristics of the object, even when phase information is available. In general both the image data and frequency data realised through an FFT algorithm could be misrepresented by false detail due to the following reasons:

i) **Sampling:** The inherent effect of sampling manifests itself as the repetition of characteristics in both domains ; severe overlap (J.J.Mc Gregor and A.H.Watt, 1983), of repeats leads to spurious features in both the object and its frequency characteristics;

ii) **Digitisation:** FFT interprets any finite structural regularity in an object as that consisting of an infinite regularity limited by an aperture of finite width. Digitisation degrades the true extent of the aperture often with a larger part of the infinite array being exposed.

Furthermore, lack of phase affects the "shape" as well as the "bounds" of the finite window aperture which limits the overall extent of the object. Since, in general digitised data are bound by a rectangular aperture, it is important to assess the manner by which this aperture is modified in the absence of phase for the purposes of zero-phase characterisation studies. As it will become evident at the end of this section, all zero-phase characterised images would not only bear the shape of this modified aperture, they will also have their characteristics extended into a region set by the new bounds of the modified aperture.

With reference to figure 4.1, consider an object function such as a continuum in the object domain, whose extent is bounded by a rectangular data window. This object can be broken down into a continuum of finite extent multiplied by a rectangular aperture. Multiplication in the spatial domain, is equivalent to the convolution of the individual frequency spectra in the Fourier domain. Hence, the overall frequency map would be the convolution of the Fourier transform of the continuum with the Fourier transform of the rectangular data window.

An ideal continuum, would generate a delta function in the Fourier domain and a rectangular aperture would give rise to a **Sinc** frequency distribution. As convolution can be envisaged as a smearing out or dealing out of one function in the position of the other, the delta function is dealt out into a **Sinc** frequency distribution. As long as the complex Fourier amplitude spectrum H(u) is available, i.e as long as the phase of the frequency spectrum is known alongside the modulus information, then upon inverse Fourier transformation of this frequency map, original object i.e the continuum would be recovered which is sharply confined to within the extent of the rectangular aperture. However, when only the intensity information is available i.e the squared modulus of Fourier components, the negative excursions of the Sinc lobe in the frequency domain are altered into positive frequency amplitudes. Such transformation not only modifies the shape of the limiting aperture but it also alters the effective extent or the sharp boundary limits of the data window.

The square of the **Sinc** ^{2} function is the frequency spectrum of a triangular data window. In addition, the negative lobes of the Sinc appearing as positive, would result in an aperture function with twice the effective extent of the original data window. Hence, the inverse Fourier transformation of the modulus squared of the Fourier spectrum would result in a new characteristics of a continuum, multiplied by a triangular data window, which has a new effective aperture of twice the previous extent.

Thus, irrespective of the shape of the original object, as long as it is bound by a rectangular data window, its zero-phase characteristics whatever shape they may be would be automatically multiplied by this triangular effect. As the aim is object characterisation as opposed to reconstruction, multiplication of the characteristics by a triangular window is of no consequence in this study.

Since many images are bounded by a rectangular aperture, the corresponding image extent in the spatial domain has to be zero-padded by a factor of two, to allow the full exposure of the zero-phase characteristics to be realised. This also allows the auto-correlation function realised from the frequency spectrum to be similar to that realised directly from the direct shift of the object in the spatial domain integral (4.18).

The next section focuses on the zero-phase characterisation study of a transmittance target using the frequency domain approach which was addressed in section 4.3.1.

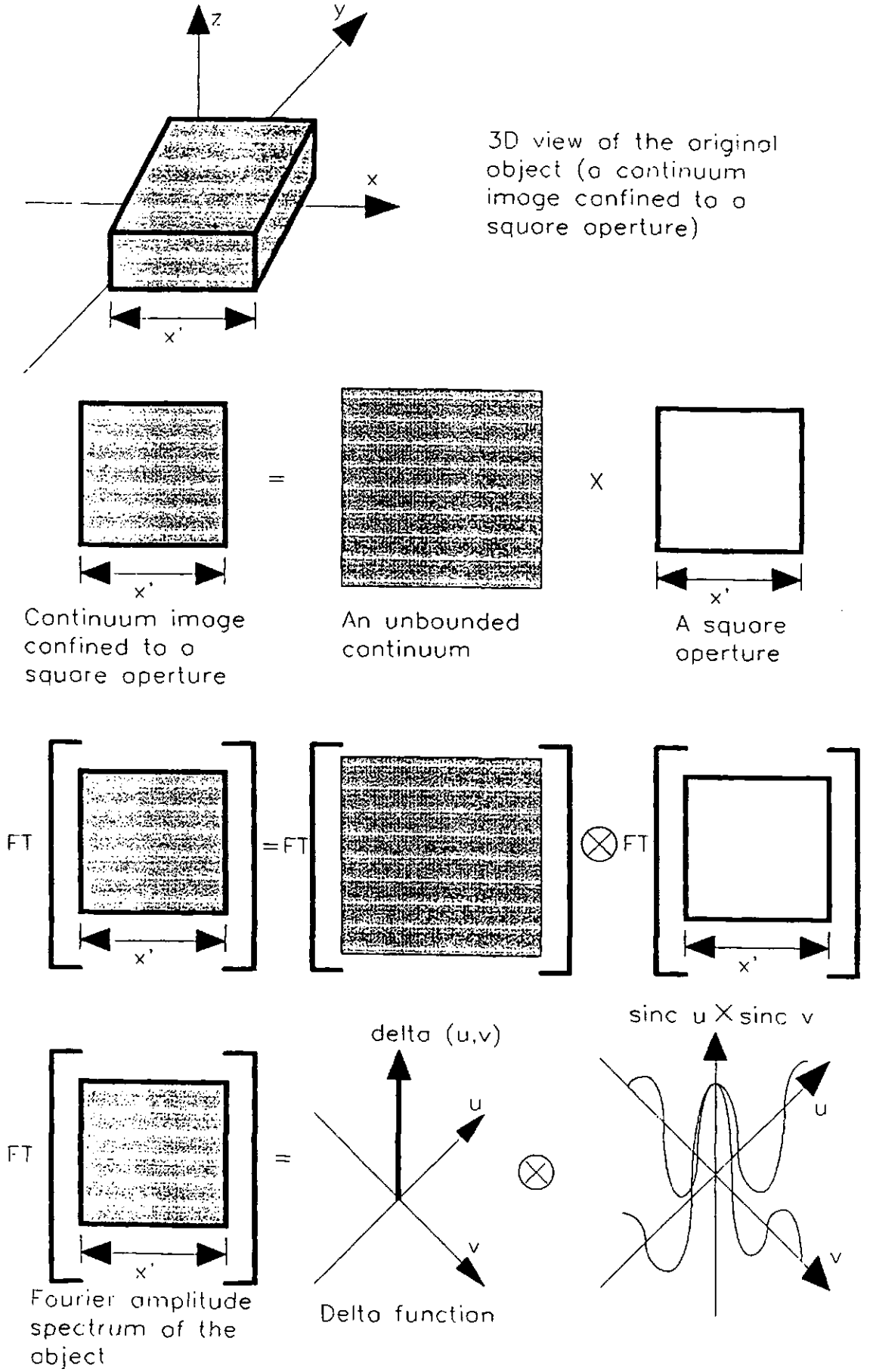

Figure 4.1: The effect of the finite window aperture on a continuum object in zero-phase characterisation. Note that the uniform amplitude profile of the object is modulated by a triangular data window as shown on page 109

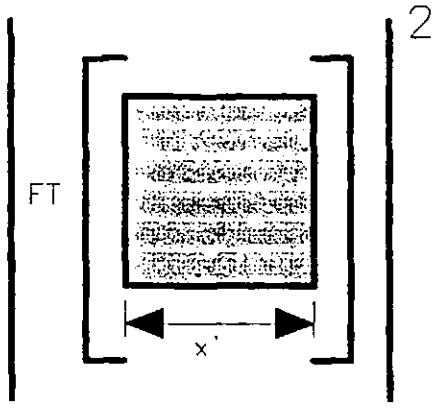

=

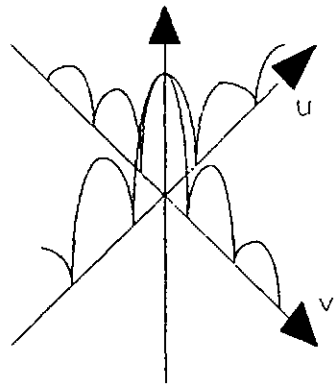

Square of the Fourier modulus spectrum of the object

$| \text{sinc}^2 u \times \text{sinc}^2 V |$

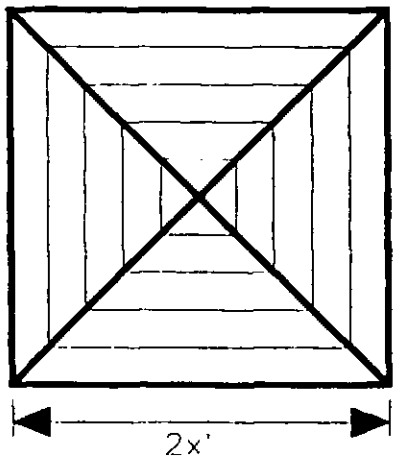

IFT

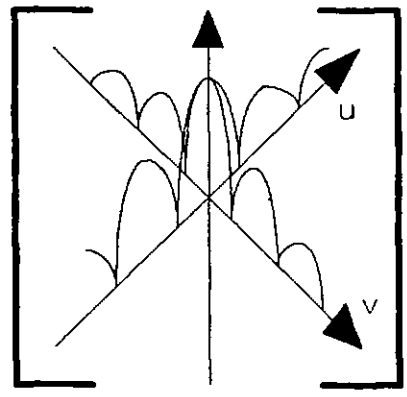

Zero phase reconstructed version of the object with twice the extent of the original and a triongular amplitude distribution

Inverse Fourier tronsform of $| \text{sinc}^2 u \times \text{sinc}^2 V |$ with zero phase

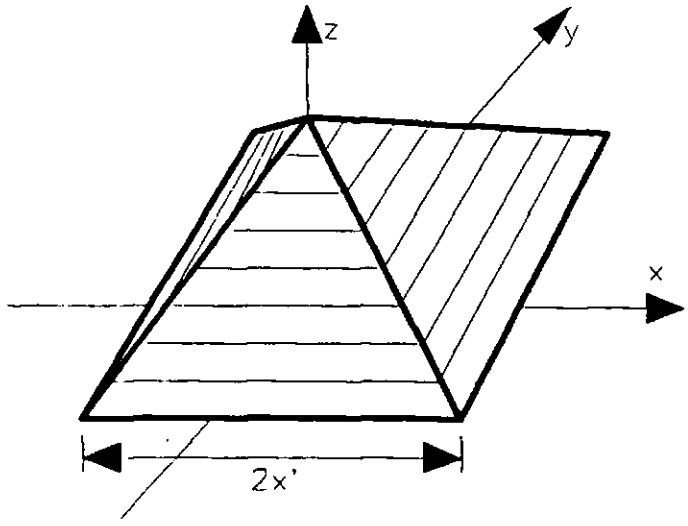

3D view of the zero-phose reconstructed version of the object

CHAPTER 4

4.4 Application of the autocorrelation function to the study of surface transmittance profiles

The transmittance target consists of an array of eighty nine circular apertures also arranged in a circular shape and with a centre of symmetry. The spatial period of the circular apertures is approximately 92μm with the overall extent of the circular aperture being 1000μm.

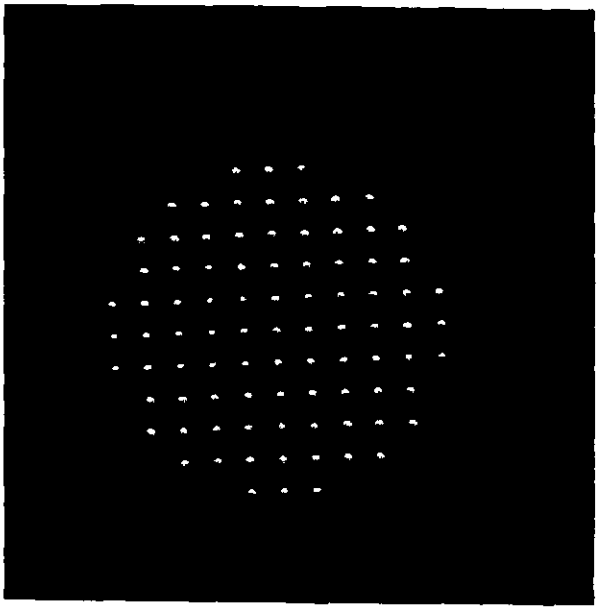

Figure 4.2 : Photo micrograph of the transmittance mask used in zero-phase characterisation study; circular apertures have a spatial period of 92μm.

Figure 4.2 is the photo-micrograph of the transmittance mask and figure 4.3a is the digitised version of this mask obtained via the travelling optical microscope and the video micro-scaler arrangement. The digitised data corresponding to the magnified image of this mask, has been used in computer simulations of zero-phase study. This data comprises of a 512 X 512 array corresponding to the digitised image of the circular lattice and appended with zeros to meet the condition of 4.3.1 to a size of 1024 X 1024 array to avoid the effects of periodic correlation of the data array (O.Brigham, 1989).

In order to comment on the restored zero-phase characteristics of this object, one needs to consider how the object's intelligence is mapped into the frequency domain and assess what fraction of the mapped intelligence is preserved under a modulus sign. The zero-phase characteristics would thus convey only that part of the object's intelligence which has not been obliterated by the lack of phase; which is the subject of investigation in the next section.

CHAPTER 4

4.4.1 Computer Generated Fourier Spectrum of the transmittance Mask

Figure 4.3c illustrates the computer generated diffraction pattern of the transmittance profile using the digitised image of figure 4.3a as the input data. The mapped diffraction pattern can be understood with reference to figure 4.3b below, which is a pictorial illustration of the equivalent form of the object array.

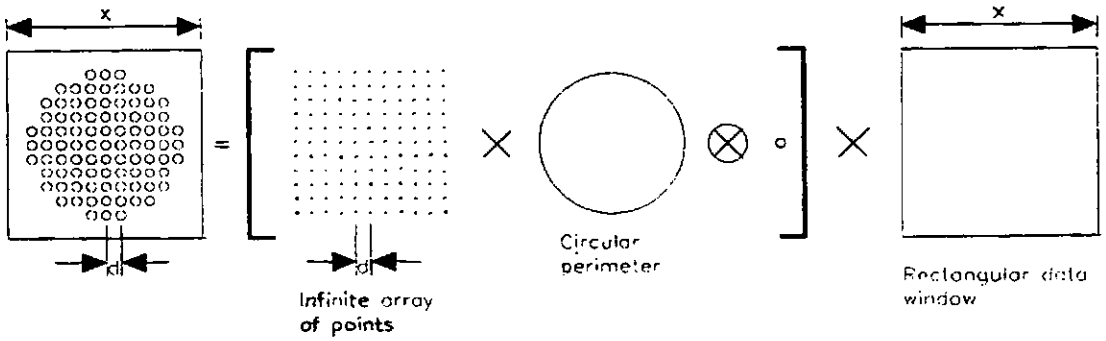

Figure 4.3b: The equivalent form of the object array used for the explanation of the Fourier modulus spectrum.

As seen, the lattice of circular apertures can be broken down into an arrangement which has resulted from an inifinte array of delta functions having a spatial period d, similar to that of the circular lattice, multiplied by a large circular aperture for limitting the arrangement to within its perimeter.

Convolution with a small circular disc would then replicate the small circular apertures in the position of delta functions. This whole scene as imaged by the camera, is then subjected to limitation by the camera iris diaphragm which has a pentagonal shape. This limitation is in the form of multiplying the captured image by a pentagonal window function. This image is further bounded by a rectangular data window, acting as a final aperture and hence limiting the overall size of the data.

With reference to figure 4.3c, in the Fourier space, the infinite array of delta functions would be transformed into another array with reciprocal spacing 1/d and convoluted with a small airy disc pattern which is the Fourier transform of the large circular perimeter. This is the operation which maps the region of existence of the object's periodicity into the frequency domain. Thus, in the complex frequency spectrum, each delta function would know that it is part of an array which is to bear a circular extent. i.e each delta function would know that the region it is bound to exist, is within a circular perimeter of 1000μm.

So far the only intelligence which has been mapped on behalf of the object into the frequency space, has been that of the object's periodicity. The actual shape of the periodic features, i.e the small circular apertures, is now coded into the frequency space, through the multiplication of the previous spectrum with a large airy disc pattern. The large airy disc pattern being the frequency transform of the small circles as seen in figure 4.3c.

The final stage is coding the characteristics of the recording device and the digitiser into the overall spectrum, which of course is not part of the object's intelligence. Thus, the spectrum is yet again convoluted by: firstly i) the transform of the pentagonal camera aperture which can be seen in figure 4.3f as the star like detail at each spectral point; and secondly, ii) the rectangular window limiting the overall size of the data.

Having explained how each aspect of the object's intelligence, i.e periodicity, shape of individual features and region of existence are mapped into the frequency space, the next section considers how the frequency information associated with each of these aspects would be affected by a modulus sign.

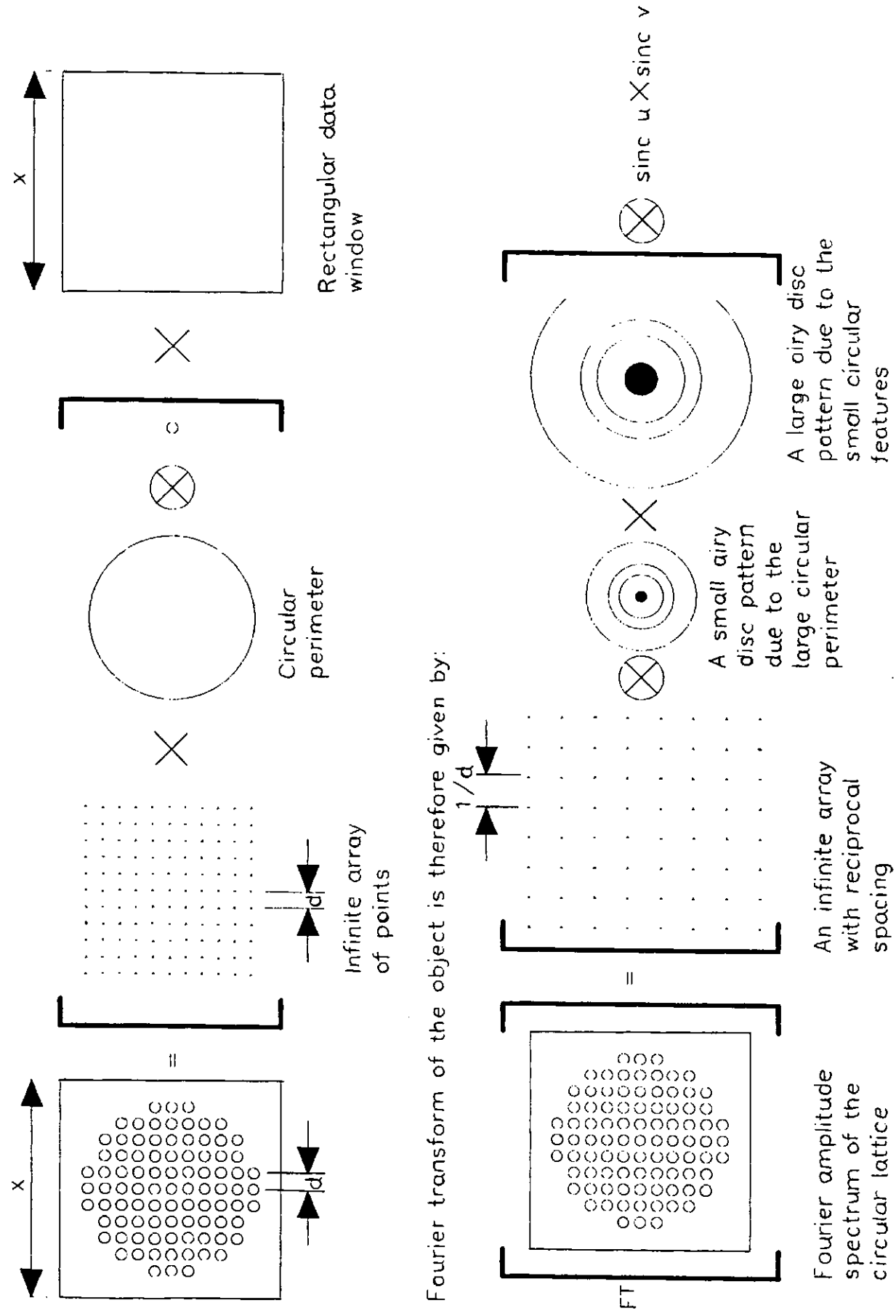

Figure 4.3c: Pictorial representation of the Fourier spectrum of the object array shown in figure 4.3b.

4.4.2 The Fraction of the Object's Intelligence Preserved Under a Modulus sign

It was addressed in section 4.2.1 that certain behaviour is favoured by the object and its frequency characteristics, if the object pattern were to be restored from only the modulus of its frequency spectrum with no knowledge of phase. This behaviour was identified as an observed symmetry in the object's geometrical shape, as well as the immunity of spectral components to a modulus sign, i.e no amplitude negations in the frequency spectrum of the object.

For the object under study, both the shape of the repetitive features, and their region of existence is circular. As already addressed, the circular aperture has a complex amplitude distribution in the frequency space which constitutes of both positive and negative amplitude variations in the form of an airy disc pattern. Whilst both the positive and negative amplitude components are present in the complex amplitude spectrum, under a modulus sign, all negative excursions transform into positive. Thus, the modulus spectrum as well as the intensity spectrum would definitely represent a different type of object behaviour altogether. For instance, the new restored characteristics of the object would appear to have extended beyond its original borders. Thus, as far as the shape of individual features and their region of existence is concerned, the intelligence associated with such detail is obliterated under a modulus sign.

Not all is lost though, since restoring object behaviour such as its periodicity, does not require a knowledge of phase information. A periodic lattice in the frequency domain, upon inverse Fourier transformation with zero-phase always restores the original periodic object with the same pace. Thus, this part of the object's intelligence is always retained under a modulus sign.

4.4.3 The Aperture Bounds of the zero-Phase Characterised Image

The aperture bounds of the characterised image of the circular lattice, would be altered from its original perimeters due to the following reasons: i) degradation of the frequency characteristics due to the digitisation of the image; and ii) loss of the phase information, i.e spectral components subjected to a modulus sign.

i) **degradation of the frequency characteristics due to digitisation of the image** What seems to confine the lattice of circular apertures, to within the circular perimeter is the large circular aperture, which transforms into a small airy disc pattern. To have this arrangement sharply bounded to within the interior of the circular perimeter, it requires a perfect airy ring distribution with an infinite number of frequency terms, in the Fourier space which would ideally transform back to a perfect circle.

As the camera does not image a perfect circle, the frequency characteristics fall short of the perfect airy pattern that they are supposed to maintain. Thus the inverse Fourier transformation would not converge to the sharp cut off of the original circle, but would somewhat be expanded leading to some spillage of the repetitive points.

ii) **loss of phase**: Though degradation due to digitisation is a possible reason for affecting the bounds of the characterised object, it is not the main reason. The spill over of the number of repetitive features originates as a direct result of the loss of the complex Fourier modulus spectrum. Similar to the aperture function of section 4.2.4, the circular aperture has a complex frequency distribution which constitutes of both positive and negative amplitude variations in the form of an airy disc

pattern. In the modulus spectrum, and equally so the intensity spectrum, all the negative excursions transform into positive, thereby having a different impact on the region of existence of the periodic features within the infinite array. This behaviour is somewhat similar to the way a Sinc amplitude distribution is altered under a modulus sign as discussed in section 4.3.2, resulting in a triangular aperture of twice the extent. In the case of the circular lattice, an airy disc distribution under a modulus sign, would appear to have a spatial frequency which is half of what it was originally. Halving the frequency, results in doubling the extent of the object in the object domain. Thus, the delta functions within the infinite array, would now have this " new information" that they are to exist in a region twice as big as the original.

4.4.4 Comparison of the Zero-Phase Characterised Images with the Original Images

Having outlined what fraction of the object's intelligence is preserved under a modulus sign, and what impact would the loss of phase have on the aperture bounds of the object, apart from the loss of its shape, one can now comment on the nature of the zero-phase characterisation for the circular lattice.

Figures 4.3a, 4.3e, 4.3f and 4.3g denote, the original object, Fourier spectrum and finally the zero-phase restored image of the object. As seen from figure 4.3g, the zero-phase image, does preserve the cyclic pitch of the object and its circular symmetry. There is also a spillage of periodic features beyond the perimeters of the 1000μm circular aperture. Though, undoubtedly, the extra repetitive features are part of the zero-phase characteristics, they are not part of the original object, and are thus referred to as image artifacts.

In the frequency domain however, such action is similarly taken by interpolating the frequency spectrum of the original object by the same factor of two. Interpolating the overall frequency spectrum by a factor of two, results in an object of the same size in terms of the number of pixels, but with an added surround of zeros. Hence, the object would appear well distinguished from the surrounding zero support.

All the processing of data has to be performed on the sampled version of h(x), i.e h(n) which has discrete values, for which the auto-correlation of the sampled signal is $R_s(k)$

$$R_s(k) = \sum_{n=-\infty}^{\infty} h(n).h(n+k) \tag{4.28}$$

where the following correlation theorem holds:

$$h(x) \otimes h(x)^* \leftrightarrow H(u).H(u)^* \tag{4.29}$$

i.e the autocorrelation can be obtained by the multiplication of the Fourier transform of the function and its complex conjugate in the frequency domain. But the discrete Fourier transform and its inverse are periodic. By a similar analogy, the discrete auto correlation is also periodic. In order that the periodic versions of the auto correlation do not overlap, the extent of the function h(x) limited to values between 0 to n-1 has to be increased to 0 and 2n-1 ; this will ensure that the individual periods of the auto correlation do not overlap i.e no end effects or wrap around errors (Brigham,1974). Therefore, the infinite summation of the above in the discrete format ranges from:

$$R_s(k) = \sum_{0}^{2n-1} h(n).h(n+k) \tag{4.30}$$

This implies that a given length of data has to be appended with zeros to accommodate the periodicity of above. The discrete Fourier of which is:

$$S(u) = \sum_{k=-\infty}^{\infty} R_s(k)\, e^{-j2\pi ku} \tag{4.31}$$

The two-dimensional operation can be realised in a similar manner from the two-dimensional spectrum.

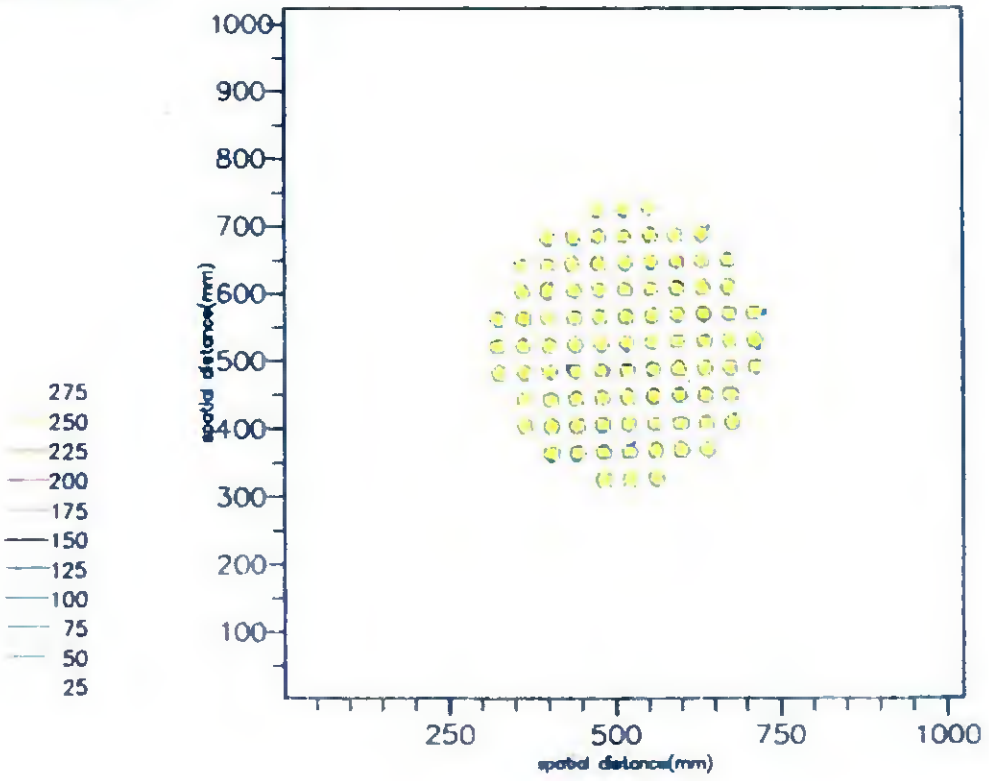

Figure 4 3a: Digitised image of the transmittance profile; the image data consists of 512x512 points which has been extended to a 1024x1024 array to avoid the effects of periodic correlation of data.

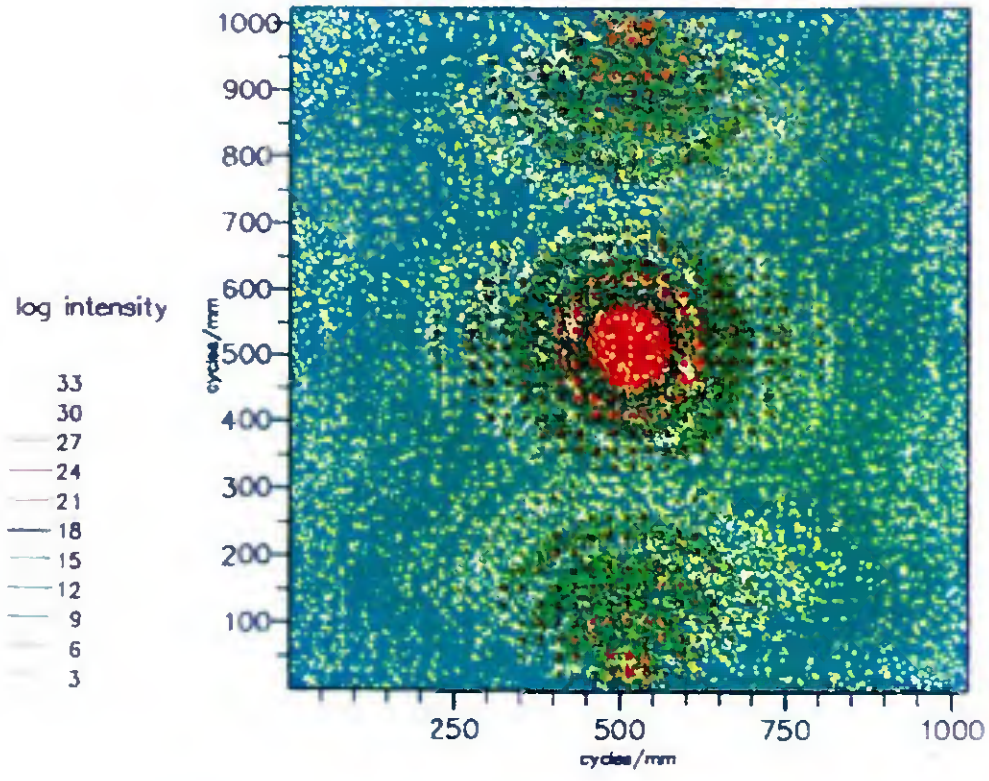

Figure 4 3e: Computer generated Fourier spectrum of the object array of figure 4.2a; note there is a slight overlap between the repeated versions of the FFT spectrum

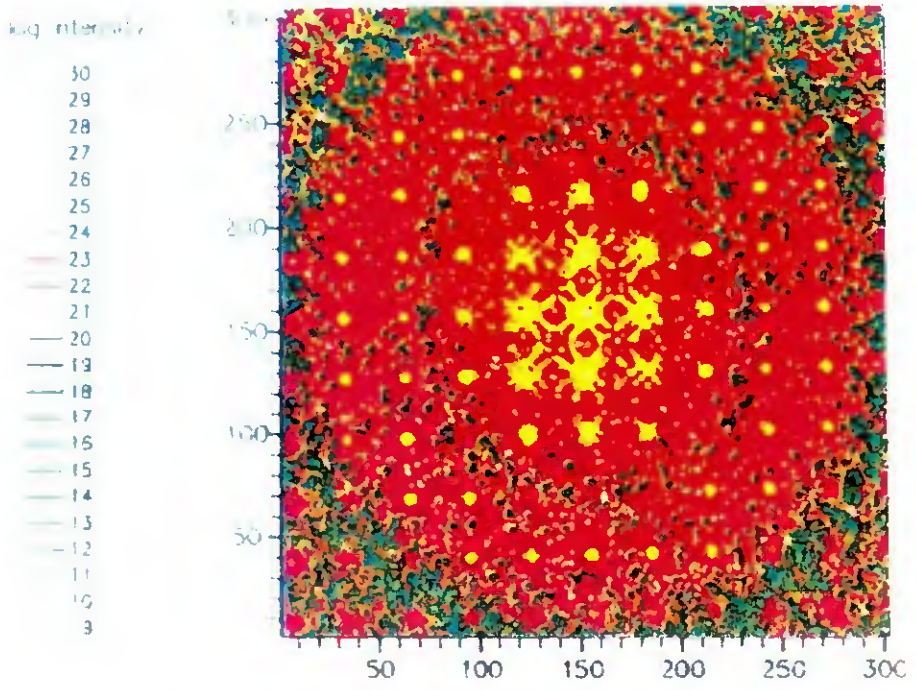

Figure 4.3f. A closer view of the Fourier modulus spectrum of figure 4.3e showing the effect of the pentagonal camera aperture, seen as the cross details as well as the finite window aperture, seen as the plus sign. Note that loss of phase data associated with the finite window aperture results in the zero phase characteristics to be multiplied by a triangular effect.

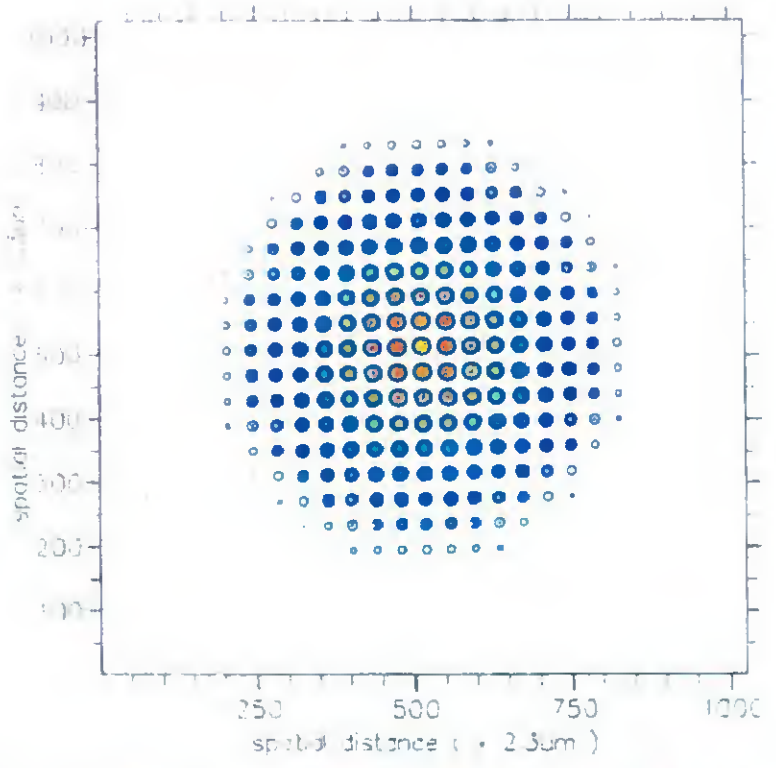

Figure 4.3g. Zero phase restored image of the object array via inverse Fourier transformation of the modulus spectrum of figure 4.3e. Note that the restored periodicity has the same cyclic pitch as the object , as well as the same circular symmetry. The increase in the number of periodic features is due to the fact that the zero-phase image has an effective aperture which exposes more of the infinite array than the object. These surplus features are labelled as artefacts since they are not part of the original characteristics.

Indeed, the nature of the restored characteristics of figure 4.3g can be explained with reference to section 4.3, via the standard integral (4.18). With regards to this integral, if the object were to be displaced with respect to itself, periodicities would only be picked up, if the periodic features in the object and its displaced version overlap.i.e at zero displacement, ($x'=0$) the object and its shifted version have 100% overlap, and the value of the function R(x')is at maximum. As the shift is introduced, only at the periodic positions i.e when $x'=x'+x$ will there be the overlap of the circular regions

Both positive and negative displacements, result in the effective extent of the recovered characteristics about the origin to be twice the extent of the original object. This is true if the object is limited to a strict region of known length i.e within the bounds of a square aperture (R. Bates and W.R. Fright, 1982), (R. Bates, 1981) (R.N. Bracewell,1986), (K. Wolf, 1979). It should be mentioned that different objects have different characteristic autocorrelation functions for which their width does not necessarily have the factor two relationship to the object (K.Dutta, 1979).

It is not difficult to see that the overlap of the periodic features in the object and its shifted version only happens for the length that the periodicity exists. Thus, this function (4.18), should only exhibit periodicity up to the length of data for which repetition exists. This is also in agreement with what has been seen in the case of the zero-phase characteristics of figure 4.3g being realised through FFT. However, it should be noted that whilst the direct method using integral of (4.18) only allows for zero-phase characteristics to be seen in a region twice as big as the original object, depending on the shape of the object, the FFT allows for more of the zero-phase behaviour to be exposed provided the rectangular data window is big enough for such exposure to be displayed. This is certainly true for periodic objects, where the spillage of repetitive features can be seen beyond a region of twice the extent of the original object.

With reference to figure 4.3g, which is the zero-phase behaviour of the circular lattice, such spillage seems to be confined to a region twice as big. However, a logarithmic display of the characteristics, to enhance the lower amplitude features, would further reveal the existence of periodic characteristics, outside the displayed region. This merely heightens the fact that an infinite periodicity in the frequency domain, is undoubtedly represented by another form of infinite periodicity in the object domain;and it is entirely up to the amplitude variations in the zero phase image as to what proportion of this infinite periodicity is to be displayed. In this case, the amplitude variations of the zero-phase image attenuate these periodic features beyond the displayed region. Since they are not part of the original behaviour in the object, their absence in figure 4.3g, is of no consequence either. With reference to section 4.2.5, the finite window aperture, limiting the overall size of the digitised image, would have its toll on the restored characteristics of figure 4.3g, in form of a triangular window modulating the amplitude of the zero-phase image. The three-dimensional view of such triangular modulation has been shown in figures 4.4.

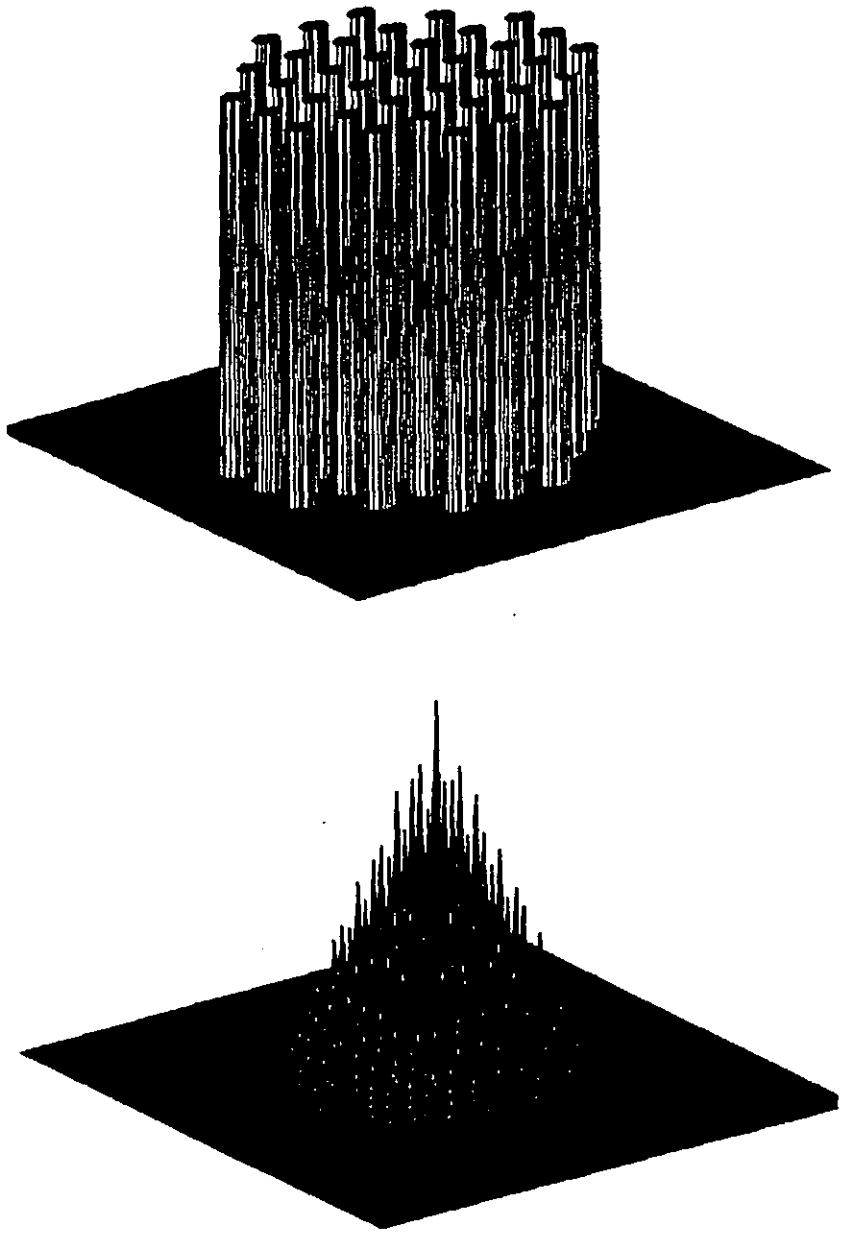

Figure 4.4: The effect of the finite window aperture on the amplitude profile of the zero-phase image.

Note that in order to display this effect in a reasonable time, the zero-phase image has been plotted for a circular lattice with a smaller number of apertures.

It is not difficult to deduce the true extent of the original array as this is half of the region of the zero-phase characterised image. In fact, iterative phase restoration techniques from the modulus of the frequency spectrum are constantly exploiting such knowledge to arrive at the true solution of the object.

However, rather than exercising this knowledge, and only displaying half of the periodic array of figure 4.3g, the author has chosen a different approach for making the periodic characteristics converge to within their original circular perimeter. This is based on windowing the lower frequency region of the Fourier spectrum and noting whether a closer version of the object image can be restored based on the strength of the lower frequency coefficients only.

With this purpose in mind, the central 256x256 spectrum in figure 4.3h, has been inverse Fourier transformed with zero phase and the characteristics of the object restored in figure 4.3. As seen, there is basically no difference between the zero-phase characteristics obtained from this selection of the lower frequency components and that of the whole region. This merely signifies the fact that there are still spectral components within this selected region that their associated phase information is yet vital in maintaining the true characteristics of the object. A further attempt however, via selecting the 129x129 region of the original spectrum, does have a remarkable effect on the nature of the restored characteristics as can be seen from figures 4.3i and 4.3k. Indeed figure 4.3k, bears a strong resemblance to the original image of the object in terms of the original symmetry of the object as well as its region of support.

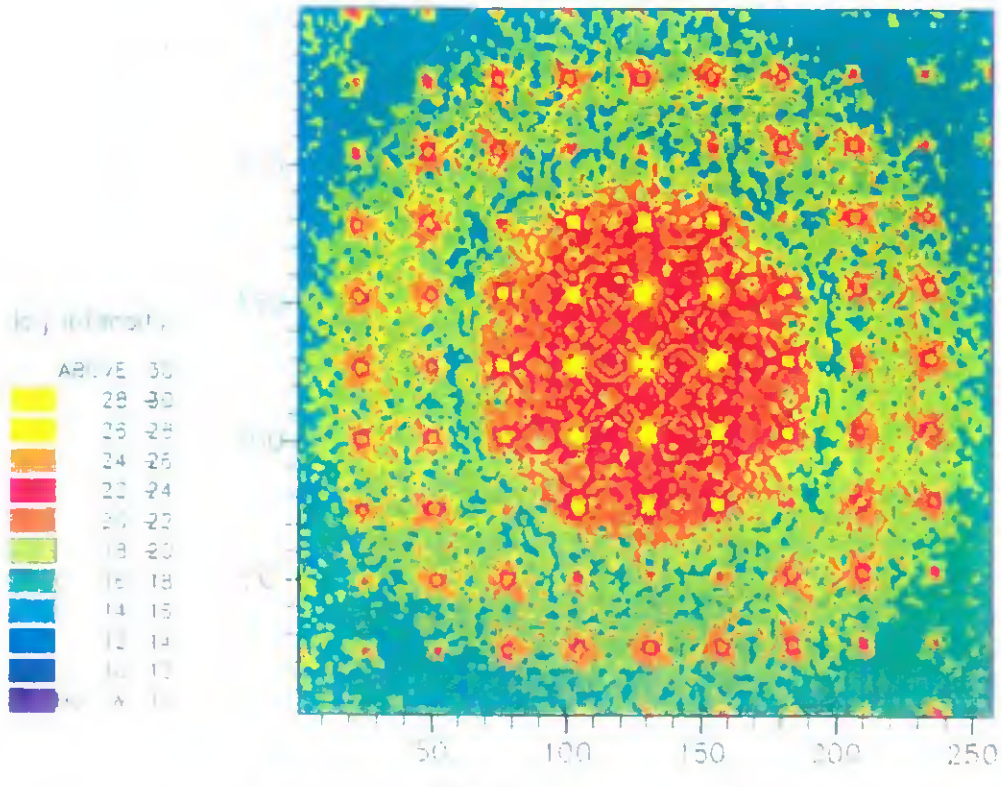

Figure 4.3h 256x256 region of the Fourier spectrum of figure 4.3e, i.e using the lower frequency region to avoid the spectral overlap of coeffiicients seen in 4.3e,as well as testing the convergence of these range of coefficients

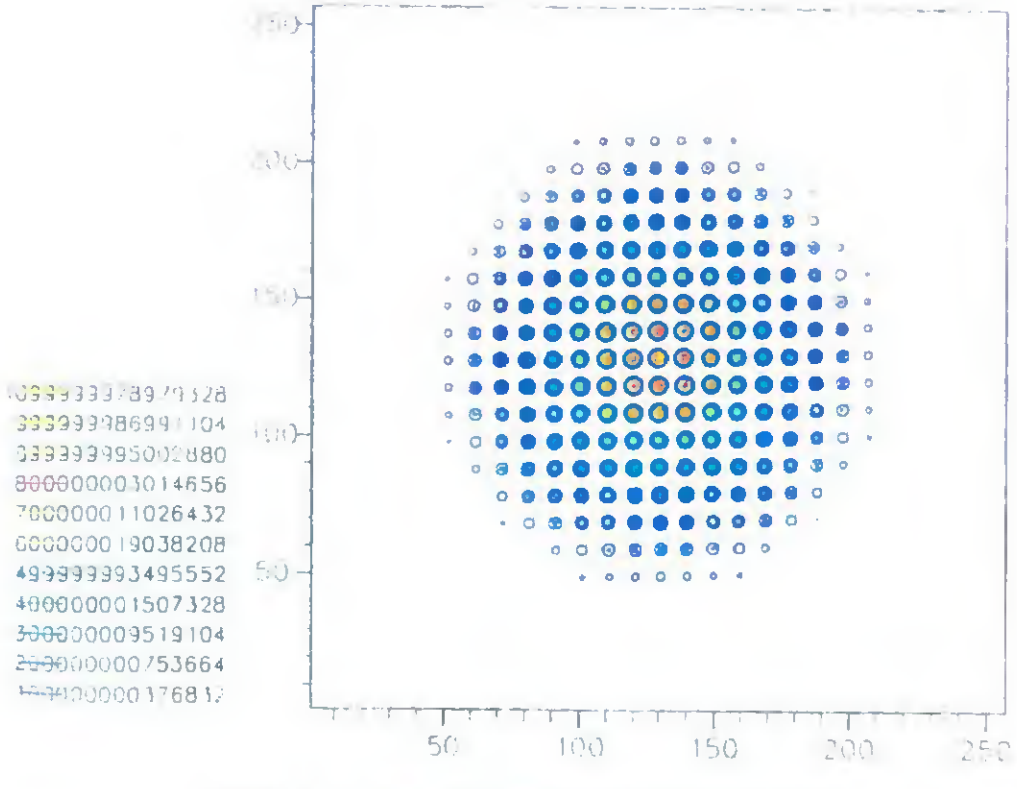

Figure 4.3i: The zero phase characterised image of the object using the Fourier modulus spectrum of figure 4.3h. Note this result is basically the same as figure 4.3g.

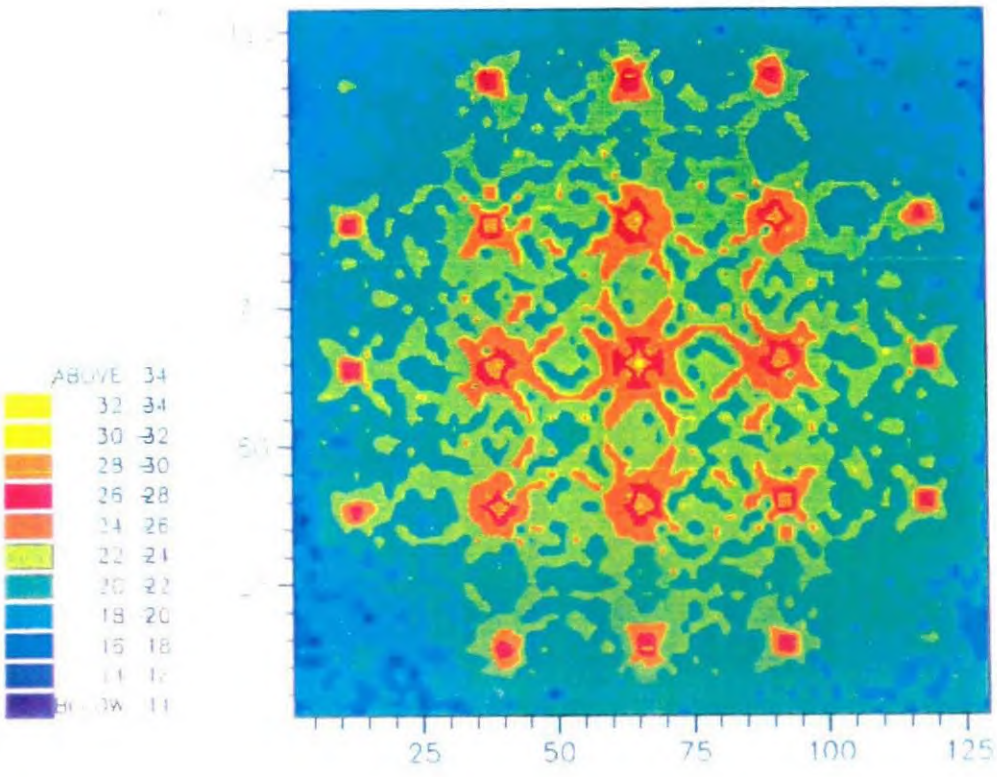

Figure 4.3j: 128x128 region of the Fourier modulus spectrum of figure 4.3e, i.e a much lower frequency region to restore object behaviour.

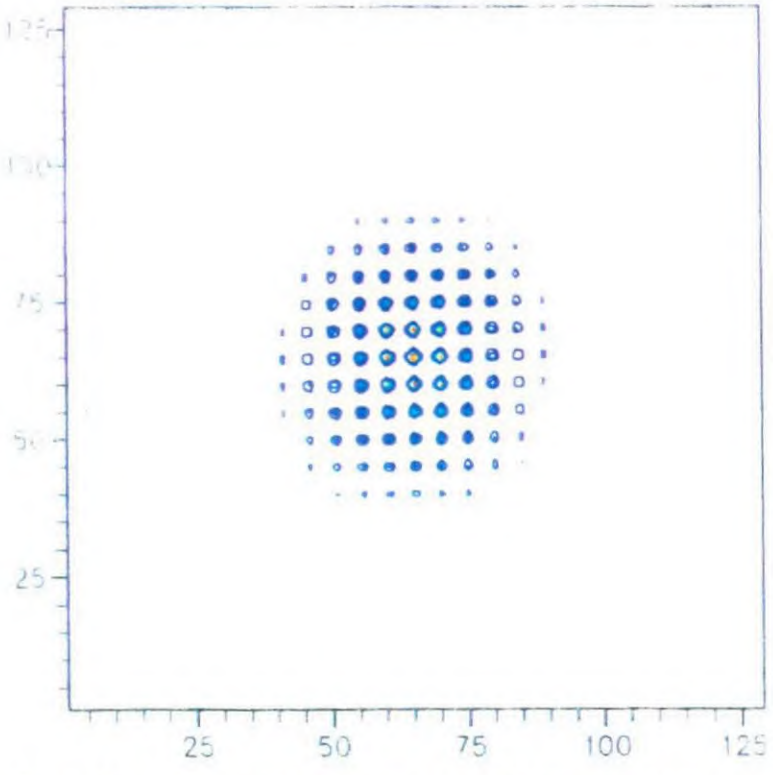

Figure 4.3k: Zero-phase characterised image using the 128x128 spectrum of figure 4.3j; note this lower frequency region does indeed possess coefficients whose phase can be regarded as zero. This can be seen from the apparent likeliness of this image to the original object

In order to disclose why selective windowing of the frequency map has favoured a closer approximation to the true object behaviour than that of the full frequency map, one needs to recall the type of object geometries which are supportive of zero-phase characterisation. This support meaning that the frequency characteristics does converge to a solution very similar to the original object characteristics when the spectral components are inverse Fourier transformed with zero phase. This is the subject of discussion in the next section.

4.4.5 Finite Windowing as a Means of "Closing in" to the true Solution

With reference to section 4.2.1, let one recall the qualifying factors in an object, as well as its spectrum, which makes its corresponding frequency characteristics amenable to zero-phase recovery and note whether the windowed version of the spectrum incorporates any of these aspects. For recollection, these qualifying factors are: i) an even symmetry; and ii) a frequency spectrum with no amplitude negations.

The roots of Fourier theory classify object functions in terms of evenness, oddness or a combination of both. This allows one to make predetermined assumptions regarding the nature of the cyclic components needed for the object synthesis. For instance profiles which are mirror symmetric about the origin, can be Fourier synthesized from cyclic components which are purely cosinusoidal in nature, because the mirror symmetry resembles that of a cosine curve.

From section 4.2.1, expressing equation (4.13) in terms of sines and cosines, the complex Fourier field can be written as:

$$H(u) = |H(u)| [\cos\theta_u + i\sin\theta_u] \tag{4.32}$$

When θ is 0, only the cosinusoidal components are energised or activated and reaching a solution rests very much on whether the original object reflectance profile bears an "even symmetry", which merely requires cosinusoidal components for mapping the overall frequency characteristics.

In crystallographic context, the atomic arrangement in a molecular compound, always have a symmetry with respect to the central atom. A zero-phase reconstruction is thus a useful guideline as to the rearrangement of the crystals. Hence, crystallographers are confronted with a three-dimensional lattice structure which is usually amenable to zero-phase characterisation.

Although there is every evidence that the transmittance target does possess a centre of symmetry and thus fulfils the evenness in structure needed in support of a zero-phase recovery, this symmetry is somewhat disrupted in the digitised version of this object. Inspection of figure 4.3a reveals that the digitised transmittance profile is not equally bright for all the circular apertures. In addition, the digitisation process has not captured the circular perimeter of each tiny circle in an identical and symmetrical format.

Hence, the true frequency spectrum of this object, would be a combination of even cosine terms and odd sine terms, i.e both the sine and cosine components are activated in equation (4.32). Since a zero-phase recovery necessitates only cosinusoidal components, the aim now is to clarify how windowing would reduce the impact of the sinusoidal components brought on by the asymmetry in the digitised image. Thus, windowing can be regarded as a means of swaying the balance, in terms of the proportion of the sine and cosine terms in equation (4.32), more in favour of the cosinusoidal components; this issue is discussed in the following section.

The digitally degraded lattice of circular features can be thought of being made of two different types of masks to account for both the sine and cosine components present. This degraded image can be considered to consist of:

i) a perfect arrangement of circular apertures giving it even symmetry;

ii) a jagged or stepped variation to account for the asymmetry in the features.

Whilst a perfect circular aperture would have a frequency distribution which consists of both high and low frequency components, the jagged or stepped components would mainly occupy the high frequency region of the Fourier space, as the dimensional range of these components is considerably smaller than the spatial extent of the perfect circles. It is therefore reasonable to associate the lower frequency region of the spectrum with spectral components which are mainly due to the larger structural variations, which are also the strongest range of frequency coefficients to account for the even characteristics in the object.

Furthermore, if the true amplitude profile of the object is irrelevant, as in characterisation studies, it is reasonable to only invoke to the very low frequency region of the Fourier map where the fundamental and the immediate spectral components reside as:

i) This is where most of the signal energy is located;

ii) if anything is to be recovered, it has to include the fundamental and its immediate neighbourhood;

iii) This will allow for the elimination of the higher frequency region from the synthesis process, which will also exclude the phase ambiguity associated with it.

Windowing eliminates the influence of the higher frequency components on the restored characteristics by excluding them from the synthesis process. This in turn allows for selecting the most significant calibre of spectral components in terms of amplitude, which are also likely to bear the even characteristics of the object. However, this is not the only reason which provokes the selected range of the frequency components to converge to a closer solution. In addition to the above, windowing also allows for a means of focusing on to the "zero-phase region" of the frequency spectrum for this particular object.

As already addressed, the frequency spectrum of the circular lattice does possess amplitude negations, the information associated with which would be lost under a modulus sign. This implies that even if the digitisation of the image had not destroyed the even symmetry of the object and the entire frequency characteristics were to be mapped by cosinusoidal components only, some cosinusoids still needed to be laterally shifted in position before they could be added to the rest of the terms.

However, in this particular case it is possible to identify the region of the spectrum whereby there would be no need for such lateral positioning. Due to the similarities of the diffraction pattern of this circular lattice to that of a single circle, it is not difficult to predict the region where the actual phases are zero. A single circular aperture gives rise to an airy ring distribution, seen as a series of concentric circles, with phases which vary between 0 and π between alternative circles. The central circular region has the widest diameter thereby maintaining zero phase over a good number of coefficients. This is also the region where the circular lattice is likely to have a good range of coefficients with zero phase.

The only penalty for excluding the higher frequency coefficients is the lack of definition in the restored characteristics seen as coarseness in the structure of repetitive features. To show this effect, the original image of the object in figure 4.3a and its zero phase restored image in 4.3g has been shown side by side for further comparison. The coarseness in the zero-phase image can be evidently seen as the rhombus like characteristics of the repetitive features.

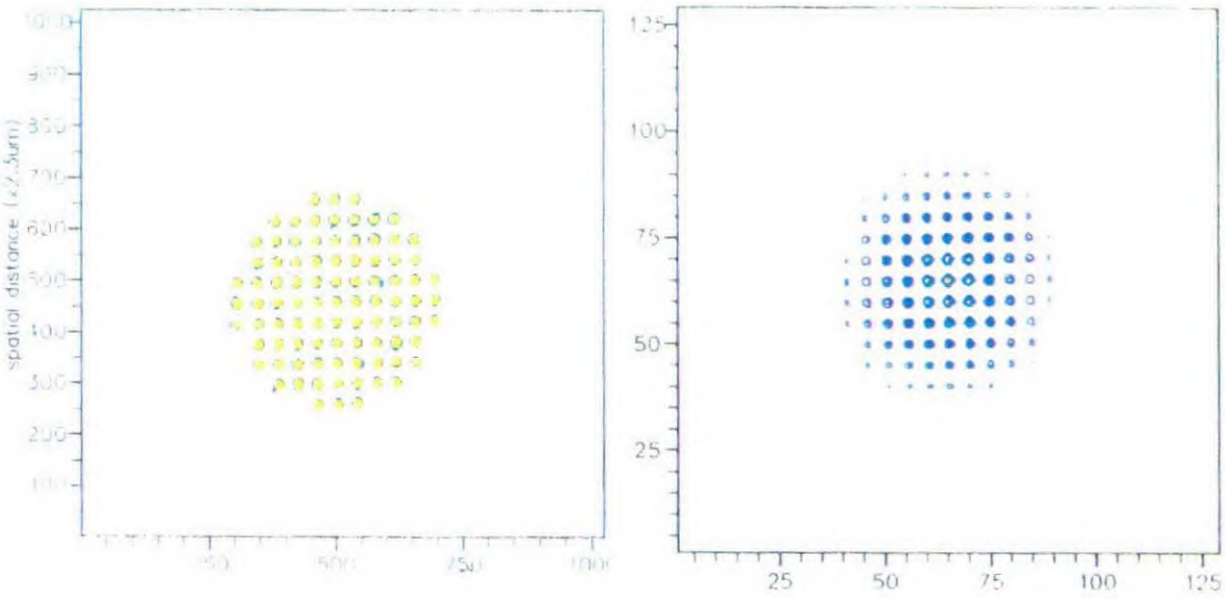

Figure 4.5:Comparison of the original object with its zero-phase restored image through selective windowing of the frequency map; lack of the higher frequency components manifests itself as the coarseness seen in the appearance of the repetitive features.

Although the argument presented in this section relates to the use of the modulus of the spectral characteristics to arrive at a zero-phase image which resembles the original image, the actual reconstructions shown in figure 4.5 has been through the utilisation of the intensity of the spectral data in the zero-phase synthesis. These results show that because of the similarities in modulus-only and intensity -only synthesis, when there are circumstances for a modulus-only synthesis to converge to a solution which is a close

reconstruction of the object, an intensity-only synthesis is also likely to capture such likeliness. One would not be doing justice if this section were brought to an end without referring to one other attribute which zero-phase is capable of preserving in an object despite the absence of phase. This is the symmetry with which the regular characteristics in an object are arranged.

4.4.6 Zero-phase Characterisation as a Means of Restoring the object Symmetry

Contrary to other attributes in an object, such as the its exact shape, or its true region of support which do rely on a supply of phase data alongside the modulus information, preserving the symmetry of the object does not demand any such knowledge. This is because the symmetry with which the regularity is arranged is always transferred to the frequency spectrum and a modulus sign does nothing what so ever to jeopardise this information. This fact has already been witnessed for the case of the circular lattice, whether zero phase is the potential solution phase or not. As seen, the repetitive regularities in the zero-phase characteristics had maintained the circular symmetry of the object even before selective windowing of the frequency spectrum was introduced.

Furthermore, to show that different type of apertures do indeed favour a zero-phase assumption without any need for selective windowing, the digitised image of the object array in figure 4.3a, has been somewhat degraded in quality by preserving only the odd fields associated with image data. Consequently, the image not only suffers from poor resolution due to the lack of pixels in the vertical direction, it also appears elongated in the horizontal direction thereby confining the repetitive features to an elliptic region instead of a circular one as seen in figure 4.6a.

This elliptic symmetry is also transferred to the frequency domain whereby, the Fourier coefficients are arranged in a similar format as can be seen from figure 4.6b. The inverse Fourier transformation of this entire frequency spectrum reveals interesting results. Firstly, this type of aperture, i.e elliptic, does favour zero-phase characterisation in the sense that the restored zero-phase image of the object has almost captured all the distinguishable features of the original object. Note that there is no spillage of repetitive features beyond the elliptic perimeter in figure 4.4c.

More so, the aperture characteristics i.e the elliptic symmetry, has been transferred from the object to frequency domain, preserved in the modulus spectrum, and once again transferred from the frequency spectrum to the object domain. As can be seen this attribute, i.e the symmetry of the aperture, has survived in the zero-phase image of figure 4.6c.

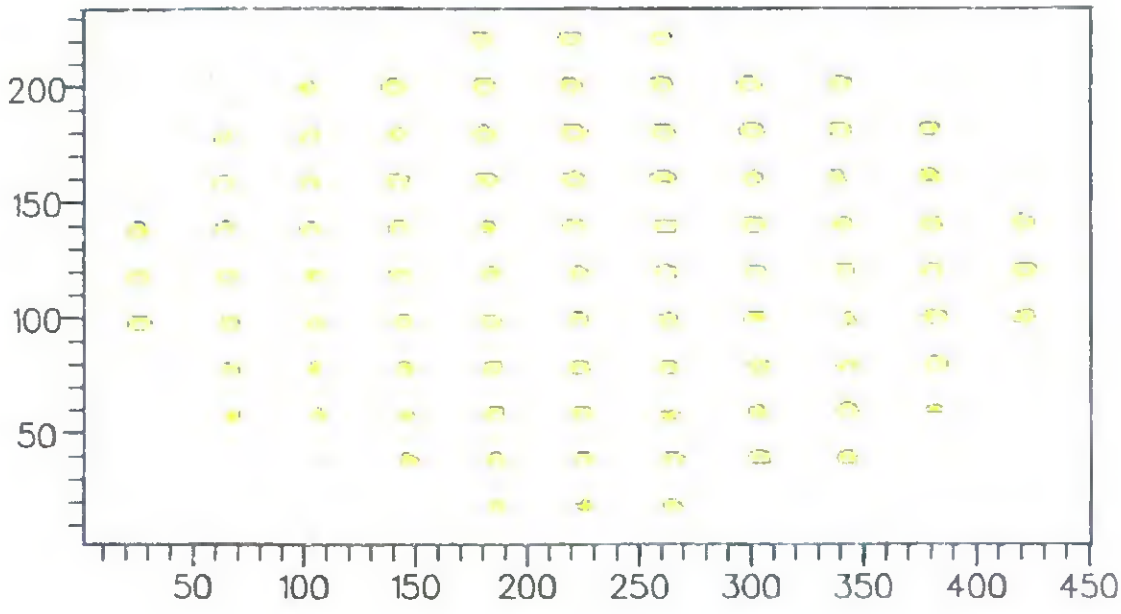

Figure 4.6a : Digitised image of the circular lattice, using only the odd field of the data; note that the previous circular symmetry is destroyed and the repetitive features are now confined to an elliptic aperture.

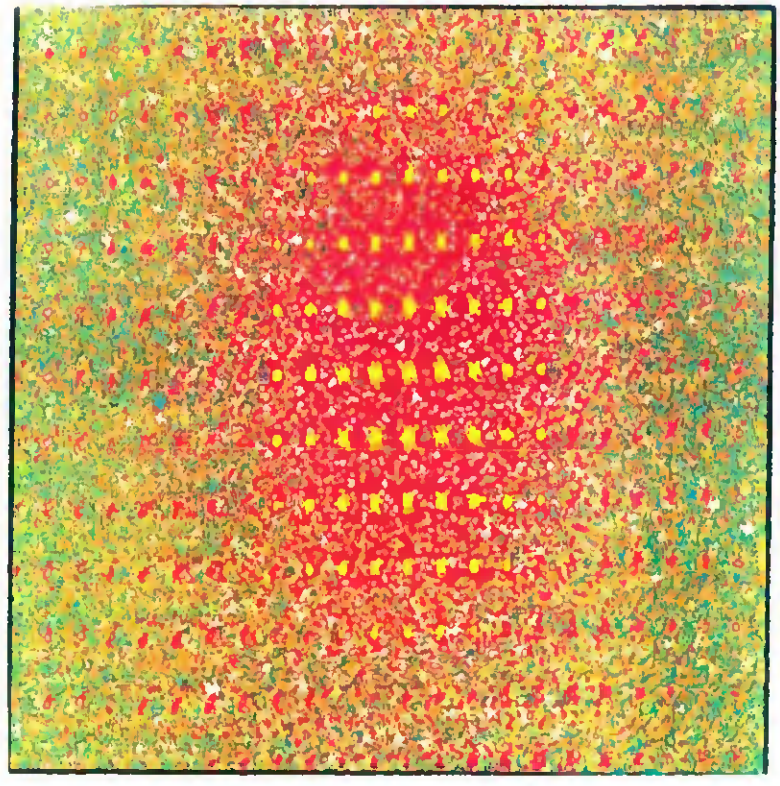

Figure 4.6b: Fourier modulus spectrum of figure 4.6a; note that the modulus data retains the symmetry of the aperture despite the absence of phase.

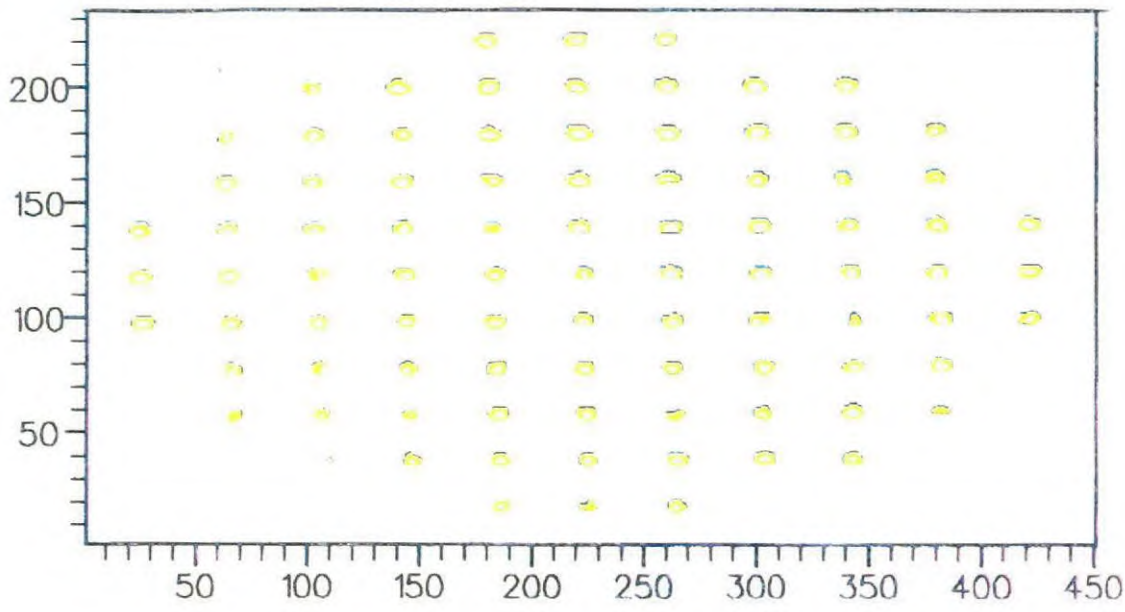

Figure 4.6a: The original image of the repetitive object illustrated once more for comparison with the zero-phase image below.

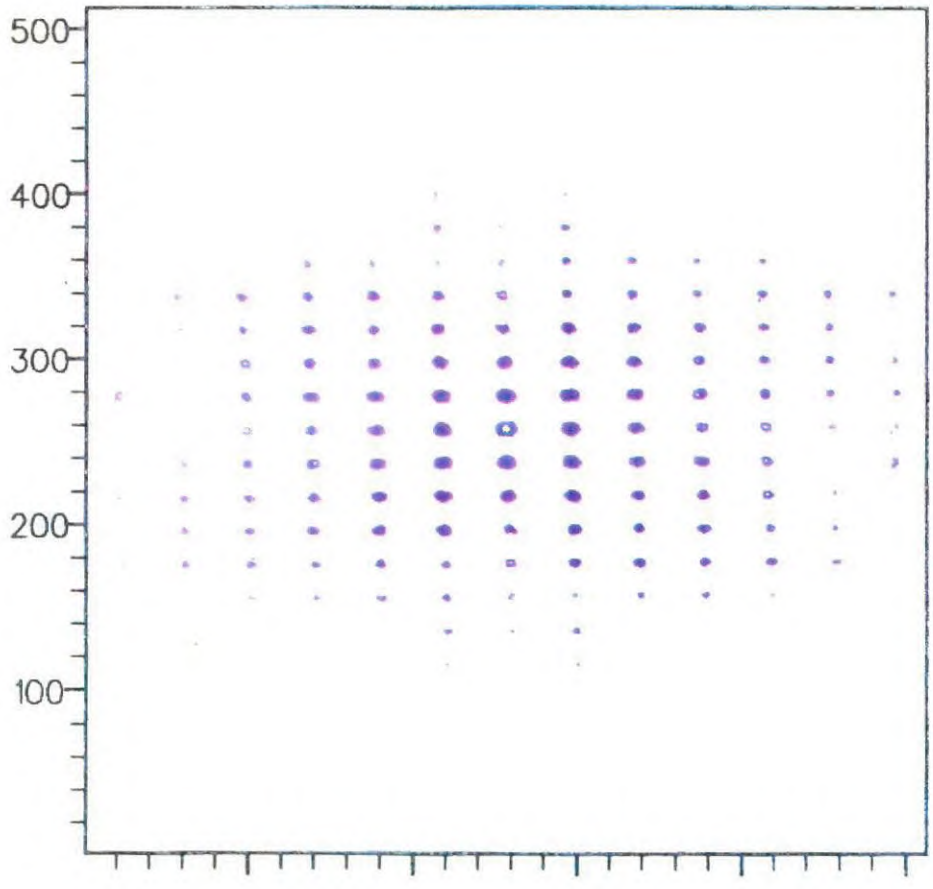

Figure 4.6c: Zero-phase restored image of the object in figure 4.6a, using the Fourier modulus spectrum of figure 4.6b. Note that this object can be regarded as a "tolerable reconstruction" of the original even without selective windowing of the Fourier modulus spectrum.

4.5 The analytical Proof of Restoring Periodicity in Zero-Phase Characterisation.

This section, provides the analytical proof of restoring periodicity in an object, through zero phase characterisation, provided that the parent object function is periodic in itself.

from (4.6) the auto-correlation of the surface transmittance profile $h(x)$ is:

$$R(x')=\int_{-\infty}^{\infty} h(x)\cdot h(x'+x)\ dx$$

the periodic version of the transmittance profile can be created by setting

$$h(x) = h(x+x_o) \tag{4.33}$$

i.e adding a period x_o to the surface profile will shift any point on the profile by a period and the profile becomes repetitive this can be seen in figure 4.7; or yet more generally, adding an integer multiple of periods nx_o, h(x) can be written as:

$$h(x+nx_o) = h(x) \tag{4.34}$$

The aim now is to prove that if

$$\begin{aligned} h(x) &= h(x+x_o) \\ R(x') &= R(x'+x) \end{aligned} \tag{4.35}$$

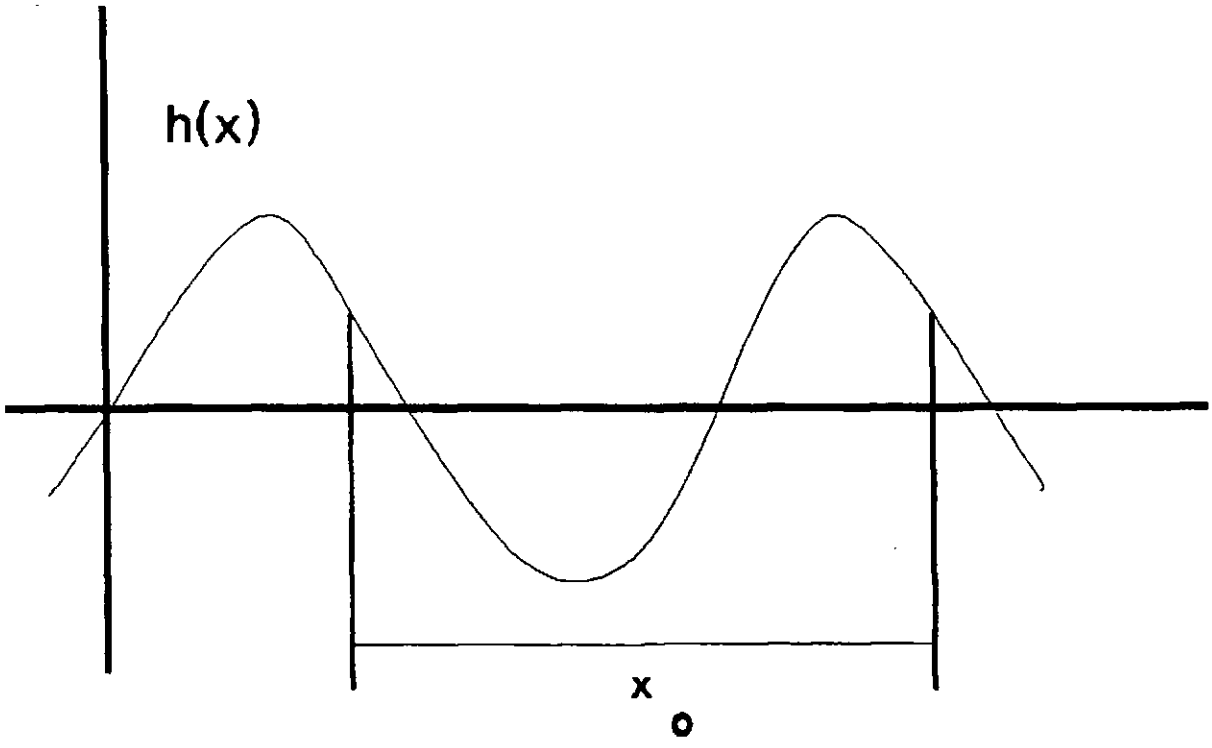

Figure 4.7:Creating the periodic version of h(x) by adding a period x_o to each point on h(x).

the new autocorrelation function for the periodic version of the R(x') can be formed by introducing periodicity of x_o into the right hand side of (4.1) and the corresponding position where the variable x' has to be made periodic i.e:

$$R(x'+x_o) = \int_{-\infty}^{\infty} h(x).h(x+x'+x_o)dx \qquad (4.36)$$

but, the periodic version of the autocorrelation by introducing periodicity into h(x) is

$$R_p(x') = \int_{-\infty}^{\infty} h(x+x_o).h(x+x_o+x')dx \qquad (4.37)$$

$$\begin{aligned} h(x+x_o) &= h(x) \\ h(x+x'+x_o) &= h(x+x') \end{aligned} \qquad (4.38)$$

so that the above two equations reduce to:

$$R(x'+x_o) = \int_{-\infty}^{\infty} h(x).h(x+x')dx \tag{4.39}$$

and $R_p(x')$ reduces to:

$$R_p(x') = \int_{-\infty}^{\infty} h(x).h(x+x')dx \tag{4.40}$$

$$\therefore \quad R(x'+x_o) = R_p(x') = R(x') \tag{4.41}$$

4.6 Reflecting on What has Been Achieved

The notion of using zero-phase for object characterisation, may appear daunting in the first instance, as common belief is that without phase there is absolutely no hope of retrieving any intelligence of the object. This belief is also heavily supported by the fact the theoretical simulations over the years has proved that the phase of the object signal conveys much of the intelligence of the object as compared to the modulus of its frequency spectrum. In most cases the modulus characteristics hardly arrives at any form of intelligence which is comparable to that of the object. With the intensity being square of the modulus characteristics, the same judgement is passed on to the utilisation of intensity-only synthesis in object characterisation. Without disputing the superiority of phase over modulus in terms of conveying object related information, the author has brought to attention the type of object geometries whose frequency characteristics definitely maps certain attributes of the object into the modulus data and equally so into the intensity characteristics. These are object structures which maintain some form of regularity to their behaviour. For such class of objects, modulus and intensity can be as valuable an entity as the phase information in terms of preserving the object's intelligence.

Although there may be circumstances where both the modulus and intensity-only synthesis would arrive at a characterised image of an object which very much resembles the original, this is not the reason that it has been pursued for in characterisation studies. Assessed on a more general level, a zero-phase synthesis is sensitive enough to reveal selective intelligence within the object which has well-defined behaviour. It has been shown in this chapter that a phase-less synthesis should be given credit for on the following accounts:

i) restoring the cyclic pitch of the regular features with the same pace;

ii) maintaining the symmetry of the object's aperture;

iii) providing a means of deducing the true aperture bounds of the object;

Although such information may not be adequate in some application areas, it is ample in characterisation studies where all that matters is a means of assessing the regular characteristics of the surface to qualify as well as classify them for certain manufacturing applications. Further more, classification and recognition of structured and patterned surfaces based on the outcome of their zero-phase characteristics, can be a concise means of assessing topographical behaviour. With such purpose in mind, zero-phase characterisation has been applied to the study of the topographical characteristics of a machined surface in the next chapter.

CHAPTER 5

ZERO PHASE CHARACTERISATION OF A MACHINED SURFACE

5.1 Introduction

This chapter investigates the prospects of zero-phase characterisation for a reflectance target from the practical point of view as well as computer simulation studies. The reflectance target is a turned machined specimen which like many other engineering surfaces, bears the tool mark embellishments and a population of repetitive components. Much of the typical characteristics expected in a zero-phase characterisation has already been met in the previous chapter. This study has not only identified the general traits associated with a zero-phase characterisation, it has also established the suitability of such technique in mapping the habitual regularity of certain engineering surfaces. Although, lack of phase deprives one of the object's positional information, as well as its exact structural configuration, other attributes are equally important and valuable in the surface manufacturing sector. In the assessment of engineering surfaces, the exact positional co-ordinates of the features is irrelevant, and such parameters can not be found through serial means of assessing surface topography either. What takes precedence is the range of spatial features and their lateral spacing. spacing. In this respect, zero-phase characterisation can always be relied upon to produce this information.

CHAPTER 5

This chapter focuses on the extraction of regularity from an optically recorded diffraction pattern, the difficulties associated in capturing the pattern, interpretation of the results in the presence of a Gaussian beam, and modification of the optical spectrum for the restoration of the finer spatial features. This work has resulted in three publications (N.Sotoudeh, *et al.*, 1989), (N.Sotoudeh, *et al.*, 1993), (N.Sotoudeh, *et al.*, 1992), with the most significant and novel contribution being the application of the scaling principle in resolving the finer spatial structures. The body of this chapter is arranged in the following manner:

Section 5.2 describes the mechanism by which a turned machined surface is generated. This gives an insight as to how the cutting process generates a predominantly regular profile of coarse variations, embedded in which are a whole set of regularities on a finer scale. It also describes how the macro variations (i.e coarse structures) themselves could be resting on an undulating surface which can influence the reflective properties of the object specimen.

Section 5.3 investigates the zero-phase characterisation of a machined surface. This study provides a basis for comparing the computer simulated diffraction pattern with the optically recorded diffraction pattern and the quality of information associated with each. The zero-phase reconstructed profile is then compared with the actual profile, and the main similarities are further highlighted.

Section 5.5 focuses on the zero-phase characterisation of the surface from the experimentally recorded diffraction pattern. Issues such as aliasing, asymmetry in the diffraction pattern and the pre-processing of the optical data have been addressed in sections 5.5.1 - 5.5.2. Section 5.5.3 provides the visual evidence for the interaction of the beam with a cosinusoidally corrugated surface and how the amplitude profile of the

surface is modulated by the Gaussian nature of the source. Section 5.5.4 discusses the nature of the restored characteristics with reference to the modulation characteristics of the laser beam, and the approximate dimensional range of the features obtained from experimental measurements. These have been identified as the coarser structural variations steeper in depth than the finer structures, by a factor of 70, and much larger in lateral spacing (approx. by a factor of 40) than the finest recorded feature.

Section 5.6 addresses the frequency domain scaling principle as a novel means of restoring the finer spatial features through the compression of the overall spectrum. Allied with the fact that not all Fourier coefficients are needed to restore object characteristics, compression of the overall frequency spectrum has been exercised in two respects:

i) spectrum contracting in size by ignoring Fourier coefficients horizontally and vertically whilst exercising care in preserving the signature of the fine details in the contracted frequency spectrum;

ii) spectrum further contracting in size by making it part of a large array acting as a background.

Section 5.6.1 displays the restored topology of the machined surface through the application of such frequency compression technique. The approximate dimensional range of these features are deduced from the scaling factor associate with the spectrum contraction, and the existence of the features are then verified with the aid of the scanning electron microscopy photo-micrographs and those of travelling optical microscopy. Section 5.6.2 ends this chapter by discussing the limitations of this principle in terms of possible loss of definition, aliasing and the computational strains of processing large data arrays.

CHAPTER 5

5.2 Characterising The Profile Of Machined Surfaces

(N.Sotoudeh, *et al.*, 1989)

Turned and shaped machined surfaces are produced by a single point cutting tool. The ratio of pitch to depth varies considerably. During the cutting process chips are detached by the tool and a drag occurs just behind the cutting edge which compresses the fragmented metal into a layer of amorphous or smear metal. The heat and pressure of the operation destroys the true crystalline structure of the metal producing a layer of low strength and weak load bearing capacity. If the tool is perfectly guided and the chips uniformly produced, the mean level of the grooves should be on a geometrical surface having the perfect form designated by the drawing. If the guiding is not perfect or the cutting not uniform, the grooves themselves will be on an undulating surface. The complete texture of the surface may be very complex with errors resulting from the feed of the tool, the cutting action, vibration and anisotropy in the crystalline structure of the metal. In general there are two important factors peculiar to the geometry of the turned surfaces which separates turning from all other machining methods (Rubert, Handbook, 1986) :

i) the geometry of the turned surfaces is almost regular and consistent. It consists of ridges of material of approximately uniform height aligned in the direction of turning (P.Sullivan, *et al.*, 1992);

ii) the basic shape of the grooves of the turned profile is almost a true negative replica of the shape of the cutting tool tip, with superimposed irregularities mainly due to the vibrations of the cutting speed, known as Prof. Olsen's rule (Rubert Handbook, 1986).

In this respect turned machined surfaces will generate the ideal diffraction pattern most suitable for the zero-phase characterisation study. In order to produce well-defined diffraction patterns, the area of the surface sampled by the laser beam needs to possess features that are comparable in size with the wavelength of light. A range of size from 1μm to 500μm is suitable. Additionally, the area sampled should be larger in diameter than the size of the largest feature of interest.

Figure 5.1: Photograph of the turned machined surface used for zero-phase characterisation study.

There are basically three main type of spatial structures present on the turned surface of figure 5.1 used for characterisation study:

i) the random component for which a Gaussian distribution of reflectance profile is obeyed following the formulation by (Beckmann and Spizicchino, 1963). It should be noted that the reflectance profile, exhibits a Gaussian pattern only if the random component of the surface can be modelled in terms of a Gaussian distribution;

ii) the structured grooves having a spatial period of 200μm-100μm.

iii) the tool-chatter components, which are a direct result of the base of the grooves being subjected to microscopic tool-chatter with a spatial period of 100μm-5μm.

Figures 5.1a and 5.1b show the grooves and the tool-chatter components. Figures 5.1c and 5.1d show the scanning electron microscopy photo micrographs of the region of the machined surface which was illuminated by the laser beam.

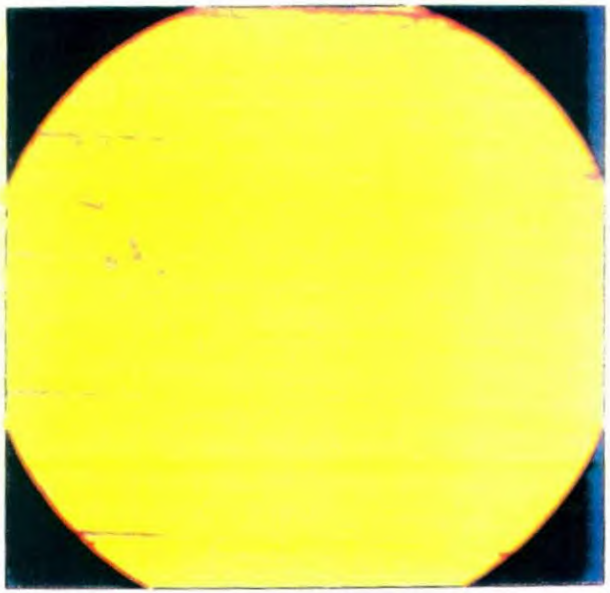

Figure 5.1a: Photo-micrograph of the machined surface showing the grooves with a spatial period of 200 μm.

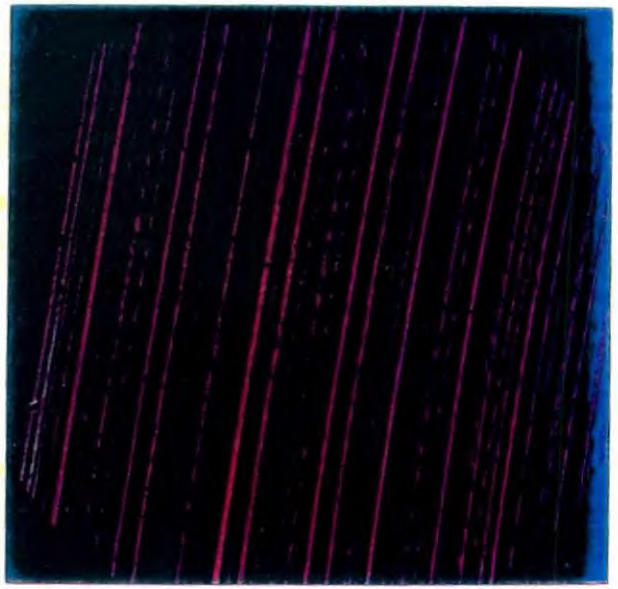

Figure 5.1b: Photo-micrograph of the machined surface at a higher magnification showing tool-chatter components ranging between 5μm-100μm.

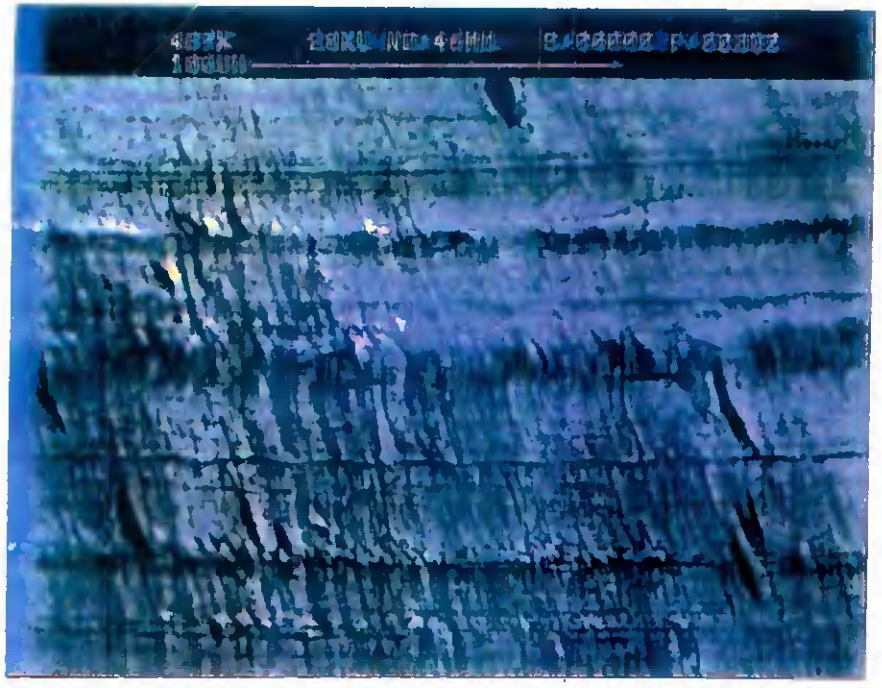

Figure 5.1c: Scanning electron microscopy photo-micrographs of the machined surface showing the presence of the tool-chatter components with a spatial period of 20μm.

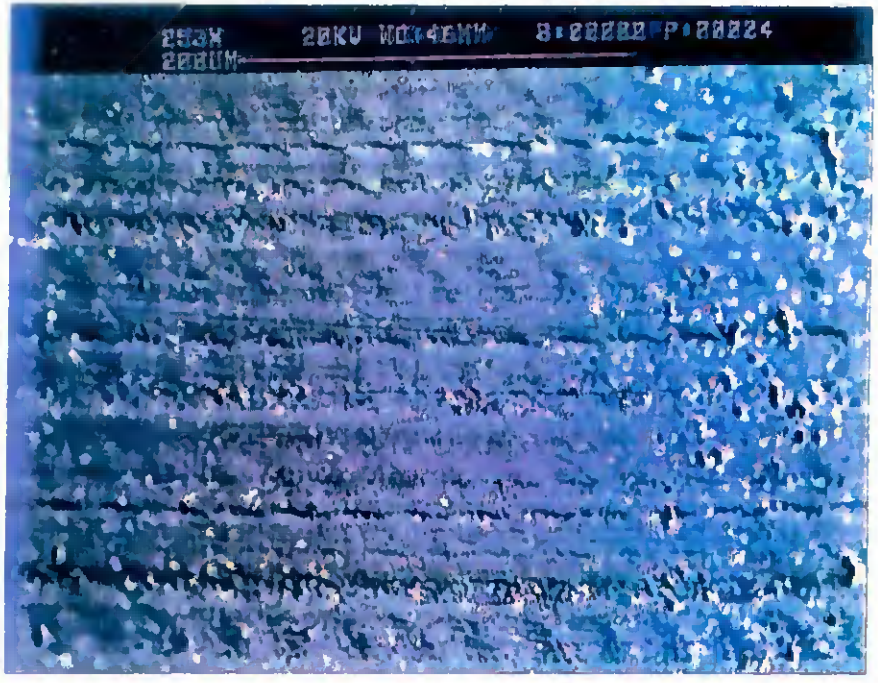

Figure 5.1d: Scanning electron microscopy photo-micrograph obtained at a lower magnification, showing a whole collection of tool-chatter components with a spatial period of 30μm.

CHAPTER 5

5.3 Computer Simulated Zero-Phase Characterisation of the Machined Surface

Figure 5.3a is the digitised image of a magnified region of the metal surface obtained by the travelling optical microscope and the camera arrangement of figure 3.6. The direction of the illumination and the plane of focusing when recording the digitised images of the machined profile play an important role when using the travelling optical microscope. The profile mainly shows three types of regularities captured at this particular plane of focus. Due to the diverse range of regularities and their corresponding variation in depth, it is not possible to integrate the whole range of features into one particular photo-micrograph.

Alpha step trace of the surface profile illustrated an average roughness of 7.27 KA for grooves as compared to the 135 A for the tool- chatter components; signifying a span in the height variations of the spatial components by a factor of 50. Thus, the digitised image of the machined surface only displays those roughness heights of similar amplitude which can be properly focused at a particular plane under the travelling microscope. It is thus apparent that magnified images of the surface do not represent the full spatial characteristics of the surface.

Figure 5.3a mainly shows three types of regularities captured at this particular plane of focus. Higher amplitude tool-chatter components have the ripple like structure to their height variations and finer tool-chatter harmonics appear as a set of broken lines in the digitised region. Note that the displayed image is only a 300x300 region out of the 512x512 image used in the zero-phase study. The three type of regularities and their spatial range are as follows:

i) the very bright regions seen as the thick lines, having the largest spatial period amongst the captured regularities i.e 56mm spacing width of 20mm;

ii) bright regions designated by the thinner lines of slightly smaller spatial period of approx. 50-52mm and width of 8-10mm;

iii) elliptic and oval shaped features of the smallest width i.e apprx 5mm,with a cyclic pitch of 45mm along the grooves and 55mm at right angles to the grooves. These features, are the coarser tool-chatter components which have been captured in this photo-micrograph,; the finest being as small as 5nm.

In order to comment on the zero-phase characterisation of this region of the surface,the contribution of each of the three characteristics to the frequency spectrum has to be considered.

5.3.1 Computer Generated Diffraction Pattern of the Machined Surface

A set of regularly spaced lines of spatial period d, produces a set of regularly spaced dots with a separation of 1/d in the frequency spectrum at right angles to the direction of orientation of these lines. The thick and thin lines are two different types of regularity. Therefore, the central region would not contain one intense row of spots which all have the same spacing; because the thick and thin regions act as two different gratings of slightly different periodicity. Consequently, in the frequency spectrum, there would be some regularity which has interacted with another regularity falling on the same line. Though difficult to see in the diffraction pattern of figure 5.3b, a high resolution plot of the rotated version of the surface signifies this fact in figure 1.12.

Since the brightest regions of the image correspond to the patterns of these two types of regularity, it is also expected that the diffraction pattern be predominantly dominated by the intense row of spots associated with such structure.

The third type of regularity is due to the elliptic or oval shaped features whose shape also influences the overall shape of the diffraction pattern. Small structural information is Fourier transformed into large detail at the frequency plane, thus the frequency contribution of this feature would be an enlarged elliptic or oval pattern at right angles to the original alignment of this feature. This effect can be clearly seen in the central region of the frequency spectrum, whereby the global arrangement of the Fourier coefficients can be seen to possess such oval symmetry.

The general influence of these features can be seen clearly in the diffraction pattern. However, the periodicity information associated with these oval features would not be so well defined and distinguished as such in the frequency spectrum. This is mainly due to the fact that though the oval features are repetitive, the repetitions are not exactly in line, i.e tool-chatter variations along one line are slightly displaced with respect to the ones along another line. This is similar to having a matrix of oval features where all the oval shapes are not exactly centred at the nodes of this matrix but they are slightly displaced in a pseudo random manner.

As opposed to a regular array of features, which would similarly give rise to regular array of bright regions separated by dark regions in between (which maintains similar regularity in the frequency domain seen as a lattice of bright points separated by dark regions), an irregular array of features would give rise to a random matrix of faint points near the lower frequency region of the Fourier map. Thus, the randomly spaced array of oval features would contribute towards the overall frequency spectrum through an intense central pattern embedded in a whole random fuzzy distribution of light. In addition, since the spatial period of the oval features is the same as the thick and thin lines, this frequency information would be mainly clustered in the central region.

Further more, since the oval features have a lower luminance and are confined to a smaller area, their associated frequency information would be "too faint" to be identified alongside the regularities of higher luminance.

If this spectrum were to be inverse Fourier transformed with zero phase, the regularity that would predominantly be displayed and picked up, would be that associated with the two sets of lines whose information is well distinguished from other points in the frequency spectrum. This fact is highlighted in the next section.

5.3.2 Comparison of the original luminance profile and the zero-phase characterised profile

Figure 5.3d is the 3D plot of the 512x512 luminance profile of the surface. Figure 5.3e is its corresponding zero-phase image generated by inverse Fourier transforming the frequency spectrum of figure 5.3b. Though not a pixel by pixel representation of the luminance profile, it bears a true resemblance to the original height variations in terms of maintaining their orientation and their predominant regularity. These height variations are again influenced by the "triangular data window" effect addressed in chapter 4 and as can be seen modulated in amplitude by the shape of this window.

As to the effect of the oval shaped features, the frequency components associated with this information are too weak to be restored. Examination of figure 5.3b reveals a logarithmic change in intensity levels of 10^{29} -10^{22} i.e an order of magnitude of 0.1 millionth difference between the yellow to red transition. With the red being the intensity level of the finer amplitude components. Thus, this information would not be recovered in the presence of the domineering structural components, shown in the yellow scale.

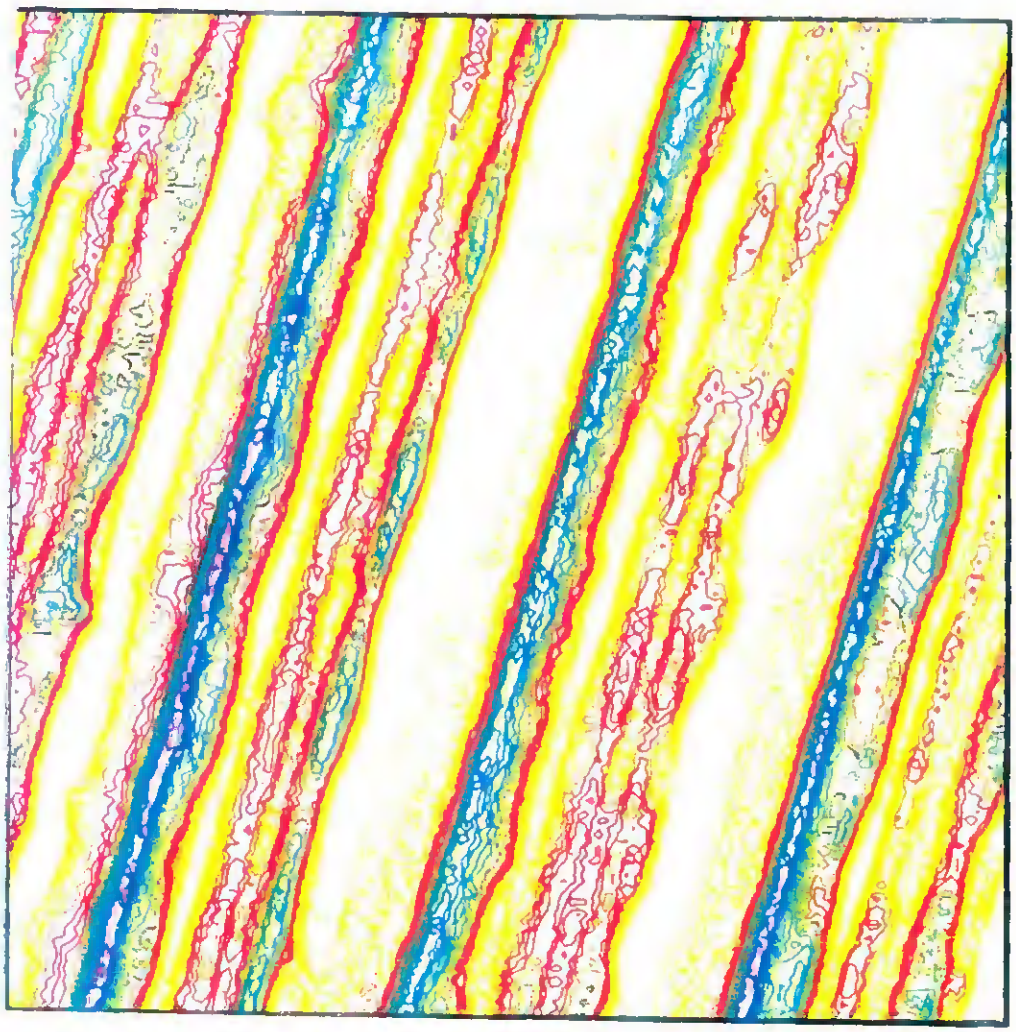

Figure 5.3a: Digitised image of the magnified region of the surface; the image displays three types of spatial regularities seen as: i) the very thick lines, ii) the thinner lines and iii) the oval shaped features.

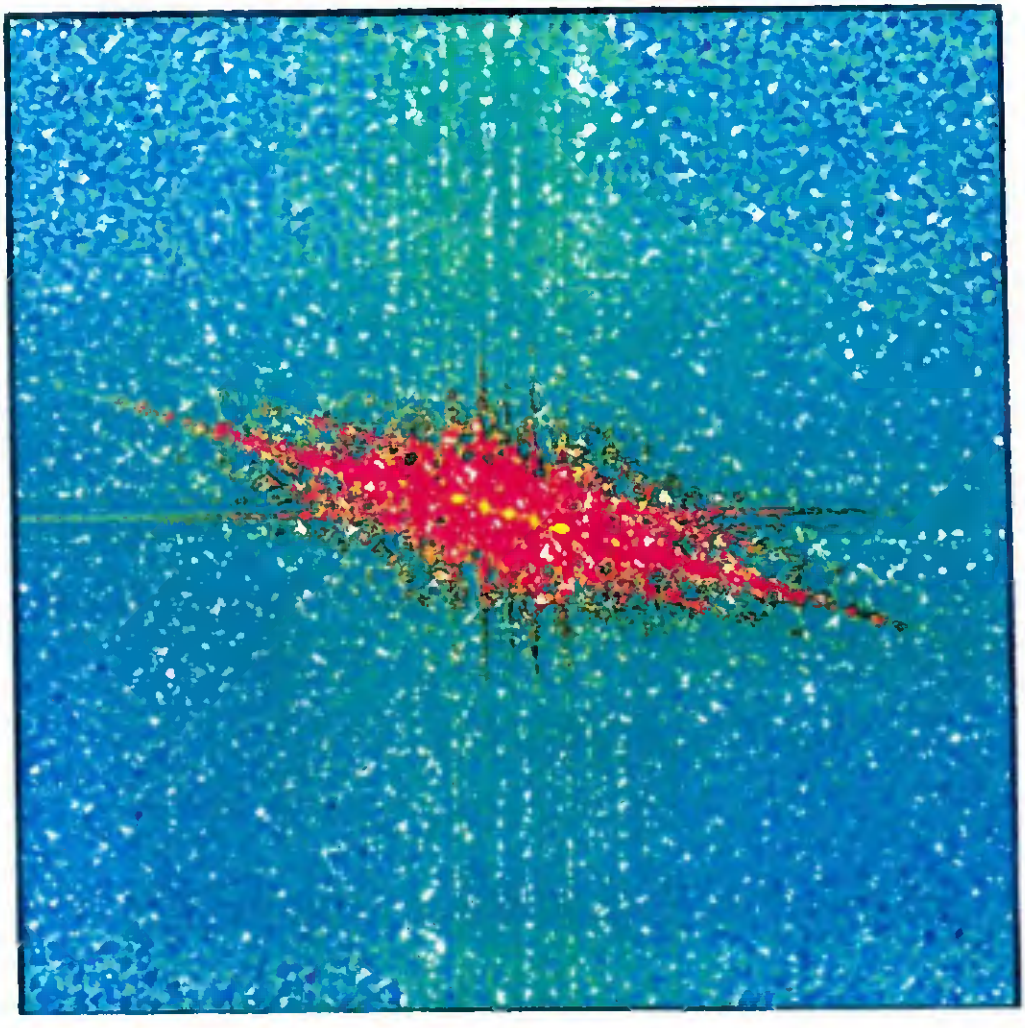

Figure 5.3b: Computer generated Fourier spectrum of the magnified image of the machined surface; the spectrum is dominated by the prominent periodicity due to the coarser features seen as the very bright points.

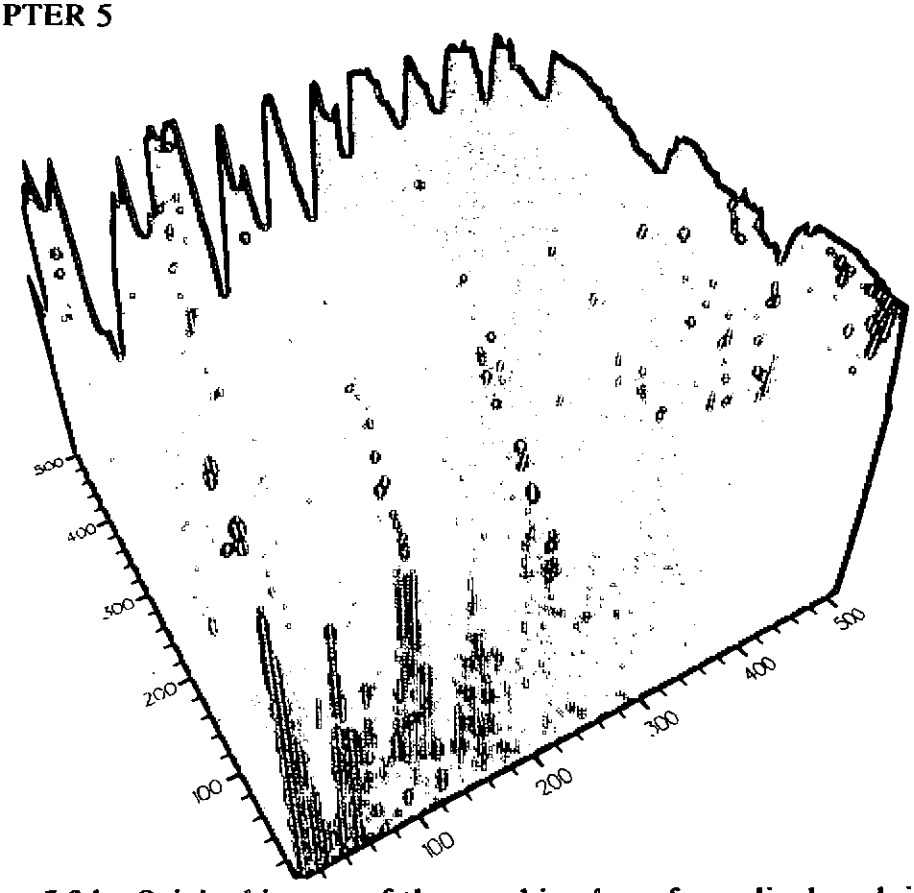

Figure 5.3d: Original image of the machined surface displayed in 3D for comparison with the zero-phase restored characteristics displayed below.

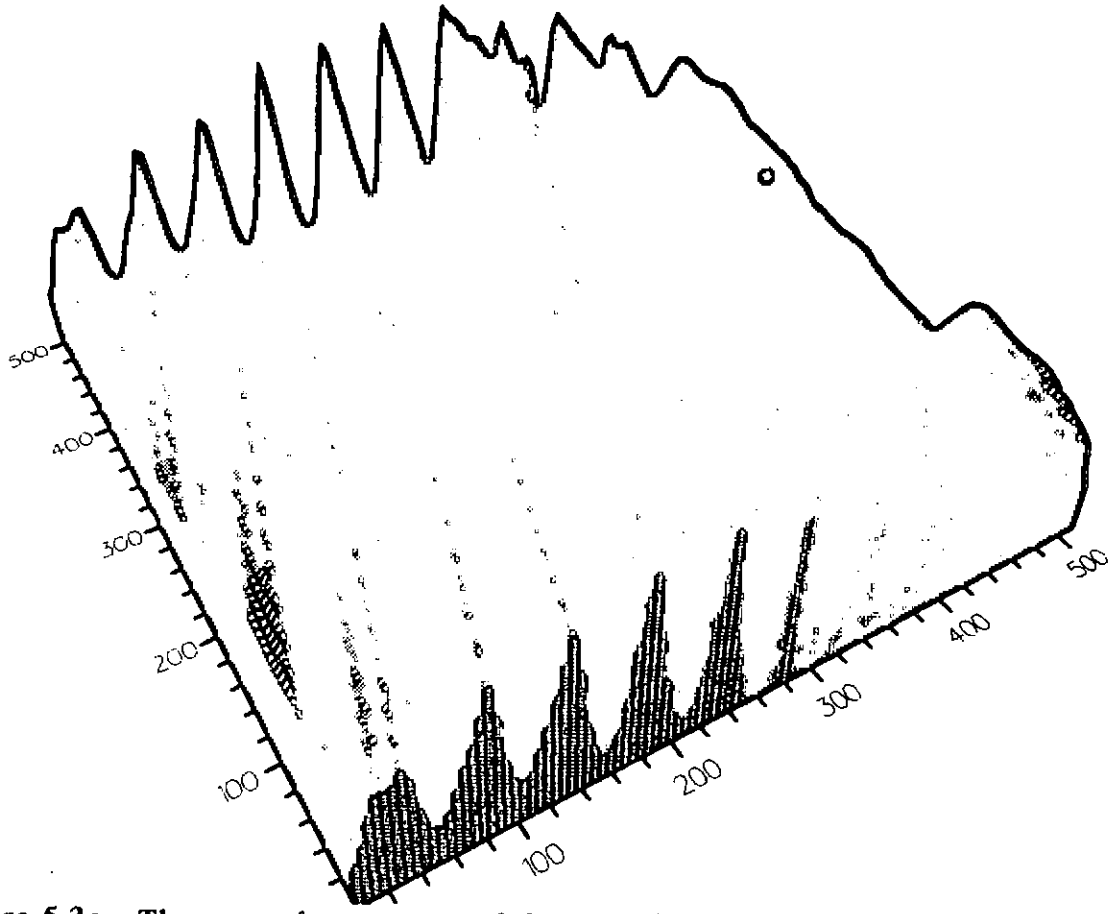

Figure 5.3e: The zero-phase restored image of the surface via using the computer generated spectrum of figure 5.3b; note that even in the absence of phase, this image bears a striking resemblence to the original.

5.4 Zero-phase characterisation of the machined surface using the experimental optical spectrum

The main difference between an optically recorded diffraction pattern and a computer generated diffraction pattern, is the influence of the laser beam intensity distribution on the optically recorded data. The following section discusses the outcome of such impact on the restored characteristics of the object.

5.4.1 The Effect of the Laser Beam Profile On the Optically Recorded Spectrum

Each point of light seen in the optically diffracted spectrum, would be convolved by a Gaussian intensity profile which is the frequency transform of the incident Gaussian beam. This would lead to:

i) modulation of the restored object characteristics by a Gaussian effect: all the experimental reconstructions will have the laser beam profile multiplied by the reconstructed surface reflectance profile. This multiplication would lead to the Gaussian intensity distribution of the beam modulating the recovered shape of the features by this effect. The presence of a superimposed Gaussian envelope on the restored surface characteristics could lead to difficulty in identifying the true geometrical structure of the surface.

ii) severe attenuation of the spatial features which fall near the edge of the beam. The rapid drop in the intensity of the Gaussian beam allows for only a limited range of the spatial features to be restored. These are mainly surface characteristics which are close to the centre of the beam when illuminated.

To illustrate the effect that the Gaussian profile introduces on to the surface characteristics, the modulation of a cosinusoid with a Gaussian distribution has been shown in figure 5.4

The impact of such modulation on the overall characteristics can be seen as:

i) loss of characteristics falling near the edge of the beam; i.e the near edge undulations are barley recognisable;

ii) loss of the circular symmetry of the Gaussian profile; i.e the circular cross section seems to be elongated in the direction of the cosinusoidal undulations.

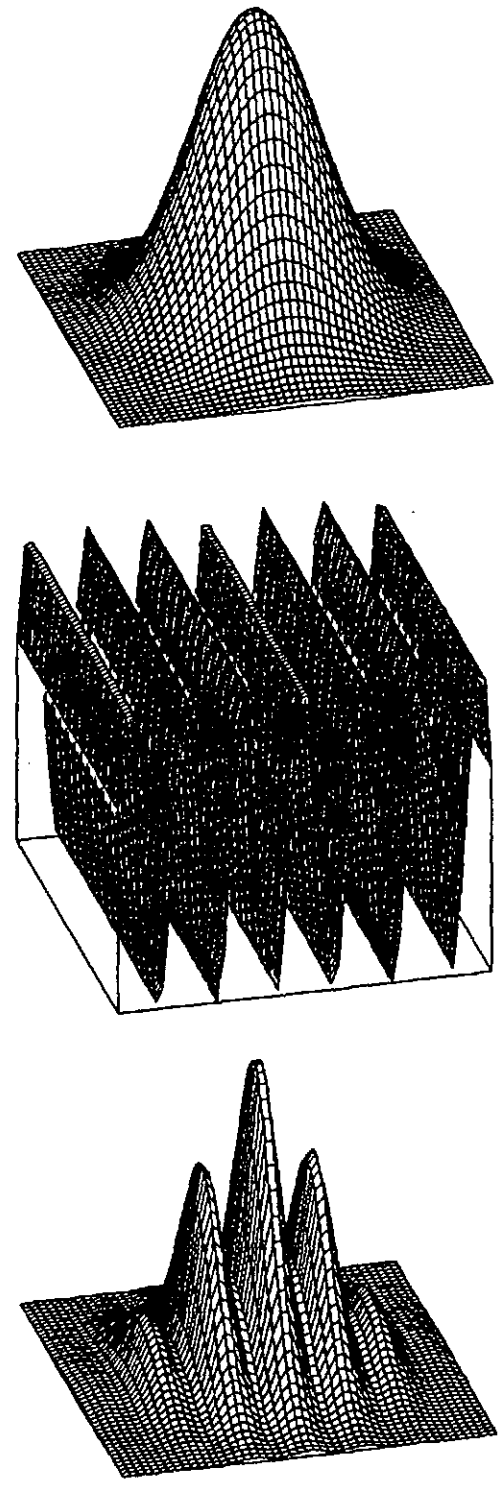

Figure 5.4 : Modulation of a Gaussian intensity distribution with a cosinusoidal undulation.

5.4.2 Capturing the Optical Spectrum

Though the optical diffraction pattern maps the whole range of spatial components present within the illuminated region of the surface, this information can not be intercepted with the same fidelity by the recording device. In particular, when the object surface possesses spatial features whose dimensional size varies considerably. Very fine spatial components give rise to frequency characteristics which are located much further from the centre of the spectrum as compared to the coarser structures. Since, the intensity of the spectral components also drops with distance from the centre, the spectral signature of the very fine spatial characteristics would be far too faint to be registered by the camera in the presence of the predominantly intense lower frequency components.

This was particularly evident in the case of the machined surface which gave rise to frequency characteristics with a very bright central region followed by lower intensity spectral lines, the overall effect of which had to be captured by the camera.

Thus a compromise had to be made between increasing the intensity of the finer characteristics to a level which could be picked up by the camera ; and maintaining the intensity of the lower frequency components at a level which did not drive the camera into saturation. In doing so, the recorded optical spectrum only displays frequency components associated with spatial features of approximately 30μm periodicity, whereas periodicities as fine as 5μm have been picked up by the Alpha-step profiler.

5.4.3 Selective Reflectivity of the Machined Surface

In general, the structural configuration of most object surfaces is such that it gives rise to a symmetrical distribution of frequency components about the optic axes. This is due to the fact that all the plane waves intercepting the object, upon diffraction leave in pairs with inclinations of $+\theta$ and $-\theta$ from the optical axis. However, in the case of the machined surface, it was noticed that the diffraction pattern did not exhibit the classical symmetry which was expected. It somewhat displayed a more intense distribution of the frequency components on one side of the spectrum as compared to the other side.

This asymmetry, is typical of the frequency characteristics associated with blazed reflection gratings used in spectroscopy, where the reflecting surface is at a carefully controlled angle to the plane of the grating (R. Newton, 1990), (R. Broadmann, *et al.*, 1985). In the case of the machined surface, the observed asymmetry is due to the tool cutting action which has introduced other effects such as grooves being cut at an angle. This results in preferential reflectance at the angle of cut, in addition to the Fourier transform of the aforementioned spatial features i.e the grooves and tool-chatter components.

This fact has been illustrated in figure 5.4a for a reflectance object for which the pattern cut on to the surface rests on a flat base and the same object for which the pattern cut on to the surface is inclined at an angle, thus giving rise to preferential reflectance. It should also be mentioned that the asymmetry in the captured optical spectrum is on occasions due to the way the camera has been positioned when recording the optical spectrum. If the camera is not looking normally on to the screen, the camera itself would capture the part of the diffraction pattern closer to it as brighter as compared to the part which is further away. Under such circumstances the experimentally recorded diffraction patterns have to be corrected for such effect. In this case however, as the asymmetry is inherently due to the geometrical structure of the surface, this information has been preserved in the recorded spectrum.

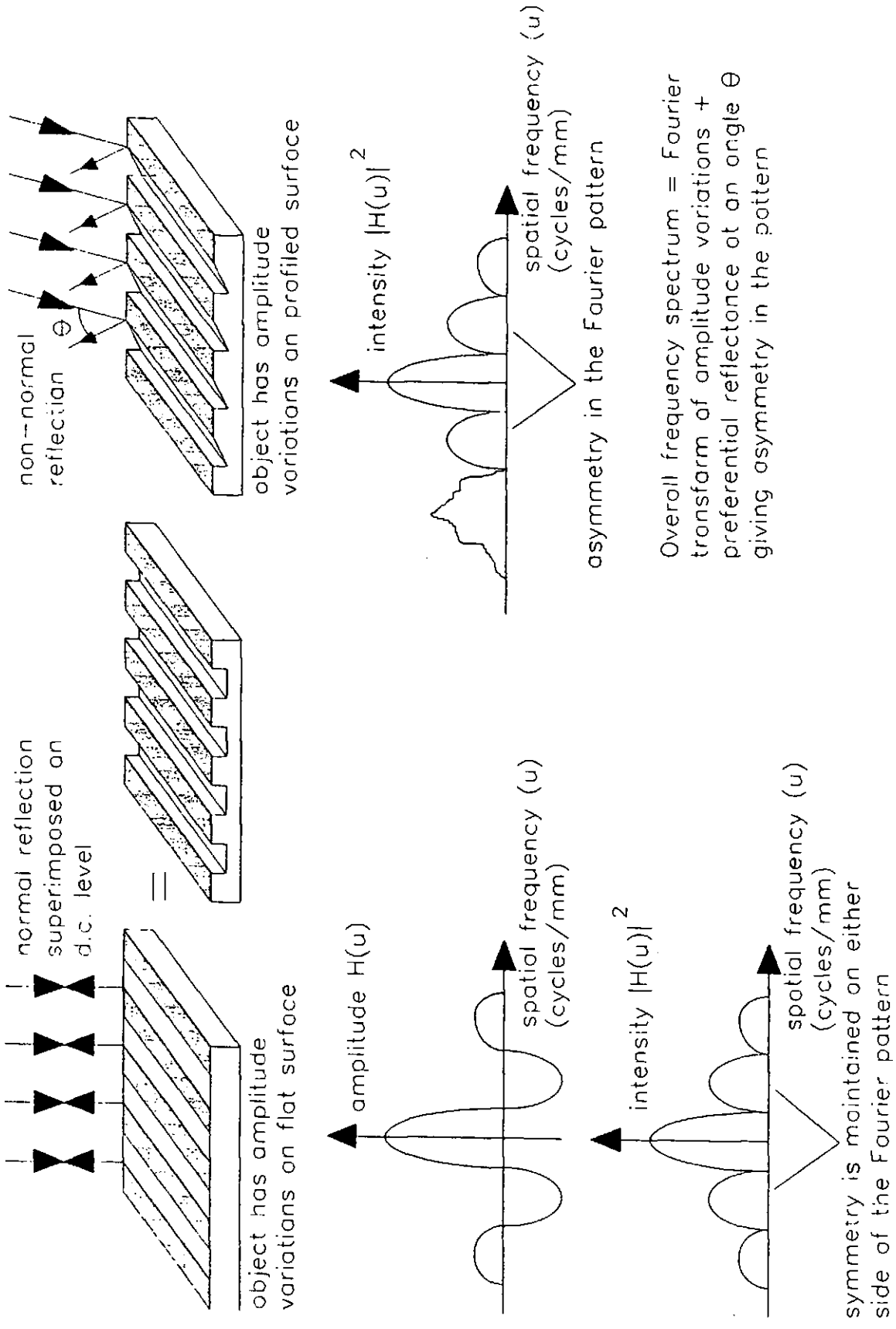

Figure 5.4a: Illustration of selective reflectivity for an object surface, giving rise to asymmetry in its associated diffraction pattern.

5.4.4 Recovery of the surface spatial characteristics

(N.Sotoudeh, *et al.*, 1991)

Figure 5.6 illustrates the experimentally captured optical diffraction pattern for the machined surface. Though, the very fine spatial periodicities have not been recorded as part of this spectrum, the optically recorded spectrum is by far more superior in mapping the structural characteristics of the surface as compared to the computer simulated spectrum of figure 5.3b. With reference to figure 5.5 and figure 5.6, the main difference is due to the way the frequency information associated with the coarse structures is mapped.

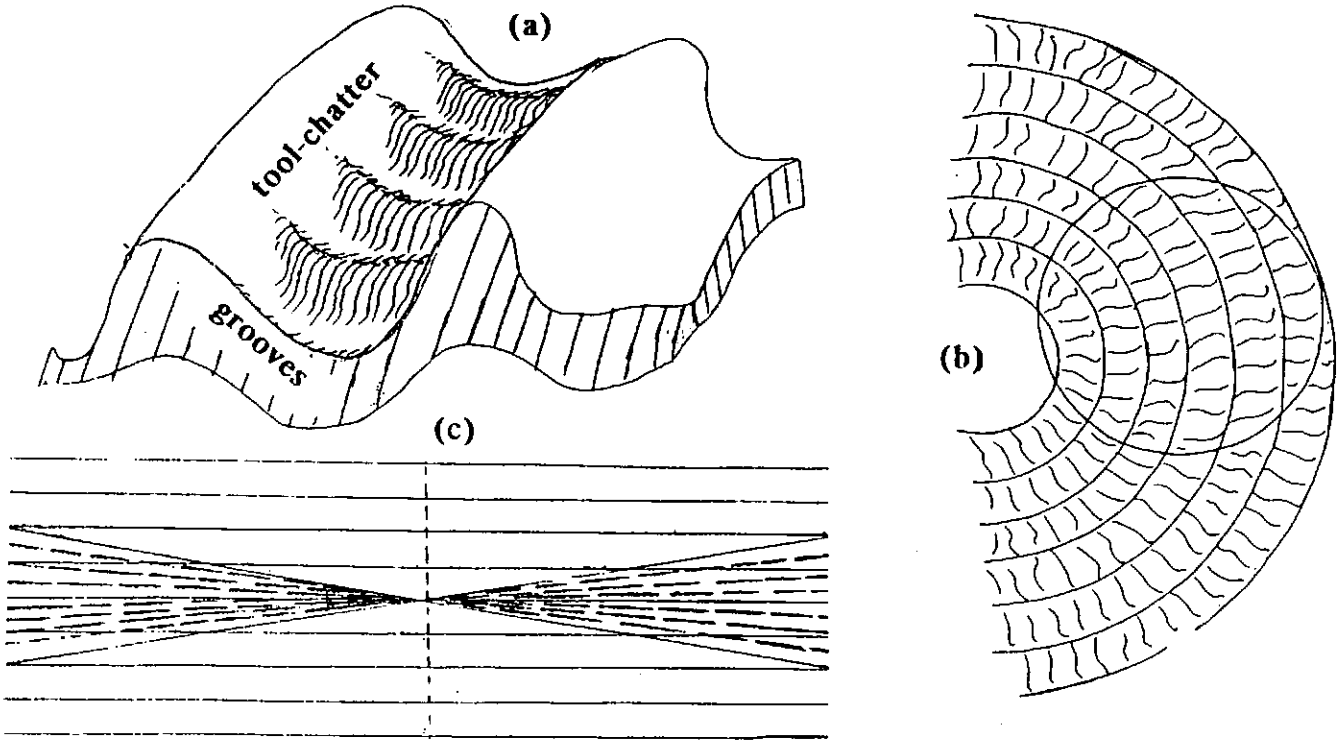

Figure 5.5: Schematic representation of the machined surface showing the orientation of the grooves and the tool-chatter components in (a); grooves appearing as semi-circular arc within the illuminated region in (b); predicted pattern for the optical spectrum from the geometrical view depicted in (a).

A series of straight lines, as was seen in the case of the digitised image of figure 5.3d, gives rise to a set of bright points at right angles to the direction of alignment of these lines. A series of arcs, which is really how the grooves are on the surface as seen by the laser beam, would generate a whole series of bright points each along a line.

Each of these lines would be at right angles to the curvature of the groove or the arc portion of the groove which is being illuminated by the beam. Thus the contribution of the grooves or the coarser spatial structures can be seen as a series of lines confined within two intersecting cones in the central region. The bright central region of the optical spectrum in figure 5.6a signifies this fact.

The extra horizontal lines indicate the abundance of the various tool-chatter components sampled by the laser beam as compared to the previous computer simulation results for which only a limited number of such components was included in the digitised photo-micrograph. Since the tool-chatter components run opposite to the variation of the grooves, their contribution would be mainly at right angles to that of the grooves. These lines indicate spatial periodicities of ≈ 100μm, 50μm and 30μm respectively.

This captured optical spectrum has been rearranged as in section (3.7) for the effective calculation of the inverse Fourier transform characteristics via the inverse Fourier transformation computer program. Figure 5.6c illustrates the inverse Fourier transformation of the captured optical spectrum. Since the diffraction pattern is the Fourier transform of the product of the laser beam reflectance profile and the reflectance profile of the surface characteristics, upon inverse Fourier transformation one would recover the autocorrelation of the product of the two functions. Hence the recovered characteristics would have the Gaussian nature of the beam superimposed on the reconstructions. The distorted shape of the recovered laser beam characteristics, is due to the reflection of the beam from the gross features which are the grooves; i.e reflection of a beam with circular cross section from a flat surface would be circular whereas the same beam reflected from a contoured surface would have its shape modulated by the surface contours. This point has already been addressed in 5.4.1.

Due to the rapid change in the scale of the recovered intensity profile over a small distance, a logarithmic display would facilitate the observation of the lower amplitude characteristics which is displayed in figure 5.6d. The approximate scale of the restored features i.e the grooves has been calculated via using the laser beam diameter as a reference. This approximate diameter was set equal to the distance for which the intensity has dropped to 1% of its maximum value. In figure 5.6d, a transition of 5-3 on the logarithmic scale accounts for a 100 fold drop in intensity. As near the edge of the beam, the intensity drops off very significantly, this distance is a good approximation for the calculation of the edge of the laser beam.

With the laser beam having a diameter of ≈ 2mm, the dimensional range of the grooves which appear to have a cyclic pitch of ≈ 4 pixels within the displayed region of 41x41 pixels in figure 5.6d can be estimated as follows:

$$C_{grooves} = \frac{4 \; x \; 2x10^{-3}}{41} mm \qquad (5.0)$$

$$= 195 \, \mu m$$

It should be noted that since in practice a Gaussian intensity profile has no sharply defined beam edge, the measures of beam width can only be used as a crude guide for distance measurement (Appendix C).

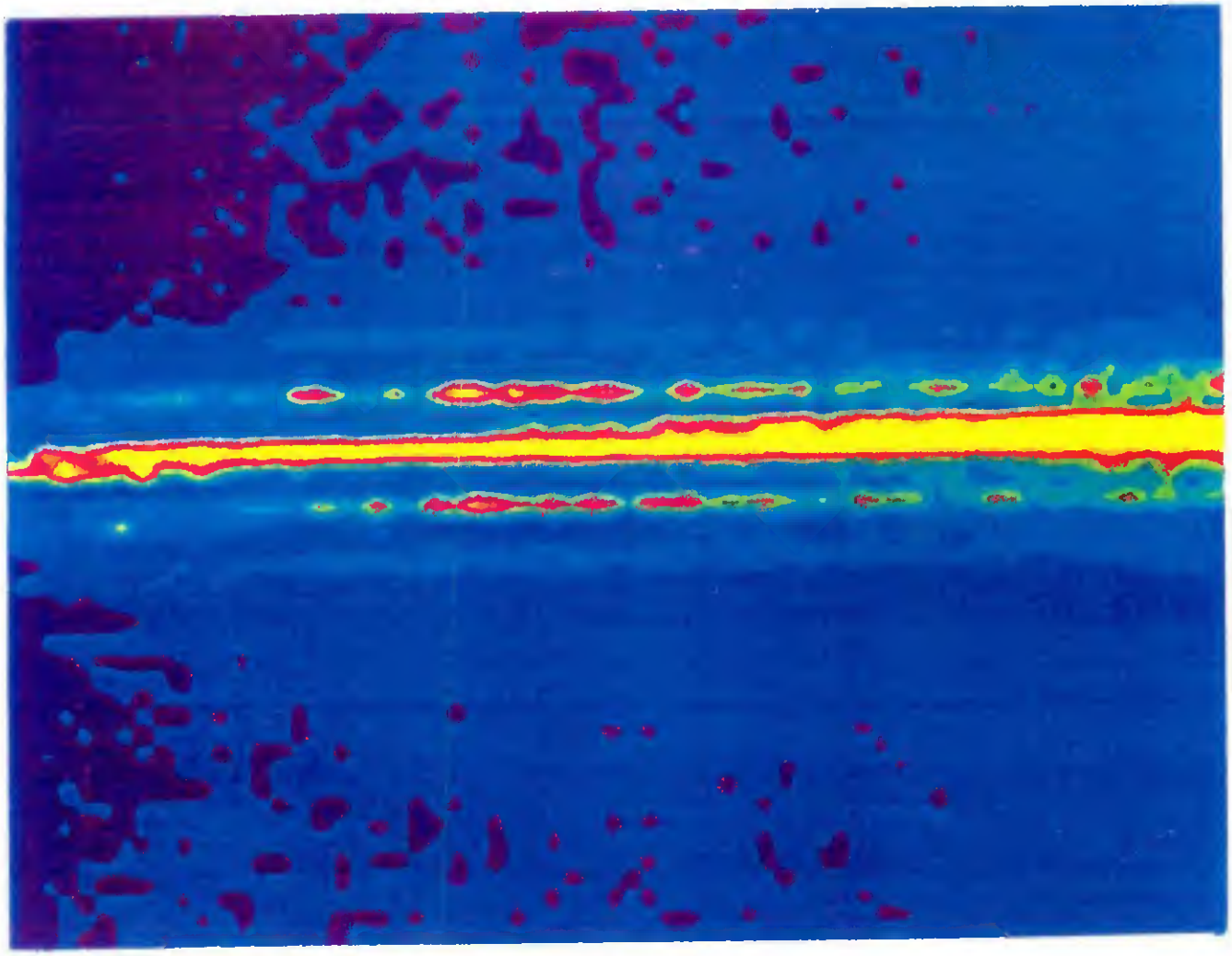

Figure 5.6a: Experimentally captured optical diffraction pattern for the machined surface illustrating the contribution of the grooves in the central region; followed by a series of horizontal lines due to the tool-chatter components.

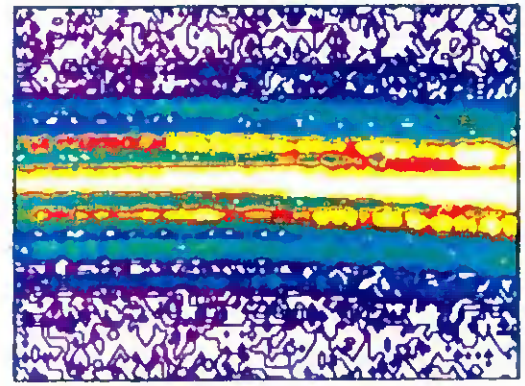

Figure 5.6b: Enhanced view of the central region of the diffraction pattern showing the spectral lines due to tool-chatter components more clearly.

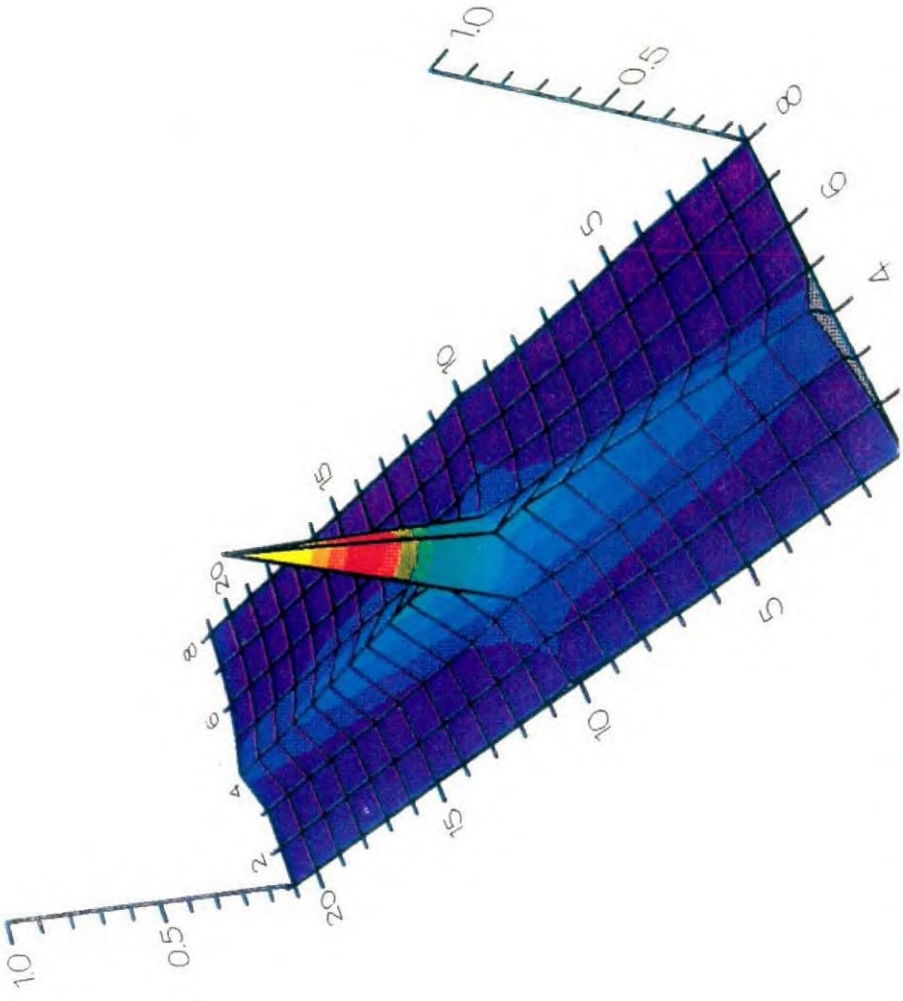

Figure 5.6c: Zero-phase reconstruction of the reflectance profile of the machined surface, without logarithmic enhancement; note that the overall profile is dominated by the Gaussian characteristics of the laser beam.

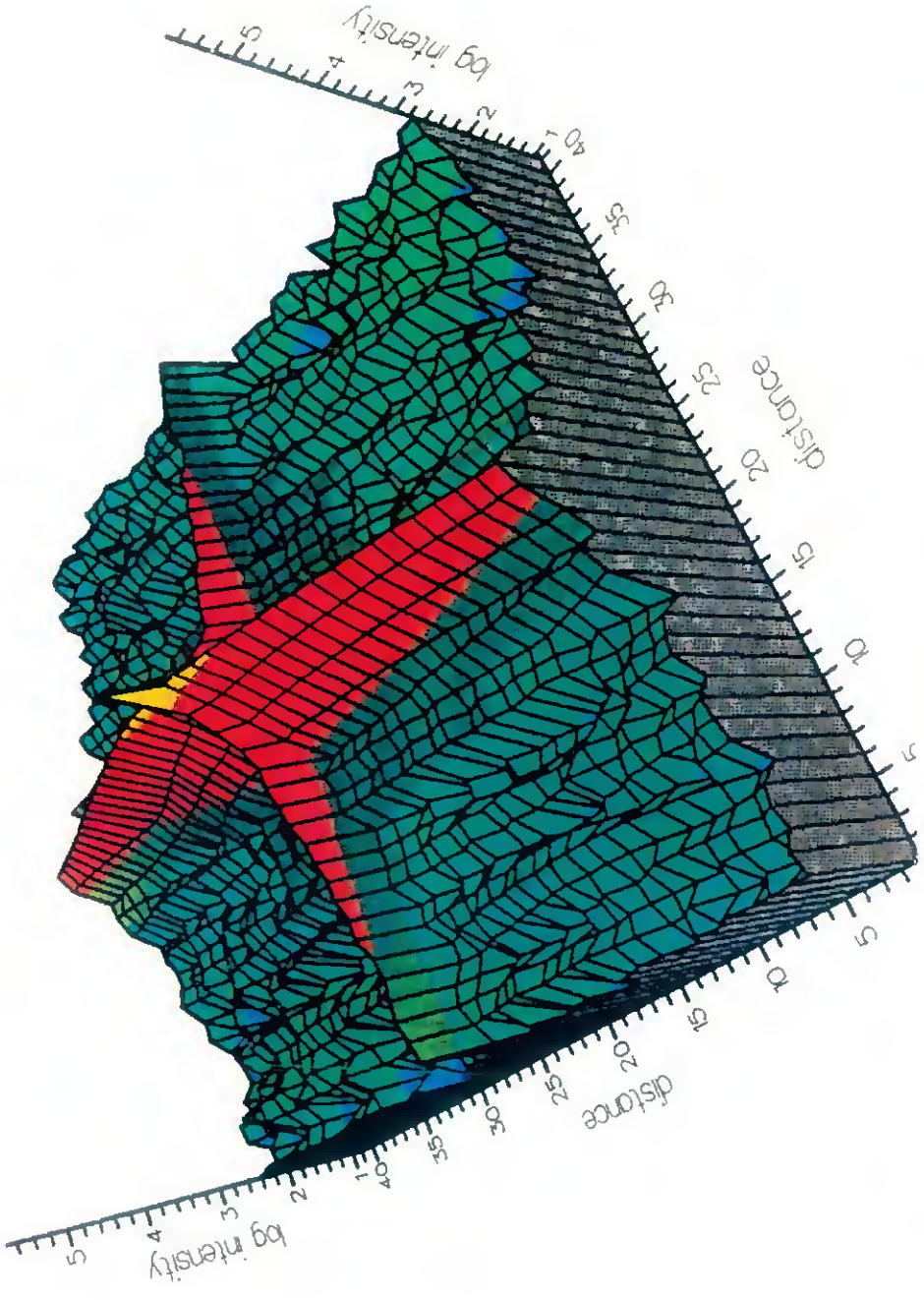

Figure 5.6d: Logarithmic enhancement of the zero-phase characterisation of figure 5.6c; the restored features are the grooves having a spatial period of ~195μm.

5.4.5 The analytical proof of restoring periodicity for an object with multiple regularities

The analytical proof that the zero-phase characterisation of the machined surface possessing a combination of surface spatial structures i.e tool- chatter and its harmonics can be recovered is as follows:

If the surface reflectance profile is to consist of tool-chatter components defined in terms of different sinusoid of arbitrary amplitudes and phases but with spatial frequencies which are harmonics of the fundamental i.e:

$$h(x) = A'\sin(\alpha x+\phi)+B'\sin(\beta x+\chi)+C'\sin(\gamma x+\psi) \qquad (5.1)$$

from equation (4.1) the standard autocorrelation function over the length -L/2 to L/2 of the object surface can be expressed as:

$$R(x')=\int_{-L/2}^{L/2} h(x).h(x+x')dx \qquad (4.1)$$

substituting for h(x) and h(x+x′) in equation (4.1), the autocorrelation function can now be expressed as:

$$R(x') = \int_{-L/2}^{L/2} \{ A'(\sin\alpha x+\phi) + B'\sin(\beta x+\chi)+C'\sin(\gamma x+\psi) \}$$
$$\{ A'\sin(\alpha x+\alpha x'+\phi)+B'\sin(\beta x+\beta x'+\chi)+C'\sin(\gamma x+\gamma x'+\Psi)\}\, dx \qquad (5.2)$$

writing out the first few terms of the product of h(x) and h(x+x′) the integral of (5.2) in expanded form would be:

$$R(x') = \int_{-L/2}^{L/2} [A'\sin(\alpha x+\phi)\ (A'\sin(\alpha x+\alpha x'+\phi)+B'\sin(\beta x+\chi)\ B'\sin(\beta x+\beta x'+\chi)$$
$$+C'\sin(\gamma x+\psi)C'\sin(\gamma x+\gamma x'+\psi)+A'\sin(\alpha x+\phi)B'\sin(\beta x+\beta x'+\chi)$$
$$+A'\sin(\alpha x+\phi)C'\sin(\gamma x+\gamma x'+\psi) + \textit{other cross product terms}]\, dx \qquad (5.3)$$

expressing the sine products in terms of cosine functions and neglecting the cross product terms (5.3) is reduced to:

$$R(x') = \int_{-L/2}^{L/2} \acute{A}^2\{\cos(\alpha x)-\cos(2\alpha x'+\alpha x+2\phi)\} + \acute{B}^2\{\cos(\beta x)-\cos(2\beta x'+\beta x+2\chi)\} + \acute{C}^2\{\cos(\gamma x)-\cos(2\gamma x'+\gamma x+2\psi)\} \quad dx \qquad (5.4)$$

which reduces to :

$$R(x') = \acute{A}^2 L\cos\alpha x+\acute{B}^2 L\cos\beta x+\acute{C}^2 L\cos\gamma x \qquad (5.5)$$

As can be seen, this function exhibits the periodicity of the three original harmonics and the periodic characteristics of the original profile is retained in its auto-correlation function.

As was seen in section 5.4.4, though the recorded optical spectrum contains spatial frequency components associated with features as fine as 30μm, this information has not been retrieved in the zero-phase restored characteristics of figure 5.6d. Further more as seen in figure 5.6d, the cyclic pitch of the grooves seems to be limited to ≈ 4 pixels from the peak of one groove to another, somewhat a poor spatial resolution. Undoubtedly, any finer characteristics which are embedded in the bottom of the grooves can not be identified at the current resolution.

Thus, in order to restore structural variations finer than the grooves, the optical spectrum needs to be modified in such a manner that it introduces the following effects:

i) firstly, an improvement in spatial domain resolution in terms of the number of available pixels, so that there are "sufficient pixels" to represent grooves as well as tool-chatter components;

ii) secondly, since the output images by the display device have a pixel resolution of ≈ 0.1mm, one has to also ensure that the spatial frequency of the tool-chatter components is brought right down to a level that matches the pixel resolution of the display device so that surface characteristics of finer dimensional range can be represented by a pixel spacing of 0.1mm.

Enhancing object definition in terms of pixel resolution and altering the scale of frequency components can be elegantly achieved through the application of the Fourier scaling principle. This has led to the most outstanding technique for the realisation of surface characteristics on a magnified scale which is also accompanied by an enhanced resolution.

CHAPTER 5

Standard techniques for magnifying digitised images can not make finer structural details visible by merely enlarging the image. Such magnification is often regarded as "empty magnification" without resolving finer characteristics. Furthermore, since unaided human eye can easily detect detail as small as 0.2mm (Goodhew & Humphreys, 1988), there is little point in enlarging what can already be picked up by the eye.

To resolve finer structural details, their frequency signature need to be enclosed alongside the signature of other spectral components which participate in the formation of the final image. Since, when using Fourier scaling principle, magnification in the scale of the object is achieved through altering the scale of its frequency spectrum, whilst enclosing the signature of interest, this type of magnification is accompanied by enhanced resolution.

The following sections which are also extracts from the published work by the author outline the basic philosophy of Fourier scaling and its application to the optical spectrum of the machined surface for the restoration of the finer variations.

CHAPTER 5

5.5 The Novel Application of Frequency Compression For Restoring Finer Spatial Characteristics (N.Sotoudeh, *et al.*, 1992)

The techniques of replication and interpolation are well known for magnifying images in the spatial domain (J.S.Lim, 1990). However, if the information is in the spatial frequency domain such as the optical Fourier transform of the surface reflectance profile of the machined specimen, frequency compression techniques could be used to resolve the spatial characteristics of a surface on a magnified scale. This can be achieved both in hardware and software by making the Fourier spectrum a much smaller part of a larger data array.

For a magnification of MxM pixel array both in the x and the y directions, each spatial frequency component in the Fourier domain must be M times smaller than the corresponding previous spatial frequency, or the intervals must be 1/M times closer. Retaining all the Fourier coefficients whilst making the spectrum smaller, and digitising a compressed spectrum as well as its surround, requires processing large data arrays with unreasonable amount of computational time.

However, it is also known that not all the coefficients in the Fourier domain are needed to reconstruct a surface satisfactorily (Raja *et al.*, 1977) and surfaces can be represented by using a fraction of the detail in the Fourier spectrum hence making the Fourier domain a concise data bank for characterising surfaces(Sherrington and Smith,1988). By combining the two effects of Fourier domain compression and Fourier coefficient removal, optically recorded data for the machined surface was compressed in the frequency domain which resulted in an expansion in the spatial domain upon inverse Fourier transformation. This expansion has resolved higher frequency spatial structures, whose physical presence has been verified by both Alpha-step and electron-scanning microscopy photo-micrographs.

Due to the lack of phase, the recovered zero-phase characteristics could either be due to the higher harmonics needed to synthesize a coarse structure or they could actually represent a physically realisable finer detail. It should be mentioned that there is a limit for further magnification set by:-

i) the number of spectral coefficients that can be ignored when compressing the data, without introducing aliasing;

ii) the extent to which zero-padding of the consequent data array can be performed without putting a strain on data storage and processing time.

5.5.1 The Fourier Scaling Operation

The relationship between the scale of the object and the spread of its frequency spectrum rests with the uncertainty principle. According to this principle, the size of the object and the spread of its frequency spectrum are reciprocally related. Thus if the object were to reduce in size until it eventually diminished to a point, its associated frequency spectrum would widen until it eventually approached a continuum. Put into a mathematical context, the change in the scale of the object and its frequency spectrum can be expressed via (5.6) -(5.8). Thus if h(x,y) is the original unscaled object whose associated frequency spectrum is H(u,v) as expressed in equation (5.6):

$$\sum_{m=0}^{m-1}\sum_{n=0}^{n-1} h(x,y)\, e^{-j2\pi(ux+vy)} <=> H(u,v) \qquad (5.6)$$

and for the scaled object h[M(x,y)], its frequency spectrum would be:

$$\sum_{m=0}^{m-1}\sum_{n=0}^{n-1} h[M(x,y)]\, e^{-j2\pi(ux+vy)} <=> \frac{1}{M^2} H\left(\frac{u}{M},\frac{v}{M}\right) \qquad (5.7)$$

therefore

$$h[M(x,y)] \; <=> \; \frac{1}{M^2} H\left(\frac{u}{M},\frac{v}{M}\right) \qquad (5.8)$$

To put the mathematical operation of above into perspective, a square object function of uniform height has been gradually reduced in size and its corresponding frequency spectrum plotted on each occasion and displayed in figure 5.7.

With reference to this diagram the change in scale, or, in this case magnification can be introduced in two ways. Firstly, an enlargement in scale of the object brought on by a mere compression of the frequency characteristics which is limited to the same data window. Note all three spectra are limited to a square data window of 256x256 pixels. Secondly, further enlargement in the scale of the object brought on by extending the surrounds of the compressed spectrum, i.e by making it appear a smaller part of a much larger data array. In application to the machined surface, these two effects i.e contraction of the spectrum and extension of its surrounds, were both introduced into the optically recorded spectrum.

5.5.2 The Advantages of Magnification Based on Frequency Scaling

Magnification often implies the immediate use of a lens. However, a lens will have a modulation transfer function which goes down to a certain cut off frequency thereby inhibiting higher spatial frequencies to participate in the image formation stage. By eliminating the use of an optical lens, and recording the available spectrum from a screen, this method in effect improves on the modulation transfer function of a lens. By including more Fourier coefficients much more of the diffraction pattern is collected as compared to a lens. Furthermore, there are many instances were a lens is not physically realisable to form an image let alone to form a magnified image, a classical example being in the case of X-ray diffraction patterns.

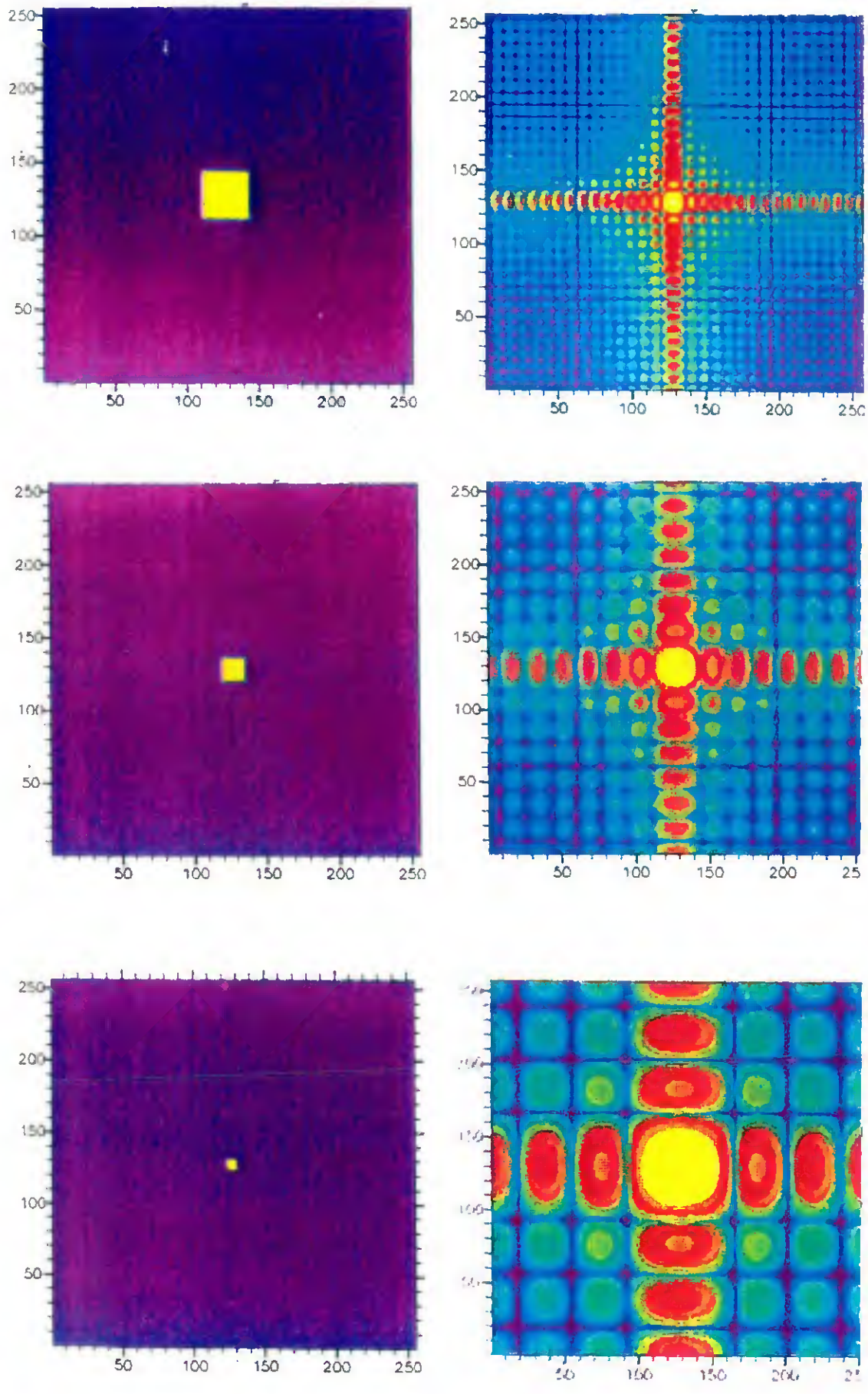

Figure 5.7: Illustration of the Fourier scaling principle; from top to bottom: compression in the scale of the object, is followed by an expansion in the corresponding frequency characteristics.

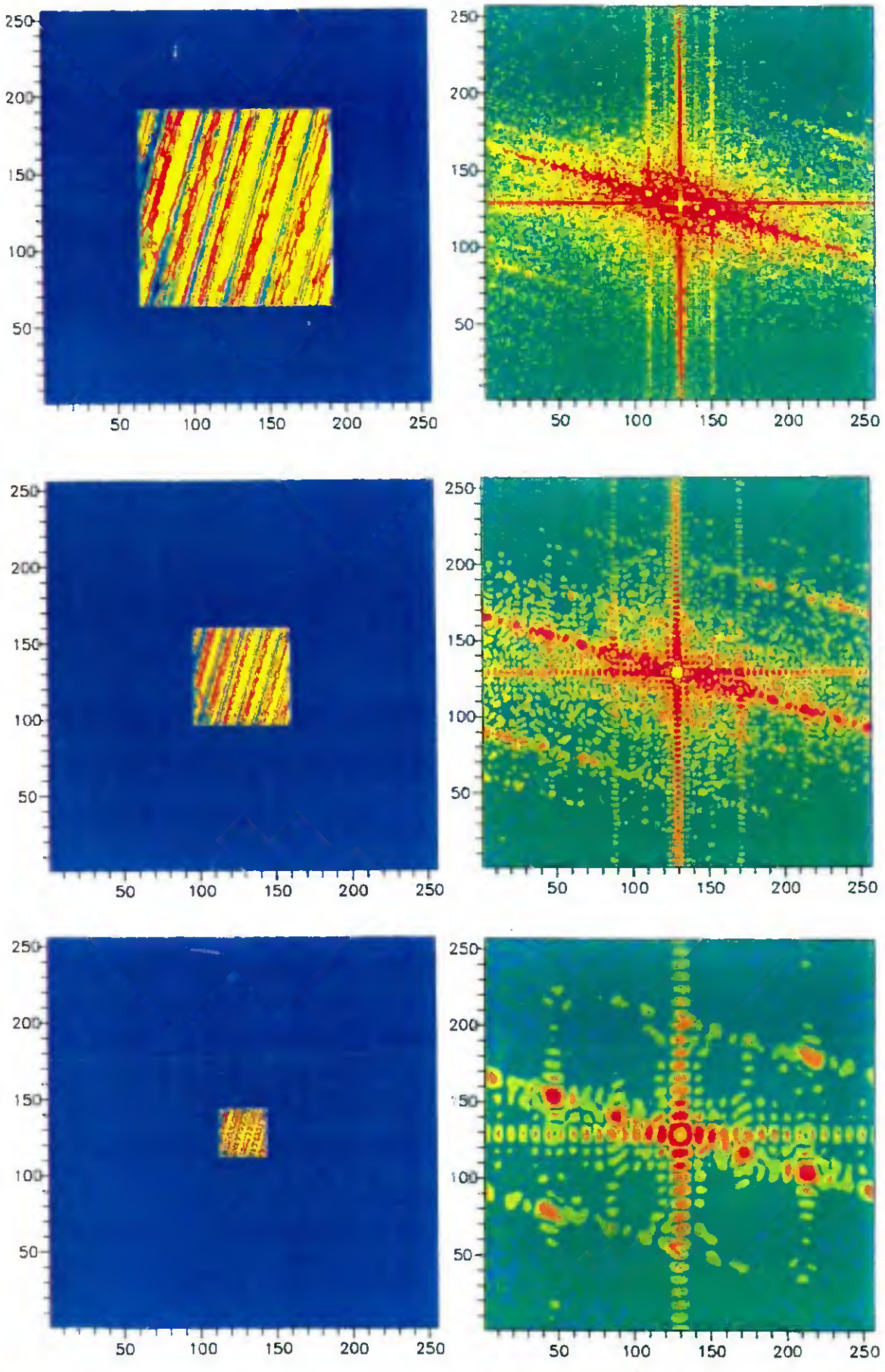

Figure 5.7a: Digitised image of the machined surface illustrating magnification characteristics; introduced through compression of the frequency this is one way of achieving object magnification.

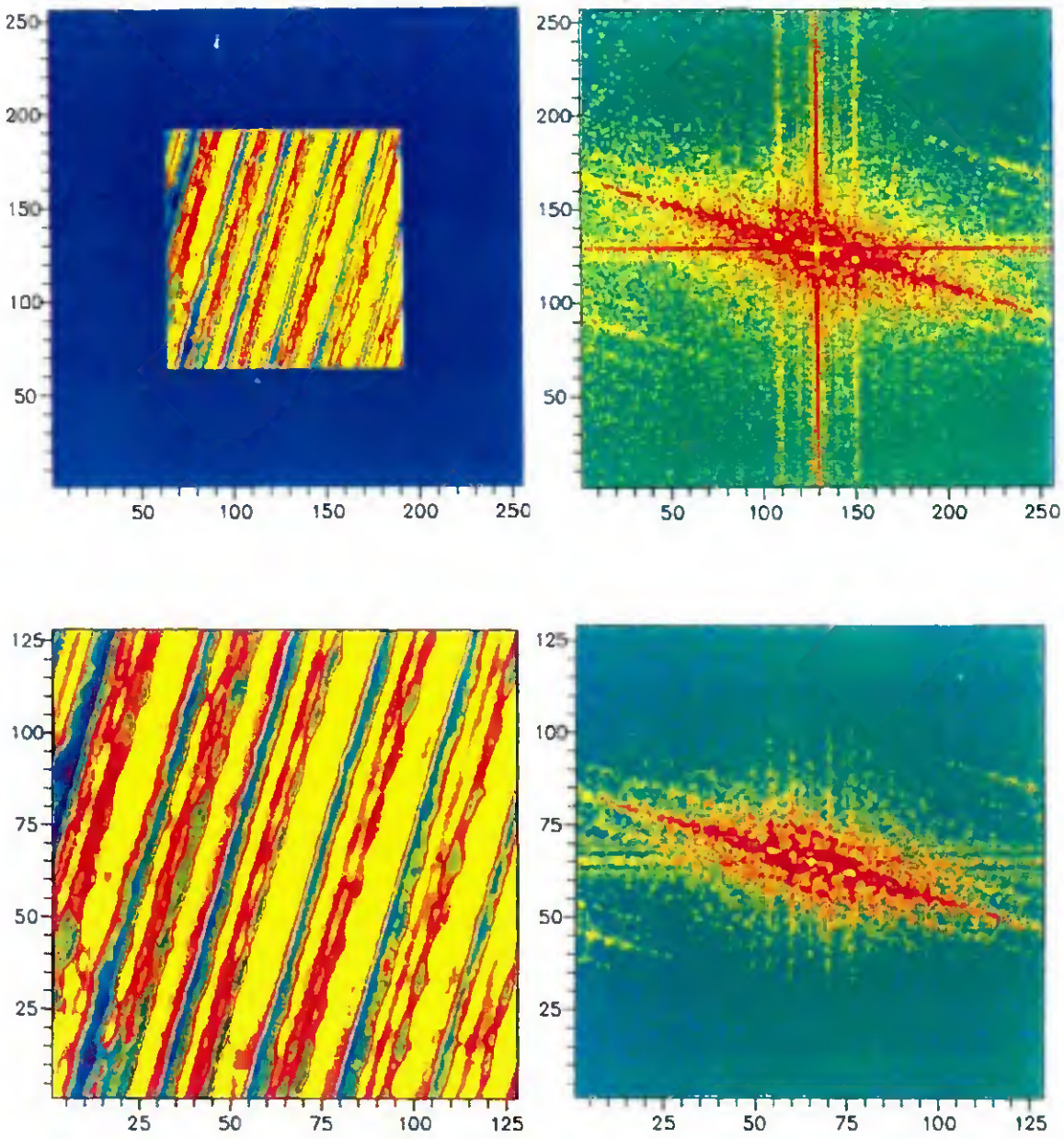

Figure 5.7b: Extending the object surrounds, interpolates the frequency characteristics, in a similar manner extending the surrounds of the frequency spectrum, interpolates the object characteristics; this is another way of achieving object magnification.

Last but not least the most attractive feature associated with a frequency scaling operation, is the freedom with which the captured spectrum can be re-scaled by either practical or computational techniques.

5.5.3 The Effect of Compression on the Frequency Characteristics of the Machined surface

With reference to figure 5.8, the compression of the optical spectrum as specified in section 5.5.1, has the following effects:

i) firstly, data residing in the higher spatial frequency region are brought in closer to the optical axis and interpreted as medium to low frequency information; this being regarded as the "scaling down" of the frequency components;

ii) secondly, by making the "scaled down spectrum" a small part of a much larger data array, upon inverse Fourier transformation the object characteristics would be enlarged by a factor with which the surrounds has been extended.

The original spectrum of figure 5.6a, consisting of 256x256 pixels has been compressed by 50% to that of 128x128 pixels. This compressed spectrum is then made part of a 512x512 data array by extending its surrounds to this value as seen in figure 5.9a.The size of the compressed spectrum with respect to its surrounds allows for an overall magnification factor in the object domain, by x4.Thus all the distances in the restored characteristics of figures 5.9b-5.9d have been enlarged by a factor of x4. As can be seen, frequency compression has not only resulted in the magnification of the characteristics, it has also resolved finer spatial periodicities. These are the very obvious cyclic features which appear in all three figures 5.9b-5.9d.

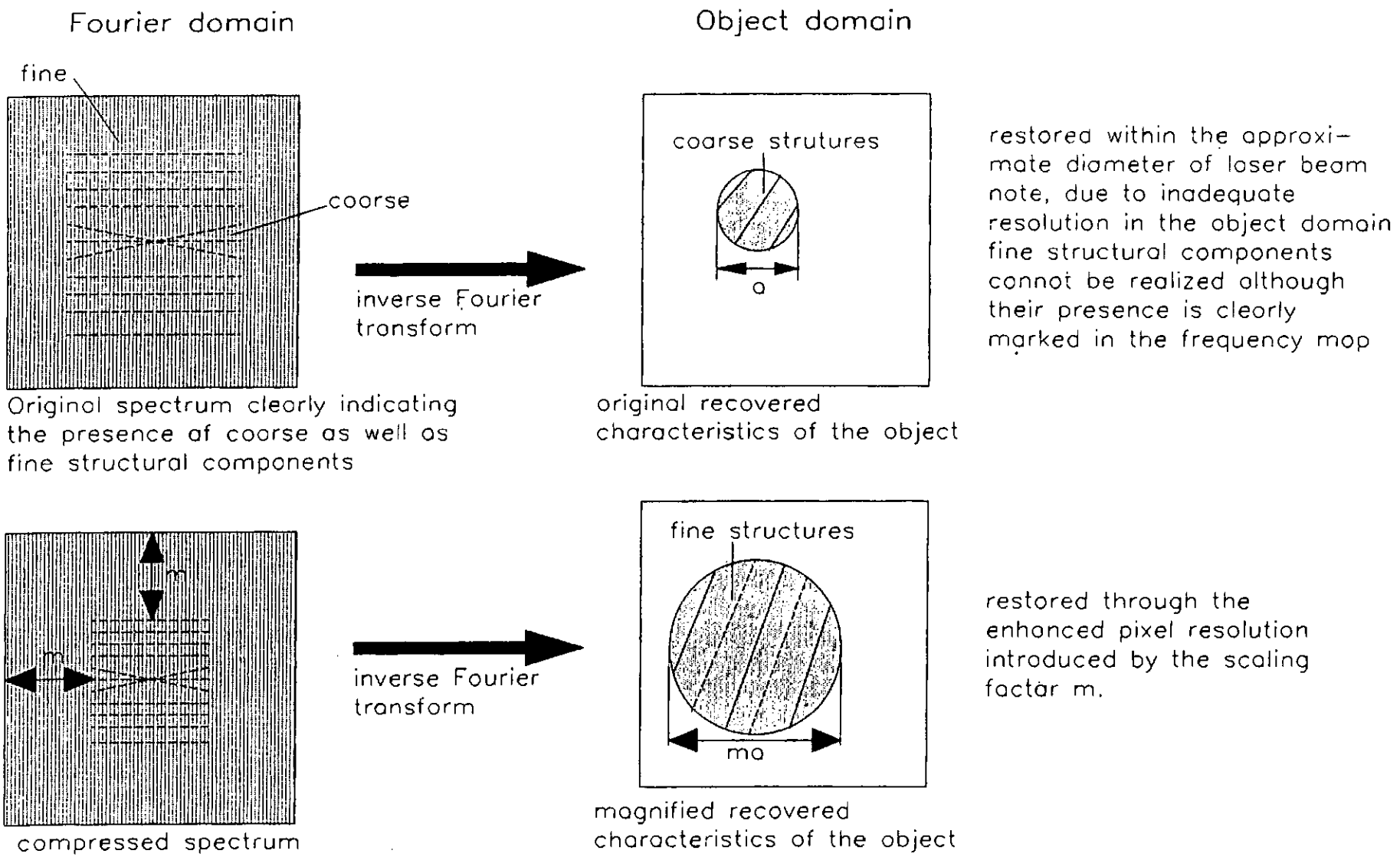

Figure 5.8: Pictorial representation of achieving magnification as well as enhanced resolution in the object domain, through compression of the frequency spectrum.

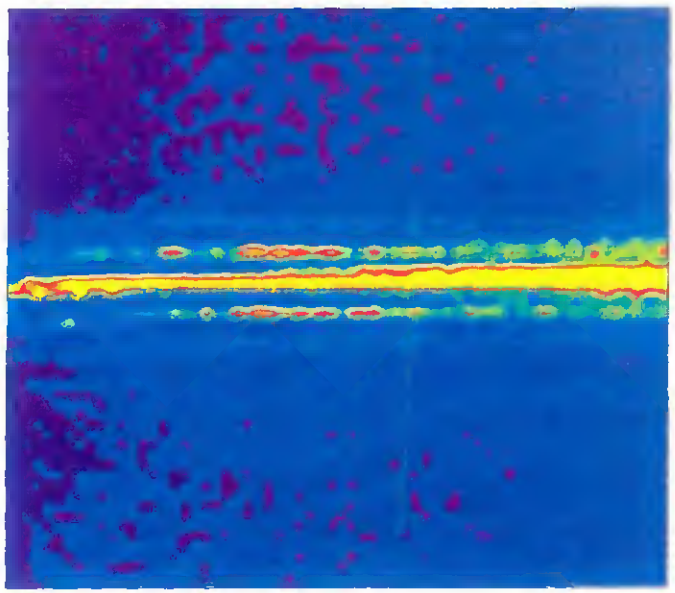

(i)

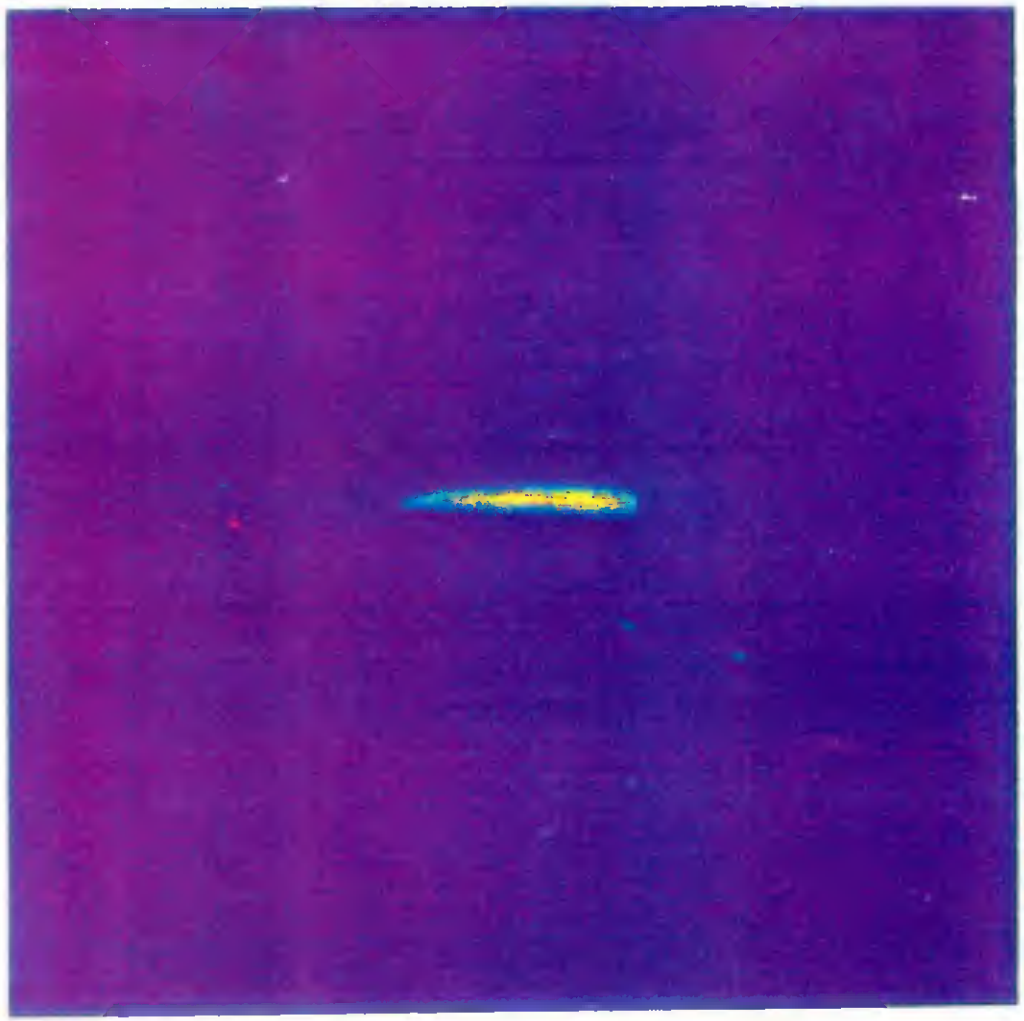

(ii)

Figure 5.9a: (i) Original image of the diffraction pattern shown prior to compression as part of a 256x256 data matrix; (ii) compressed diffraction pattern as part of a 512x512 data matrix.

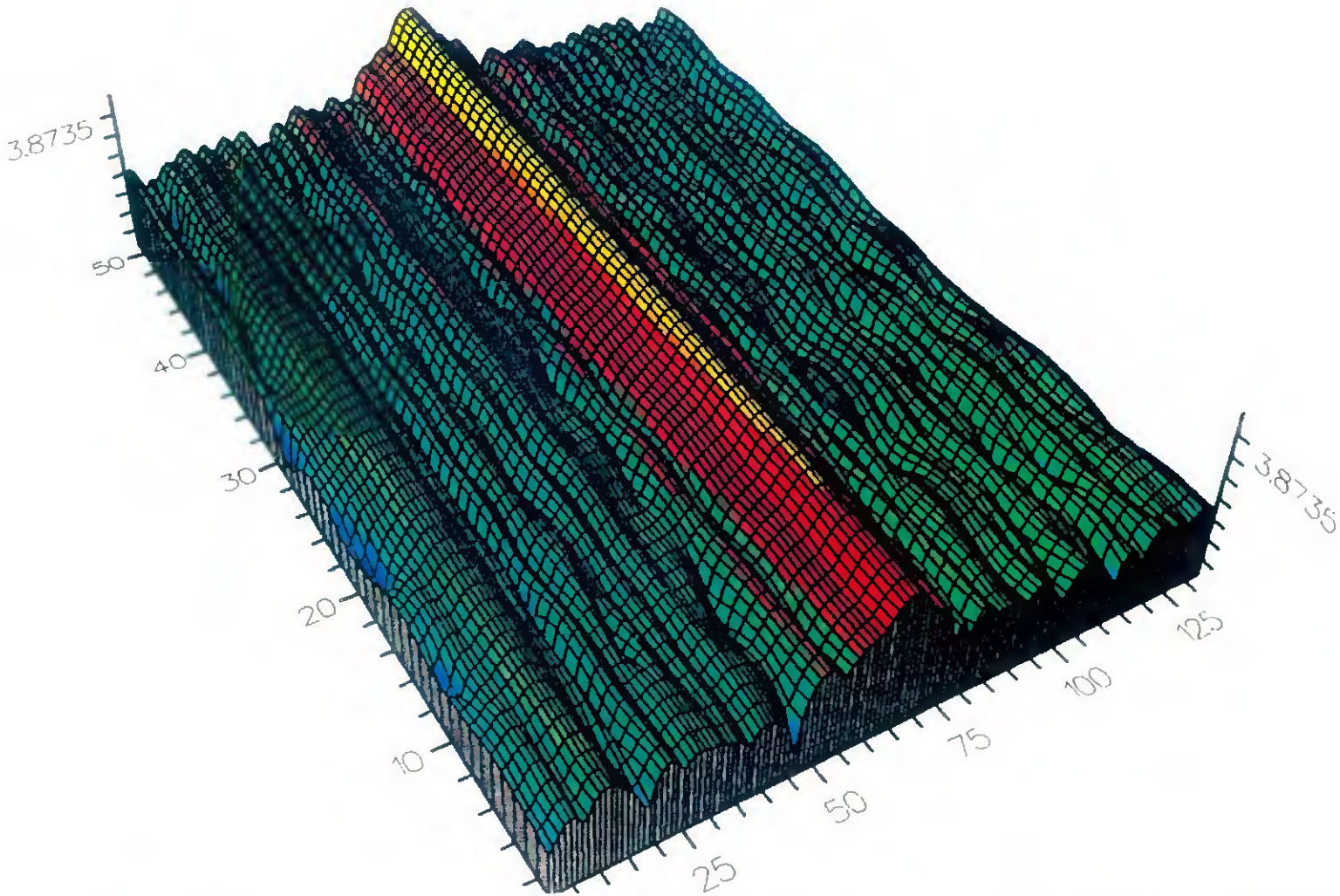

Figure 5.9b: Zero-phase restored characteristics of the machined surface from the compressed optical spectrum of figure 5.9a; this region displays cyclic regularities in the vicinity of the peak of the laser beam.

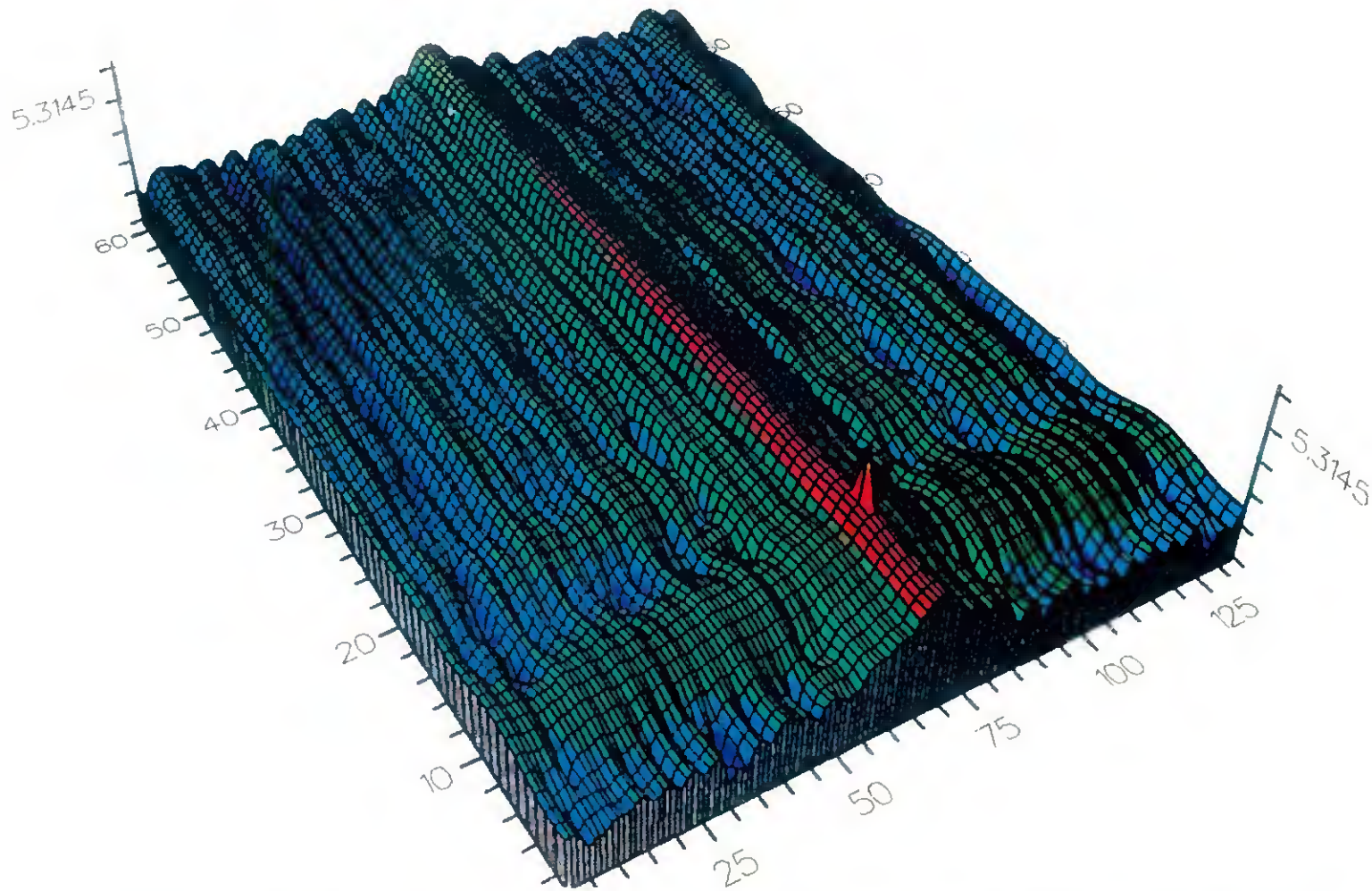

Figure 5.9c: Displaying the magnified region of the surface which also includes the peak of the laser beam; as seen, the presence of the cyclic undulations i.e the tool-chatter components is more pronounced.

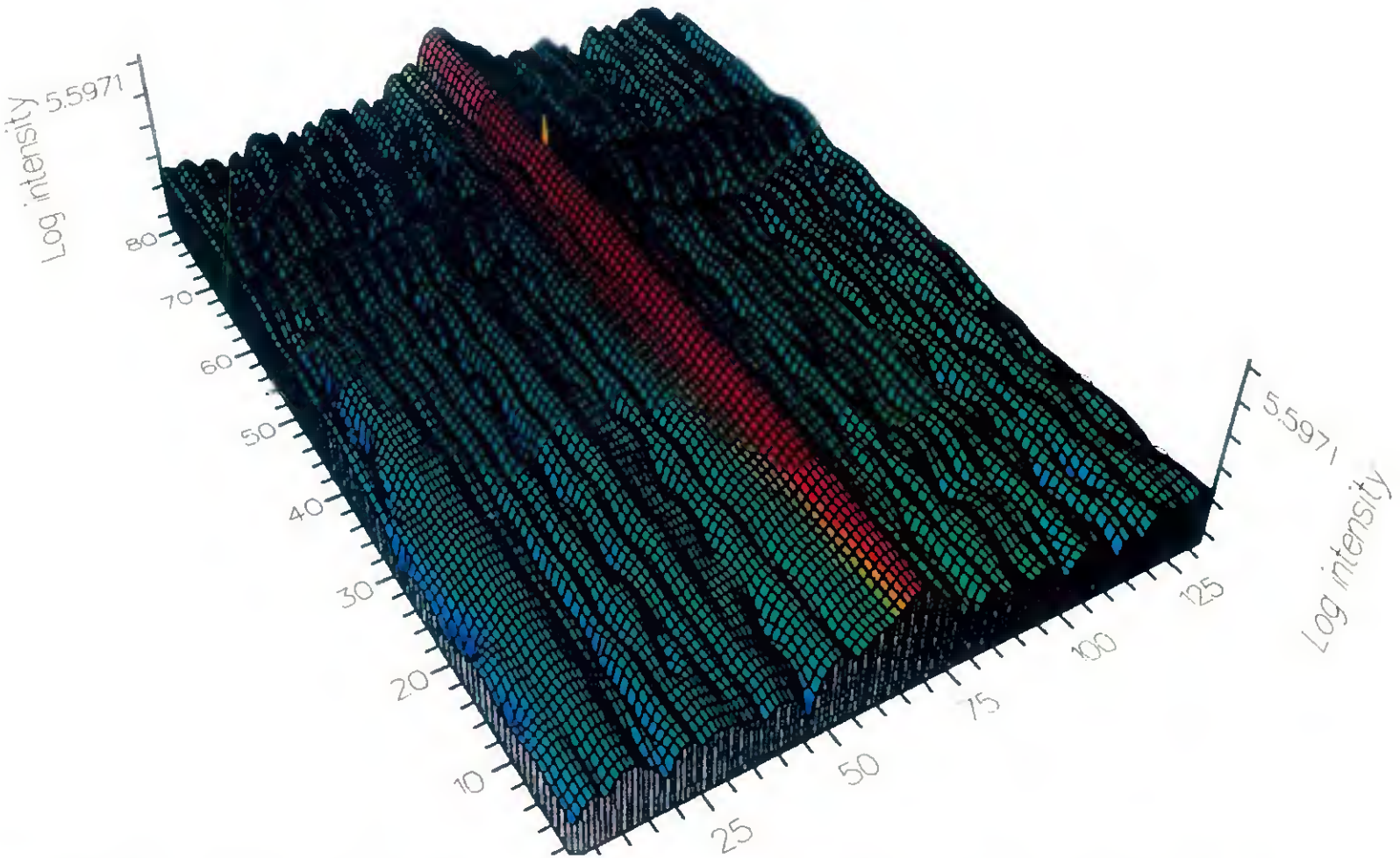

Figure 5.9d: Displaying the magnified region of the surface, further down the peak of the laser beam; the rippling effect in this restored characteristics which is due to the tool-chatter components, can also be seen in the actual photo-micrograph of the surface in figure 5.10.

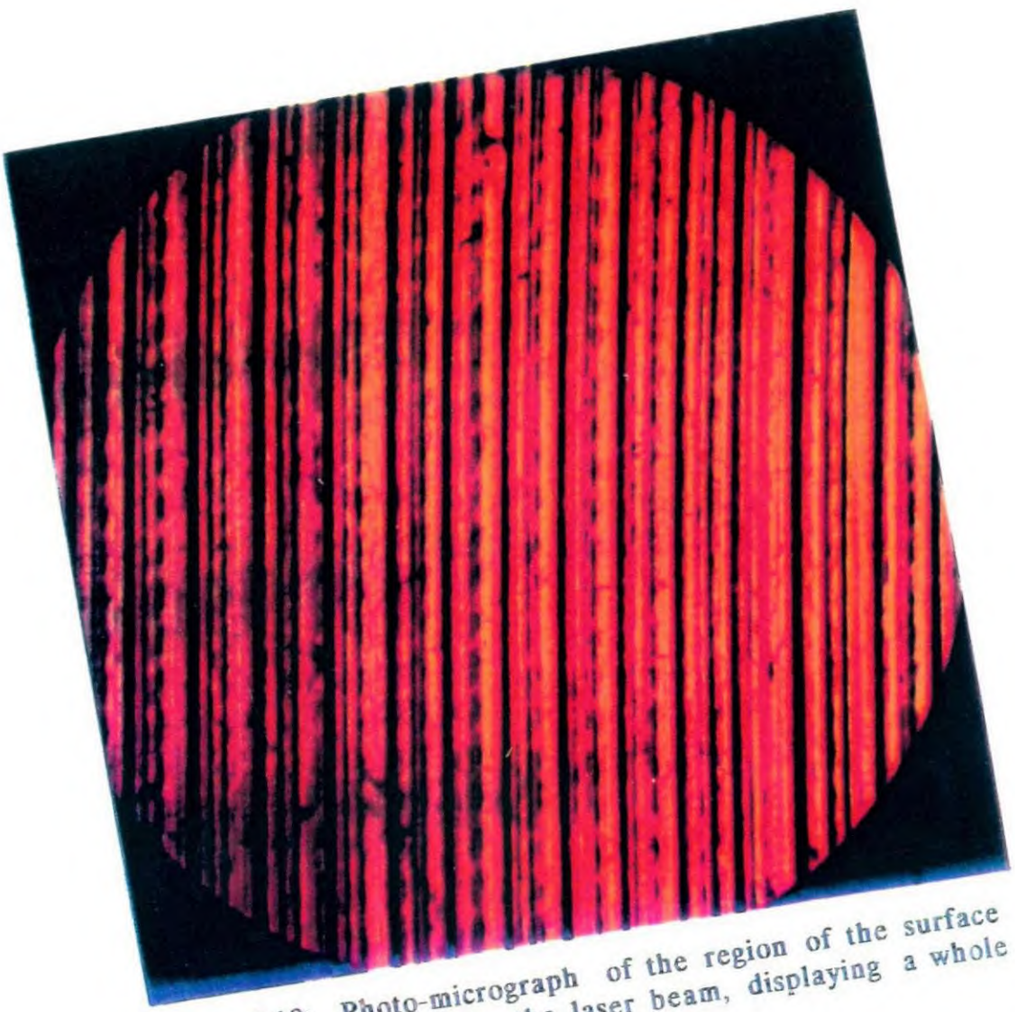

Figure 5.10: Photo-micrograph of the region of the surface which was illuminted by the laser beam, displaying a whole collection of cyclic undulations.

The only other evidence as to the existence of such cyclic behaviour, can be seen in the magnified image of the machined surface shown in figure 5.10. This image displays a large population of cyclic components which very much resembles the cyclic characteristics restored in figures 5.9b-5.9c.

5.5.4 The Effect of Ignoring Fourier Coefficients On The Reconstructions

The extent to which the Fourier coefficients can be ignored depends on the distribution of the information in the spatial frequency domain for the machined surface and noting that the signature of interest is still part of the data in the compressed spectrum. As it has already been addressed in section 5.4.4, the information regarding the finer details i.e tool-chatter and the harmonics lie at right angles to the spectral lines of the grooves, and form the set of horizontal lines on either side of the central region. The compact packing of frequency information along horizontal axis allows more freedom for the frequency components to be ignored along this direction as compared to the distinct set of lines vertically. Hence, by ignoring coefficients on the vertical scale, the information related to the finer details might be lost as compared to the extent of coefficients ignored on the horizontal axis.

More importantly, care should be exercised in maintaining the minimum sampling rate i.e the Nyquist rate whilst compressing the spectrum through ignoring frequency coefficients. Calculations carried out in chapter 3, indicate that the captured spectrum of 256x256 pixels at the camera distance can only afford to be compressed by 50% to a 128x128 spectrum whilst satisfying the Nyquist criterion with the digitiser used. As already mentioned in chapter 3, it is the frequency information associated with the large structural variations which would be at the risk of being undersampled. This technique will certainly have its limitations beyond which further improvements cannot be obtained.

5.6 Reflecting on what has been achieved in the zero-phase study

The machined surface has not been an easy specimen to characterise. Not only does it possess a random distribution of spatial components it also carries many scratches and flaws which impedes the overall frequency spectrum with their corresponding signature. Imperfections in general, being random in nature, also contribute in a random manner to the overall frequency spectrum and it is highly unlikely to restore any information regarding the existence of such features in the absence of phase. The same applies to any other roughness variations which are randomly distributed.

However, what has undoubtedly been preserved in the absence of phase, is the regular characteristics of the surface. As seen, provided that the signature of the regular components is captured at a sufficient sampling rate in the frequency domain, the object's regularity can be restored in the object domain, solely on the strength of such components. One should emphasize on the fact that restoring object's regularity through zero-phase characterisation, does not necessarily mean restoring exact geometrical structure.

Being an intensity-only synthesis, it can never be said that the restored zero-phase characteristics are a true representation of surface behaviour. However, having seen the evidence that the surface undulations resemble cosinusoidal/sinusoidal variations, and that cyclic behaviour as such is not affected by the lack of phase, it is reasonable to say that the restored characteristics are a "tolerable reconstruction" of the geometrical pattern of the surface.

This study is now extended further by introducing phase alongside modulus data to fully reconstruct the object surface as opposed to characterising it. To eliminate any

speculations as to how the exact shape of the surface is, a simpler structure was chosen whose exact geometry was known and the effectiveness of the method could be tested when the reconstructions were compared against actual surface. This is the subject of investigation in the next chapter.

CHAPTER 6

RECONSTRUCTION OF SURFACES USING PHASE INFORMATION

6.1 Introduction

This chapter extends the work beyond zero-phase characterisation of surfaces by introducing phase alongside the intensity values to arrive at a true reconstruction of the object reflectance profile rather than its characterisation. The types of surface chosen for this study were once again reflectance targets but with exact geometric shapes. The phase extraction technique is the non-iterative method of logarithmic Hilbert transform which is applied to the two- dimensional Fourier spectra of the reflectance targets under study.

Whilst application of Hilbert transformation is linked with well-behaved object functions, this research takes a different perspective by applying logarithmic Hilbert transform to object surfaces which deviate from such definition. In this respect both the study conducted on the object types as well as the methodology proposed for modifying the frequency characteristics of such objects are novel and original.

The ingenuity of the work rests with the **scaling principle** which has been exercised in a completely different manner to that of chapter 5. This principle has been fully exploited to modify the spectra of object surfaces, to bring out the continuity and the well-behavioral which is favoured by the Hilbert integral; and yet maintain the full intelligence of the object, only at the expense of perceiving it on a smaller scale.

CHAPTER 6

Remodification of the frequency envelope to display continuity and less oscillatory behaviour, is the most valuable and powerful asset that can be possessed by the Fourier spectrum of any real object to make phase extraction practically viable. The series sum of a whole group of frequency components which display continuity as well as a gradual reduction in the amplitude of frequency components converges more rapidly to the object function than the series which show a discontinuous trend and the spectral components do not "diminish" or "die out" in a uniform fashion. This rapid convergence, also brings on the advantage of requiring a fewer number of terms to describe the original object with a reasonable degree of accuracy (H.Baher, 1990).

If **"enhanced continuity"** and **smoothing out** the spectral behaviour, is a means of improving the convergence, then this factor is valuable so far as any signal restoration or object retrieval problem is concerned. The unknown object can be more confidently relied upon if it is restored from the information extracted from a continuous trend of frequency samples, than one which endures many discontinuities, seen as isolated regions as part of its spectral characteristics.
The breaking up of the spectral characteristics into many isolated lobes, is an indication of non-uniform convergence of the spectral terms (A.V.Oppenheim, 1979) and the need for the inclusion of more frequency components for synthesising the object; a fact which is not welcomed in many practical circumstances.

The arrangement of spectral components, also ties in with how effectively phase can be realised from the modulus characteristics. Since the unknown phase has to be inferred from the modulus characteristics, one has to ensure that the modulus spectrum is in its most amenable form to reveal the information which is to be retrieved from it.

This most amenable form of spectral behaviour has already been identified with, for example one which entails enhanced continuity and smooth out characteristics. It thus follows that the phase information can be more faithfully redeemed from modulus data when spectral components have been rearranged to reveal enhanced continuity.

However, whilst there are many object functions which can be fabricated to yield the desired continuity as part of their spectral behaviour, object surfaces in general do not display such characteristics. Certain behaviour associated with their spectral characteristics poses major problems so far as restoration algorithms are concerned even before one can go about extracting the unknown phase, let alone improving upon the outcome. In particular, unless the frequency characteristics of "real type" object surfaces are modified, algorithms based on Hilbert transformation cannot be utilised to retrieve such structures. The aim of the next section is to highlight how the spatial behaviour of a "real object" can influence the intelligence which is captured in a typically recorded spectrum of it. Ill behaved spectral information would be detrimental in any object retrieval exercise irrespective of the nature of the algorithm used.

6.1.1 Spectral behaviour of real type object surfaces

In utilising the phrase "real" one is referring to the structure and definition associated with the nature of the object. Whether the surface is the outcome of a typical manufacturing process, such as the previously studied machined surface or a well established technology such as integrated circuitry, it retains well-defined features, regions or distinguished patterns which can be in repeated form.

Any sharp and abrupt features in the geometrical structure of the object not only symbolise the presence of high spatial frequency components but they also signify the spread of the frequency information in the form of isolated lobes. "Real type" object surfaces contain many such features which map as regions of discontinuity in their Fourier spectra.

When complexity of structure and repetition of the pattern are entwined, such as in integrated circuitry, frequency characteristics are even more strained in the sense that more isolated regions and minima are packed into the spectral behaviour. Repetition also provokes oscillatory behaviour amongst spectral components consequently causing the spectrum to appear populated with numerous maxima and minima. The question is how can such behaviour impair our perception of the unknown object? The intelligence captured in a typical recorded version of such characteristics could be affected due to any or a combination of the following:

i) limitations of the detecting device;

ii) masking of the spectral data due to the impulsive characteristics of the spectrum;

iii) an upsurge of minima and discontinuities;

keeping pace with the rapid fluctuations of the frequency envelope, demands a detecting scheme with finer sampling intervals and more quantisation levels for the digitisation of data. With fixed sampling intervals and limited quantisation levels, this is a luxury which often cannot be met under practical circumstances. From a restoration point of view, due to the lack of continuity, the convergence of spectral components to the object function requires inclusion of spectral data well into the higher frequency regions of the spectrum.

But is the information in the higher frequency region always accessible? for highly reflective surfaces, the diffracted intensity information in this region is usually masked by the high intensity of the strongly reflected component in the centre of the pattern (M.James, 1987). Figure 6.1 -6.2 is one such example where the computer generated diffraction pattern of an object array has been shown alongside an actually recorded diffraction pattern in the optical laboratory. As seen, a great deal of information is missing in the outer regions of the spectrum, and even with the help of a spatial filter to attenuate the central region, the recorded spectrum is mainly that of low frequency data.

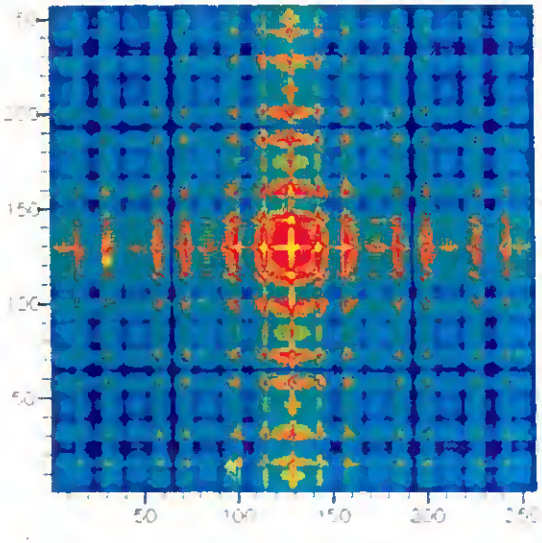

Figure 6.1: Computer generated diffraction pattern of a repetitive object.

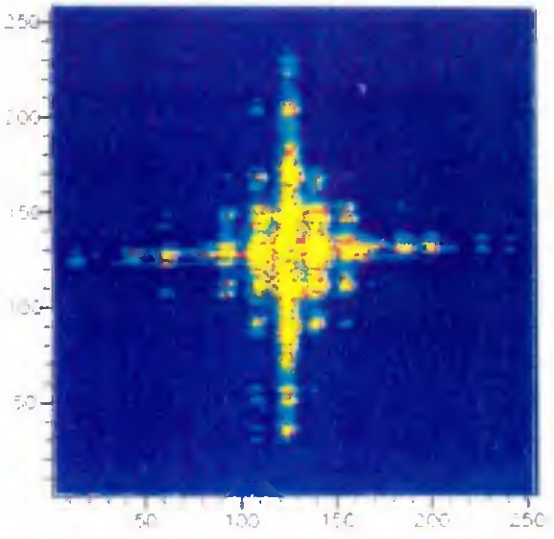

Figure 6.2:Optically recorded diffraction pattern of the same object; the palpable blobs show how the intense regions of the spectrum have overshadowed the more subtle details elsewhere.

It is not only a question of intercepting the information, it is also a question of how reliable the recorded characteristics are. Minima and discontinuities are potential sources of "ambiguity". Repetitive profiles display a handful of such regions in their frequency characteristics.

If what is deemed to be ambiguous is to contribute towards the identity of the unknown object, it is unlikely that the retrieved object will resemble the original.

Isolated zeros, when few, may not pose as a serious problem. It is when chunks of the spectrum are inhabited by a whole colony of minima and zeros that the problems start to surface. This is characteristic of multi-dimensional repetitive signals whereby lines of discontinuity or "cuts" form a prominent part of their spectral behaviour. Figure 6.4 shows the position of such cuts in the Fourier modulus spectrum of the repetitive object in figure 6.3. With few spectral components surviving in the lower frequency region and parts of the spectrum buried in almost total darkness (cuts and minima), the chances of retrieving the unknown object are quite slim.

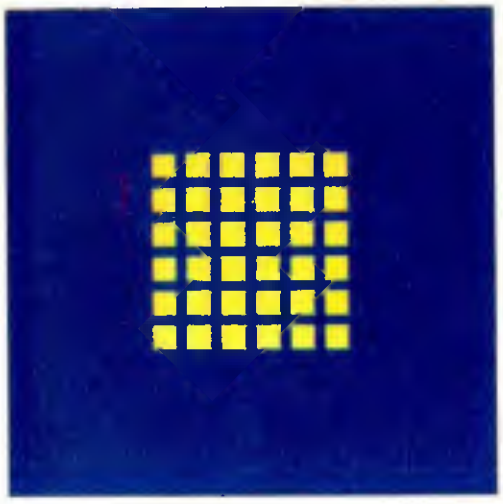

Figure 6.3: Digitised image of a repetitive object whose frequency spectrum has been shown in figure 6.1.

Figure 6.4: Position of the cuts in the Fourier spectrum of the object of figure 6.1. Note that all other frequency components have been suppressed to allow the cuts to stand out.

The question that remains to be asked is whether it is possible to remove the cuts, reduce the minima, enhance continuity and still expect the modified characteristics to be representing the same object signal? The answer is "yes" but at a price.

CHAPTER 6

Changing the whole outlook of the spectral characteristics, in the above sense, is only perpetuated by a scale related operation. Thus, the price that is paid in due course, is to do with a change in the overall scale of the retrieved object. This fact will become evident at a later stage when the scaling philosophy is described in more detail and its usefulness explained in connection with the aforementioned changes. However, before committing oneself to the particulars of the scaling principle, one needs to look into the existing techniques of object retrieval to identify some of the difficulties surrounding these methods as well as to appreciate the contribution that the scaling philosophy can make towards alleviating some of these difficulties.

CHAPTER 6

6.2 The Current State of the Art of Extracting Phase Information

There are basically two methods to arrive at an estimate of the object phase starting from the Fourier modulus information. There are iterative techniques (J.R.Fienup and A.M.Kowalczyk, 1990), (T.R.Crimmins, *et al.*, 1990), (W.Kim and M.H.Hayes, 1990), (G.Yang *et al.*, 1994),(A.H.Ahn and Yagle, 1994), initiated by (Gerchberg and Saxton, 1972) whereby some knowledge of the object and its support are required in advance. An acceptable solution , or set of solutions, is eventually arrived at by iterating back and forth between the object domain and Fourier domain and imposing the known constraints in each transition. The problem with iterative techniques, is the large number of computations performed without any guarantee of success, if the initial phases are chosen on a totally random basis. Any prior phase knowledge would be extremely valuable to aid the convergence of these iterations and successful reconstructions are usually commenced with the so called seeded iterations, embedding the prior phase knowledge.

The most surprising issue is that in a span of more than two decades since the first practical algorithm was initiated by Gerchberg and Saxton in 1972, there seems to be no improvement at the rate for which the algorithms converge , in terms of a reduction in the total number of iterations before a solution is reached. Iterations well into hundreds (H.Ahn & A.E. Yagle, 1994) and over or in the region of one thousand (J.R.Feinup, 1990) are still common practice so far as iterative approaches are concerned. Supplementary knowledge, such as a low resolution image alongside the known Fourier data (J.R.Feinup, 1990) and non-negativity constraint on the object behaviour, all in aid of convergence(H.Ahn, A.E. Yagle, 1994), still necessitate 900-1000 iterative loops before an acceptable solution can be reached.

Even then the quality of reconstructions, or the so called converged solution, is not very impressive. One would expect that after the 900th iteration, if a solution is reached it should at least bear a good resemblence to the original signal. In this context, some simulation results have been shown from a paper by (Ahn & Yagle, 1994) where even with their more improved algorithm the output does not look anything like the input at the 900th iteration. A major pitfall for iterative techniques is the stagnation problem. This is a condition whereby an estimate of the signal changes little from one iteration to another and the iterations seem to be stuck at an estimate of the object which shows no resemblence to it at all. Although the authors, Ahn & Yagle, have improved upon this condition, i.e to restore the iterations from stagnation and thus aid the algorithm to converge, never the less it does not seem to converge to the right solution.

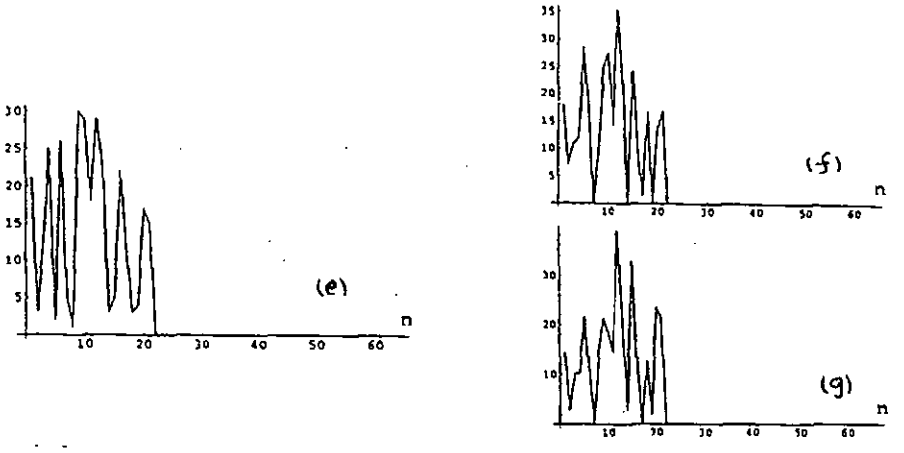

Figure 6.5e-6.5g: Results from Ahn & Yagle for the restoration of an unknown signal iteratively.(e)-original unknown signal; (f)-estimated signal at the 100th iteration with the algorithm going into stagnation; (g)-converged estimate of the signal at the 900th iteration using Ahn & Yagle algorithm.

Figure 6.5e shows the original unknown signal which is to be restored iteratively from only a knowledge of the Fourier modulus and a random estimate of the signal to start the iterations. Figure 6.5f shows the reconstructed signal at the 100th iteration, were the conventional iterative algorithm used went into stagnation and continued to do so well into the 500th iteration. This estimated signal is at best

what can be offered by a standard itertive algorithm (J.R.Feinup, 1982), because the algorithm has gone into stagnation and it is not capable of finding better estimates. To aid the stagnation problem, the reconstructed signal of 6.5f was fed into the iterative algorithm proposed by Ahn & Yagle, to be used as a starting estimate. However at the 900th iteration, it converged to the signal shown in figure 6.5g, which still bears no resemblence to the original signal of figure 6.5e.

Another iterative based approach by (W.Kim & H.Hayes, 1993) using Gerchberg and Saxton algorithm, succeeds to restore the signal after the 100th iteration, but as quoted by the authors, only the most important features of the signal have been restored. Apart from a lateral shift, a closed comparison of the two signals shows marked differences between the two. These results which have also been extracted from their paper are shown below in figures 6.5h and 6.5i. In fact looking at the two signals there are considerable differences between the amplitude of the individual peaks in each graph. Had an error metric such as the total squared error between the reconstructed signal and the original signal been utilised to assess the closeness between the two numerically, its value would have been quite large due to the notable differences between the displayed amplitudes in each graph.

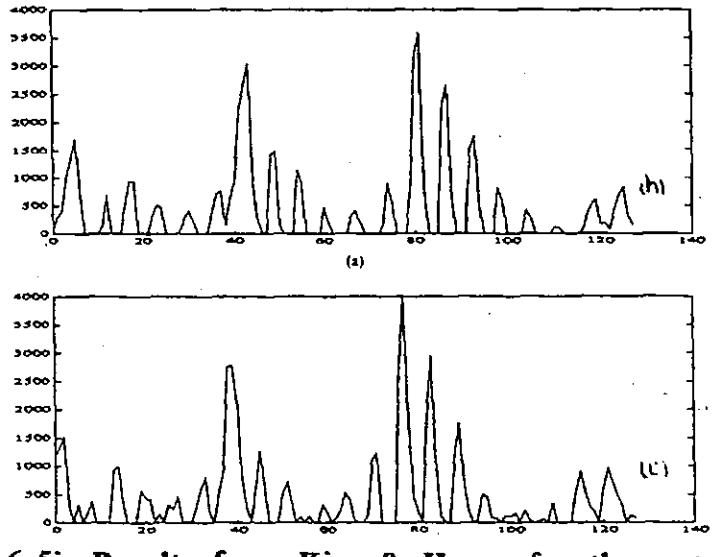

Figure 6.5h-6.5i: Results from Kim & Hayes for the restoration of an unknown signal iteratively.(h)-original unknown sequence; (i) reconstructed sequence.

Iteration is, and has been quoted, as a brute force. It should only be applied to solving problems when all other intelligent methods fail to reach a valid solution. Sometimes with certain modifications, existing methods become amenable to phase extraction with remarkable success.

The logarithmic Hilbert transform is one such method. It is a non-iterative technique which can be applied to object functions classed as entire functions. Two basic requirements place the object function in that class. Firstly the object is to be of finite extent, and secondly a transform relationship should exist for the object function (Nakajima & Asakura, 1986). Experimentally these two requirements are satisfied; as the source of illumination covers a finite area of the object, and the object itself can be mounted on a background surface to clearly limit the extent of the object when the whole scene is illuminated. Furthermore as long as the dimensional range of the features is comparable to the wavelength of the illumination, the diffracted stream of information is the Fourier transform of the object reflectance profile.

The term "entire functions" however, calls for well-behaved object functions in that both the object itself and consequently its Fourier transform are well-behaved and continuous. This is why real object geometries whose frequency characteristics runs into many discontinuities are the type of structures which are far from appropriate as regards the Hilbert integral. Since the phase data are extracted from the logarithm of the modulus of the Fourier components via an integral relationship where:

$$Ln\ modulus = \log_e |H(u)| \tag{6.0}$$

any isolated discontinuities would render the Ln (modulus) infinite. Any connected discontinuities or cuts in the Fourier plane would pose as an impossible path for the integration to take place.

If the structure of the object allows, it may be possible to exclude discontinuities from the path of integration, and rely on the central region of the spectrum to restore the object. However, this may not be feasible as the object may suffer from lack of definition due to the exclusion of the higher frequency components; or it may not maintain continuity over a good number of samples for this approach to be worth while. This is most certainly the case for repetitive profiles, whose impulsive characteristics hardly allows the spectrum to retain a continuous composure for a reasonable number of sample points.

Certainly there are other ways round removing discontinuities from the path of integration apart from selective windowing. However, the outcome is not so favourable as these techniques mainly result in the level of the discontinuities to be raised to that of minima. Thus, the spectrum would appear no different other than being inhabited by a large population of minima.

Whereas removal of discontinuities rectifies the problem in the sense that it allows the logarithmic integration to take place, never the less participation of a whole group of such minima in the extraction of the unknown information will undoubtedly strain the accuracy of the retrieved data. In addition, nothing has been done to improve upon the composure of the spectral components in terms of enhancing the continuity. The yet impulsive appearance of the spectrum, would lead to poor convergence of the terms to the original object as compared with the type of characteristics which maintains continuity for a good range of coefficients. In this context, research conducted by (R. Bates and D. Mnyama, 1987) using iterative techniques, has also reported the most successful reconstruction of the object to have stemmed from the most continuous supply of frequency samples.

Consequently, unless the removal of discontinuities is accompanied by some other method which not only lessens the overall minima in number but also improves upon the continuity amongst spectral components, the extracted phase information would be highly inaccurate. Before proposing how such changes can be brought on, it is important to identify ways round clearing the path of integration from existing discontinuities for the Logarithmic integration to take place. Figure 6.5 shows two techniques proposed by the author which have been used to raise the level of discontinuities in the frequency spectrum of a structured object. These two approaches which have been adopted throughout this study are:

i) the addition of an impulse function in the object domain,

ii) the addition of a constant background level in the frequency domain.

It should be emphasized that the restored shape of the object as seen in figures 6.5b and 6.5c has only been possible, when its spectral behaviour was modified to appear more continuous as well as enclosing less minima through the novel methodology proposed by the author. The concept of such methodology has been disclosed at a later stage in section 6.4. There is no significant difference between the two methods apart from the fact that the addition of an impulse can act as a "reference point" denoting a particular edge associated with the object. This is valuable for referencing purposes, where a distinct mark or a flaw on the surface of the object can be located with regards to the position of the impulse itself. In figure 6.5c, the amplitude of the impulse was deliberately chosen to be higher than the object signal, figure 6.5a, so that it could be clearly distinguished from rest of the object characteristics.

Adding reference positions as such is only possible when the object specimen itself is accessible, otherwise any inherent discontinuities in the frequency spectrum have be to removed via the addition of a constant background to the frequency characteristics. This method however, would not fix a particular edge of the object with respect to a reference signal.

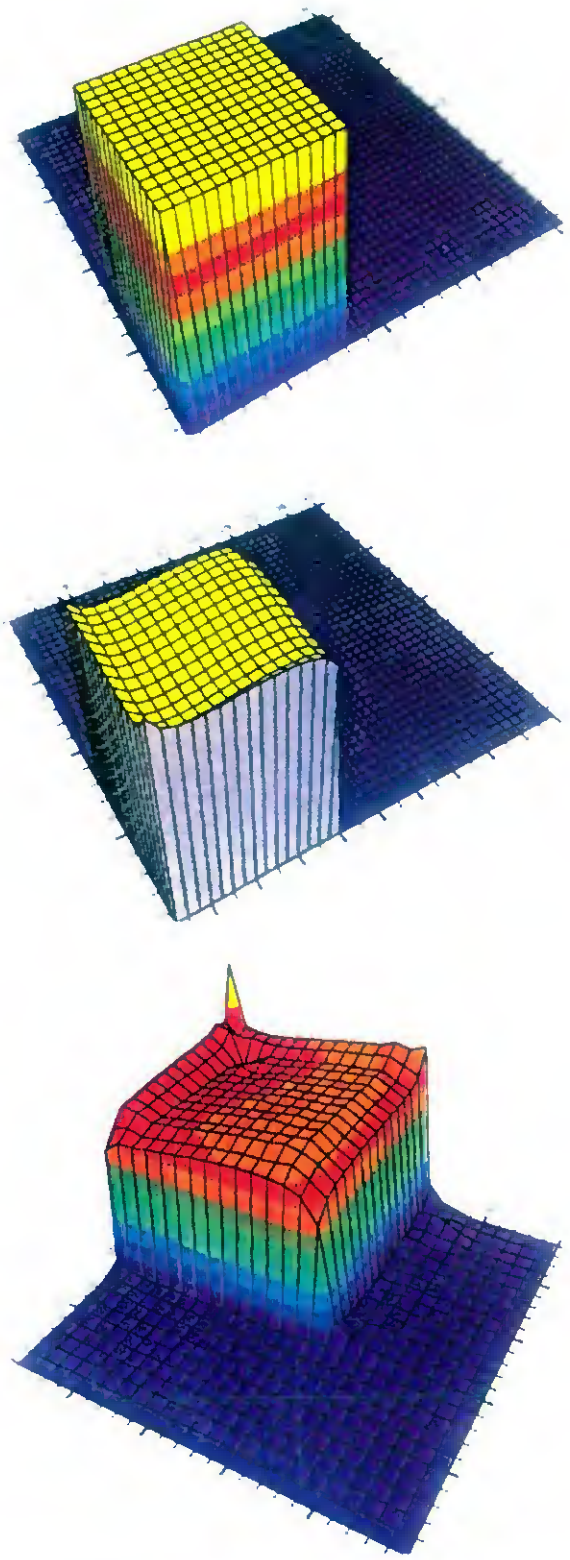

Figure 6.5:Illustrating the changes in the structure of the restored object through the addition of a continuum (b), the addition of an impulse (c).

To sum up, impulsive behaviour, rapid excursions of the spectral components and a high proportion of minima are all dangerous pitfalls as far as the extraction of phase information is concerned. As emphasized, this never the less is the manner with which repetition chooses to manifest itself in the frequency domain. At fixed sampling intervals and limited data size, the ever rapid excursions of the modulus spectrum do not prove to be a reliable medium for the extraction of the unknown phase.

Figures 6.6-6.8 show the price paid in terms of the complete loss of the object signal, when the original object endures more and more companions in repeated form. As a means of comparison, the original object, its Ln Hilbert restored version and its corresponding frequency spectrum have been shown in each set. Note how the single object in figure 6.6a has been restored faithfully in figure 6.6b from the Fourier modulus spectrum of figure 6.6c.

A figure of quality for judging the faithfulness of reconstructions is the total squared error $\sum E_{total}$ as defined in (6.33), which reveals the difference between the two signals numerically. This relationship which also appears on page 226, has been reinstated below, where h(x) is the original signal and $h_{hil}(x)$ is the retrieved Hilbert signal.

$$\sum E_{total} = \sum \{ h(x) - h_{hil}(x) \}^2 \qquad (6.33)$$

It is difficult to attach a numerical value to $\sum E_{total}$ which can be used to recognise the closeness between the retrieved object and the original and thus the quality of reconstructions. There are not set borderlines as such but there are approximate measures as to when a reconstruction is likely to show a good correlation with the original. In this context, previous work by Hayes *et al.*,(M.H.Hayes, *et al.*, 1983) in which a particular unknown sequence has been restored through iterative means has shown good correlation between the two signals when $\sum E_{total}$ is in the region of $\sum E_{total} \approx \underline{6.792 \times 10^{-2} \text{ to } 9.109 \times 10^{-2}}$.

At the expense of excessive computation brought on by longer length FFTs as well as a large number of iterations namely a thousand, an excellent match between the two signals surfaced when $\sum E_{total}$ bottomed to $\underline{4.118 \times 10^{-5}}$.

Although a smaller total squared error guarantees better numerical accuracy, and thus a better match, it is not always necessary to engage in time consuming computations in an attempt to make $\sum E_{total}$ extremely small or drive it to zero. In fact as a matter of economy in iterative reconstructions, the practice is to stop iterations before $\sum E_{total}$ reaches zero (J.R.Fienup, 1987). What is deemed to be an acceptable match can occur well before $\sum E_{total}$ is made extremely small.

In this respect to assess the quality of reconstructions, a visual examination of the signal is as important as a numerical evaluation. This happens to be the case for the retrieved object of figure 6.6b which shows no noticeable degradation as compared with the original object of figure 6.6a. With reference to table 6.1, this excellent visual fidelity between the two signals has resulted when the total squared error has a value of $\sum E_{total} \approx 7.089 \times 10^{-4}$, which is within the margins of a satisfactory reconstruction without being unnecessarily small. A pixel by pixel comparison of the two sets of data corresponding to figures 6.6a and 6.6b which has been listed in Appendix A also confirms the excellent correlation between the object and its retrieved version at this value of total squared error.

type of object	non-repetitive object	object with repetition	object with increased repetition
$\sum E_{total}$ total squared error between the original signal and the restored signal	7.089×10^{-4}	1.732	8.137

Table 6.1: Illustration of the total squared error for the retrieved versions of an object which shows : (i) no repetition, figure 6.6a ; (ii) repetition, figure 6.7a; and (iii) increased repetition, figure 6.8a.

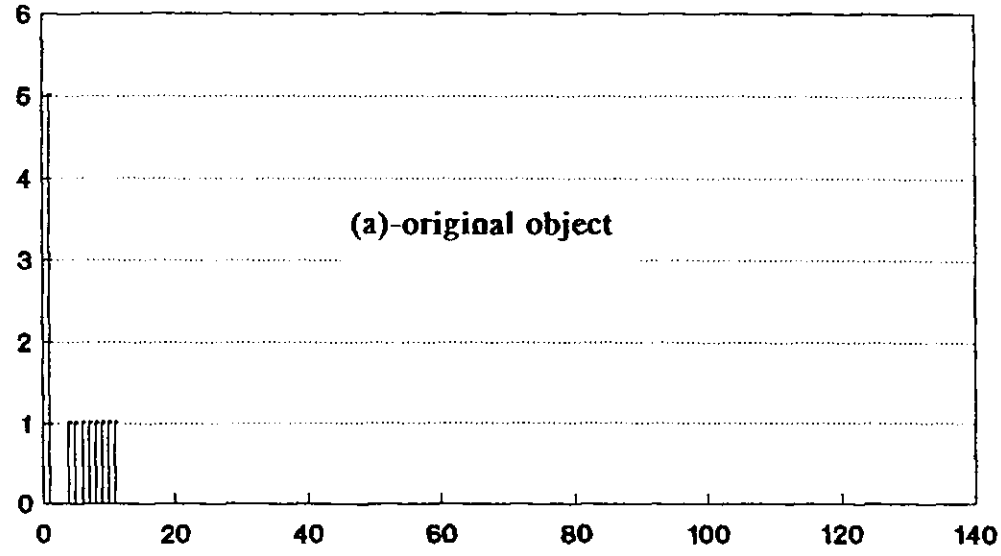

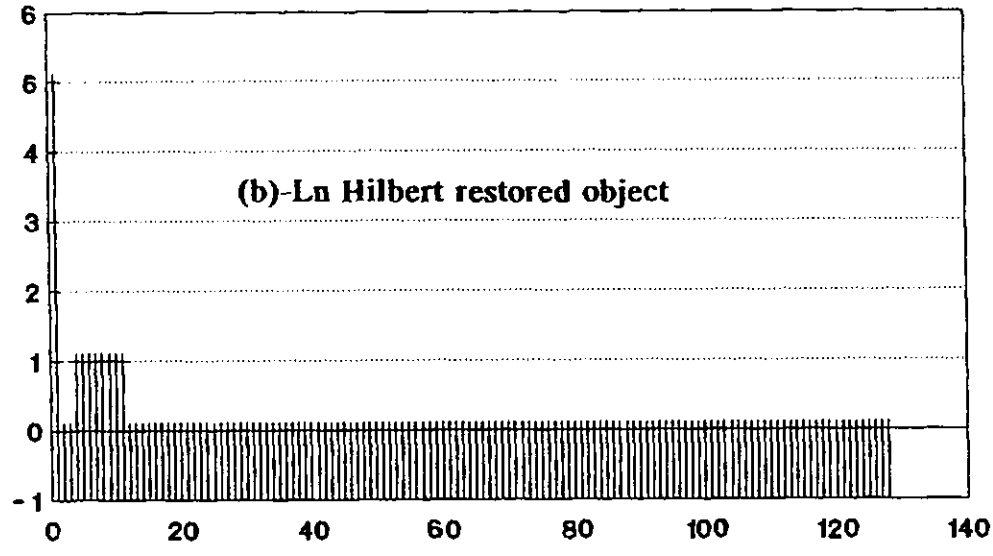

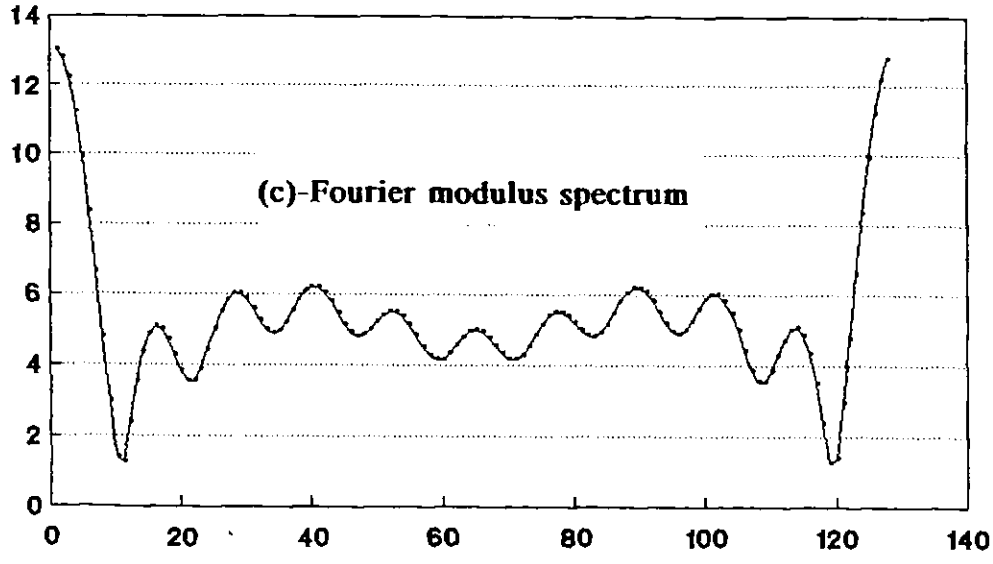

Figure 6.6: The distribution of the frequency components and its effect on the restoration of the object signal for a single object. (a)-The original object, (b)-The log Hilbert restored object, (c)- the Fourier modulus spectrum utilised for extracting the unknown phase.

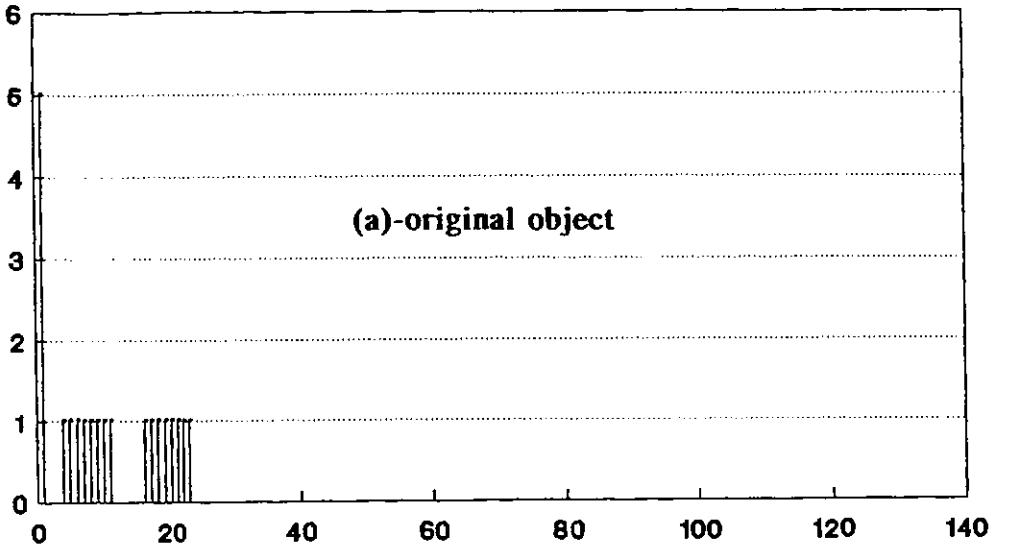

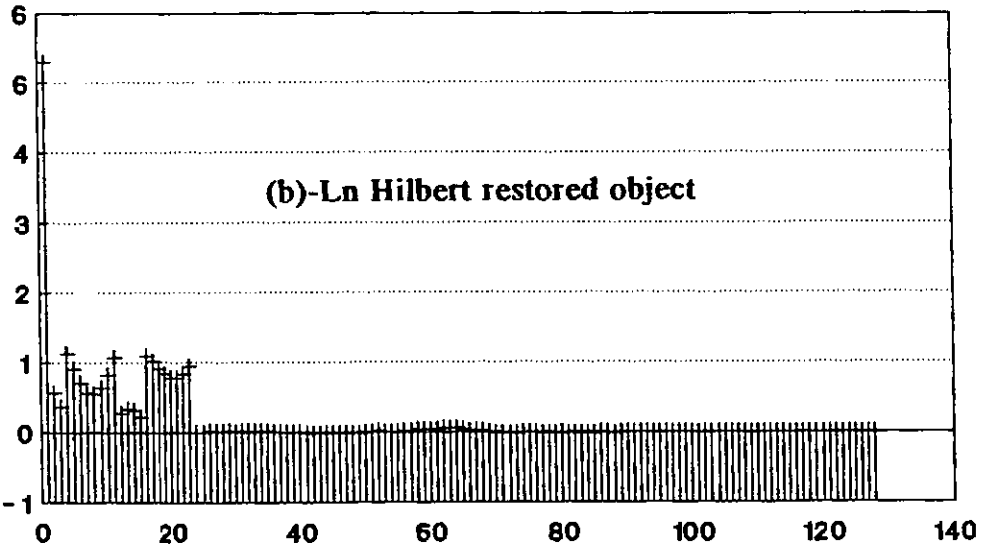

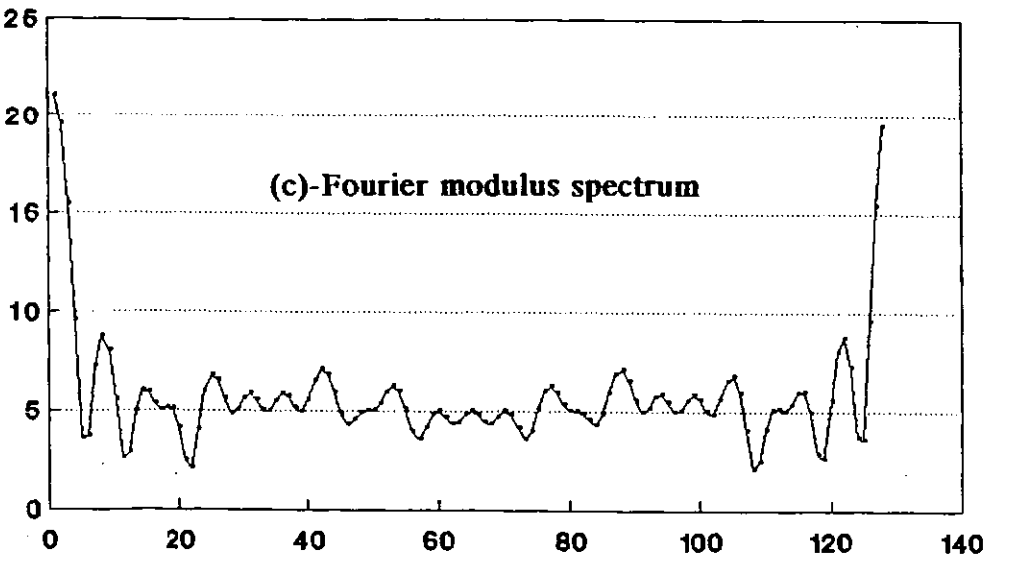

Figure 6.7: The distribution of the frequency components and its effect on the restoration of the object signal for an object with repetition.(a)-Object in repeated form, (b) The log Hilbert restored object, (c)- Fourier modulus spectrum utilised for extracting the unknown phase.

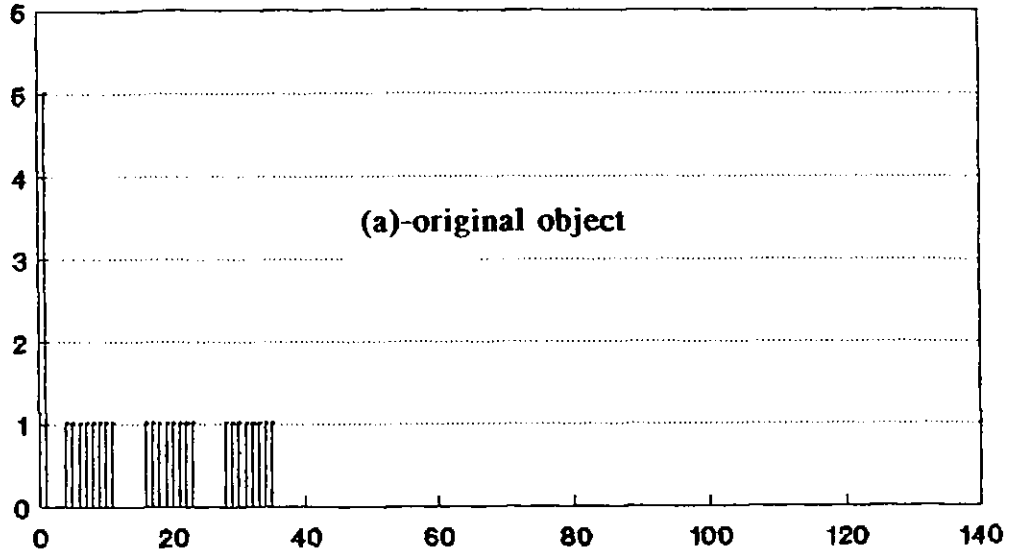

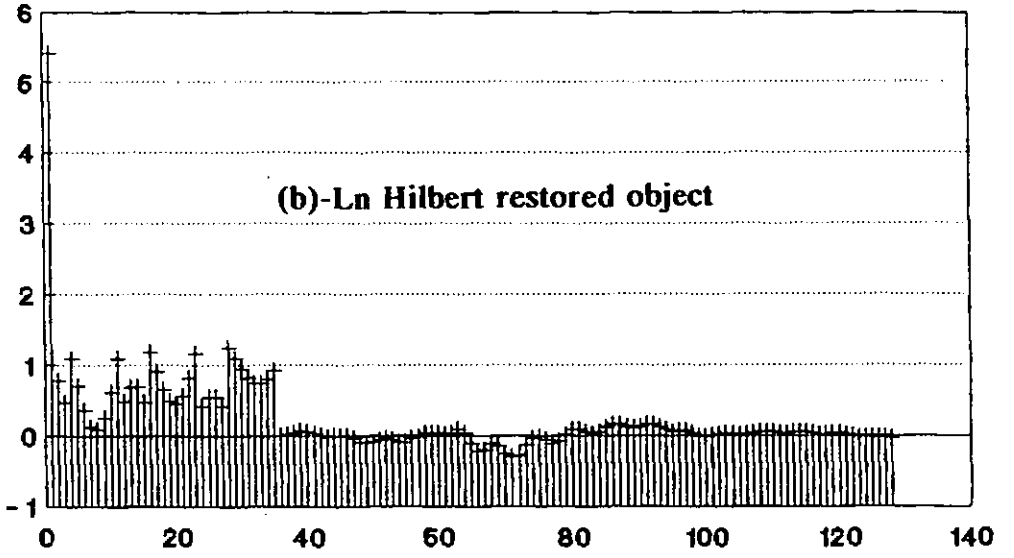

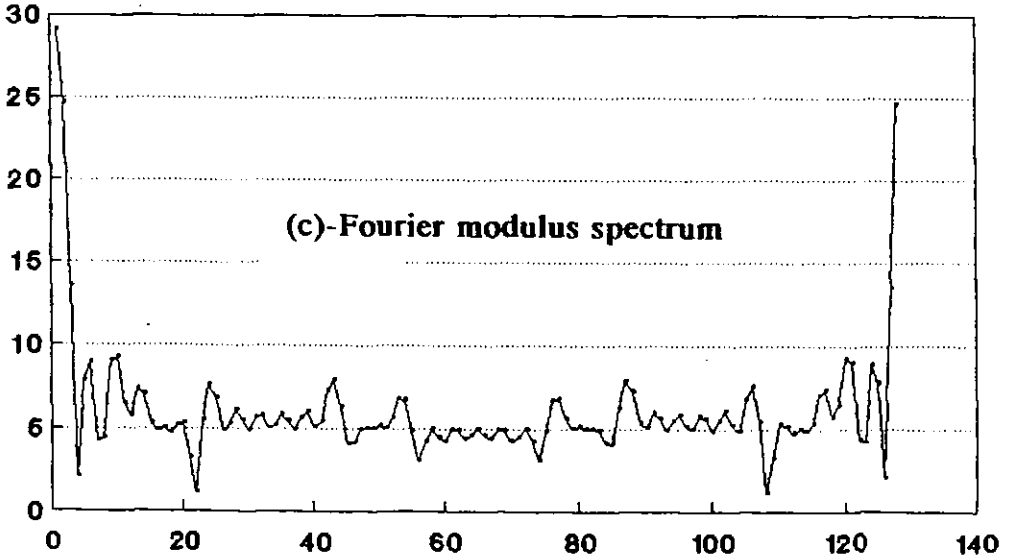

Figure 6.8: The distribution of the frequency components and its effect on the restoration of the object signal for an object with increased repetition. (a) Object with increased repetition, (b) The log Hilbert restored object, (c)-Fourier modulus spectrum utilised for extracting the unknown phase.

Looking at the trend for the total squared error in table 6.1, it is quite obvious that the retrieved reconstructions of the object, when it shows repetition, are bound to be distorted. The severity of such distortion can be seen in figures 6.7b and 6.8b, which are the reconstructed signals from the Fourier modulus spectra of figure 6.7c and 6.8c. Note how the better continuity in figure 6.6c, is violated in figures 6.7c and 6.8c at the onset of repetition; which in turn has affected the convergence of the reconstructions. A numerical listing of the two sets of signals in figures 6.7a and 6.7b; and 6.8a and 6.8b can also be seen in Appendix A.

It is possible to improve upon the appearance of the objects in figures 6.7c and 6.8c through interpolating spectral components and minimising rounding-off errors. Interpolation requires zero-padding in the object domain, an exercise which increases the burden on storage and processing. Besides, interpolation does not alter the arrangement of spectral components other than to provide extra frequency samples in between. Thus, the minima and discontinuities would not part with the spectral characteristics but they would still remain as part of the interpolated package. Besides, how severe should the interpolation be before the outcome is satisfactory?

Studies conducted by (Hayes *et al.*, 1983) reveal that an unknown sequence of length 8 pixels was zero-padded to a data size of 128 pixels before there was a reasonable match between the original and the retrieved version. Zero-padding, increases the amount of computation involved in a typical FFT evaluation. For instance an FFT operation on an NxN array (H.Baher, 1990), requires a total of $2N^2\log_2 N$ additions and $N^2\log_2 N/2$ multiplications, whereas an array zero-padded to 4 times this size i.e 4Nx4N, requires 24 times more additions and multiplications. This definitely takes its toll on the processing time (M.P.

Lamourex, 1993). From author's own experience a 1024x1024 forward and inverse Fourier transformation required in excess of 4 hours on the mainframe utilising Vax-11/ 750 machines, including the time for writing the data into a file.

6.2.1 A New Methodology

The methodology proposed by the author however, is unique in many respects. It does not require altering the overall size of the data, i.e an NxN array which includes the object and its surrounding information remains an NxN array. It recasts the whole spectral behaviour by having control over the "spread" of frequency components. Thus the spectral behaviour sustains an entirely different image in terms of the arrangement of spectral components. It cultivates continuity, reduces minima, removes and lessens discontinuities. Apart from making the spectrum amenable to Hilbert techniques, the profound continuity makes it a more reliable and solid source from which the identity of the object can be extracted. All the above changes are brought about by utilising the Fourier scale change property which relates the "spread" of the frequency behaviour to the "scale" of the object in the spatial domain. This work has also resulted in two more publications by the author during the period 1992-1994 (N.Sotoudeh, *et al.*, 1992), (N.Sotoudeh, *et al.*, 1994).

Since the key philosophy is based on altering the size of the object it is important to examine how a change in size for a repetitive object influences its frequency spectrum. The next section takes a detailed look at repetition through showing the relationship between the size of the features in a repetitive arrangement and its effect on spectral behaviour. It would then become more evident as to how a size related operation brought on by the "scaling principle" can work in the way of reducing many undesired aspects of a repetitive spectrum. Parts of the work presented in the following sections are extracts from the published work by the author.

6.3 Fourier modulus spectrum of repetitive objects

It has been stressed throughout this thesis that repetition provokes oscillatory behaviour and an unfavourable trend amongst the frequency components so far as retrieval of the unknown object is concerned. Figures 6.9-6.11 illustrate how the spectrum is influenced by repetition and what role the overall size of the object plays in remapping the frequency characteristics so that it exhibits the type of continuity that is favoured by the Hilbert integral. Figures 6.9a-6.9h is the dissimilated spectrum of two rectangular objects. The overall spectrum of the two rectangular objects, is obtained by the multiplication of the amplitude spectrum of a single rectangle in figure 6.9b, with the amplitude spectrum of the two delta functions in figure 6.9d. The amplitude spectrum of two delta functions is a cosinusoid whose frequency is reciprocally related to the separation of the delta functions.

If the distance between the repeats is large, it is thus apparent that amplitude spectrum of the single object would be modulated by a very high frequency cosine. This would result in the frequency characteristics to be oscillatory in nature with many subsidary maxima and minima. This trend can be seen in figures 6.10-6.11 where the seperation between the repeats has been increased from d, to a distance of 2d and 4d respectively. If the single object is large in itself, its amplitude spectrum would he compressed, resulting in a narrower overall spectral characteristics. Thus, the combination of large individual features as well as large separation in between the the features, would call for a highly impulsive and fluctuating spectrum.

All the evidence suggests that if the object characteristics were to be reduced in size, and compressed in the overall scale, then its spectral characteristics would be more well behaved, with much of the oscillatory behaviour phased out.

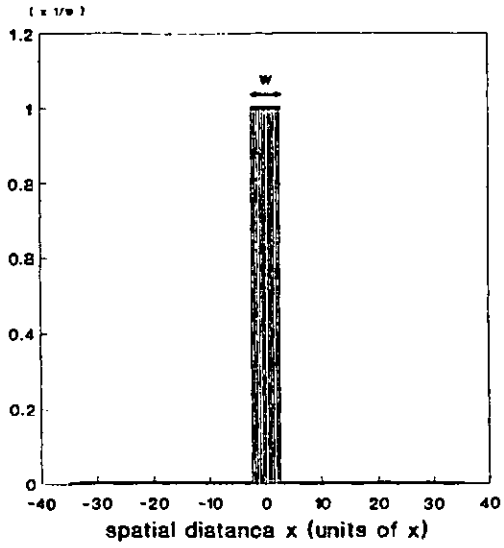

Figure 6.9a : A rectangular object.

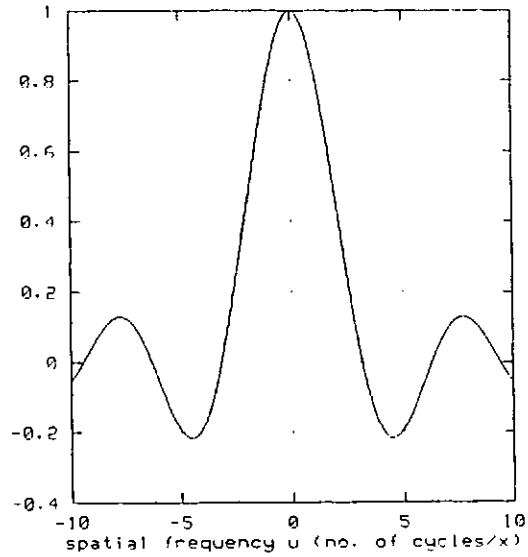

Figure 6.9b : Fourier amplitude spectrum of the single rectangular object.

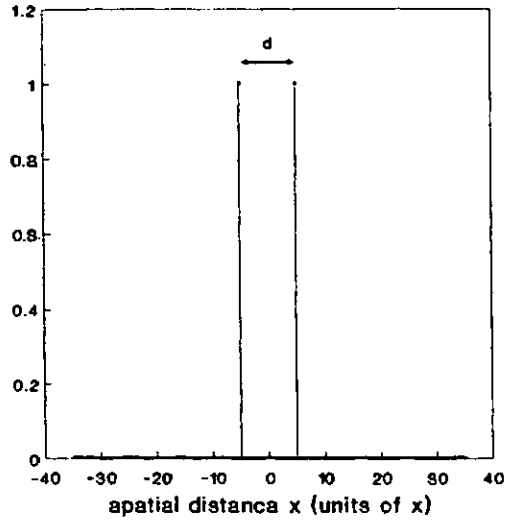

Figure 6.9c : Two delta functions separated by a distance d.

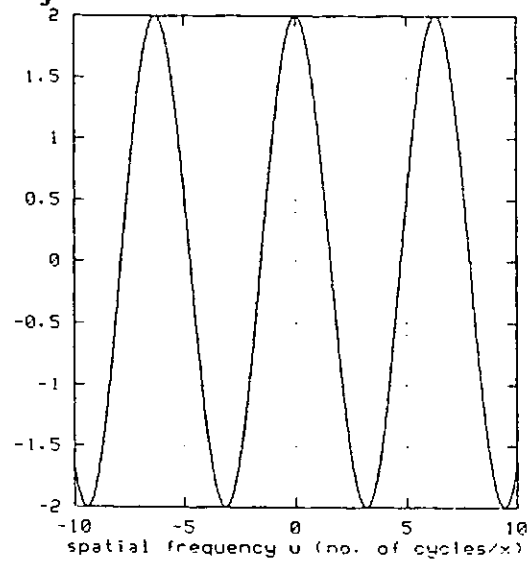

Figure 6.9d : Fourier amplitude spectrum of the two delta functions seen as a cosinusoid of frequency 2/d.

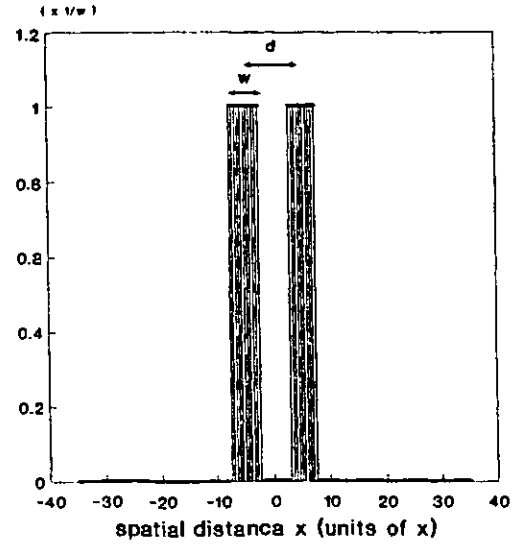

Figure 6.9e : Two rectangular objects formed by the convolution of a single rectangle with two delta functions.

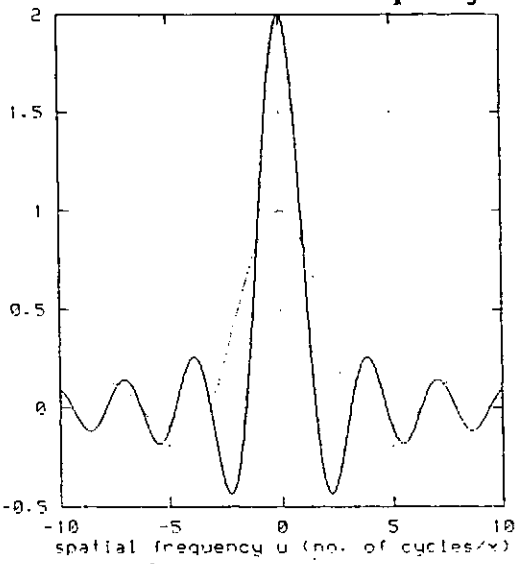

Figure 6.9f : Fourier amplitude spectrum of the two rectangular objects formed by the product of Figures 6.9b and 6.9d.

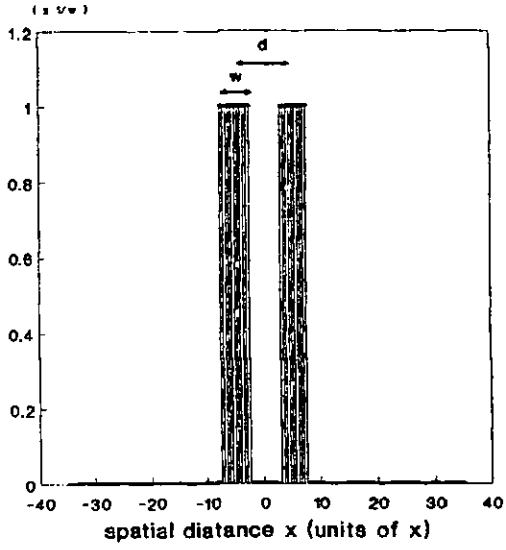

Figure 6.9g : The two rectangular objects separated by a distance d.

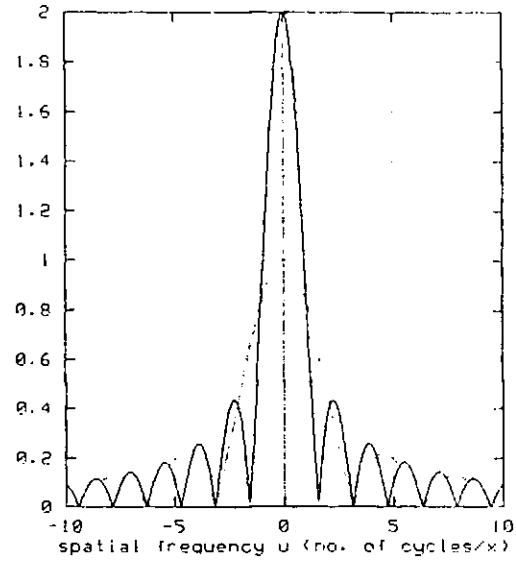

Figure 6.9h : Fourier modulus spectrum of the two rectangular objects seen as the modulation of the frequency envelope of a single rectangle with a cosinusoid of frequency 2/d.

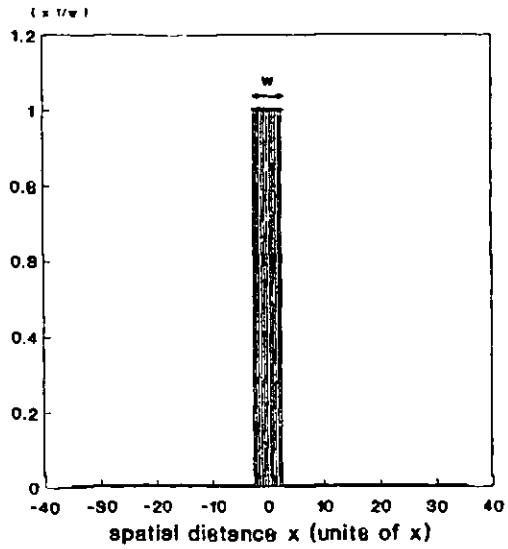

Figure 6.10a : The rectangular object of figure 6.9a maintained with constant width w.

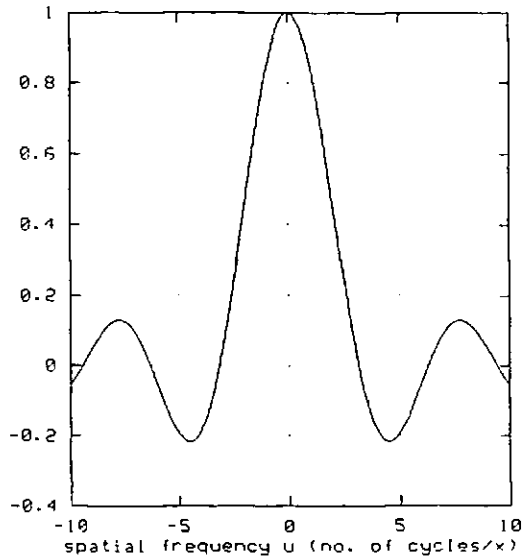

Figure 6.10b : Fourier amplitude spectrum of the single rectangular object.

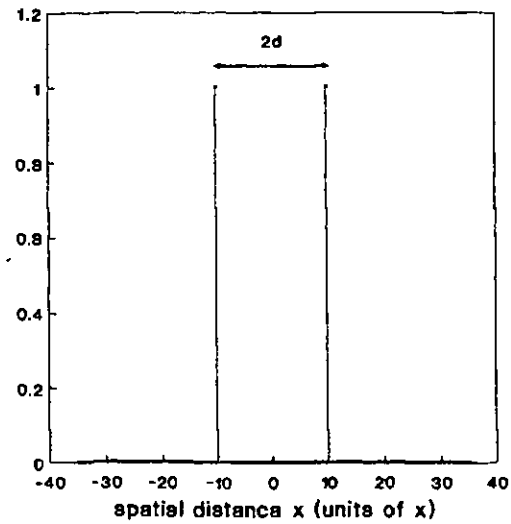

Figure 6.10c : Two delta functions separated by a distance 2d.

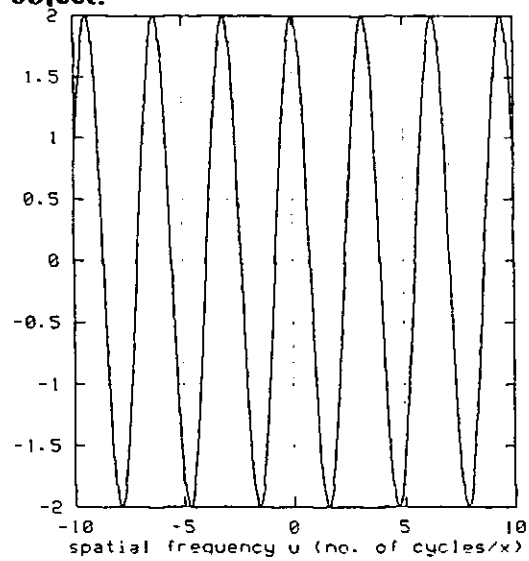

Figure 6.10d : Fourier amplitude spectrum of the two delta functions seen as a cosinusoid of frequency 1/d.

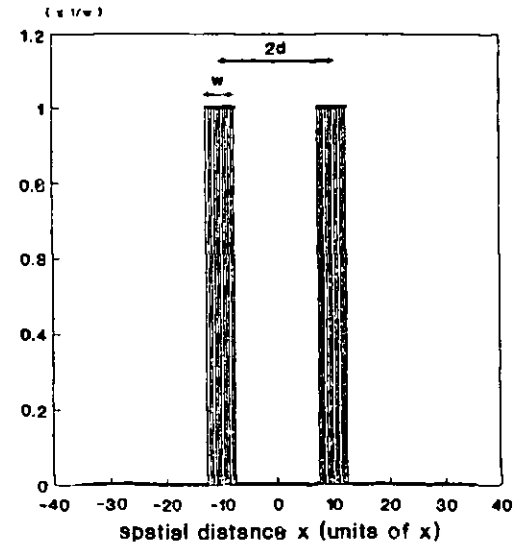

Figure 6.10e: Two rectangular objects at a separation of 2d formed by the convolution of a single rectangle with a set of delta functions 2d apart.

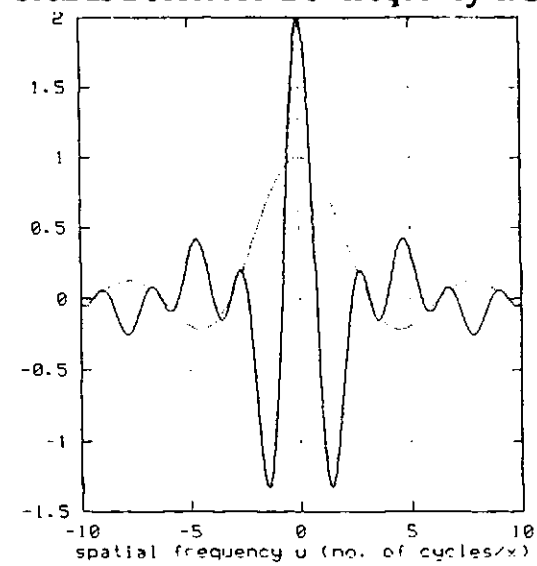

Figure 6.10f : Fourier amplitude spectrum of the two rectangular objects formed by the product of Figures 6.10b and 6.10d.

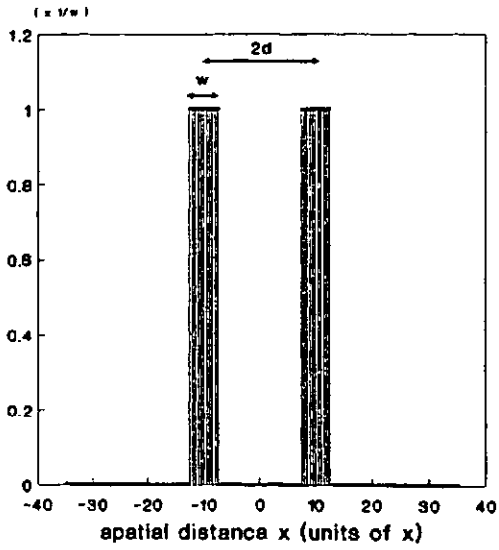

Figure 6.10g : The two rectangular objects separated by a distance 2d.

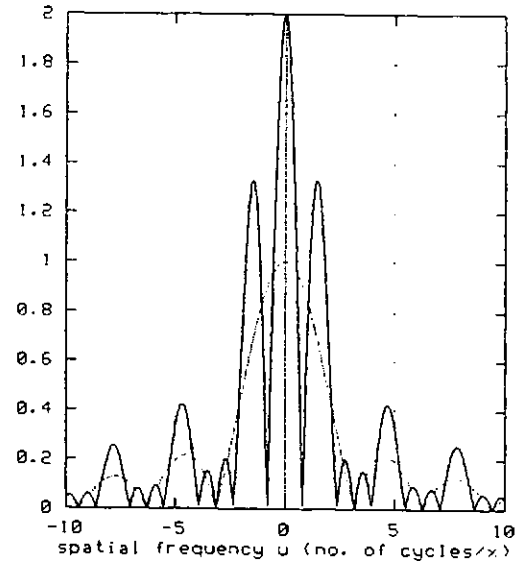

Figure 6.10h : Fourier modulus spectrum of the two rectangular objects seen as the modulation of the frequency envelope of a single rectangle with a cosinusoid of frequency 1/d.

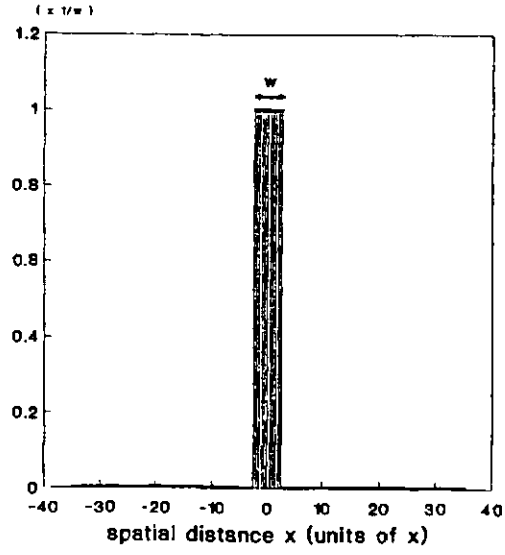

Figure 6.11a : The rectangular object of figure 6.9a maintained with constant width w.

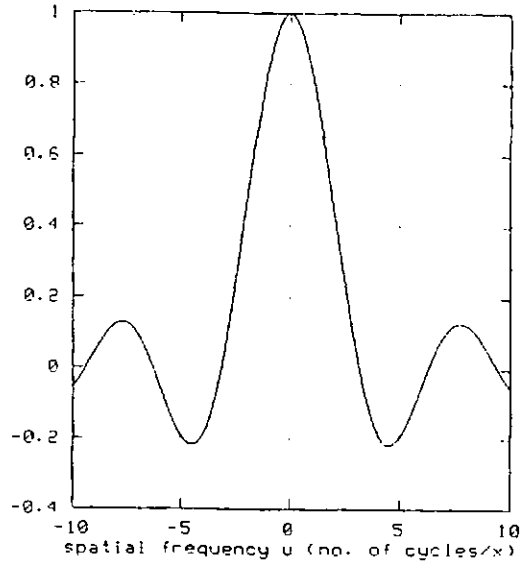

Figure 6.11b : Fourier amplitude spectrum of the single rectangular object.

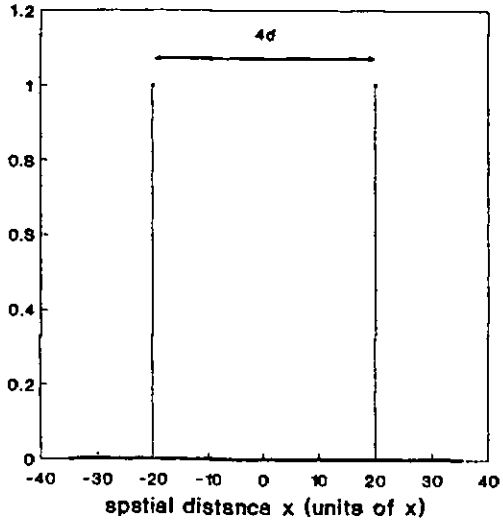

Figure 6.11c : Two delta functions separated by a distance 4d.

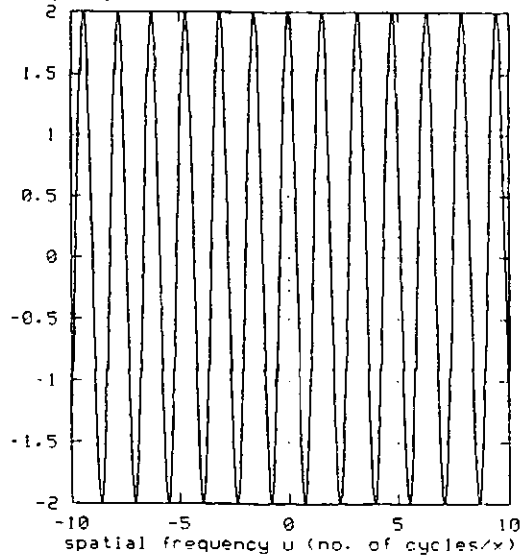

Figure 6.11d : Fourier amplitude spectrum of the two delta functions seen as a cosinusoid of frequency $\frac{1}{4d}$

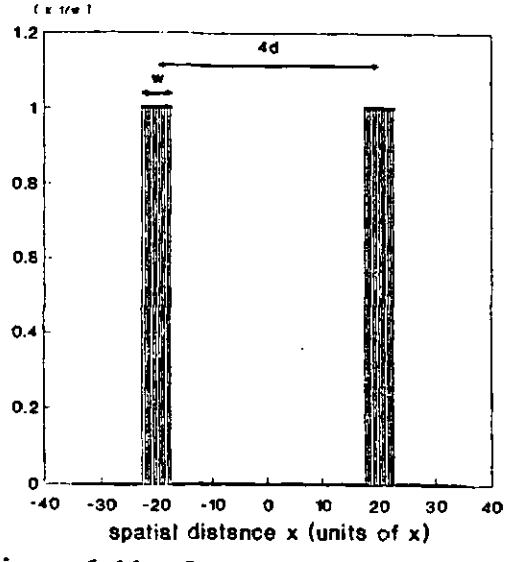

Figure 6.11e: Two rectangular objects at a separation of 4d formed by the convolution of a single rectangle with a set of delta functions 4d apart.

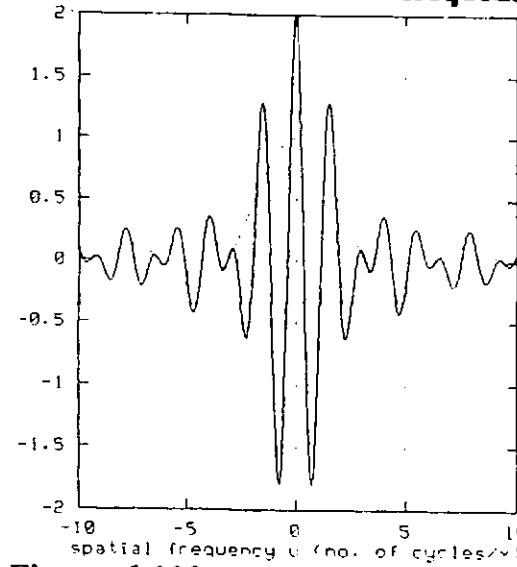

Figure 6.11f : Fourier amplitude spectrum of the two rectangular objects formed by the product of Figures 6.11b and 6.11d.

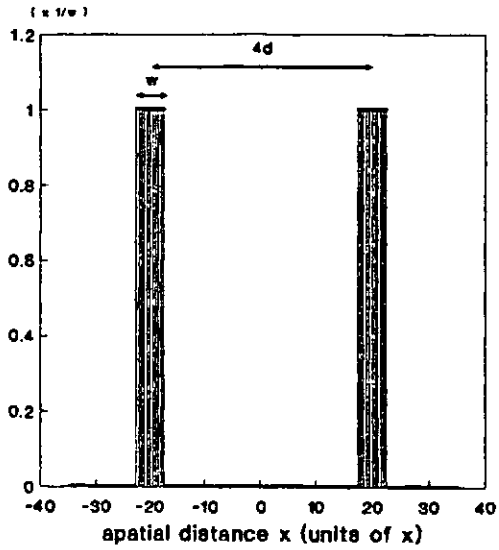

Figure 6.11g : The two rectangular objects separated by a distance 4d.

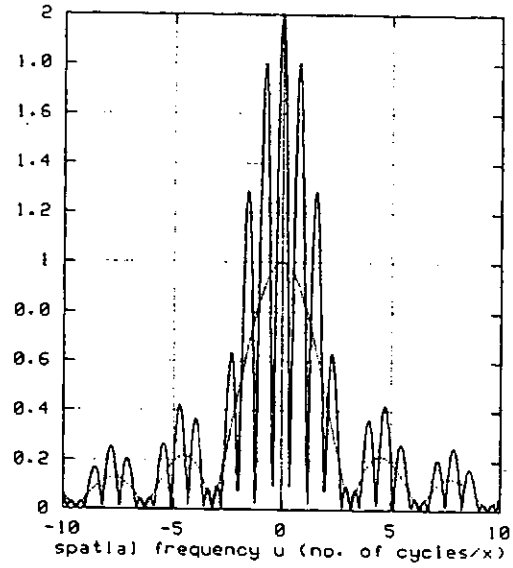

Figure 6.11h : Fourier modulus spectrum of the two rectangular objects seen as the modulation of the frequency envelope of a single rectangle with a cosinusoid of frequency 1/2d.

Not much can be done in the way of altering the physical size of the object specimen, i.e the size of the object specimen itself is fixed, but what about the size of its retrieved image? The size of the retrieved image of the object, very much depends on the scale of its frequency spectrum, that is one can enlarge or reduce the size of the retrieved image by compressing or expanding the spectral behaviour accordingly. Thus, the sought for reduction in the scale of the object which perpetuates better continuity and smoother transitions between spectral components, can be brought on through re-arranging the spectral characteristics in the frequency domain, via a "scale" related operation.

6.4 The Concept of Scale

The notion of scale has already been met in chapter 5 but for an entirely different purpose. This section brings out the importance of such concept once more in connection with the continuity requirements which is favoured by the Hilbert integral. It was addressed in section 5.5.1, that as the object is reduced in size until it ultimately diminishes to a point, its associated frequency characteristic expand until it approaches a continuum. When the object is reduced in size, this raises the frequency of the fundamental and the rest of the harmonics. Raising the frequency of the fundamental, causes this component to be positioned further away from the centre of the spectrum, thereby expanding the central region. This repositioning also takes place for the higher harmonics of the fundamental, resulting in a global expansion of the pattern. Note that with a gradual reduction in the scale of the object in the spatial domain, the many individual lobes in the frequency spectrum would be disposed of in favour of redistributing the new spectral information amongst fewer lobes.

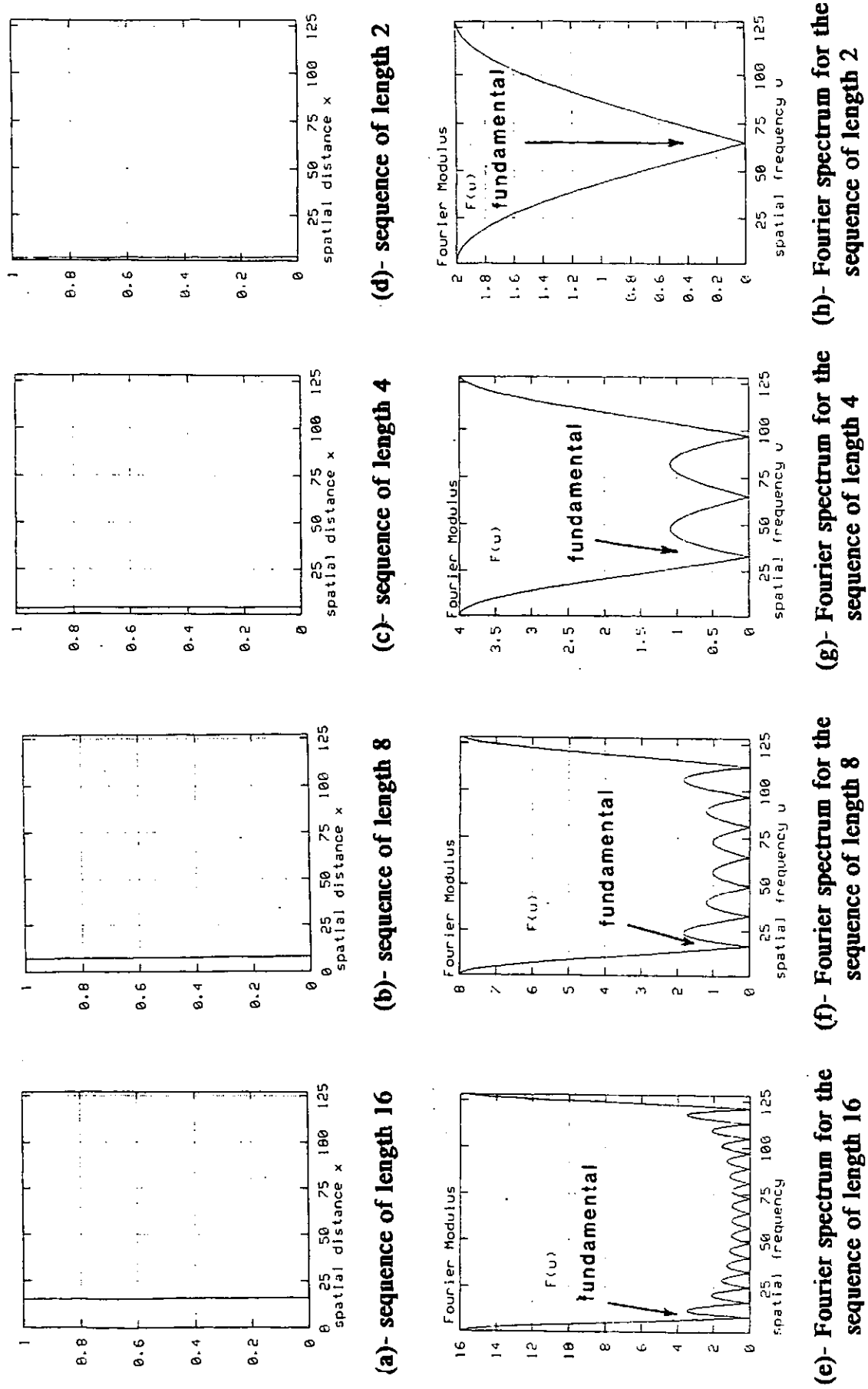

Figure 6.12: Illustration of the scaling concept with reference to the movement of the fundamental component following a reduction in the duration of the object.

With reference to figure 6.12, the movement of the fundamental from the centre of the spectrum can be seen, with a reduction in the length of the sequence. Note that the higher order lobes are phased out, until eventually the sequence of length 2 pixels, has retained all the objects structural information under one lobe.

6.5 Hilbert Transformation

This section provides an insight into the origins of Hilbert transformation and Logarithmic Hilbert transformation (B.Gold, *et al.*, 1970), (V. Cizek, 1970), (A.V. Oppenheim and Schaffer, 1975), (H.Toyoshima and S.Takahashi, 1992). As opposed to quoting the standard formulation in integral form, this section traces back this integral relation to its connections with the original object function. This helps to clarify both the digital implementation of such operation as well as identifying the sensitivity of this integral in phase evaluations.

The theoretical concept behind logarithmic Hilbert transformation has been outlined in the following order:

i) a generalised object function is expressed in terms of its even and odd parts;

ii) the Fourier transform of such object function is identified as the sum of the transform of the even and odd parts of the object;

iii) by defining the object function as a causal sequence, the object has been shown to be obtainable from only the knowledge of its even part or the knowledge of its odd part;

iv) in a similar manner, a causal object function can be extracted from only the knowlegde of the Fourier transform of the even part of the object or only the knowledge of the the Fourier transform of the odd part of the object;

v) in terms of the real and imaginary components of the Fourier transform, (iv) can be restated that a causal object function can be obtained from only the knowledge of the real part of its Fourier transform or only the knowledge of its imaginary part of its transform;

vi) following the reasoning in (v) a complex frequency function can be defined to comprise of a real part which is equivalent to Ln modulus of the Fourier data and an imaginary part which is equivalent to the phase of the Fourier data; it is thus possible to map the original causal and stable object from only the knowledge of Ln modulus of Fourier data.

6.5.1 Definition of Object Surfaces

As already seen in chapter 4, equation (4.5), any function can be separated into the sum of two other components : i) an even component and ii) an odd component. For the surface function of h(x) this can be considered to be as:

$$h(x) = h_e(x) + h_o(x) \tag{6.1}$$

where the even part $h_e(x)$ can be expressed as:

$$h_e(x) = \frac{1}{2} [\, h(x) + h(-x) \,] \tag{6.2}$$

and the odd part $h_o(x)$ can be written as:

$$h_o(x) = \frac{1}{2} [\, h(x) - h(-x) \,] \tag{6.3}$$

In a similar manner the Fourier transform of any real function would have a real part and an imaginary part which are the individual transforms of the even part and the odd part of the original function as seen in section 4.2.1.
i.e, in the Fourier domain the transform of h(x) is:

$$\mathcal{F}\ [h(x)] \leftrightarrow H(u) \tag{6.4}$$

where H(u) comprises of a real part and an imaginary part i.e:

$$H(u) = R + jI \tag{6.5}$$

or H(u) can be written in terms of an even part and an odd part of two frequency functions:

$$H(u) = H_e(u) + j\ H_o(u) \tag{6.9}$$

where the even $h_e(x)$ and odd $h_o(x)$ terms of the general object function now appear as the real $H_e(u)$ and imaginary $j\ H_o(u)$ parts of the Fourier transform in the Fourier domain. The aim now is to create a condition for which h(x) can be solely determined from the knowledge of its even part $h_e(x)$ or the knowledge of its odd part $h_o(x)$. The above condition can be created when h(x) is defined to be a causal function.

6.5.2 Object Functions Realised as Causal Sequences

For any causal sequence, the following relationships exist:

$$h(x) = \begin{pmatrix} 2h_e(x)\ , & n>0 \\ h_e(x)\ , & n=0 \\ 0\ , & n<0 \end{pmatrix} \tag{6.7}$$

$$h(x) = \begin{pmatrix} 2h_o(x)\ , & n>0 \\ 0\ , & n<0 \end{pmatrix} \tag{6.8}$$

by defining another sequence U(x), such that

$$U(x) = \begin{pmatrix} 2\ , & n>0 \\ 1\ , & n=0 \\ 0\ , & n<0 \end{pmatrix} \tag{6.9}$$

then the above definitions can be regarded as:

$$h(x) = \begin{pmatrix} h_e(x).U(x) \\ h_o(x).U(x) + h(0) \end{pmatrix} \tag{6.10}$$

Parallel to the above derivation of the complete object function h(x) from the knowledge of the even part $h_e(x)$ of a function, with a similar reasoning, the complete Fourier spectrum H(u) can be obtained from a knowledge of the even part or the odd part of the Fourier transform. As mentioned earlier these are the real and imaginary parts of the Fourier amplitude spectrum H(u).

$$H(u) = H_R(u) + j\,H_I(u) \tag{6.11}$$

and

$$\mathcal{F}\{h_e(x)\} = H_R(u) \tag{6.12}$$

$$\mathcal{F}\{h_o(x)\} = H_I(u) \tag{6.13}$$

This can be done by inverse Fourier transforming the real part of the complex Fourier spectrum $H_e(u)$, to arrive at the even part of the original sequence $h_e(x)$, and multiplying the even part of the original sequence by the sequence U_n to get back at the entire sequence h(x) constituting of both an even part and an odd part as seen in (6.10).

Whilst it is possible to arrive at the original complete sequence from the knowledge of the even part or the odd part of the complex Fourier spectrum, the real part and the imaginary parts for such sequence also maintain a relationship with one another through the Hilbert transform operation as such:

From examining equations (6.7) and (6.8) it can be seen that the even part of the original sequence $h_e(x)$ equals the odd part of the sequence $h_o(x)$ for the part of the sequence for which $n>0$ i.e:

$$h_e(x) = h_o(x) \qquad for \quad n>0 \tag{6.14}$$

and

$$h(-x) = 0 \qquad for \quad n<0 \tag{6.15}$$

the relationship between the odd part and the even part of the original sequence can now be expressed with the aid of another function which satisfies the above two requirements such that:

$$h_e(x) = h_o(x) . sgn\, x \tag{6.16}$$

$$h_o(x) = h_e(x) . sgn\, x \tag{6.17}$$

where the signum function sgn x , is defined as:

$$sgn\,(x) = 1 \qquad for \quad n>0 \tag{6.18}$$

$$sgn\,(x) = -1 \qquad for \quad n<0 \tag{6.19}$$

which has the standard Fourier transformation of :

$$sgn(x) \leftrightarrow \frac{2}{ju} \tag{6.20}$$

hence the real part of the complex Fourier amplitude spectrum

$$H_R(u) = \mathcal{F}\ [h_o(x).\ sgn(x)] \tag{6.21}$$

using the frequency convolution which states the Fourier transform of the product of two functions as the convolution of the individual Fourier transforms, equation 6.21 can be written in terms of a convolution of individual Fourier spectra: from the frequency convolution theorm, this can be written in the following manner:

$$h(x).\ h(y) \leftrightarrow \frac{1}{2\pi}\ H(e^{jux}) * H(e^{juy}) \tag{6.22}$$

$$H_R\ (e^{ju}) = \frac{1}{2\pi}\ jH_I(u)\ *\ \frac{2}{ju} \tag{6.23}$$

$$H_R(u) = \frac{1}{\pi} H_I(u) * \frac{1}{u} \tag{6.24}$$

The operation of Hilbert transformation , is the convolution operation above, of the imaginary part of the complex Fourier spectrum with the function 1/u, which can be rewritten in terms of a standard convolution integral as:

$$H_R(u) = \frac{1}{\pi} \int_{-\infty}^{\infty} \frac{H_I(\mu)}{u-\mu} d\mu \tag{6.25}$$

in a similar manner the imaginary part of the complex spectrum can be obtained from the knowledge of the real part of the complex Fourier spectrum as:

$$jH_I(u) = -j\frac{1}{\pi} H_R(u) * \frac{1}{u} \tag{6.26}$$

which once again can be expressed in terms of a convolution integral of:

$$H_I(u) = -\frac{1}{\pi} \int_{-\infty}^{\infty} \frac{H_R(\mu)}{u-\mu} d\mu \tag{6.27}$$

the two equations (6.25) and (6.27) relate the real and imaginary part of the complex Fourier amplitude spectrum H(u) through a Hilbert transform operation expressed by the two integrals. Therefore the real and imaginary part of the complex Fourier spectrum constitute a Hilbert transform pair.

Much of the effort put in extracting the original sequence from a knowledge of its even or odd part mapped as real and imaginary components of its Fourier modulus can only be of use if a similar relationship could be found to relate the modulus and the phase of the Fourier spectrum. This is the immediate need of the data gathered experimentally, as it is the time-averaged intensity which is recorded

at optical frequencies from which only the modulus is obtainable.

6.5.3 The Logarithmic Hilbert Transform

The previous section laid the foundations upon which the spatial frequency function H(u), can be extracted from a knowledge of the real part or odd part of its Fourier spectrum through Hilbert transform operations (6.25) or (6.27). This section reveals a similar expression for evaluating the phase of a frequency function $H^*(u)$, where $H^*(u) = \text{Ln}\{H(u)\}$, from the knowledge of the ln modulus of the complex function i.e $\text{Ln}\{|H(u)|\}$.

In this case however, the ln modulus and phase form the real and imaginary parts of this new complex function ln{H(u)}. Expressing H(u) in terms of the modulus and phase:

$$H(u) = |H(u)| e^{j\angle H(u)} \tag{6.28}$$

taking the natural logarithm, of equation (6.28) it is possible to relate the magnitude and phase of the complex frequency spectrum i.e:

$$\ln\{H(u)\} = \ln\{|H(u)|\} + j\angle H(u) \tag{6.29}$$

where the real part of the function equals:

$$R(u) = Ln|H(u)| \tag{6.30}$$

and the imaginary part of the function equals:

$$I(u) = \angle H(u) \tag{6.31}$$

where ln {H(u)} = H*(u), is the complex sequence relating the log magnitude and phase. Now that the logarithm of modulus and the phase are each part of a complex function H*(u), they can be related to each other in the manner that the real and imaginary parts of the Fourier spectrum were related but this time through a logarithmic Hilbert transform operation as:

$$\angle H(u) = \phi(u) = \frac{-1}{\pi} \int_{-\infty}^{\infty} \frac{\ln|H(\mu)|}{(u-\mu)} \, d\mu \qquad (6.32)$$

equation (6.32) can be interpreted as a convolution integral, whereby phases at each point, are obtained from the convolution of the log modulus of the frequency samples i.e ln |H(u)| and the function 1/u.

Following the same reasoning which was set out in section 6.5.3, it is possible to obtain the entire complex spectrum H*(u) by using the available ln modulus information. The phases specified via the integral relationship (6.32), has been obtained by means of the digital implemetation of the procedure for obtaining the unknown phases in the following manner:

i) The real part of this complex function, which is the Ln modulus of the Fourier spectrum H(u), when inverse Fourier transformed, will yield the even part of the original object function;

ii) multiplication of this by the sequence Un, restores the entire of the object function;

iii) Fourier transforming the entire object function, would yield the complex Fourier spectrum with a real part that is equal to the ln $\{|H(u)|\}$ and an imaginary part which is equal to phase.

The program, which has been developed by the author is an implementation of the aforementioned steps.

6.5.4 Evaluation of the 2D Phases

Integral equation of (6.32) denotes an expression, for evaluating one-dimensional phases. Although the one-dimensional phases have been generated in the case studies for a 1-D object sequence, the object specimen i.e the reflectance target has a 2-D structure for which the 2-D phases have to be restored.

For a two-dimensional frequency function, H(u,v), the two-dimensional phases $\phi(u,v)$ are obtained as a series of one-dimensional phases along a certain direction. For an array of MxN where M=0...m-1 and N=0...n-1 elements, phases along every horizontal strip nc, i.e $\phi(u,nc)$ are obtained independently as specified by the integral relation (6.32). To convert these independent one-

dimensional phases into a coherent pattern of two-dimensional phases, phases along another line through an orthogonal direction are obtained i.e $\phi(0,v)$. The two-dimensional phases are then obtained via the addition of $\phi(u, nc)$to the $\phi(0,v)$ which goes through the corresponding point. This operation has been shown in figure 6.13 below.

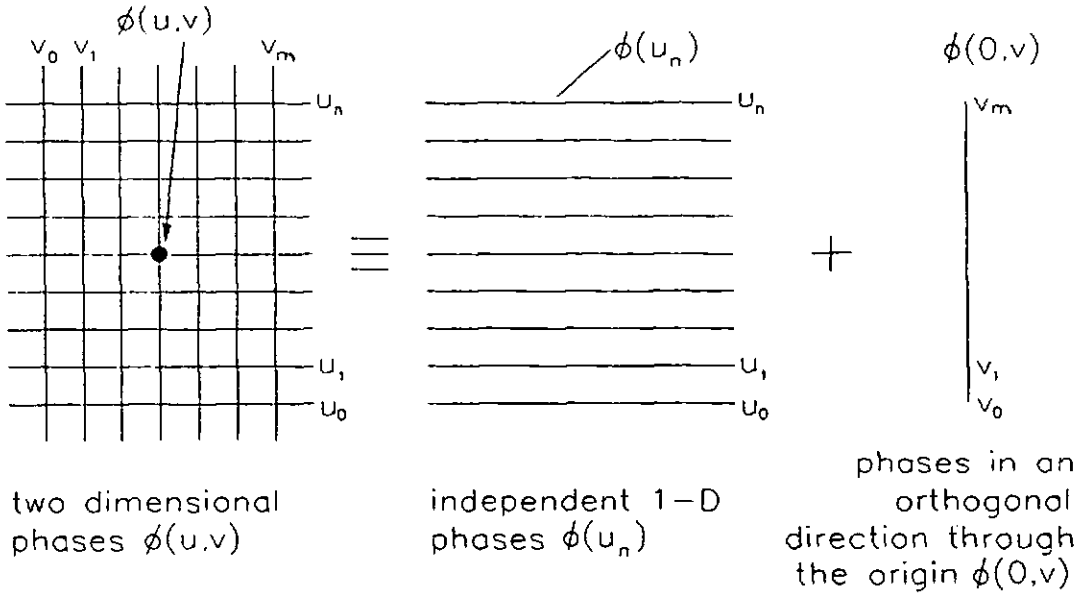

Figure 6.13: Generation of 2D phases from a series of independently evaluated 1D phases.

6.6 Case Study : Restoring a 1-D Object Sequence through Application of Fourier Scaling Principle

This study illustrates how compression in the scale of the object allows for an improvement in the restored pattern for a one-dimensional object sequence. The object sequence is a rectangular function, whose duration has been gradually reduced to re-scale the frequency characteristics. The shape of the object gives rise to many discontinuities in the spectrum which need to be altered if data are to be exposed for evaluation through the Hilbert integral. To rectify the problem, an impulse has been added to the beginning of the sequence which automatically raises the level of the data in the frequency domain by a constant amount depending on the level of the impulse function. As already addressed in section 6.2, this method was preferred to the other alternative i.e the addition of a continuum to the modulus data, since adding an impulse in the object domain, fixes the position of the object with respect to the impulse function. This function can also be used as a reference to identify the start of the sequence. In all the forthcoming figures of 6.14-6.18 an impulse of 5 has been added to the beginning of the object function.

The change in scale has been brought on four times. The data presented in this section thus comprises of the original unscaled object, and four other versions of it which have undergone a change in scale. Graphical data associated with each version of the object in figures 6.14-6.18, serves to illustrate:

(i) Original object h(x) versus the retrieved object $h_{hil}(x)$;

(ii) Fourier spectrum and the population of zeros (*identified by individual impulses*);

(iii) Original phases versus the retrieved phases;

Apart from the data presented in graphical form, a figure of quality for tracking the closeness between the restored signal and its original version has been defined via the total squared error $\sum E_{total}$. This error shows the total sum of the squared differences between the original object h(x) and the retrieved Hilbert $H_{hil}(x)$ object defined as:

$$\sum E_{total} = \sum \{ h(x) - h_{hil}(x) \}^2 \qquad (6.33)$$

The trend in the total square error $\sum E_{total}$ with each compression in the scale of the object has been put in tabular form in table 6.2, which can be found at the end of this section.

(a)-The uncompressed sequence: figures 6.14a-6.14g

Figure 6.14a, illustrates the original unscaled sequence having the largest duration amongst this series, followed by the Ln Hilbert restored sequence in figure 6.14b. As can be seen from figure 6.14b, it is quite difficult to deduce the starting edge of the object with certainty and the retrieved object is highly distorted.With reference to table 6.2, the total squared error $\sum E_{total}$ as defined by equation (6.33) between the original and the restored signal is as large as 13.88. A close look at figures 6.14c and 6.14d reveals the cause of such distortion. The spectrum starts off with a large swing to the first minimum, and it is not until the thirtieth pixel that it eventually levels off.

Lack of continuity amongst the most significant calibre of frequency components, leads to poor convergence of Ln modulus of the frequency components to the function from which the phase data is extracted.

In addition, participation of a whole group of minima also impairs the accuracy with which phase data is evaluated, through rounding off errors. Although the spectrum does not possess any true zeros, as they have now been raised to minima, the position of the zeros has been indicated to clearly illustrate the large population of minima that it entails at this stage.

An alternative way of assessing the discrepancies between the original object and its restored version, is through the comparison of the extracted phases with the original. The reconstructed characteristics would only be similar to the true object, if the extracted phases closely approximate the original phases. Thus any error in the retrieved phase data would strongly influence the shape of the recovered sequence. Figures 6.14e and 6.14f show the original phases and the Ln Hilbert restored phases. As can be seen there is considerable difference between the two especially in the lower frequency end of the spectrum. As already addressed the Hilbert integral runs into grave errors for very sharp and rapid transitions in the amplitude of the frequency components. This is also the observed behaviour in the lower frequency range of the frequency spectrum in figure 6.14c.

Since the most significant spectral components reside in the lower frequency region, when accompanied by phase information which is highly inaccurate, the restored behaviour is bound to be highly distorted. As seen the phase difference which is the error in calculating the true phases almost levels off or reaches a plateau in the medium to higher frequency region, in harmony with the modulus spectrum which also levels off in this region.

(b)-Sequence compressed by a factor x2; figures 6.15a-6.15g

The compressed version of this sequence by a factor of 2, can be seen in figure 6.15a. There is slight improvement in the restored object, in figure 6.15b, in the sense that the starting edge of the sequence is now clearly identifiable as compared to the previous case signifying the fact that better continuity amongst higher frequency components has led to preservation of the edge information in the restored object. This fact is also reflected in the value of the total squared error $\sum E_{total}$ which has come down to 5.091 a reduction in the total suquare error by ~ 63% as compared to the previous case. However, the lower frequency region, still entails large phase errors, figures 6.15e and 6.15f. Note that the overall population of zeros in figure 6.15d, has been reduced by approximately a factor of 2.

(c)-Sequence compressed by a factor of x4: figures 6.16a-6.16g

Further compression in the scale of the original object by a factor of 4 as seen in figure 6.16a presents slight improvement in its restored behaviour round the edges figure 6.16b, but still noticeable distortion in its general structure. With reference to table 6.2, $\sum E_{total}$ now reaches a value of 1.732, a reduction in the total squared error by ~87.5% . When the edges of the recovered object become well defined as in figure 6.16b, one has reason to believe that the retrieved phases are reproducing phase variations in the higher frequency region. The comparison of the original phases with Ln Hilbert restored phases shows very good replication of the phase pattern by the Hilbert integral in this region.

(d)-Sequence compressed by a factor of x8 : figures 6.17a-6.17g

Marked improvements can be seen in figure 6.17b, when the original sequence is compressed by a factor of 8. This spectrum has few zeros figure 6.17d, has smooth transition between the maxima and the minima, and the Ln Hilbert phases are perfectly duplicating the profile of the original phases.

The phase difference now shoots up to a maximum of 0.08 radians as compared to the few radians in the previous cases, and there is no reason whatsoever for the restored characteristics to be much different from the original behaviour. In fact, there is a dramatic improvement in the total squared error $\sum E_{total}$ having a value of 2.083×10^{-3} a reduction in total square error by ≈99.98% as compared to the original case.

(e)-Sequence compressed by a factor of x16: Figures 6.18a-6.18g

Finally, optimal perfection, backed up by a total squared error of $\sum E_{total}$ of 1.857×10^{-9}, can be seen when the original sequence is compressed by a factor of 16 in figure 6.18a. In this case the Ln Hilbert phases follow the pattern of the original phases with a maximum phase difference of 4×10^{-5} radians. There is undeniably a 100% match between the two sequences. Lastly, the population of zeros has been dramatically reduced in number. Figure 6.18d shows that this spectrum would have only possessed one zero if it had not been raised in level by the impulse function. Clearly, compression in the overall scale of the object has led to a significant reduction in the total square error namely an initial error of 1.388×10^{1} between the restored sequence and the original sequence has been reduced to that of 1.857×10^{-9}. A detailed listing of the total squared errors for the original sequence and its compressed versions can be found in table 6.2a.

scale of the object	object without compression	object with ×2 compression	object with ×4 compression	object with ×8 compression	object with ×16 compression
$\sum E_{total}$ total squared error	1.388×10^{1}	5.091	1.732	2.083×10^{-3}	1.857×10^{-9}

Table 6.2a: Showing the trend in the total squared error parameter with the compression in the scale of the object.

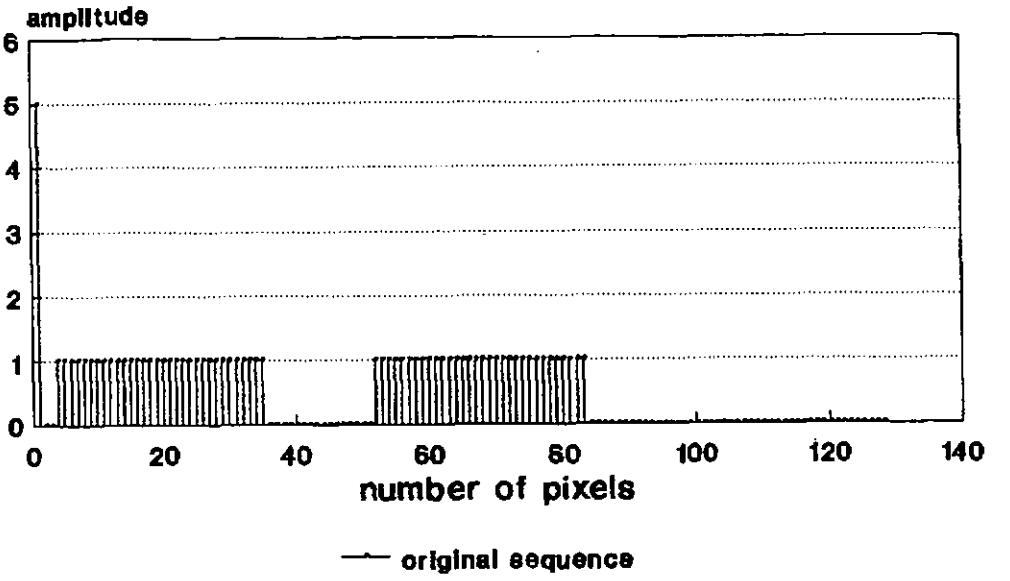

Figure 6.14a: The original object sequence prior to compression.

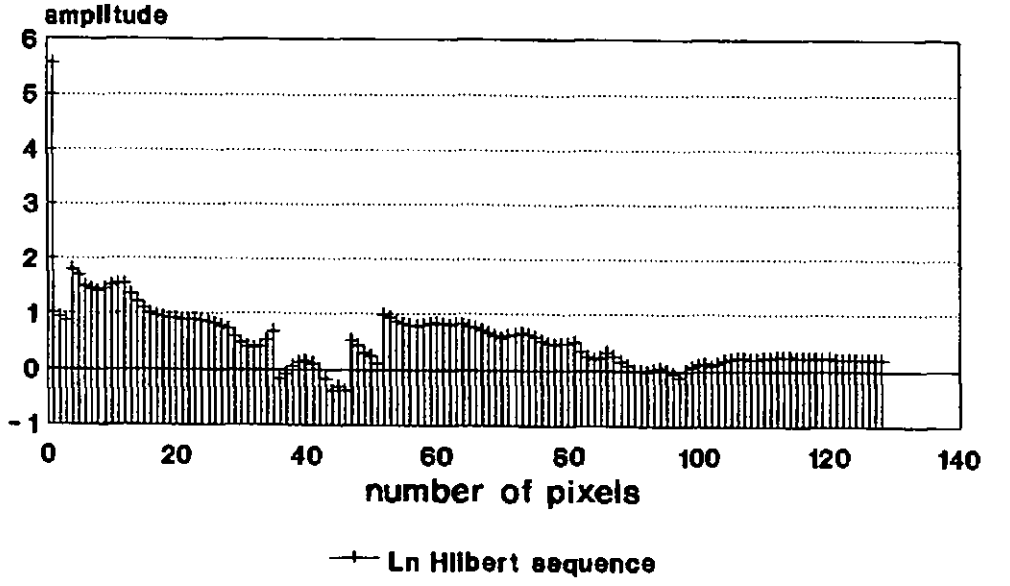

Figure 6.14b: Ln Hilbert restored version of the object, from the Fourier modulus spectrum of figure 6.14c.

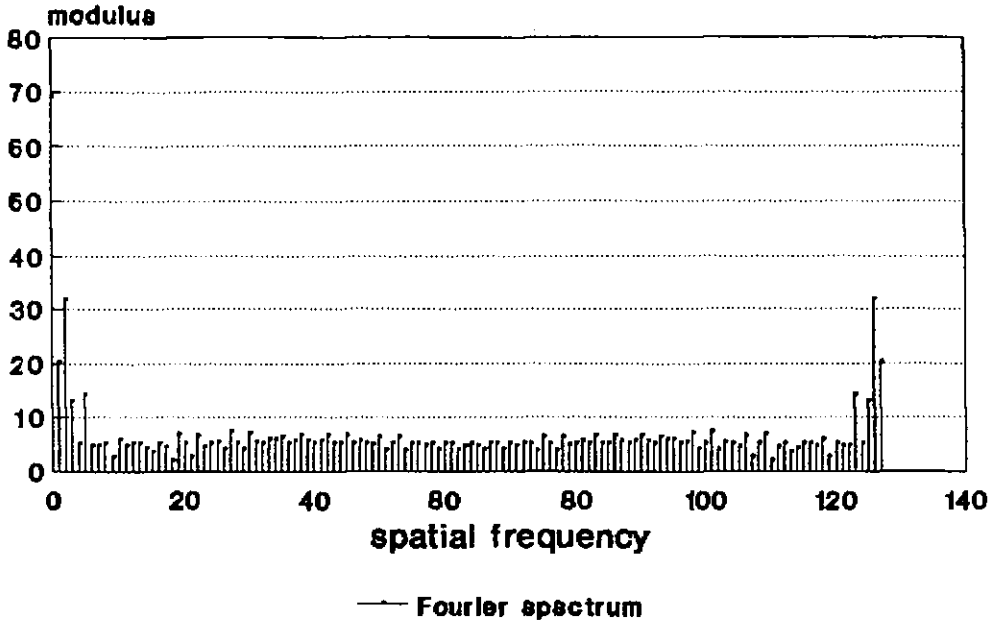

Figure 6.14c: Fourier modulus spectrum of the uncompressed object of figure 6.14a.

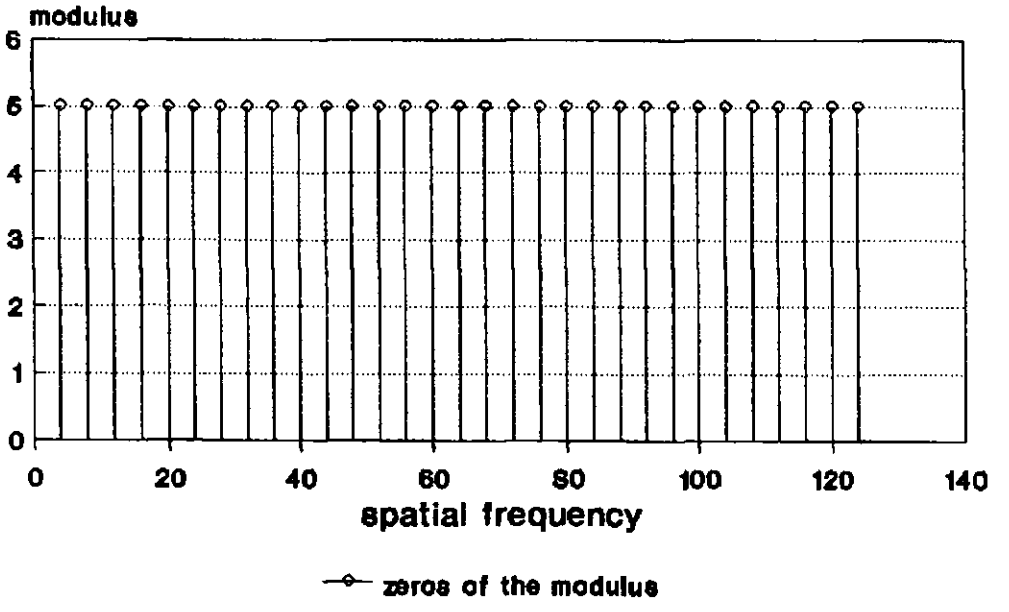

Figure 6.14d: Population of zeros in the Fourier modulus spectrum of figure 6.14c which have all been replaced by minima. To clearly indicate the position of zeros, all spectral components in figure 6.14c have been suppressed.

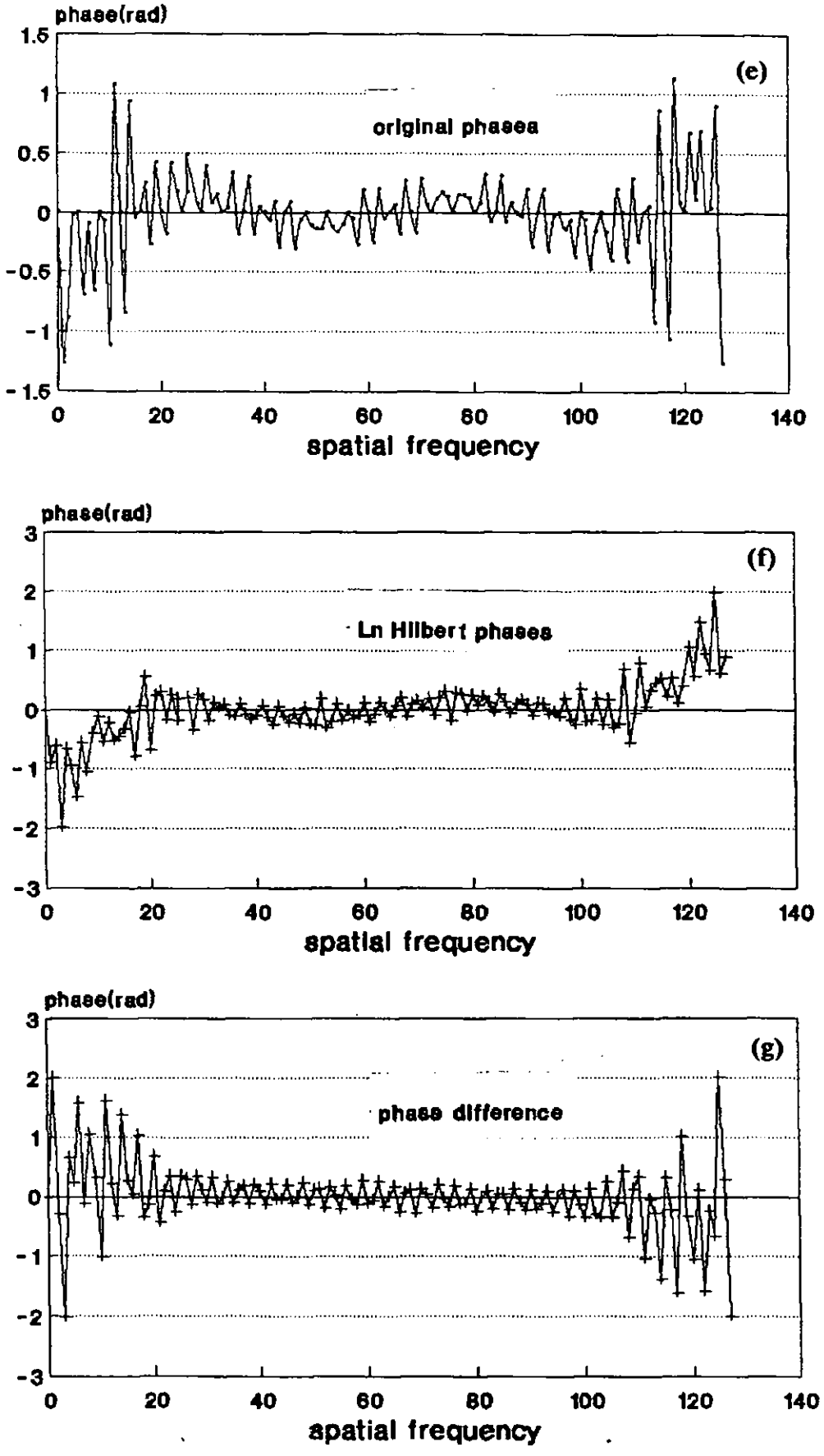

Figure 6.14: (e)- Original phases ; (f)-Ln Hilbert restored phases from the spectrum of figure 6.14c; (g)- Difference between the original phases and the restored phases.

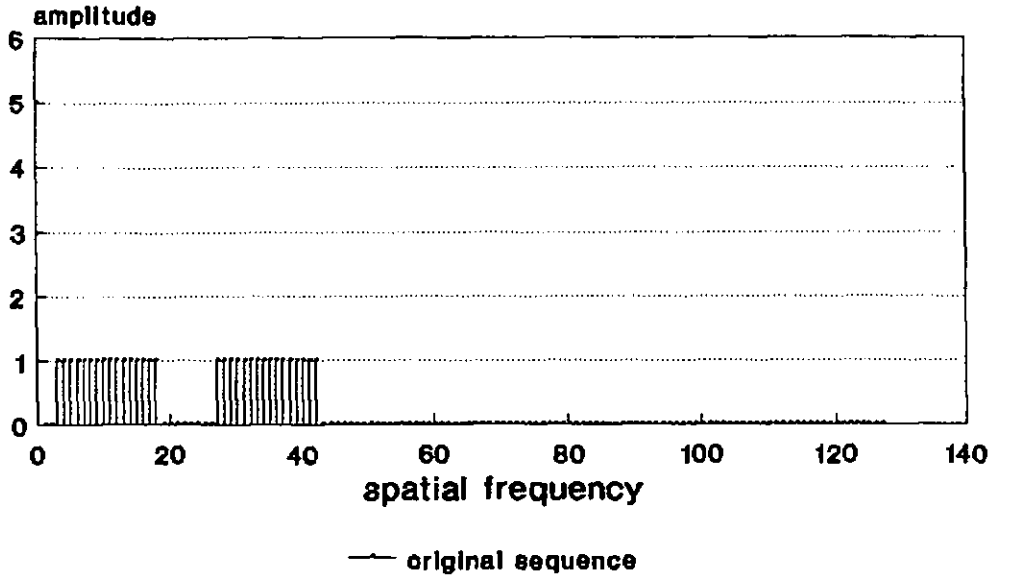

Figure 6.15a: The original object sequence compressed by a factor of 2.

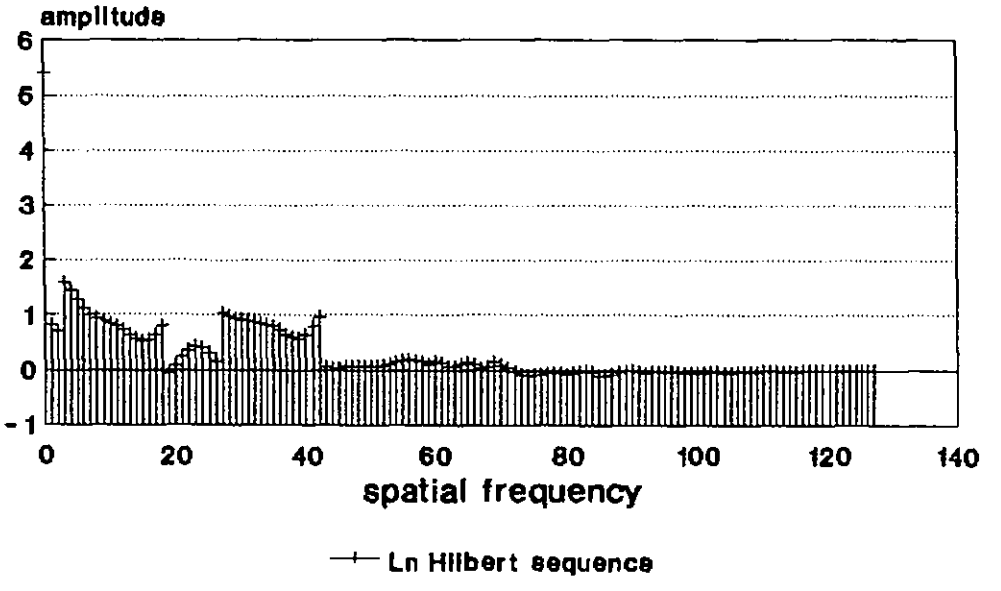

Figure 6.15b: Ln Hilbert restored version of the object, from the Fourier modulus spectrum of figure 6.15c.

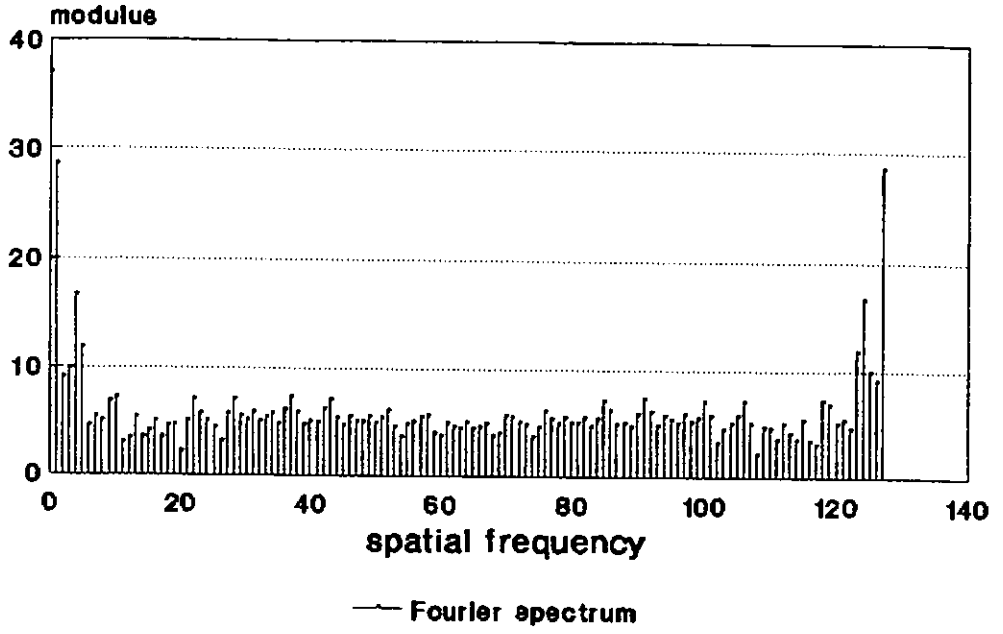

Figure 6.15c: Fourier modulus spectrum of the compressed object of figure 6.15a.

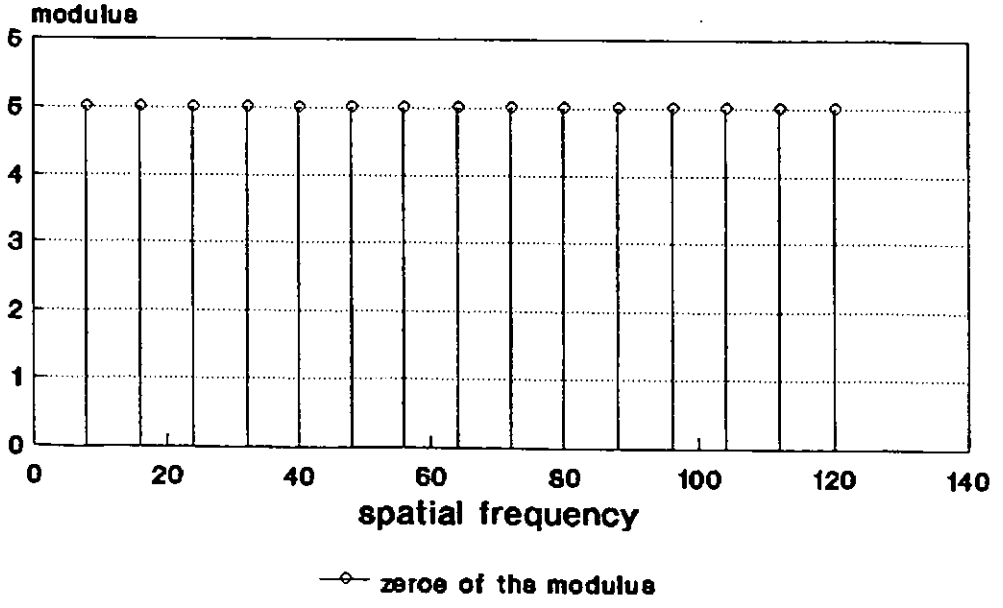

Figure 6.15d: Population of zeros in the Fourier modulus spectrum of figure 6.15c which have all been replaced by minima. To clearly indicate the position of zeros, all spectral components in figure 6.15c have been suppressed.

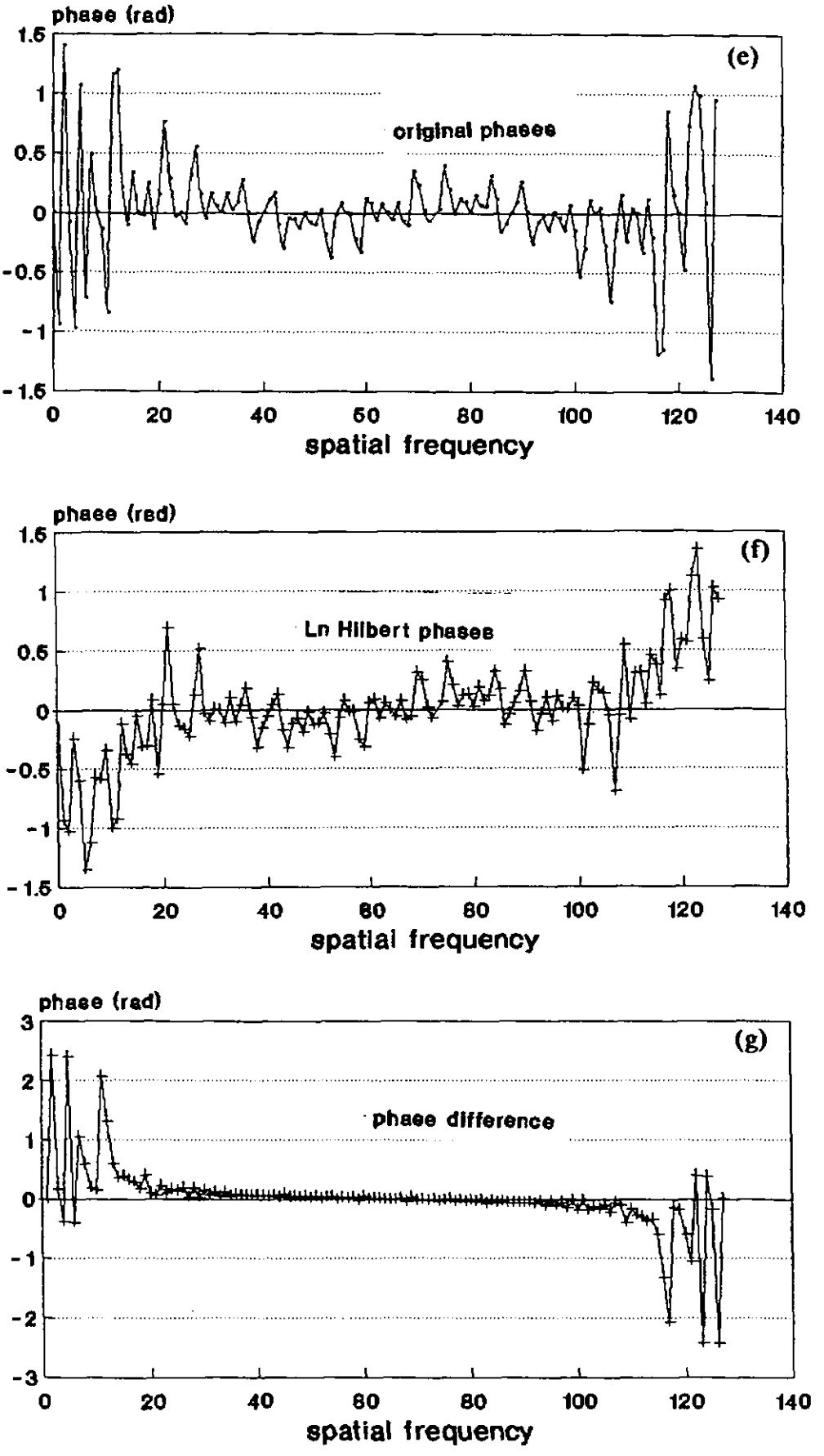

Figure 6.15: (e)- Original phases; (f)-Ln Hilbert restored phases from the spectrum of figure 6.15c; (g)- Difference between the original phases and the restored phases.

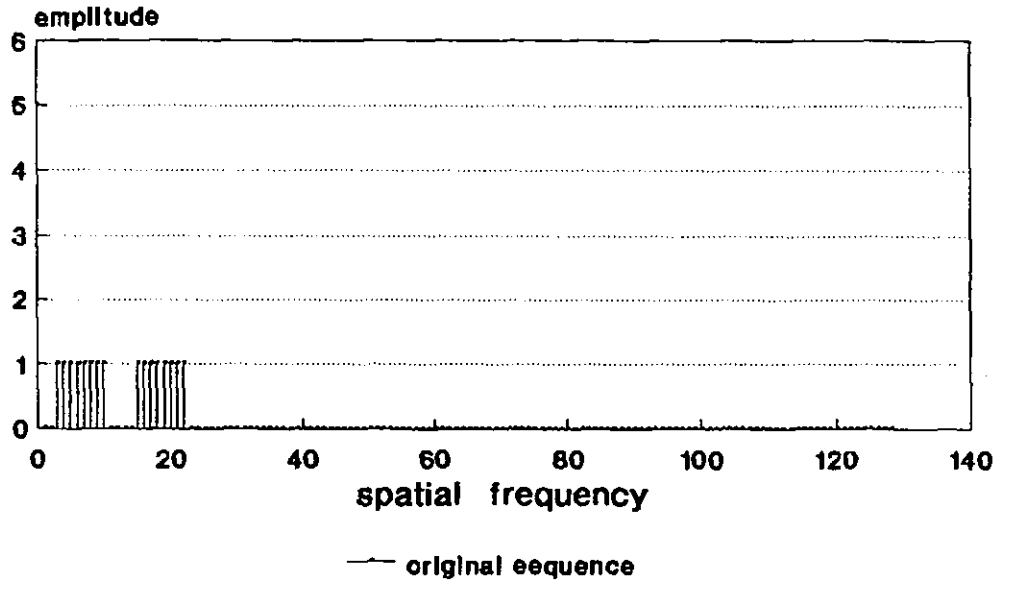

Figure 6.16a: The original object sequence compressed by a factor of 4.

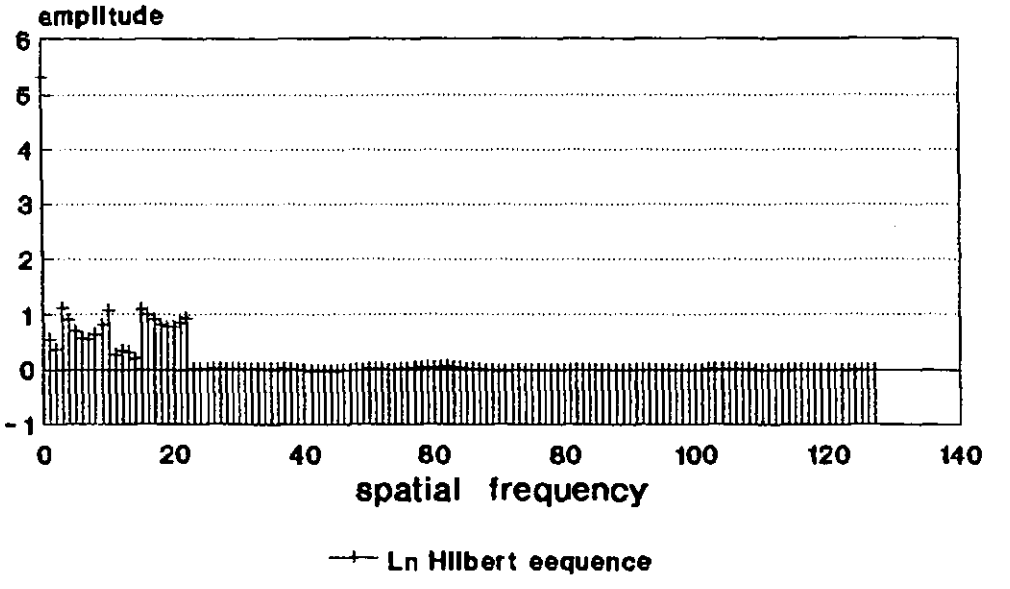

Figure 6.16b: Ln Hilbert restored version of the object from the Fourier modulus spectrum of figure 6.16c.

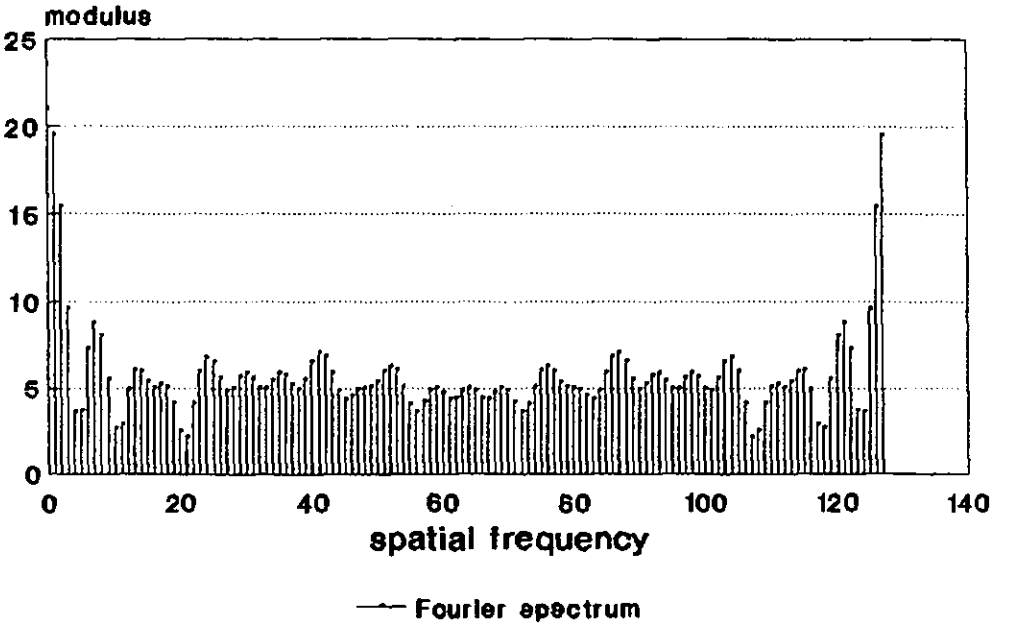

Figure 6.16c: Fourier modulus spectrum of the compressed object of figure 6.16a.

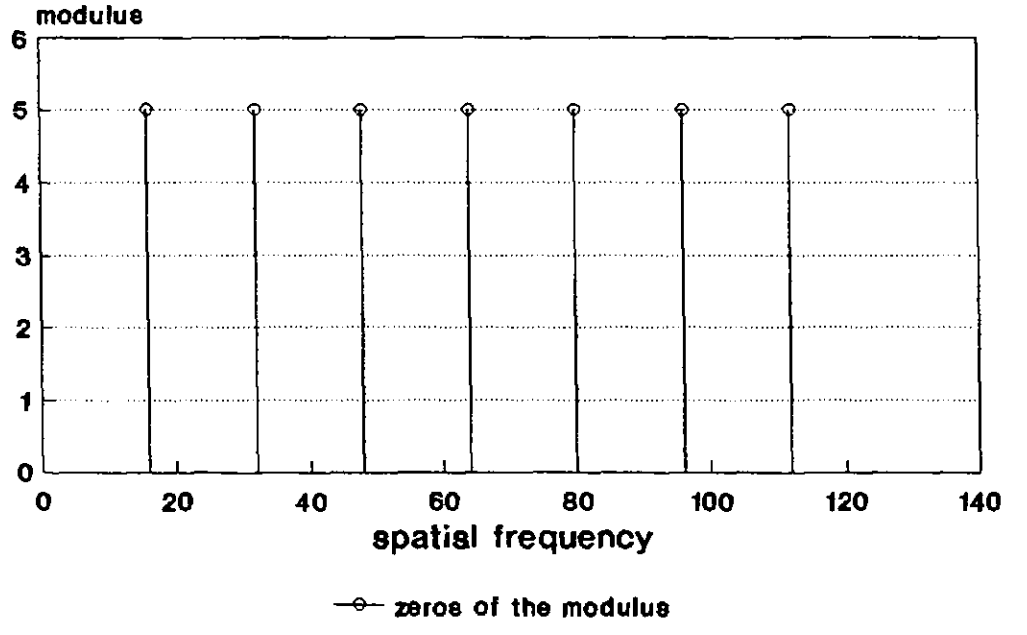

Figure 6.16d: Population of zeros in the Fourier modulus spectrum of figure 6.16c. which have all been replaced by minima. To clearly indicate the position of zeros, all spectral components in figure 6.16c have been suppressed. Note the considerable reduction in the population of zeros as compared to that of figures 6.14d and 6.15d.

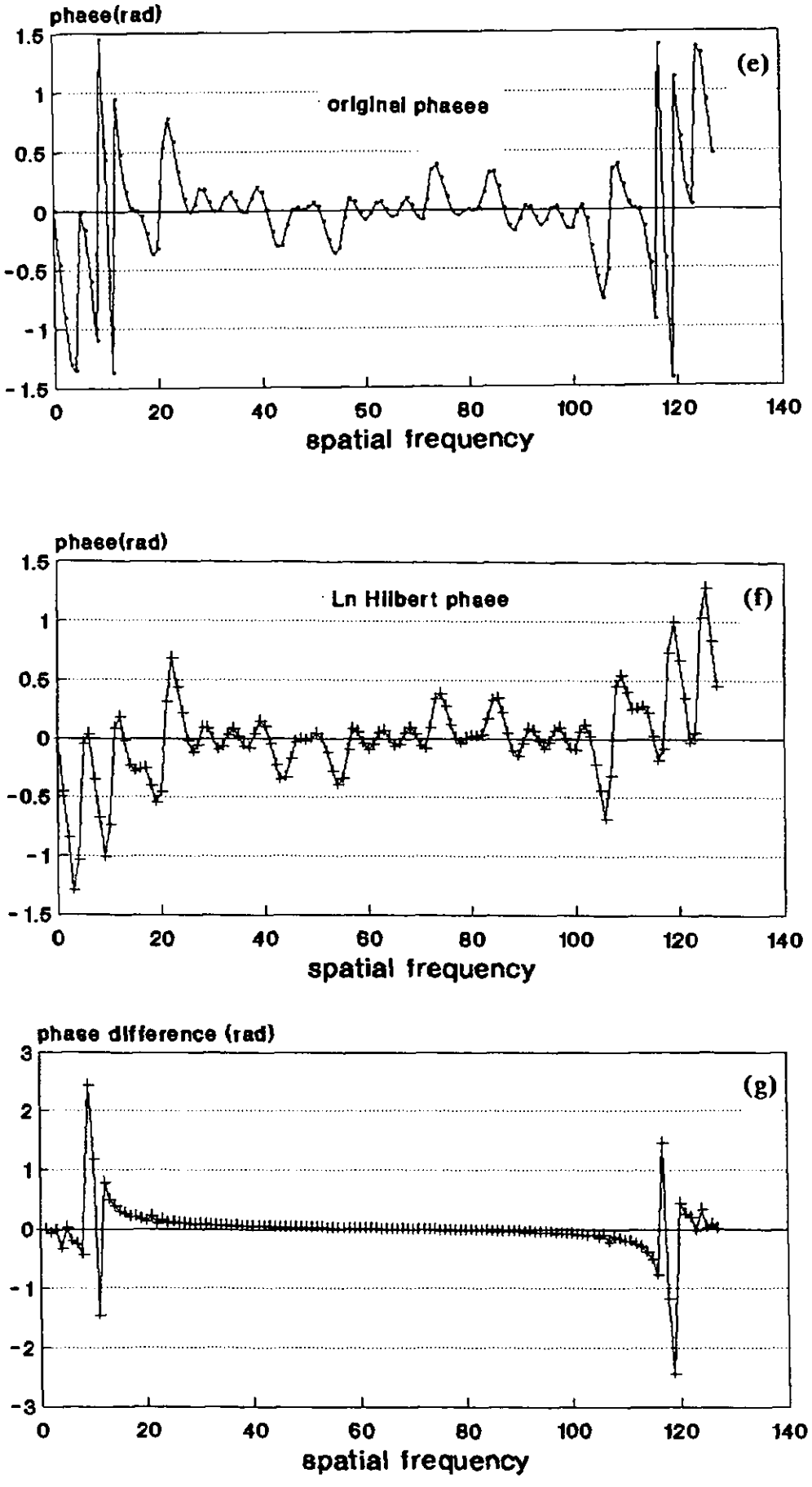

Figure 6.16: (e)-Original phases; (f)-Ln Hilbert restored phases from the spectrum of figure 6.16c; (g)-Difference between the original phases and the restored phases.

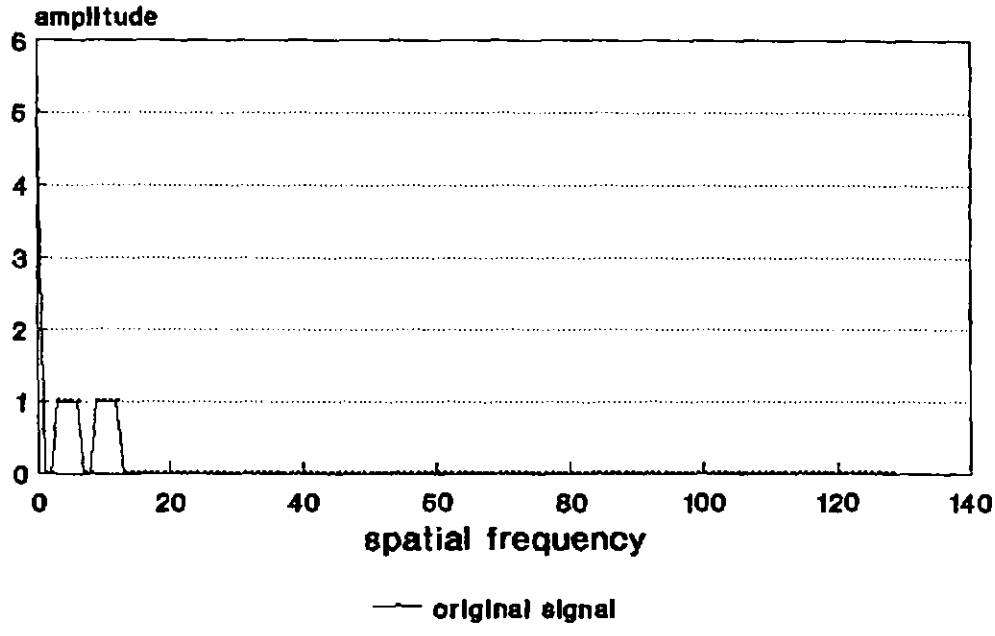

Figure 6.17a: The original object sequence compressed by a factor of 8.

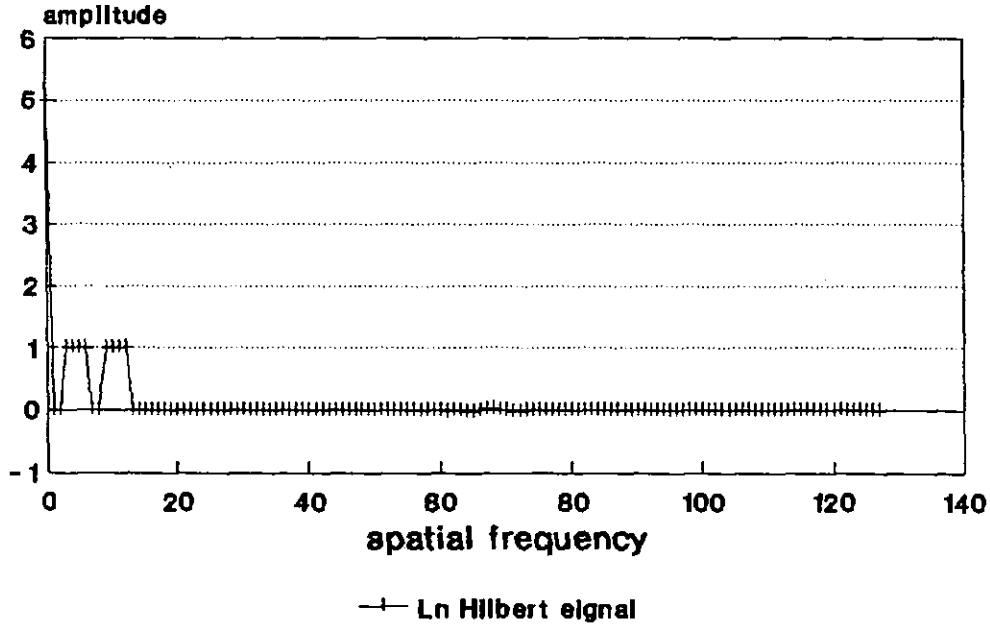

Figure 6.17b: Ln Hilbert restored version of the object, from the Fourier modulus spectrum of figure 6.17c.

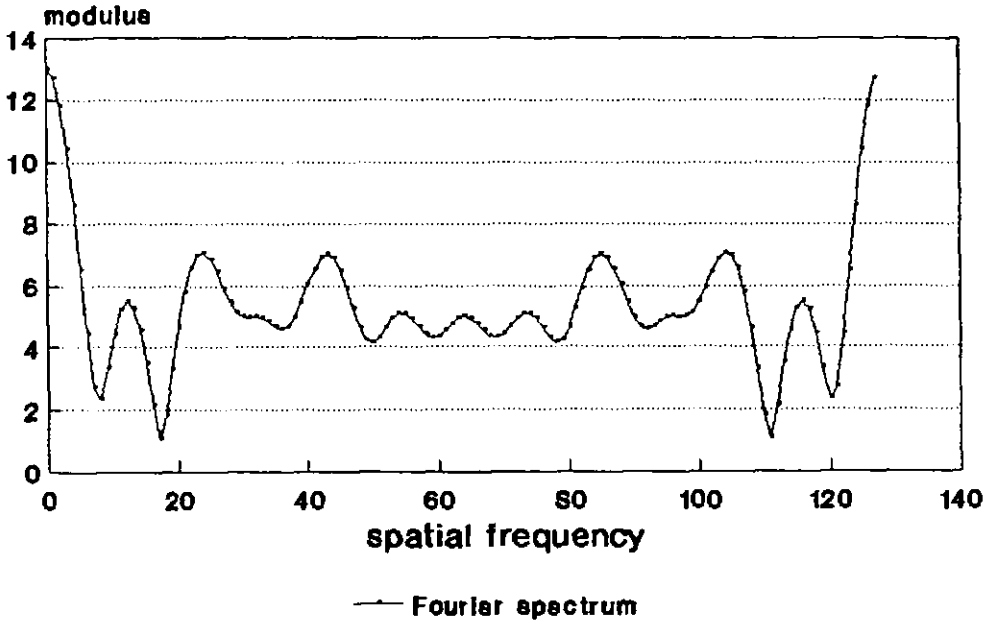

Figure 6.17c: Fourier modulus spectrum of the compressed object of figure 6.17a.

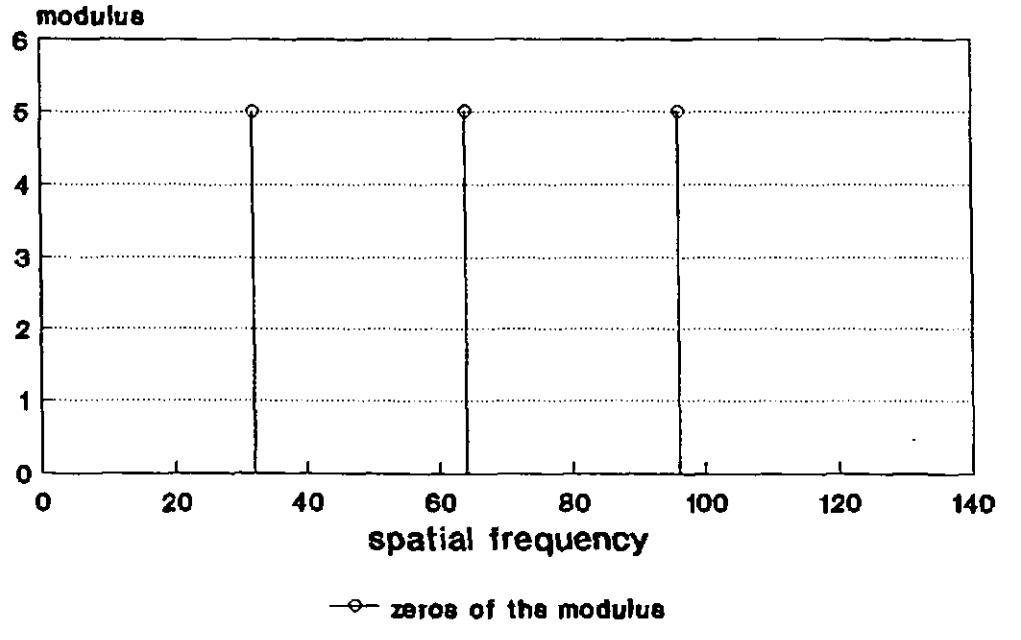

Figure 6.17d: Population of zeros in the Fourier modulus spectrum of figure 6.17c which have all been replaced by minima. To clearly indicate the position of zeros, all spectral components in figure 6.17c have been suppressed.

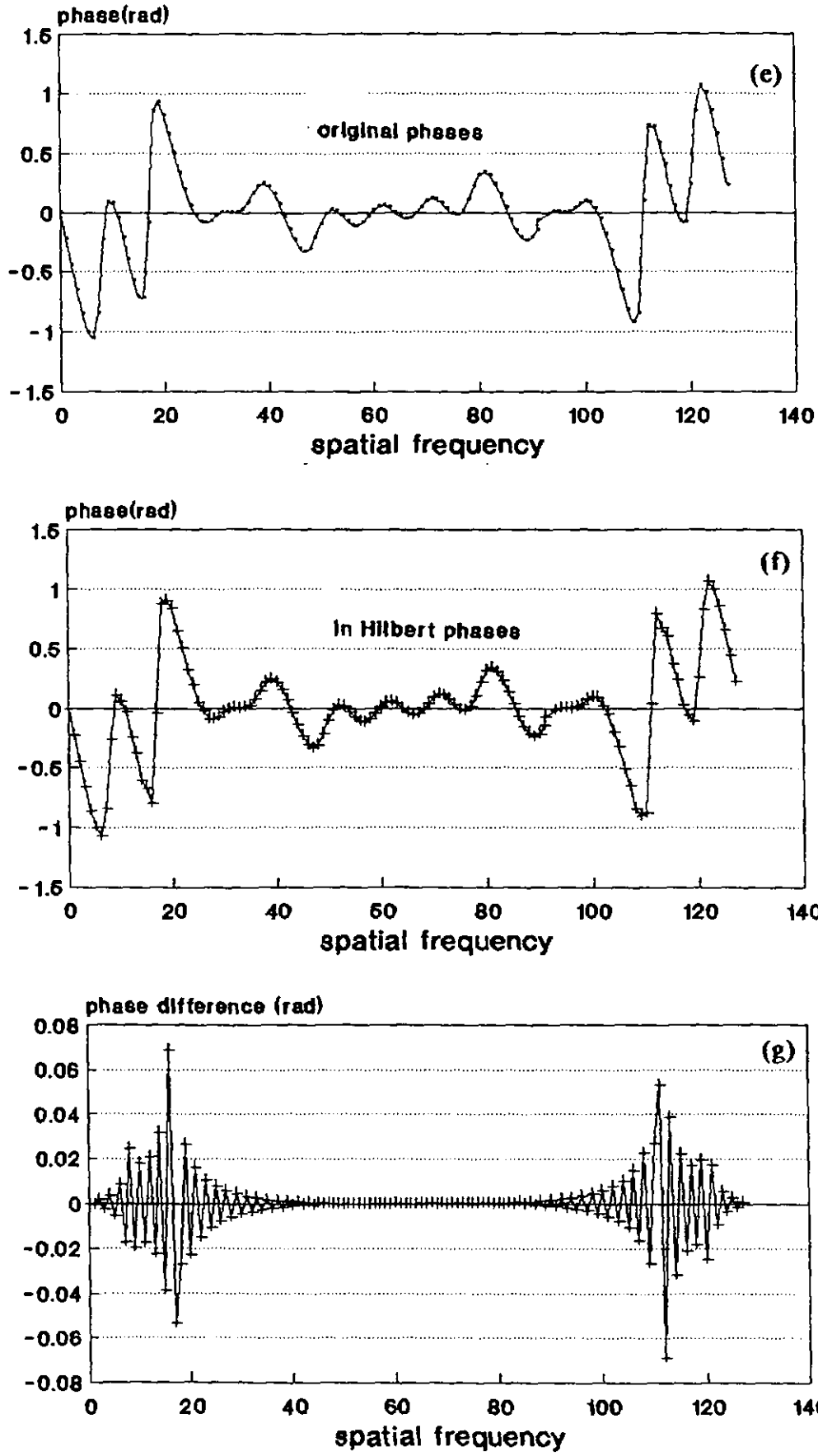

Figure 6.17: (e)-Original phases; (f) Ln Hilbert restored phases from the spectrum of figure 6.17c; (g)-Difference between the original phases and the restored phases.

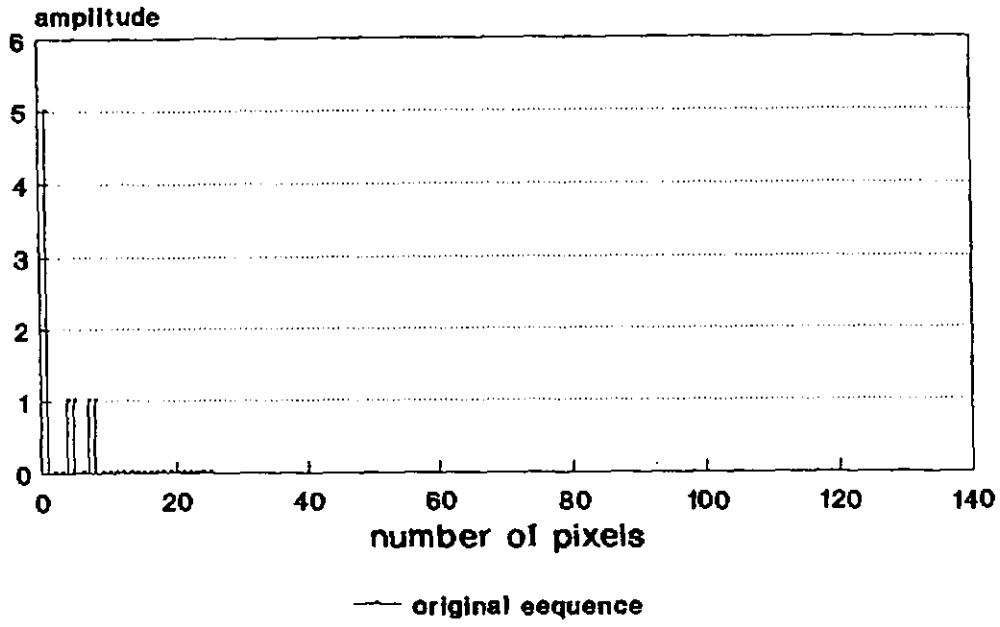

Figure 6.18a: The original object sequence compressed by a factor of 16.

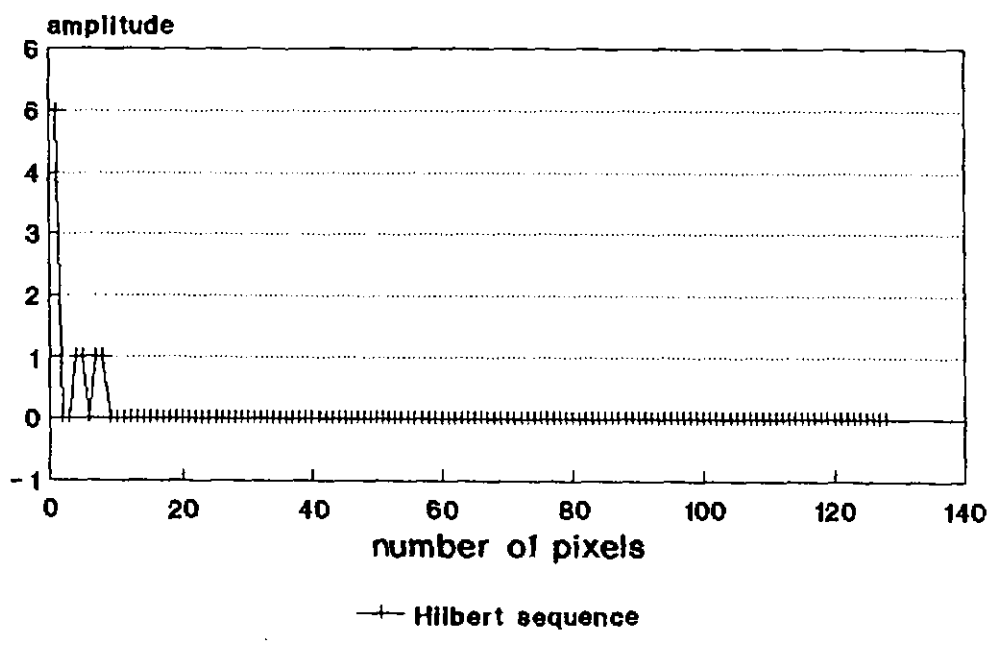

Figure 6.18b: Ln Hilbert restored version of the object, from the Fourier modulus spectrum of figure 6.18c.

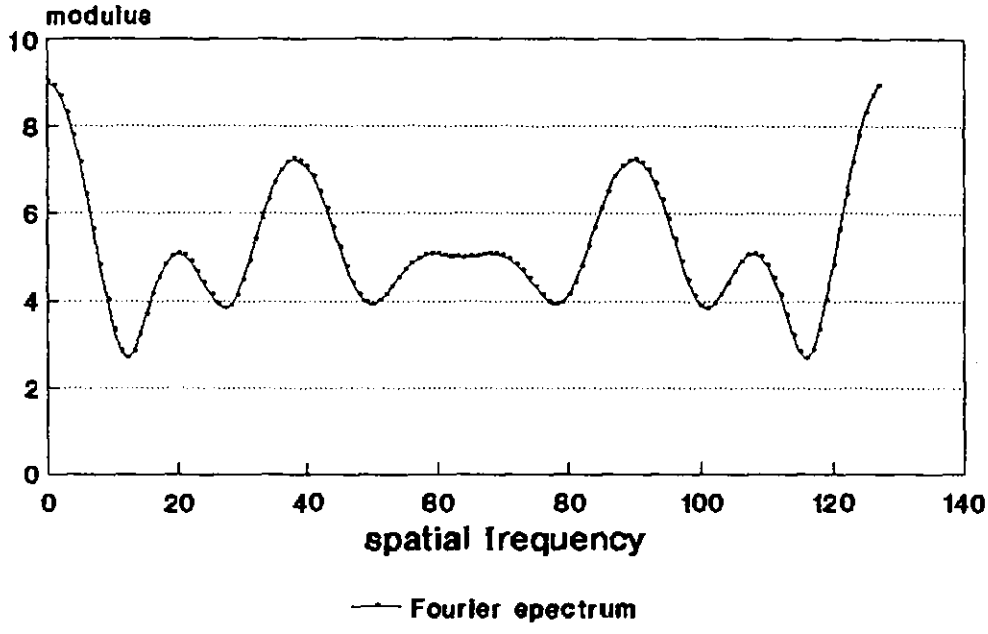

Figure 6.18c: Fourier modulus spectrum of the compressed object of figure 6.18a.

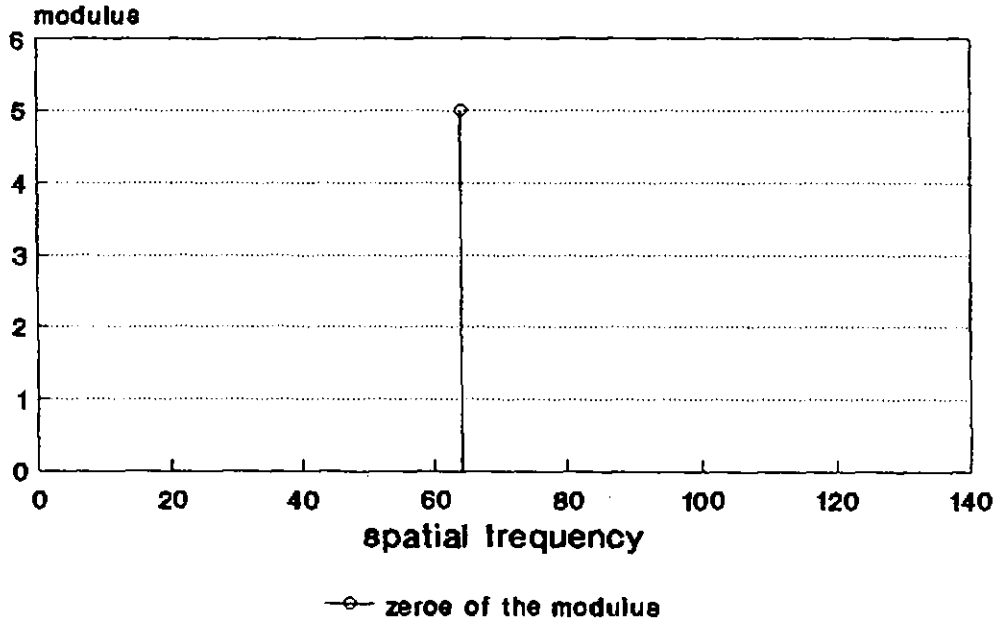

Figure 6.18d: Population of zeros in the Fourier modulus spectrum of figure 6.18c which have all been replaced by minima. To clearly indicate the position of zeros, all spectral components in figure 6.18c have been suppressed. Note that the zero population bas almost disappeared.

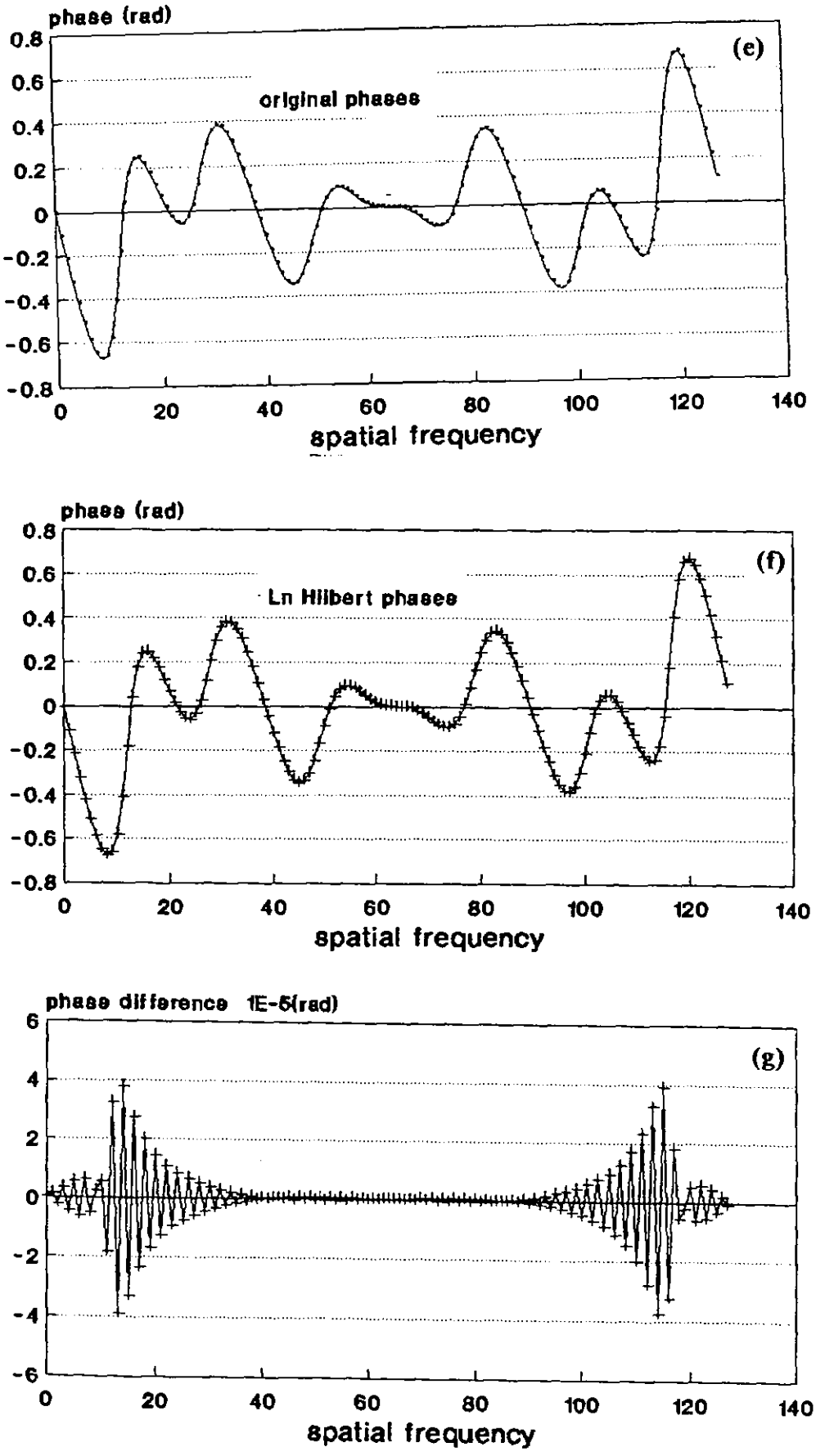

Figure 6.18: (e)-Original phases; (f) Ln Hilbert restored phases from the spectrum of figure 6.18c; (g)-Difference between the original phases and the restored phases.

6.6.1 Application of the Fourier scaling principle to the restoration of non-repetitive objects

Compression factors of x16 may seem rather harsh on the original object as the object itself would suffer from lack of definition, due to the reduction in the overall pixel resolution across its profile. The point that needs to be raised at this stage is that any repetition in the object characteristics would be a sign that the spectrum needs to undergo a higher compression factor as compared to a single object. This fact has already been explained in section 6.3, where the influence of repetition on the modulus characteristics was described in detail.

This section, performs another case study for the restoration of a 1-D object sequence but not in repeated form. The study reveals that although the spectrum does possess discontinuities, its envelope appears less impulsive than the repeated version of a similar sequence. This study proves that, depending on the geometrical structure of the object, non-repetitive profiles need not undergo severe compression in order to be restored.

Figures 6.19-6.22 present the original object sequence and the Ln Hilbert restored sequence which has been superimposed upon it for better comparison. The object is adequately recognisable in figure 6.21 after only experiencing a scale change of x4 without further need for reduction in its overall extent. However, for a repetitive sequence, whose repeats maintain the same number of pixels across, it can be inferred from the previous study, that a scale change of at least x16 needs to be introduced to initiate a reasonable reconstruction of the object. Table 6.2b illustrates the values of the total squared error in the retrieved object signal, both prior to scaling and also after consecutive change of scale. Note that although not leading to a perfect match, a total squared error of 1.532×10^{-1} still puts the reconstruction in a recognisable format.

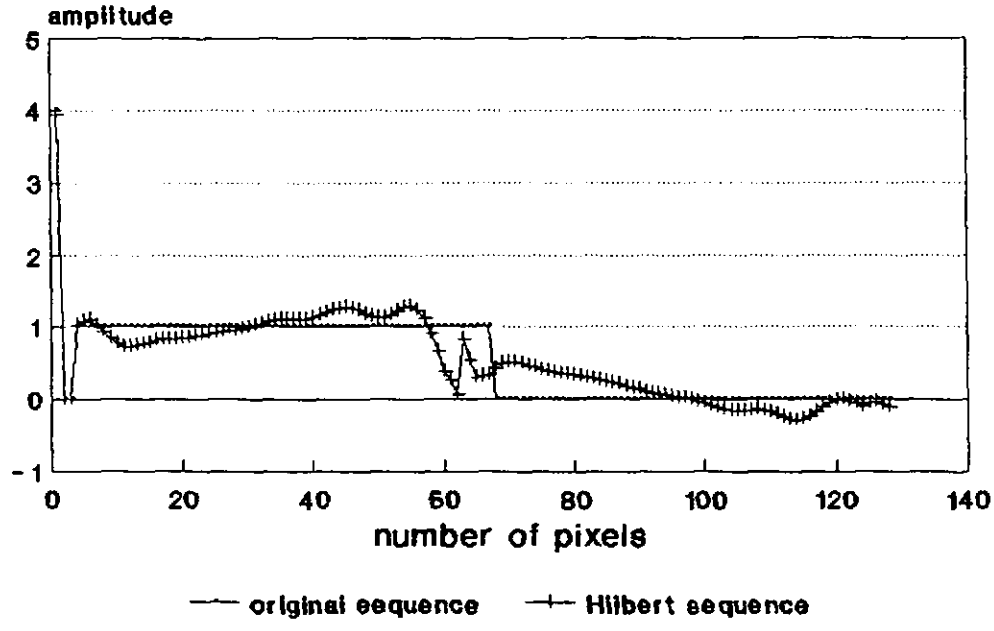

Figure 6.19: Comparison of the original sequence with the Ln Hilbert restored sequence prior to changing the scale of the object.

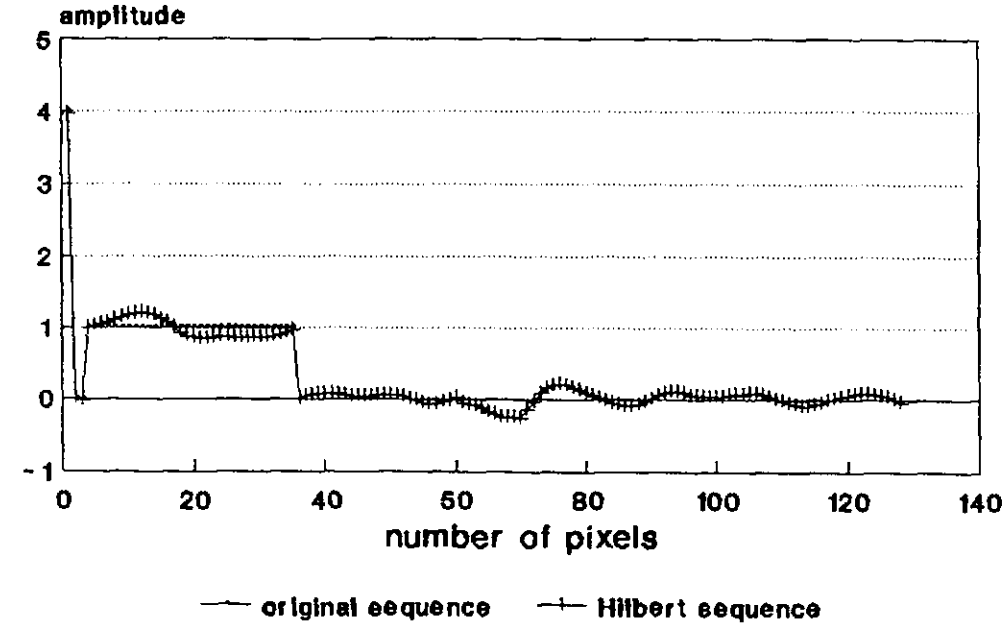

Figure 6.20: Comparison of the original aod the restored characteristics of the object after being reduced in scale by a factor of 2.

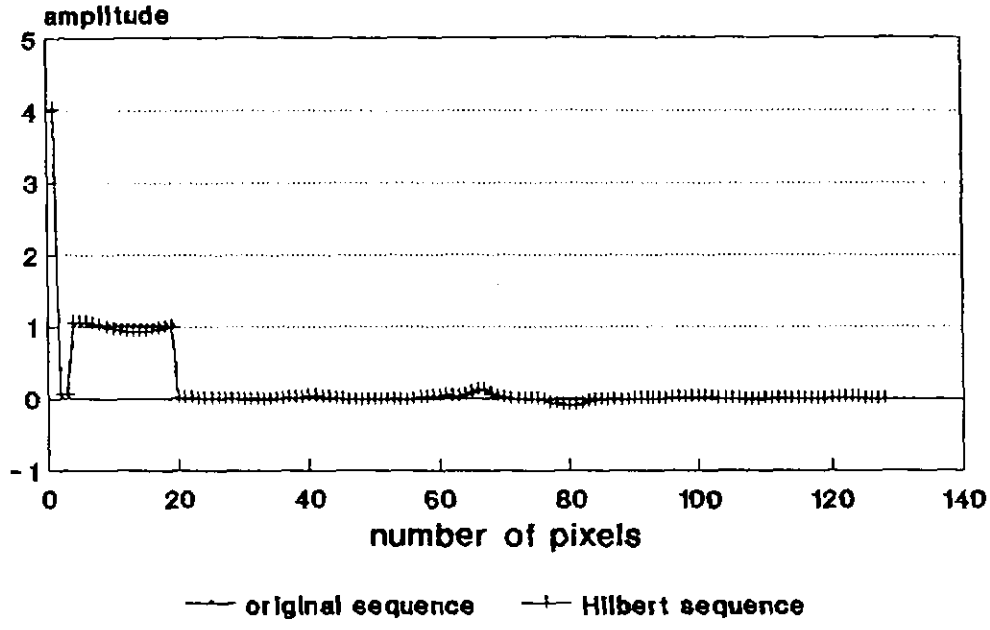

Figure 6.21: Comparison of the original and the restored characteristics of the object after being reduced in scale by a factor of 4.

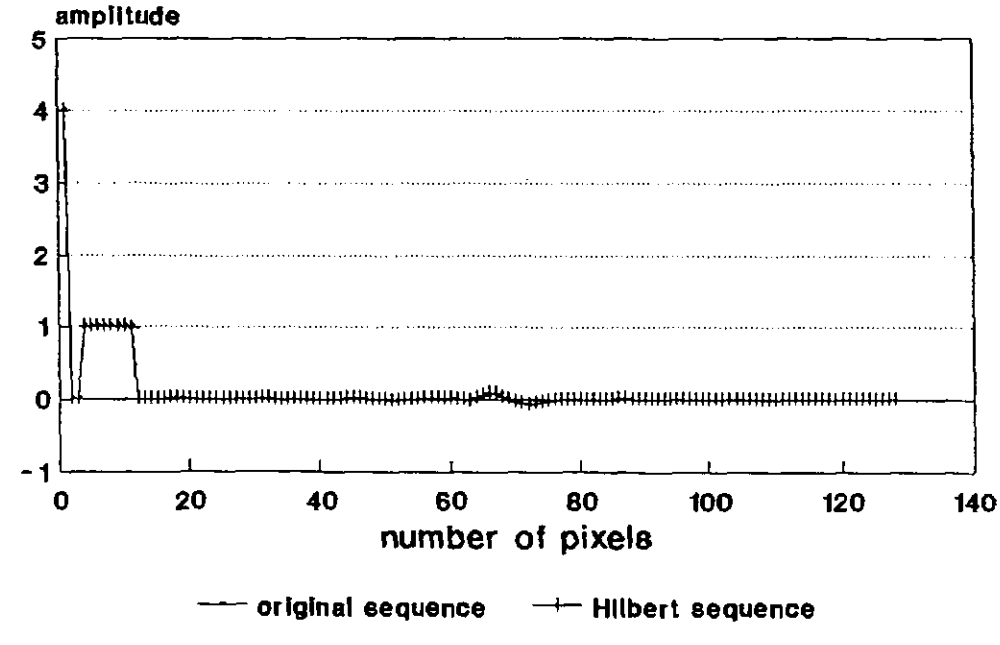

Figure 6.22: Comparison of the original and the restored characteristics of the object, after being reduced in scale by a factor of 8.

scale of the object	object without compression	object with ×2 compression	object with ×4 compression	object with ×8 compression
$\sum E_{total}$ total squared error	8.768	1.336	1.532×10^{-1}	3.595×10^{-2}

Table 6.2b: The trend in the total squared error for a non-repetitive object with consequent compression in its scale.

So far, the study has been centred around one-dimensional object sequences whose overall change in scale has been represented in graphical form. For multi-dimensional objects, it is informative to visualise the relative size of the object with respect to its surrounds before the change in scale is deemed effective. Figures 6.23a-6.23i is the application of the scaling principle, to a non-repetitive multi-dimensional object. The restored versions of the object in figures 6.23h and 6.23i are equally acceptable. It is inevitable that every reduction in the scale of the object takes us one step further in improving the reconstructions, however in an attempt to obtain a perfect match through progressive compression, the restored object would be so small that it would be barely recognisable as part of a large surround.

What should also be emphasised is that the modulus characteristics are completely blind to where the object is located. In figure 6.23, although the object is located in the centre of the large surrounding data window this information is not coded into the modulus spectrum. Consequently, the restored version of the object would have no sense of position and can appear anywhere within the surrounding perimeter. In figures 6.23g, 6.23h and 6.23i the retrieved versions of the object are in the bottom left hand corner of the data window as opposed to the central position that they originally occupied. Provided the overall integrity of the object is maintained in its concise form, loss of size or possible difficulty in locating the object, are trivial matters particularly when the unscaled information is unlikely to result in a favourable outcome.

Repetition and impulsive behaviour go hand in hand. When confronted with highly impulsive characteristics, it would be more advantageous to enforce a correct reconstruction of the object even at the expense of perceiving it on a smaller scale than to settle for a reconstruction that undermines the true behaviour of the object.

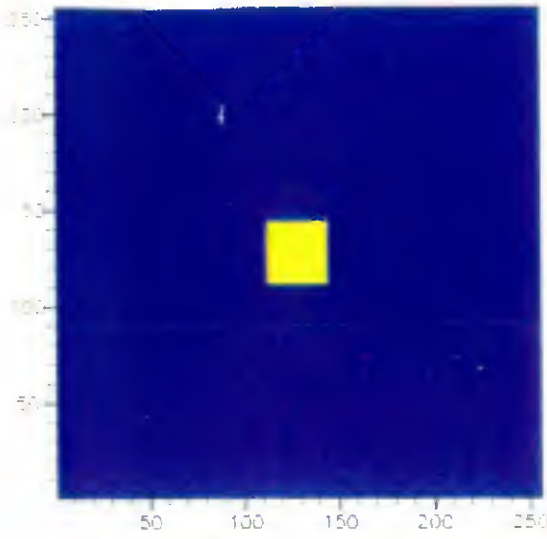

Figure 6.23a: Original object.

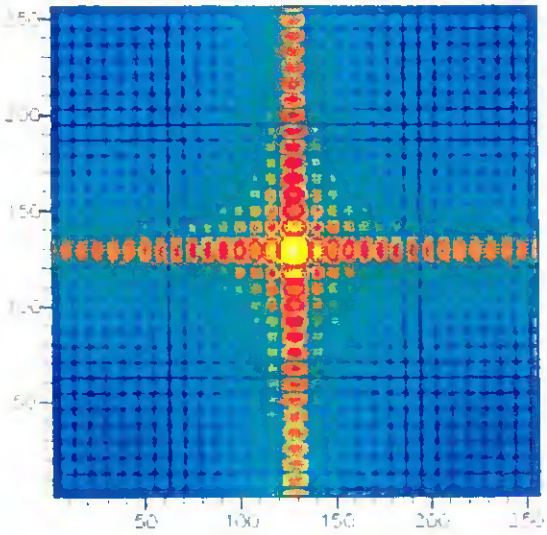

Figure 6.23b: Fourier spectrum of the object in figure 6.23a.

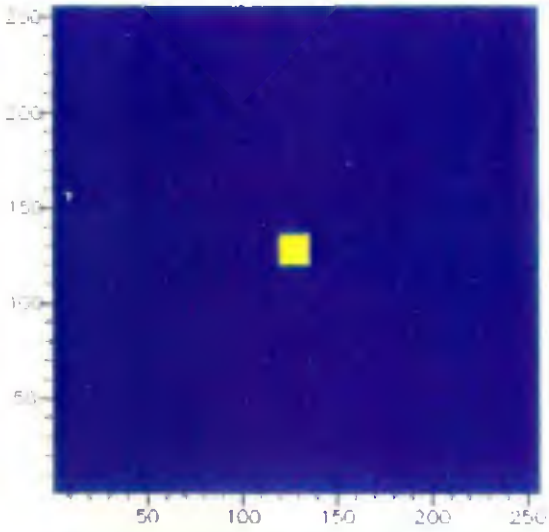

Figure 6.23c: Object compressed a factor of 2.

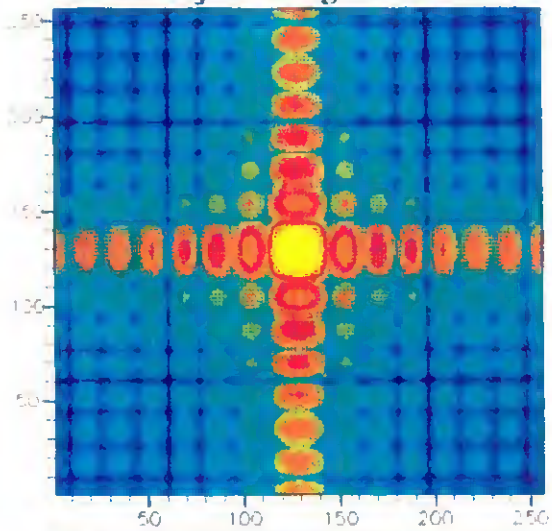

Figure 6.23d:Fourier spectrum by of the object in figure 6.23c

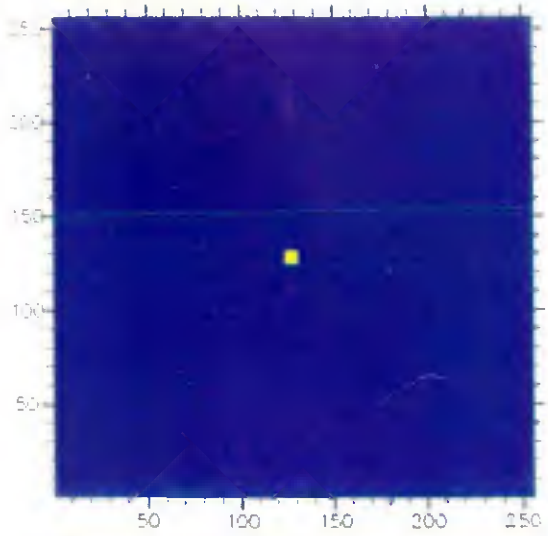

Figure 6.23d:Object compressed a factor of 4.

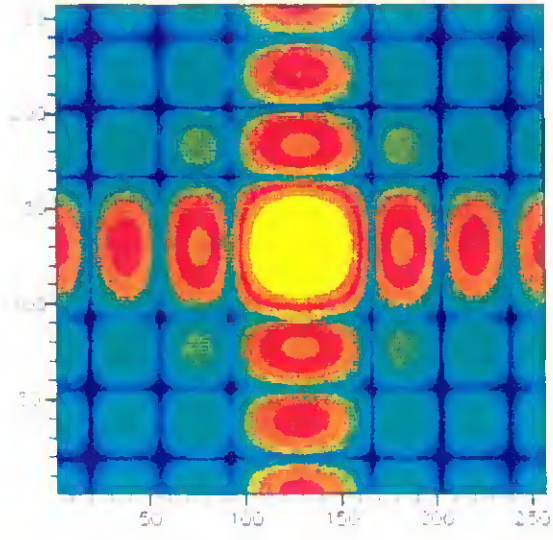

Figure 6.23e:Fourier spectrum by of the object in figure 6.23d.

Figure 6.23:Application of the scaling principle to the restoration of a multi-dimensional object. Figures 6.23a-6.23i illustrate the relative size of the object with respect to its surround before the change in scale is deemed effective.

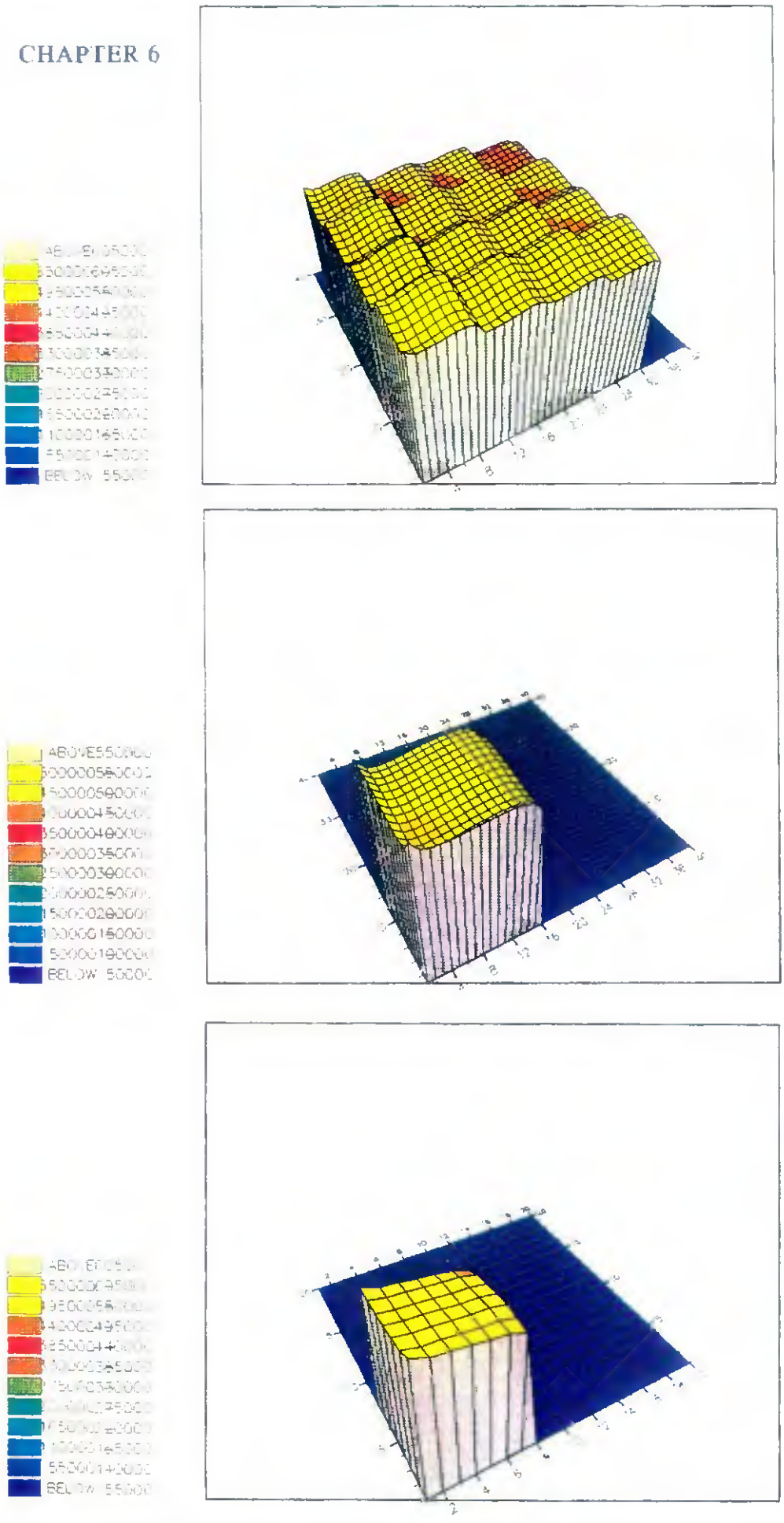

Figure 6.23: (g)- Restored version of the original object from spectrum of figure 6.23b; (h)- Restored version of the object from the expanded spectrum of figure 6.23d; (i)- Restored version of the object from the expanded spectrum of figure 6.23f.

Reduction in size is not too high a price to pay, particularly when the lost resolution can be revived through interpolation. This philosophy has already been exercised in chapter 5.

The next section, puts the scaling philosophy into a final test, i.e the restoration of the geometrical structure of a real object specimen from the modulus of its frequency characteristics.

6.7 Putting the Philosophy into test: Application of the frequency scaling principle for the restoration of a repetitive object specimen (N.Sotoudeh, *et al.*, 1994), (N.Sotoudeh, *et al.*, 1993)

Figure 6.24 shows the photo-micrograph of the reflectance object which is to be restored via the logarithmic Hilbert transform integral. The bright regions consist of chromium which has been deposited on to a glass background. The dimensions of square features are 100μm x100μm with a 50μm spacing. The image of this object was then digitised via the travelling optical microscope and used for generating the two-dimensional Fourier modulus spectrum. In order to achieve optimum contrast for the object, the background contribution for the square array in the spatial domain has been set to zero. The computer generated Fourier modulus spectrum has many discontinuities appearing as cuts in the Fourier plane. As mentioned earlier on any isolated discontinuity would appear as a singularity to the modulus and any connected regions of discontinuities appearing as cuts can not be handled by the Hilbert integral. In order to restore the continuity of the logarithm of the modulus, a constant level has been added to the modulus data.

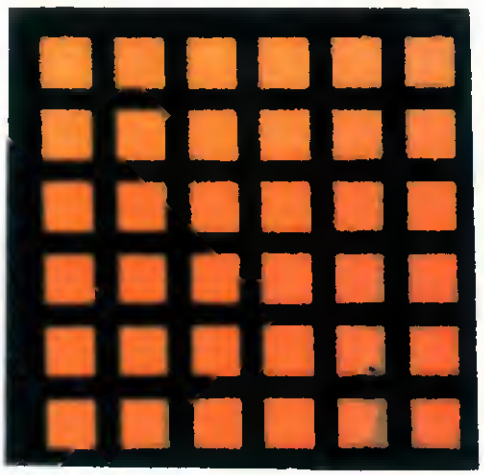

Figure 6.24: Photo-micrograph of the reflectance array. Square features are 100μm x 100μm with a 50μm spacing.

The logarithmic Hilbert transform integral is then applied to each strip of the Fourier modulus spectrum $|F(u,nc)|$ for the whole array to evaluate the phases along each line. In order to convert these one-dimensional phases $\phi(u,nc)$, into a

coherent pattern of two-dimensional phases, the phases along an orthogonal direction through the origin are evaluated $\phi(0,v)$, and added to the phases of each horizontal strip passing through the corresponding vertical point. The two-dimensional phases are then inverse Fourier transformed with the available moduli to arrive back at the object's reflectance profile.

Figure 6.25a shows the digitised image of this array prior to being compressed. Figure 6.25b is the corresponding Fourier spectrum. The spectrum contains many regions of discontinuity whose level has been raised. The restored object profile, is distorted due to many errors arising from phase variations for a spectrum which has many minima. In particular, when the intensity lobes have very rapid variations sampled by few pixels across, inaccuracies in phase values are imminent.

Figure 6.26a is the same array of reflectance objects compressed by a factor of x3 in the overall size but retained as part of a data matrix of size 256x256 pixels. The immediate expansion of the new Fourier spectrum can be seen in figure 6.26b. A comparison of the expanded spectrum with the original in figure 6.25b, reveals how the new spectrum appears as an interpolated version of the previous characteristics, which mainly incorporates the lower to medium range of the previous spectral data.

Although the restored object in figure 6.26d is undoubtedly a very close reconstruction of the original behaviour, there is still room for further improvement by subjecting the object specimen to yet another change of scale, whilst bearing in mind that the compressed versions of the object entail fewer imaging pixels across. Reduction in the number of imaging pixels across the object, would only pose as

a problem when the sampled information falls short of the minimum required rate i.e the Nyquist rate. Provided the object is sampled by sufficient pixels, so as to comply with the minimum rate depicted by the sampling theorem, it is worth a while compressing the characteristics until a perfect match is achieved.

A further compression of the object scale by a factor of x6, in figure 6.27a, which is also the final limit for bringing on a change of scale in this case, would still cultivate the continuity amongst spectral components and install a more faithful reconstruction as seen in figure 6.27d. Apart from a slight shift in the position of the restored object in figure 6.27d, the original pattern and its retrieved version are virtually indistinguishable. However, as previously noted, by reducing the overall size of the object, pixel resolution in the spatial domain would be degraded. This implies that one cannot enhance resolution optimally in both domains (R.Ramirez, 1985). Much enhanced resolution in the frequency domain, is accompanied by a loss of resolution in the object domain in terms of the available pixels. Therefore, object compression can only be afforded up to a point whereby a reasonable fraction of the object characteristics are still preserved when subjected to an overall scale change. For the type of object specimen being studied such degree of compression has been exercised with the assumption that chromium regions were free from any structural characteristics, such as a flaw or scratch whose structural detail would not survive through severe compression of the object scale.

Finally, to provide a clear image of the enhanced continuity amongst the spectral components, the central region of the frequency spectrum of figures 6.25b, 6.26b and 6.27b has been plotted on both linear and logarithmic scale. Figures 6.28 and 6.29 show the three spectral characteristics corresponding to the object and its compressed versions. Enhanced continuity has also been accompanied by an overall

reduction in the population of the zeros in the expanded frequency spectra. This can be seen in figure 6.30 whereby lines of zeros shown as cuts have been reduced and pushed out of the frequency characteristics which then can be conveniently ignored.

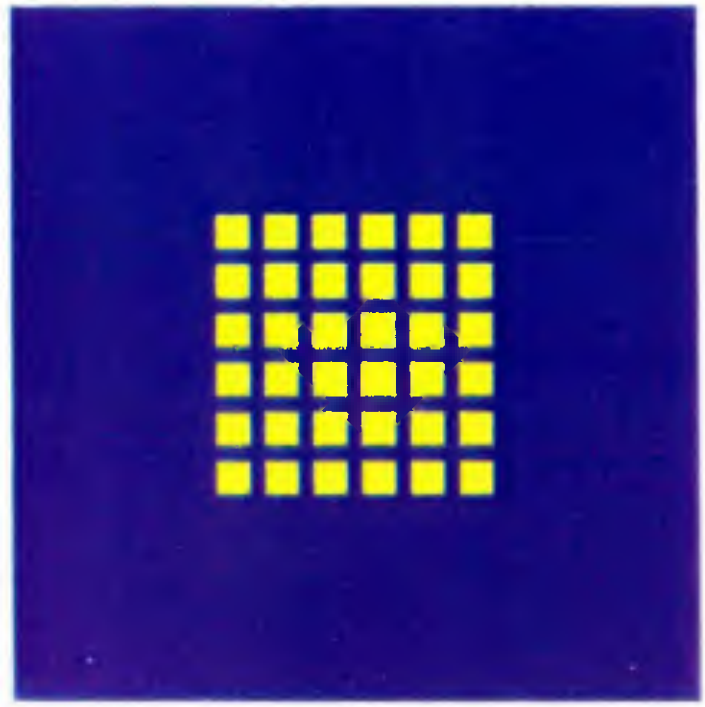

Figure 6.25a Original reflectance profile without compression.

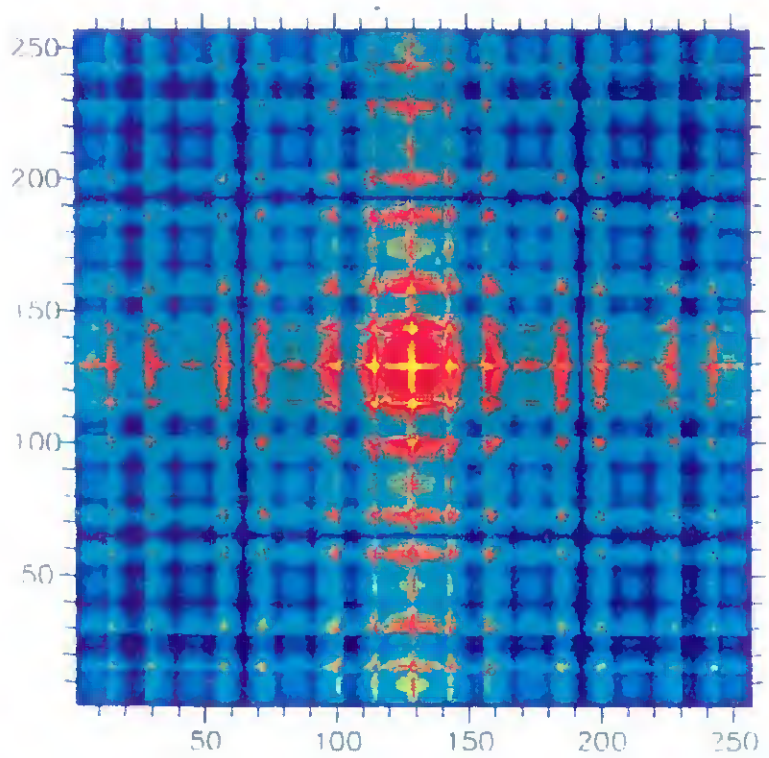

Figure 6.25b Fourier modulus spectrum of the original object of Figure 6.25a

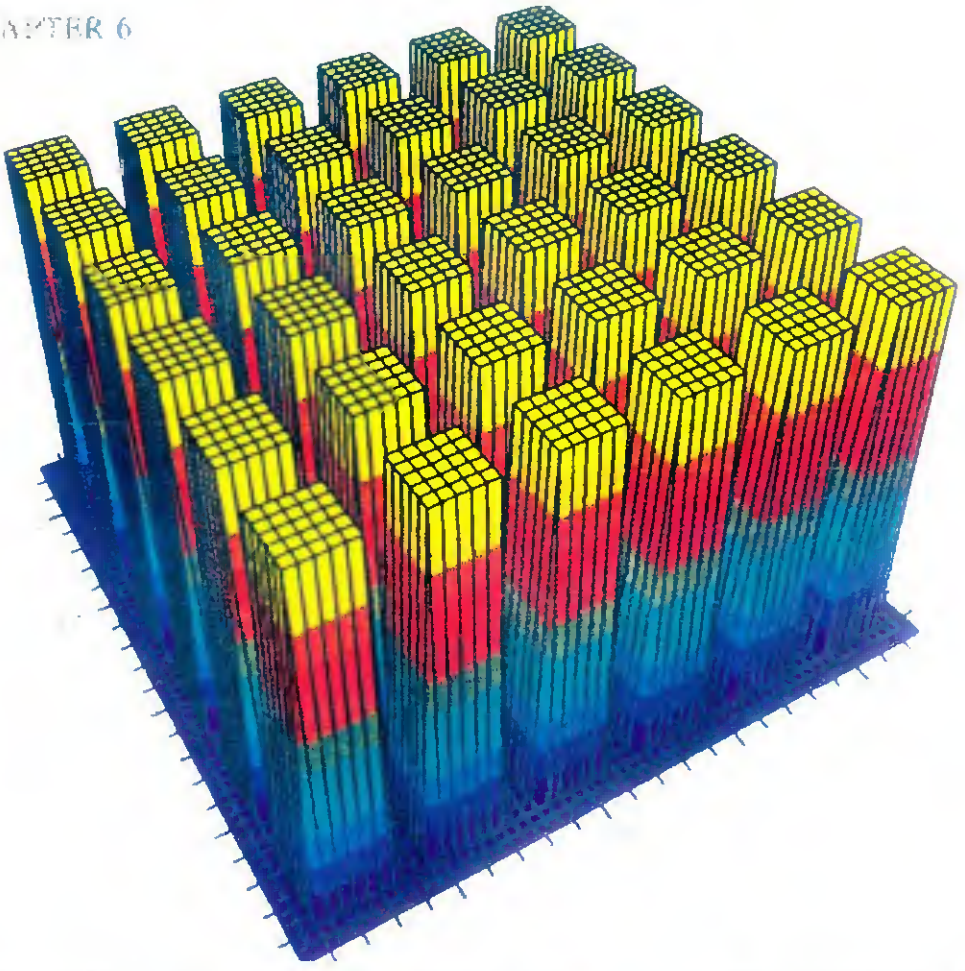

Figure 6.25c : 3D view of the original reflectance profile of Figure 6.25a.

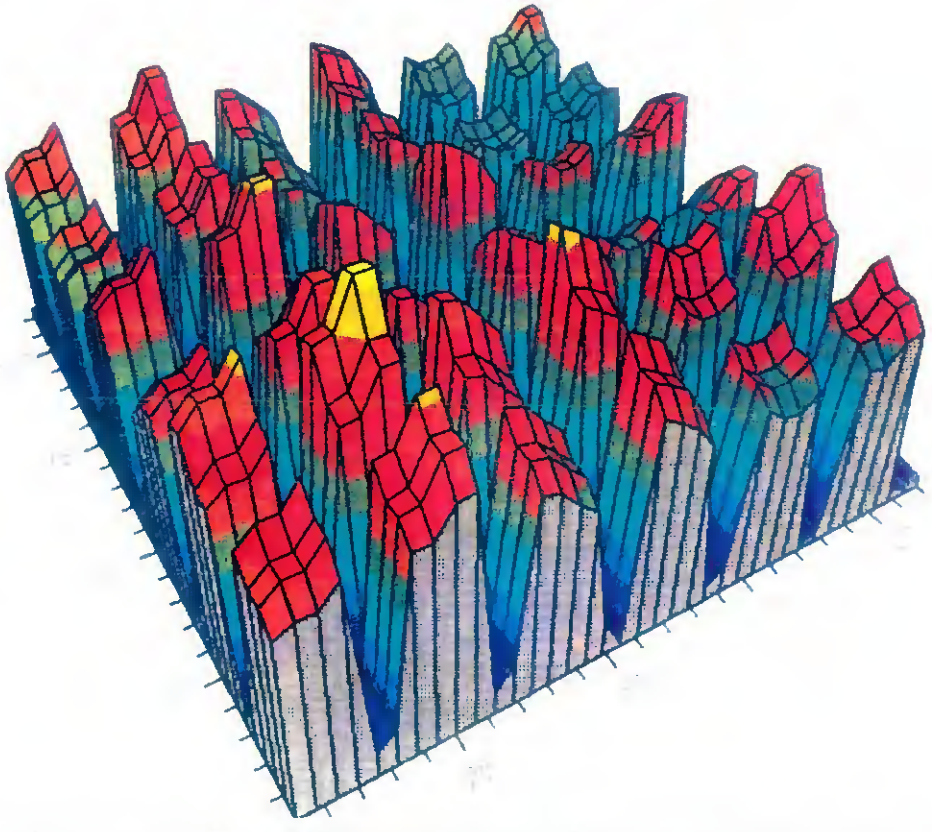

Figure 6.25d : 3D view of the reconstructed reflectance profile of the object from the Fourier modulus spectrum of Figure 6.25b

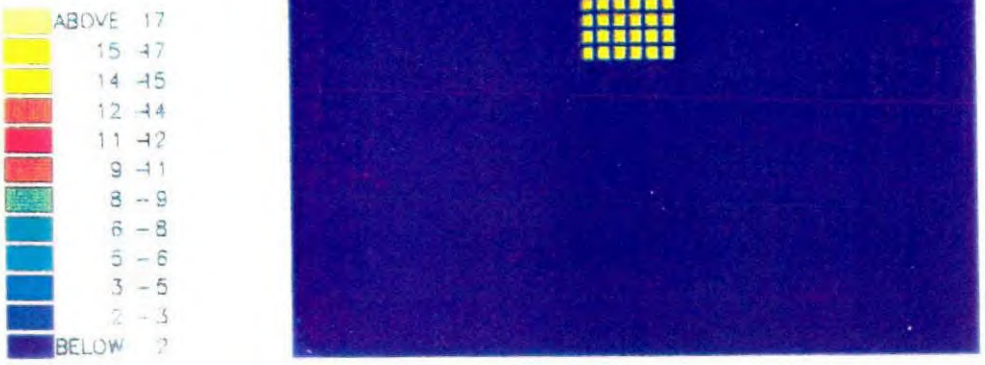

Figure 6.26a : Original reflectance profile compressed in size by a factor of 3.

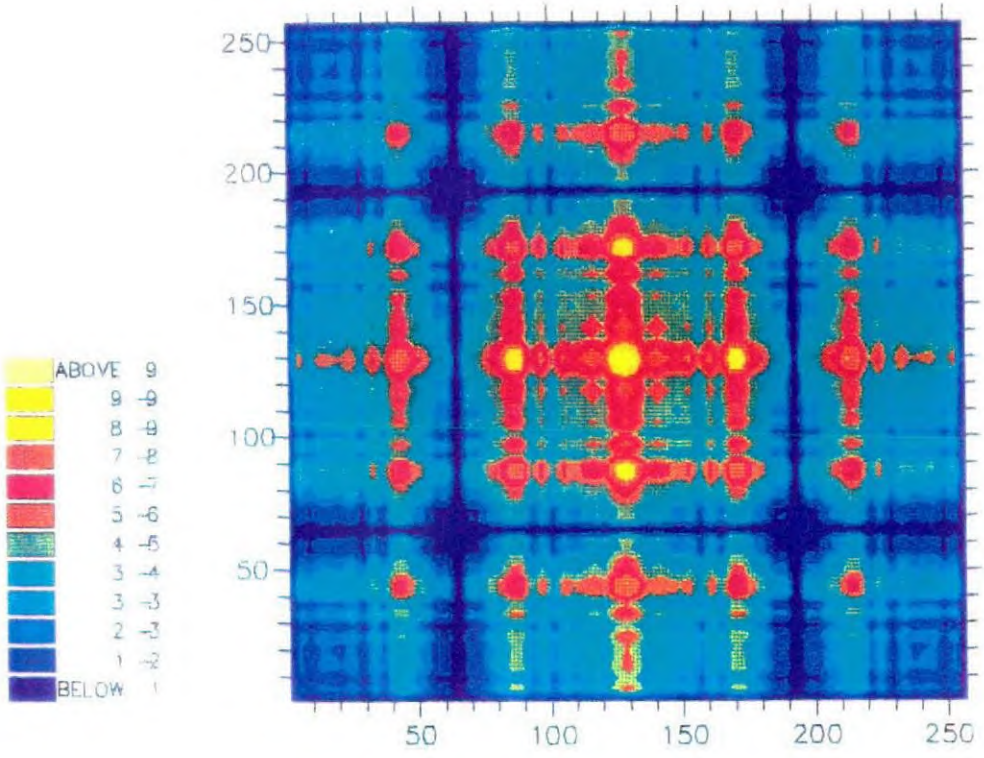

Figure 6.26b : Fourier modulus spectrum of the compressed object of Figure 6.26a.

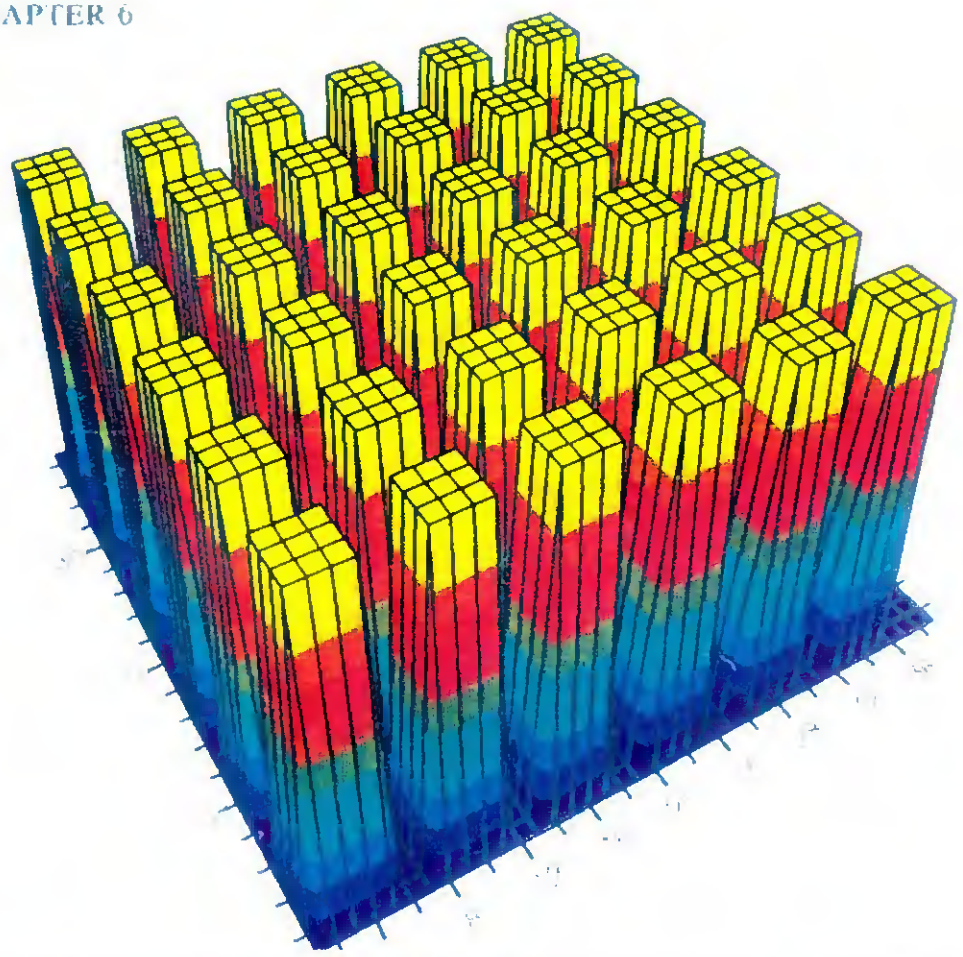

Figure 6.26c : 3D view of the original reflectance profile of Figure 6.26a.

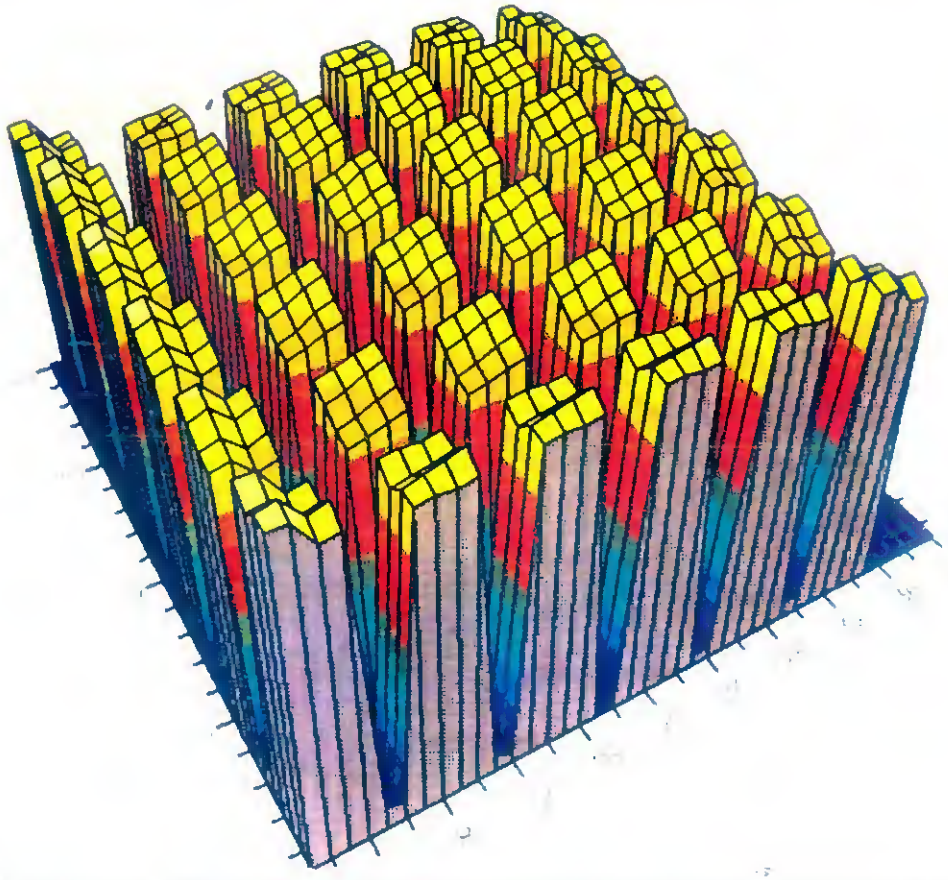

Figure 6.26d : 3D view of the reconstructed reflectance profile of the object from the Fourier modulus spectrum of Figure 6.26b

Figure 6.27a Original reflectance profile compressed in size by a factor of 6

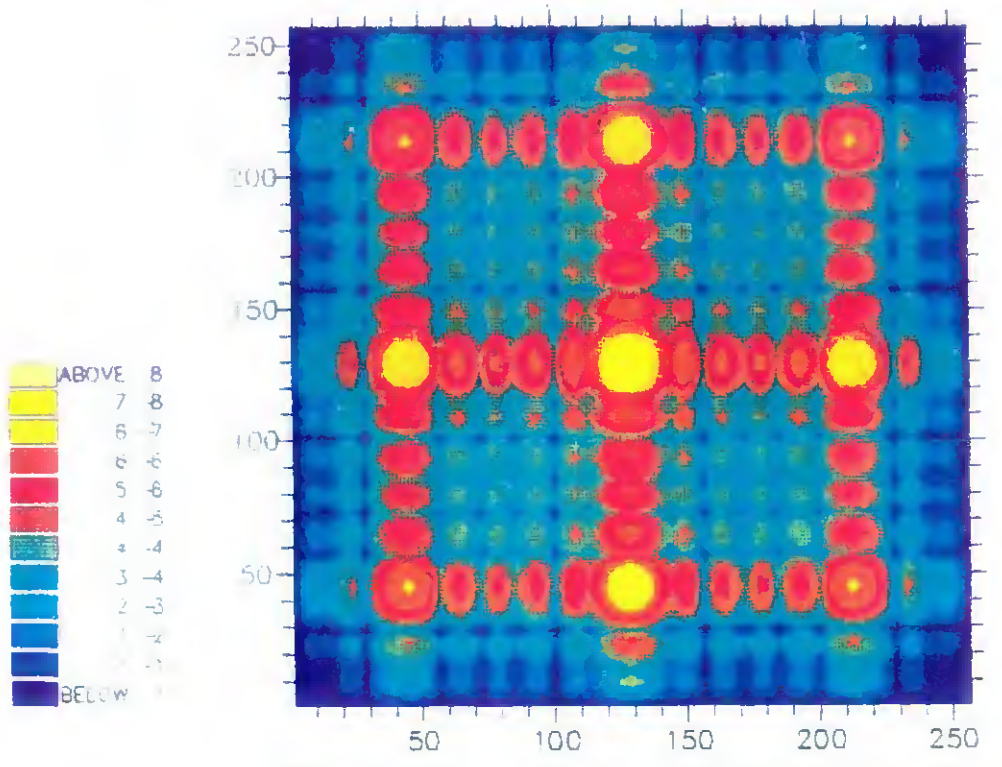

Figure 6.27b Fourier modulus spectrum of the compressed object of Figure 6.27a

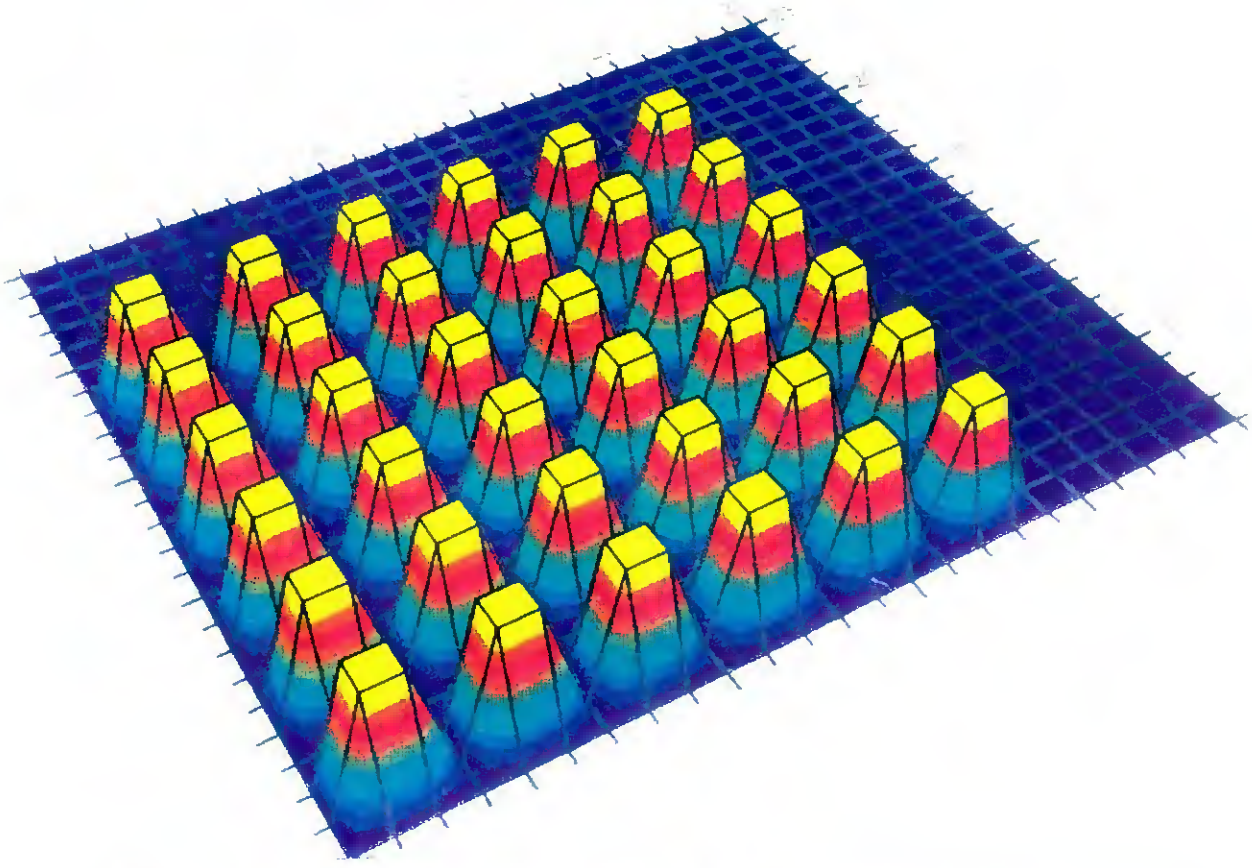

Figure 6.27c 3D view of the original reflectance profile of Figure 6.27a

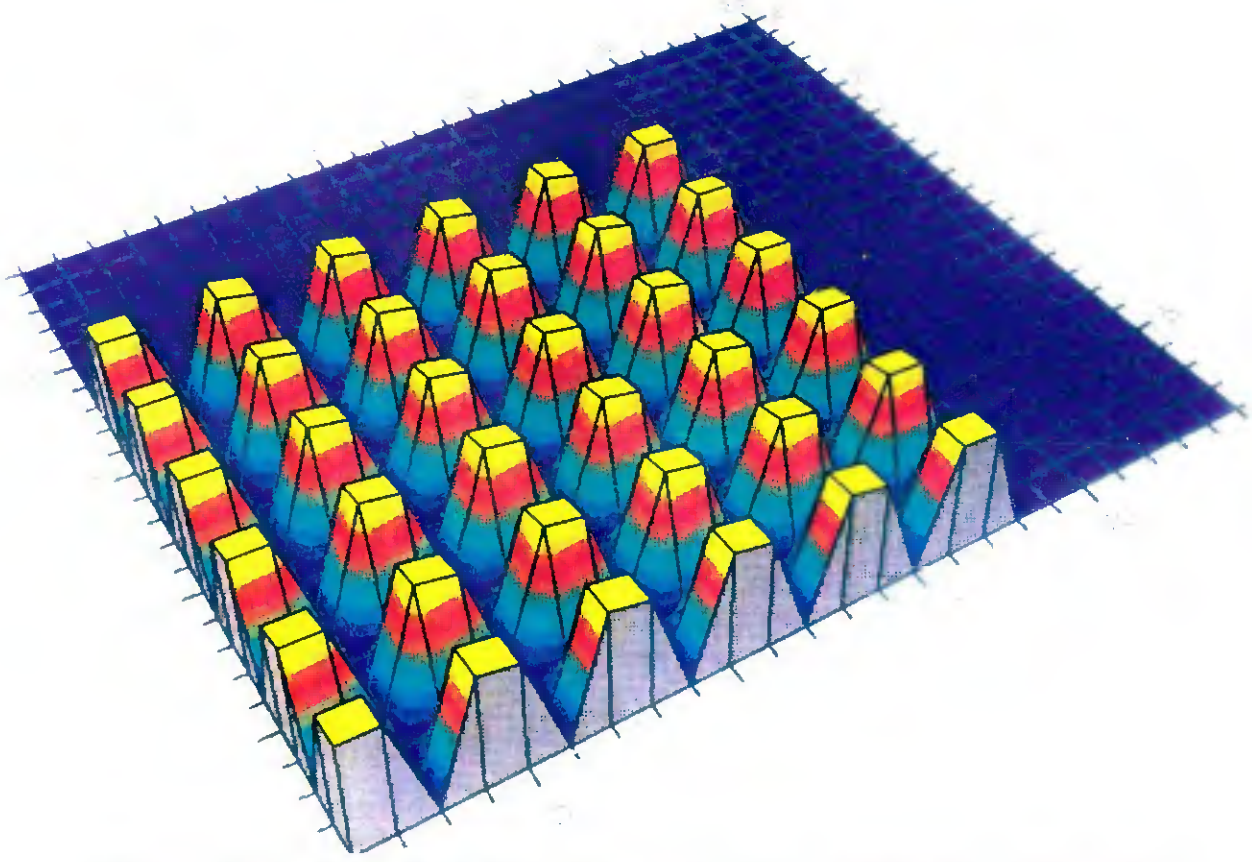

Figure 6.27d 3D view of the reconstructed reflectance profile of the object from the Fourier modulus spectrum of Figure 6.27b

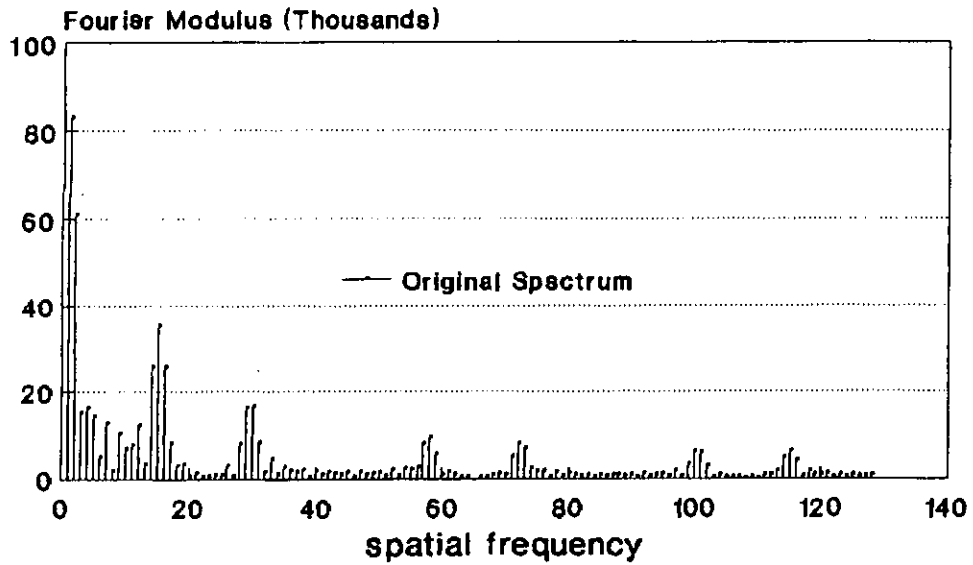

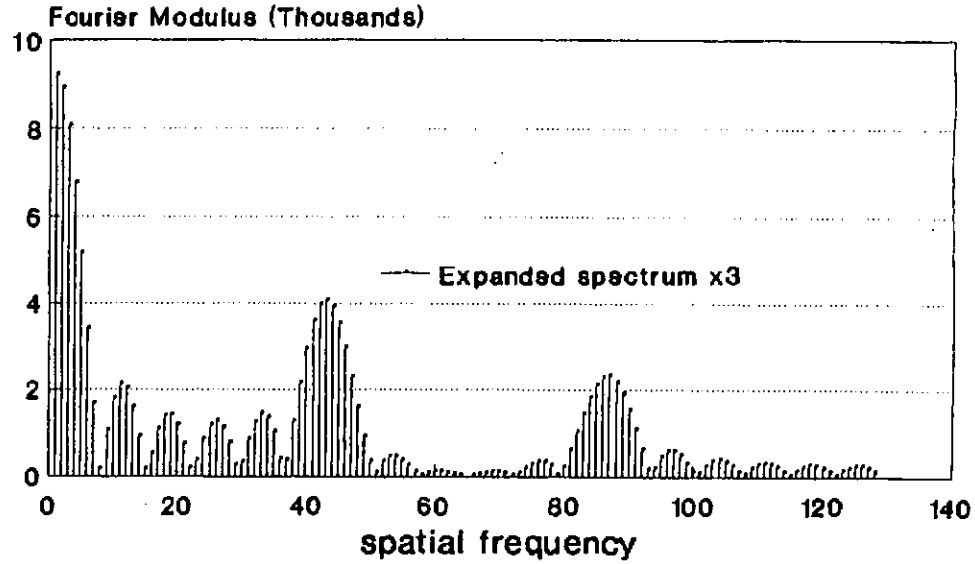

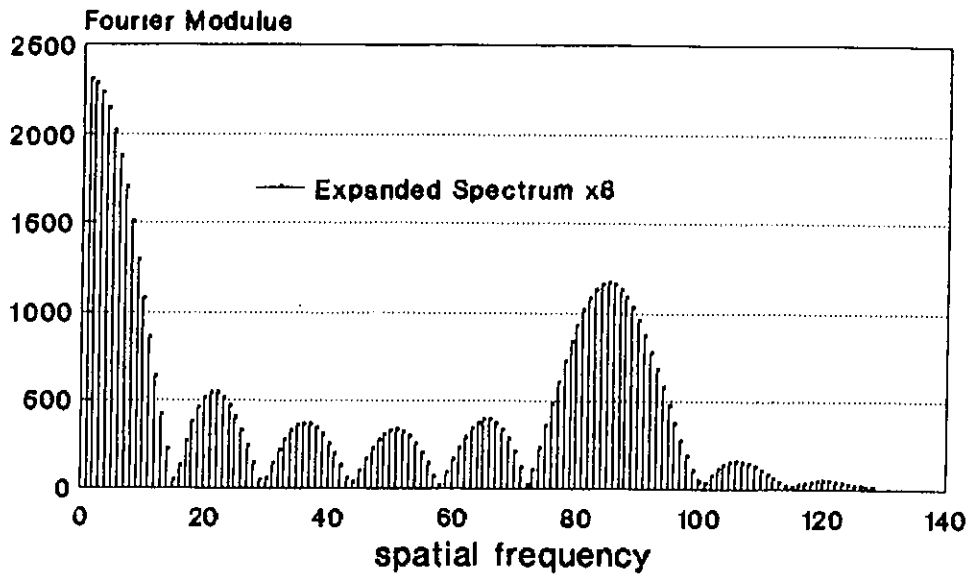

Figure 6.28: Cross section of the central region of the Fourier modulus spectrum for the object array and its compressed versions on linear scale.

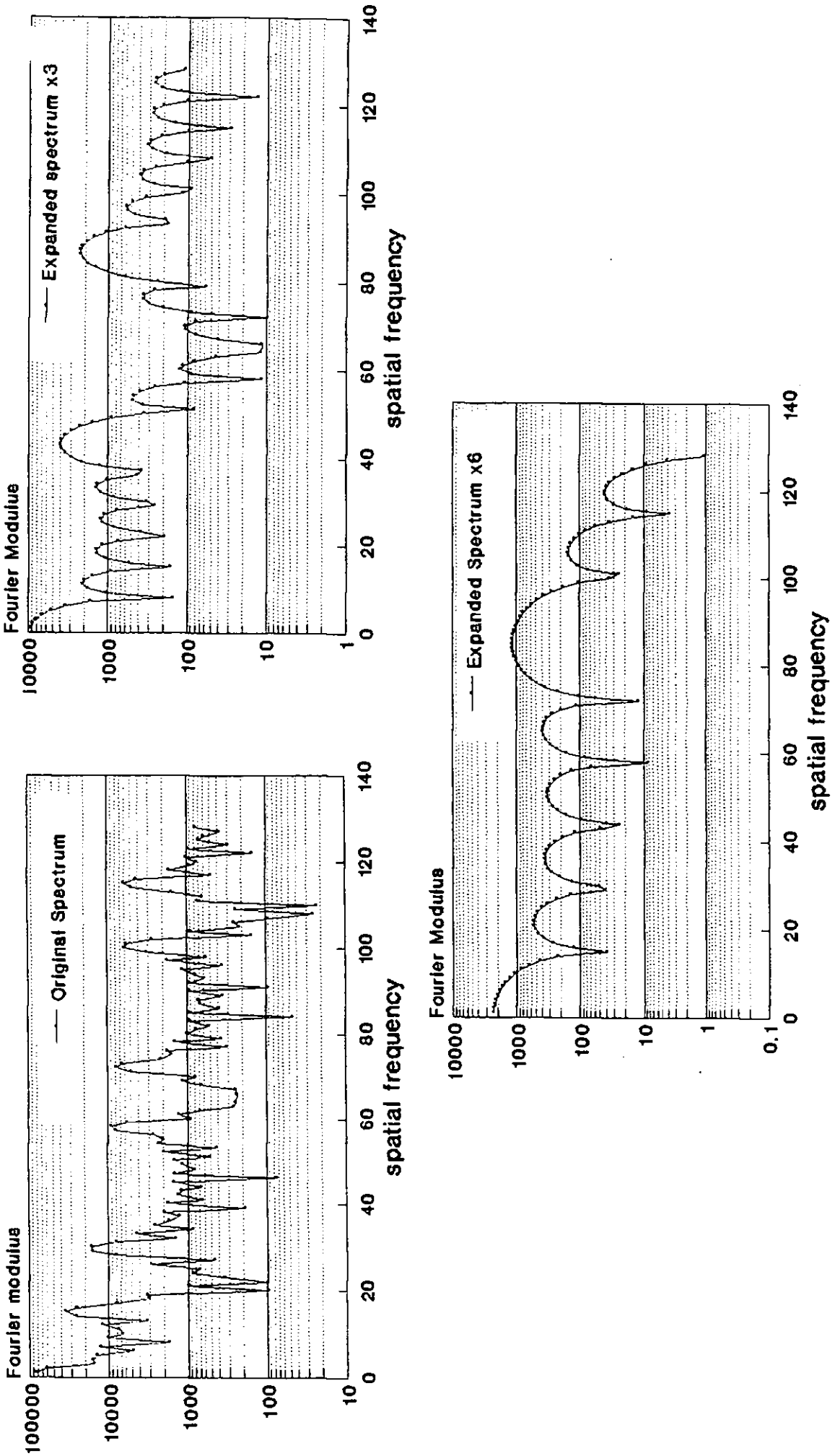

Figure 6.29: Cross section of the central region of the Fourier modulus spectrum for the object array and its compressed version on logarithmic scale.

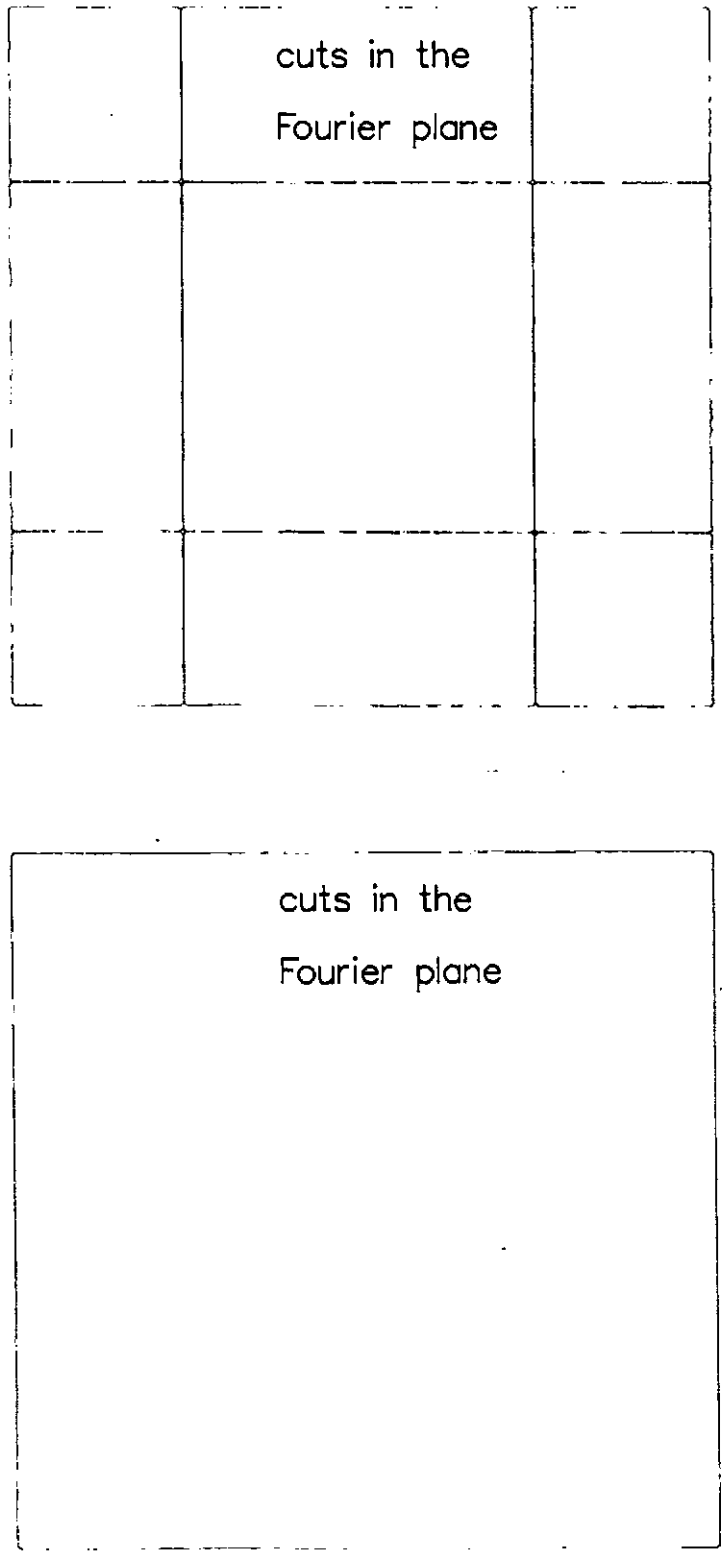

Figure 6.30: (a)- Population of zeros for the original spectrum of figure 6.25b and (b)- Population of zeros for the expanded spectrum of figure 6.27b; all other spectral components have been suppressed to show the connected discontinuities or cuts more clearly.

6.8 Reflecting on what has been achieved

Many researchers have come to realise that the success of phase retrieval cannot be pinned to one single technique. It is likely to be more effective when a number of disparate techniques are combined together, instead of exhausting one single method. To extend the scope of Hilbert transformation beyond its current use, the **"scaling philosophy"** has been put forward as a novel means of outcasting the many undesired features of the spectral characteristics of real type object surfaces. These object surfaces can have many isolated regions as part of their spectral characteristics which defies the basic needs for continuity which are demanded by the Hilbert transformation.

Complementing the non-iterative qualities of Hilbert transformation, the scaling philosophy has shone new light into the retrieval of real type object geometries which would have otherwise been impossible to recover through the conventional use of Hilbert transformation alone. The most desirable and outstanding aspect of a "scale related " operation is that whilst it promotes continuity and well-behaviour, which are much sought for qualities in favour of a Hilbert related operation, it does so entirely without undermining the intelligence of the retrieved object in any form. Compression or expansion of the spectral data merely readjusts the scale of the object via an inverse dimensional relationship. Therefore all the geometrical details of the object remain intact but just appear different in size in proportion to the rest of the object which has undergone a change in scale.

However, the consequent expansion of spectral characteristics has been rewarding in the sense of smoothing out the spectral variations, reducing minima and isolated regions, and enhancing the continuity amongst spectral components.

Indeed, this rearrangement of the spectral components ***has*** proved to be a more reliable configuration for extracting the unknowm phases (N.Sotoudeh, *et al.*, 1992), (N.Sotoudeh, *et al.*, 1994).

This fact has been shown extensively by the author in a number of independent studies on both one-dimensional and two-dimensional sequences. The improvement and faithfulness in the retrieved phases and consequently the restored object has been shown numerically, in terms of an error metric defined as the total squared error, $\sum E_{total}$. This parameter shows the sum of the squared differences between the original and the retrieved version of the signal. Reasonable recoveries usually happen when $\sum E_{total}$ is in the region of $6.7x10^{-2}$-$9x10^{-2}$ (M.Hayes, *et. al*, 1983) or ideally much lower. In two studies conducted on a repetitive and a non-repetitive object, prior to re-scaling, there were large discrepancies between the original and its retrieved version, which was also reflected in the high value of $\sum E_{total}$, namely $\underline{1.388x10^{1}}$ for the repetitive object and $\underline{8.768}$ for the non-repetitive object.

However, at the on set of re-scaling, the total squared error $\sum E_{total}$ was reduced from a value of $\underline{1.388x10^{1}}$to an exceptionally low value of $\underline{1.857x10^{-9}}$ for the repetitive object; and from a value of $\underline{8.768}$ to $\underline{3.595x10^{-2}}$ for the non-repetitive object. Both improvements were brought on fairly rapidly by merely re-scaling the spectral characteristics a few times, a major issue when one compares this approach with iterative techniques. Many iterative reconstructions run well into one hundred and one thousand of iterations before they are brought to an end depending upon the nature of the outcome. Similar to the total square error parameter used in this study to evaluate the nature of the outcome, in majority of iteratively based studies, a mean square parameter is used as a performance criterion.

Evidential facts (Feinup, 1978, 1987) reveal that this parameter, is reduced by a factor of 2 in every one hundred iterations. In the quest for minimising this parameter, one might be installing more and more iterative loops, only to find that the outcome is unsatisfactory. This happens to be the case when, apart from the modulus information, there is no other additional information available prior to commencing the iterations. Why indulge in time consuming computations not knowing the outcome, when a mere rearrangement of spectral components can pilot a reasonable reconstruction of the object with limited effort ?

In fact, a point which is most captivating about the scaling principle is that excellent recoveries can be achieved with very limited effort through "progressive re-scaling" of the spectral characteristics, knowing that every change in scale is productive in its own right. That is every change in scale makes the reconstruction one step closer to a perfect match. As has been shown by way of example for the non-repetitive and repetitive objects, such perfect match happens within the third and the fourth attempts of re-scaling with every attempt being an improvement upon its predecessor.

However, the outlook is quite different as far as iterative techniques are concerned. There is no guarantee that every iteration is productive. Although iterations are made to navigate in the direction to minimise the mean square error, this does not necessarily lead to a perfect match. The algorithm would be stuck at a point where it cannot minimise the error any further without having have reached a solution. When stagnation sets in, the algorithm has usually exhausted few hundred of such iterative loops; a seemingly worthless effort at the expense of excessive computer run time.

CHAPTER 6

The final testament to the effectiveness of the scaling principle has been the successful restoration of a real object specimen, namely an array of chromium features in the shape of 100um x100um squares, deposited on to a glass background occupying a total area of $0.85mm^2$. All in all, "three" attempts were made to retrieve the geometrical structure of this specimen on a three-dimensional scale.

A most remarkable recovery resulted just by exercising the re-scaling of the spectral characteristics of the object for the first time. Having witnessed the outstanding improvement by this one single operation, it was inevitable that a further change of scale brought on by a higher compression factor would lead to an exceptionally good reconstruction of the object. Apart from a slight lateral shift, the results show an excellent match between the retrieved structure of the object and the original version to the extent that is difficult to tell the two apart.

A note of warning regarding this technique however is that this is not a fully embracing theory, i.e, it would cease to be effective, when excercised to its extreme. This extreme is provoked when a solution is far from satisfactory, and the object is not capable of undergoing further compression to be improved upon. This border line was almost reached, when this object specimen was subjected to a compression factor of x6, in an attempt to perfect its reconstruction. Although, the chromium features have been restored in all faithfulness after undergoing quite a severe compression in size, had this not have resulted in an acceptable reconstruction, it would have been impossible to subject this pattern to a further change in scale.

There are limitations to how severely the object can be compressed, or equivalently its spectral characterictics expanded. The very principle as to how the scaling philosophy operates is a sound reminder of this. Taken to the extreme, when the scale of the object is reduced until it eventually diminishes to a point, its spectral characteristics expand until it ultimately reaches a continuum".

The message is that optimal resolution cannot be achieved in both domains. At the expense of losing pixel definition across the object in the object domain, one is gaining enhanced definition across its frequency samples in the sense of occupying a great deal more in the available frequency space. Thus, due to the very limited number of pixels across the compressed object, there might not be enough imaging pixels to describe the fine details of the object. Although, this is something that one should be aware of, it most certainly is not a set back. One can zero-pad the spectral characteristics in the frequency domain to interpolate the restored object in the object domain, thereby encouraging more pixels across the object.

What should also be noted, is the fact that excellent reconstructions have been made without altering the overall size of the data. Throughout this study, the number of the samples in the object domain and consequently, the number of the samples in the frequency domain have always been fixed. This implies that one need not necessarily increase the size of the frequency samples to foster a better reconstruction. The key to the success of scaling is merely the "rearrangement" of the spectral components within the existing frequency space. One need not insert extra samples in between, when the whole intelligence of the object is adequately preserved amongst the rearranged frequency data.

Finally, left last to be commented on, which is also the most pleasing aspect about the scaling principle, is the ease with which it can be implemented practically. Many ideas put across for solving problems are merely feasible under perfect simulation conditions, whereas problems start to surface when their usefulness is questioned under practical circumstances. This is not the case for the scaling philosophy. It has already been shown that such change in scale can be brought on in a number of ways, one of which i.e (i), has been thoroughly investigated and proved fully operational, these are:

(i) altering the scale of the transform via hardware, i.e the positioning of the camera;

(ii) altering the scale of the transform via software;

(iii) altering the scale of the transform by changing the illumination.

Up until now, the only propositions for bringing on a change in scale has been that involving methods (i) and (ii). A very novel approach is the use of the source of illumination to implement a scale sensitive operation in the Fourier space. Whilst in methods (i) and (ii) the re-arrangement of spectral data requires intervention on behalf of the operator, the third method automatically rearranges the spectral information in response to a change in the wavelength of illumination. This aspect of the work will be further discussed in plans for future developments of this technique in chapter 7.

CHAPTER 7

CONCLUSIONS AND FURTHER WORK

7.1 Summary and Conclusions

There are many imaging applications where one is faced with insufficient information to enable a faithful picture to be obtained. The insufficiency usually lies in the lack of phase information. Typical imaging applications where phase information is lost are in electron microscopy, space object imaging, speckle imaging and spatial frequency techniques based on diffraction throughout the whole electromagnetic spectrum.

As regards the reconstruction of a faithful image it is unfortunate that the phase information produced by the object is far more important than the information contained in the modulus of the spatial frequency spectrum of the object. Even in terms of capturing any identifiable aspect of the object, the modulus data on its own proves incapable of revealing the most simple distinguishing features of the object such as its borders, edges and corners all of which can be easily recovered from the phase information alone.

In the past, the inability of imaging systems to capture phase information coupled with the firm belief that phase, once lost, was irrecoverable has inhibited the investigation of techniques whereby meaningful phase might be substantially recovered from modulus information. Even if a faithful image cannot be achieved it might be possible to recover sufficient information for the characteristic features of the object to be classified. Such classification would find application in the assessment of surface objects.

CHAPTER 7

This research has been concerned with the feasibility of extracting phase related information from the intensity of the spatial frequency characteristics of the object. This research has demonstrated that in special circumstances it is possible to achieve high quality images which closely reproduce the three-dimensional structure of the original objects.

Even if the circumstances do not allow the recovery of phase information, there are certain applications where the modulus data can yield valuable information about the object even though a faithful image cannot be reconstructed.

Certain aspects of an object such as any form of regularity, collection of similar patterns or well defined behaviour, are directly coded into the frequency spectrum of the object and can be identified as part of the object behaviour without any recourse to the phase information. This opens up the possibility of object surface characterisation from the intensity of spectral components in the complete absence of phase information. This issue has already been raised in chapter 1 as part of the review of the existing literature and more comprehensively in chapter 2 through the pictorial representation of zero-phase characterisation.

A phase-less synthesis has several implications for surface feature characterisation. The advantages are that it is non-contact, non-destructive, area sampling, suitable for on-line assessment of many manufactured surfaces with regular features and is by far superior to any spatial means of surface imaging due to the higher resolution harboured in a typical frequency map. This form of assessment has been carefully labelled as "characterisation", because the characterised images are not a true reconstruction of the object surface. They are merely an image of the most dominant behavioural characteristics portrayed by the surface . There is however the possibility that the image of the most dominant behaviour portrayed by the surface is very closely related to the actual shape of the asperities which portray such dominant behaviour.

Two different independent studies conducted on an object function with a known geometrical structure and an unknown machined surface confirm this fact. In the first instance, studies related to the zero-phase characterisation of a transmittance profile as part of the investigation in chapter 4, revealed that the intensity information in the typical spectral characteristics of the object would yield a characterised image of the object which very closely resembles the original spatial distribution of the object. Although the spatial distribution of the characterised image is very similar to the actual image, the number of the repetitive features in the image is almost inevitably in excess of the original number in the object. This is because for objects with even symmetry, the zero-phase characterisation when using the intensity of the spectral characteristics is the self convolution of the image of the object.

This self convolution always results in the number of the imaged features being in excess of the original number in the object domain. However, it has been shown that for this particular object, there is a region of the frequency spectrum where the phase of the frequency components is highly likely to be zero. Selective windowing of this spectral region has confirmed this fact and zero-phase characterisation of this selected group of spectral components has indeed arrived at a spatial arrangement which very much resembles the original object not only in the general form but also in terms of the number of features present. This striking similarity has been brought about through an inverse Fourier transformation of a selected group of spectral data, even though the intensity of spectral components was utilised in the synthesis process. These results, once again, support the notion of utilising zero-phase characterisation as a means for assessing regular behaviour in surface related studies, namely the characterisation of machined surfaces.

In this context more elaborate findings come to light when zero-phase characterisation was utilised to reveal surface related information for a machined surface which quite remarkably possessed a whole range of different regularities. The regularities resulted from a typical finishing process namely turning, which generated almost identical periodicity as a direct result of the material being detached from the surface by the cutting edge of the tool. The vibration of the tool also leads to a whole array of periodic components known as tool-chatter components, along side the dominant periodicity produced by the tool marks. The two-dimensional optical spectrum of this surface clearly contained the signature of such spatial features in the form of well distinguished and distinct spectral components, making it an ideal subject for zero-phase investigations.

In chapter 5, two types of study have been performed to assess the outcome of zero-phase characterisation for this particular surface. The magnified and digitised image of the surface obtained via a travelling optical microscope was used to generate the two-dimensional spectrum of the surface.

The intensity of the spectral components was then inverse Fourier transformed with zero phase and the outcome compared with the actual image. Although merely a characterisation, the similarity between the two images in the absence of phase was striking. An inevitable part of the zero-phase characteristics, the effect of a finite data window aperture was notably present in the zero-phase image of the surface. However, even with the effect of a data window being present, the dominant characteristic features of the surface topography namely the cyclic pitch and the lay of regularity, remained intact in the intensity profile. The second study was based upon the utilisation of the diffracted optical spectrum to recover zero-phase characteristics. Optically recorded information has the characteristics of the illumination incorporated in it and these characteristics would evidently be present as part of the zero-phase behaviour. However, the presence of the beam profile did not impede the identification of the dominant regularity, which was very much recognisable as part of the characterised image.

Although both the dominant regularity and the tool-chatter components were present as part of the captured spectral characteristics of the machined surface, due to the lack of pixel resolution, the zero-phase behaviour initially recovered only one type of regularity, namely that of the grooves. A unique and exceptional methodology adopted by the author, however, led to the recovery of the finer spatial variations. The sensitivity of the frequency domain to the scale of the object, prompted the idea that a scale sensitive operation can be introduced to magnify or enlarge the zero-phase characteristics in the object domain with the benefit that there would be more imaging pixels across the magnified image which can then represent finer variations.

The outcome of the scaling operation was highly successful. By merely extending the surrounds of the spectrum in the frequency domain, the zero-phase characteristic image of the object was enlarged accordingly revealing the much finer spatial variations of the surface.

Although magnification of images is common practice in the spatial domain, there is however no gained resolution through such an operation. However, a magnification brought about by the utilisation of spatial frequency components has the merits of revealing much finer details if these have been captured as part of the frequency map. In this respect many surface related studies based on the use of the spatial frequency map would inevitably benefit from utilising such a technique to track down finer spatial structures present in the surface.

Although the scaling technique has been identified as a way of obtaining digital magnification which quite remarkably is accompanied by enhanced resolution, there are other changes which can be brought about through a scale related operation which prove extremely valuable in the reconstruction and full recovery of object surfaces in general.

CHAPTER 7

To fully appreciate the contribution that the scaling technique has made to this investigation, it is important to distinguish the different ways that scaling can be put into use and to acknowledge clearly the purpose it has to fulfil in each application. A change in scale can alter the spectral behaviour in two different ways:

i) expansion or compression of the spectral behaviour through interpolating the existing spectral components with the effect that the overall arrangement of the spectral components is not changed. For example, frequency envelope is retained but extra samples are inserted or removed to make the spectrum expand or contract;

ii) expansion or compression of the spectral behaviour through the rearrangement of the spectral components with the effect that the overall arrangement of spectral components is completely altered. For example, the frequency envelope is completely altered with the lobes stretched out or compressed to compensate for the change in the scale of the object.

A note of explanation will clarify the purpose that either technique is to serve so far as the findings in this research are concerned. In the first instance i), when the size of the object is fixed and its surrounds are extended, this merely results in the interpolation of the frequency behaviour. The general format of the spectral behaviour will not vary but the spectrum will be enlarged or interpolated because additional frequency samples have been inserted.

Because of the inverse dimensional property that operates between the spatial domain and the spatial frequency domain, this philosophy can be activated in reverse. This is exactly the reason for which the scaling philosophy was used in chapter 5, in order to interpolate the spatial behaviour in the object domain, thereby supplying extra imaging pixels to track finer variations , namely the tool chatter components of the machined surface.

The second way i.e, ii), by which a change in scale is brought about has more weight to it and is fundamentally important to the findings in this investigation so far as a full reconstruction of a real object surface is concerned. The importance of this aspect of the scaling philosophy is that through re-modification of the whole spectral envelope, it allows a means for extracting the unknown phase information through the utilisation of the non-iterative techniques of logarithmic Hilbert transformation which would have otherwise been impossible to perform.

Such change in scale as addressed in ii), is brought about by fixing the surrounds of the object and then changing the size of the object itself. In this case the general format of the frequency behaviour is completely different with every change in the scale of the object. The frequency behaviour appears expanded or enlarged not because the previous frequency spectrum has been interpolated, but because, every smaller version of the object has its fundamental and higher harmonics placed further away from the centre of the spectrum resulting in the spectral lobes appearing to be stretched out or expanded. The two principles by which the scaling philosophy can be invoked have been shown in figure 7.1.

This global expansion enhances the continuity amongst spectral components, reduces spectral excursions such as maxima and minima, reduces zero-crossing of the spectral behaviour, and reduces or removes the discontinuities that are present along the path of integration for evaluation of the unknown phases.

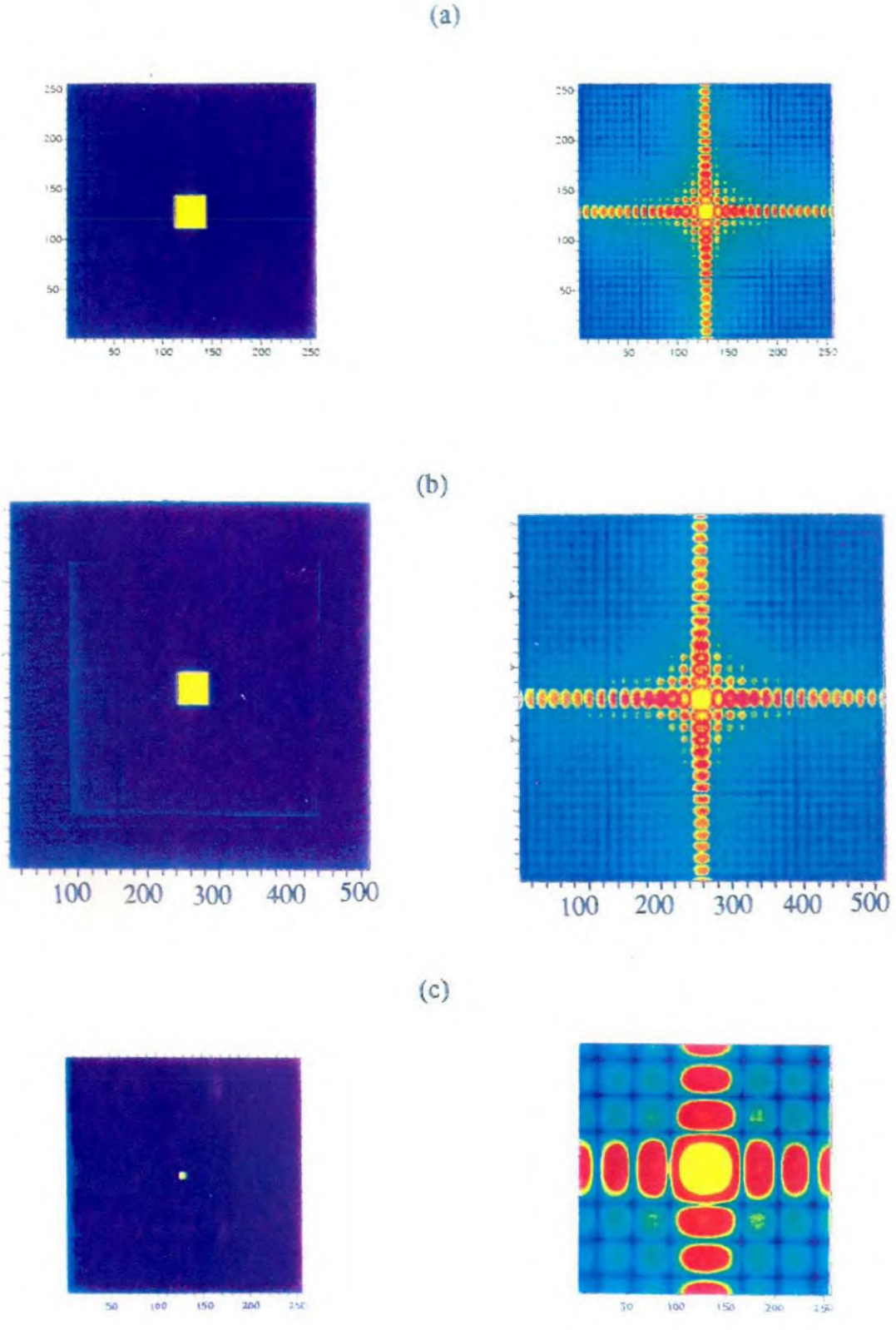

Figure 7.1: Two ways by which the scaling philosophy can be invoked; (a)- the original unscaled object; (b)- object the same size but scaled background gives rise to interpolated spectral behaviour with the general arrangement of spectral coefficients remaining the same; (c)- scaled object but background the same size gives rise to a completely new arrangement of spectral coefficients.

This aspect of the scaling philosophy is exactly what is required for modifying the spectral characteristics of real object specimens. These are object surfaces which have repetition, structure. Inevitably, they give rise to impulsive spectral behaviour with a whole population of maxima and minima, lack of continuity, and a whole colony of zeros as part of their spectral characteristics. The unique way round modifying such spectral characteristics is through cultivating continuity, phasing out impulsive behaviour, and removing discontinuities from the spectrum, all of which are neatly brought about through a scale sensitive operation.

The elegance of this approach is that whilst the overall spectral behaviour undergoes a thorough re-arrangement to make it amenable to phase extraction via a logarithmic Hilbert transform operation, the whole intelligence of the object remains intact and there is no loss of object related information, even though, the whole emblem of the frequency behaviour has undergone a dramatic change ! The only change that the object is going to experience is that the software reconstructed version of it will be on a smaller scale. Also, looked at from another angle, spectral behaviour which possesses continuity, converges more rapidly to the object signal and by the virtue of such rapid convergence is a better medium for the extraction of the unknown phases than is the spectral behaviour which has an impulsive character.

The whole of chapter 6 has been devoted to substantially prove how this aspect of scaling philosophy has not only allowed for a non-iterative approach for extracting the unknown phases, but has significantly aided and improved the accuracy with which the unknown phase values have been extracted. There is mountable evidence which justifies the changes and the improvements brought on by the scaling operation in the extraction of unknown phases. These have been presented by way of simulated reconstructions for both 1-D and 2-D object signals both prior to and after progressive re-scaling of the spectral characteristics.

All the reconstructions have been evaluated on the basis of the total squared error parameter $\sum E_{total}$, which reveals the extent of the discrepancy between the original and the recovered object signals numerically. Prior to the application of the scaling principle the infidelity between the original and the reconstructed version was revealed by a value of $\sum E_{total} = 1.388 \times 10^{1}$ for the total squared error parameter. However, with the aid of re-scaling this figure was progressively reduced until it reached a value of $\sum E_{total} = 1.857 \times 10^{-9}$ when the original signal was compressed in size by a factor of x16. Repetition in the object characteristics does provoke oscillatory behaviour and in turn calls for a higher compression factor in the scale of the object in order to reduce or remove the impulsive characteristics. In this respect it did take five attempts of re-scaling for the reconstruction to yield a perfect match between the original and the retrieved signal. Similar improvements were also sought for a non-repetitive object fairly rapidly at the third attempt of re-scaling which yielded a reasonable match between the original and the reconstructed version when the $\sum E_{total}$ dropped from $\sum E_{total} = 8.768$ to $\sum E_{total} = 3.595 \times 10^{-2}$.

The final testament to the effectiveness of the scaling principle came when it was used to successfully recover the structural geometry of a 2-D real object signal. The object features constituted of 100 μm x100μm square regions deposited on to a glass background with a 50 μm spacing. The magnified digitised images of these features was progressively compressed and the resulting frequency spectrum was utilised to extract the unknown phase information. All in all, three attempts were made before the outcome resulted in an exceptional match between the original and the reconstructed version.

7.2 The Impact of the New Methodology on Phase Retrieval

The application of the Fourier scaling principle in conjunction with Logarithmic Hilbert transform, has led to a powerful and unique principle for extraction of the unknown phases of real type object structures which would have otherwise been impossible to retrieve through the application of Hilbert transformation alone.

Being non-iterative in principle, it is far superior to other orthodox means of phase retrieval which rely on iteratively based approaches. The results emerge fairly rapidly from only a few applications of the scaling concept where as with the iteratively based approaches, there is no guarantee that there would be a solution even after several hundred attempts have been made at the iterations. In this context quoted statistics has it that the mean square error, which is a figure of quality for assessing the reconstructions seems to drop by a factor of 2 every one hundred iterations, and iterative reconstructions do start at an extremely high value for this parameter.

It should be mentioned that the combination of the logarithmic Hilbert transform and the scaling principle does not lend itself to a fully embracing theory. Despite the sheer power of this approach, there are inevitably limitations beyond which the scaling principle would cease to be effective. Optimum resolution cannot be achieved in both domains. At the expense of enhancing spectral information in terms of gaining continuity amongst spectral components through a more subtle spread of spectral characteristics, one is losing pixel resolution across the object. Consequently, there are a number of drawbacks. Firstly, pixel degradation in the object domain might lead to part of the spatial information not to be accounted for. For instance a smaller sized object might lack definition. Secondly, it may well be that a solution is far from satisfactory, and yet it is not possible to re-scale the spectral characteristics any further to improve upon it.

7.3 Suggestions for Further Research

Although one should be aware of the aforementioned limitations of the scaling principle, these are by no means setbacks. The size of the object can always be altered through interpolating the spatial domain behaviour, similar to the approach adopted in resolving the spatial characteristics of the machined surface. More so, if the object cannot be further compressed in size, to foster a more continuous form of spectral behaviour, why not utilise the existing not so perfect reconstruction of it in iterative algorithms and let iterations complete the task of finding a matching solution. After all iterations starting from randomly seeded data are known to be unsuccessful in finding a reasonable match but they do appear promising when initial information regarding the object is supplied alongside the modulus information. In this respect an uncompleted, reconstruction from a Hilbert transform and scaling operation, is by far a better estimate of the object behaviour than any other initial random estimate which is fed to iterative algorithms. This is one possible area of work which should be looked into.

Many hypothesis are functional under purely ideal conditions usually in simulation studies, where as their effectiveness is questionable when the theory is assessed from the point of view of its practical feasibility. This is definitely not the case for the scaling philosophy. It can easily be implemented under practical circumstances as it can be initiated through software. It has already been suggested that a change in scale can easily be brought on through the repositioning of the recording device or through selective enlargement of the digitised images.

Of central importance, is that the notion of scaling can be taken even further. That is rather to reposition the recording device to view a smaller or larger diffraction pattern or to induce this change of scale through software, the compression or expansion of spectral data in full accordance with the theory of scaling, can be most elegantly perpetuated through a change of wavelength of incident illumination. Figure 7.2 shows how such change in scale can take place.

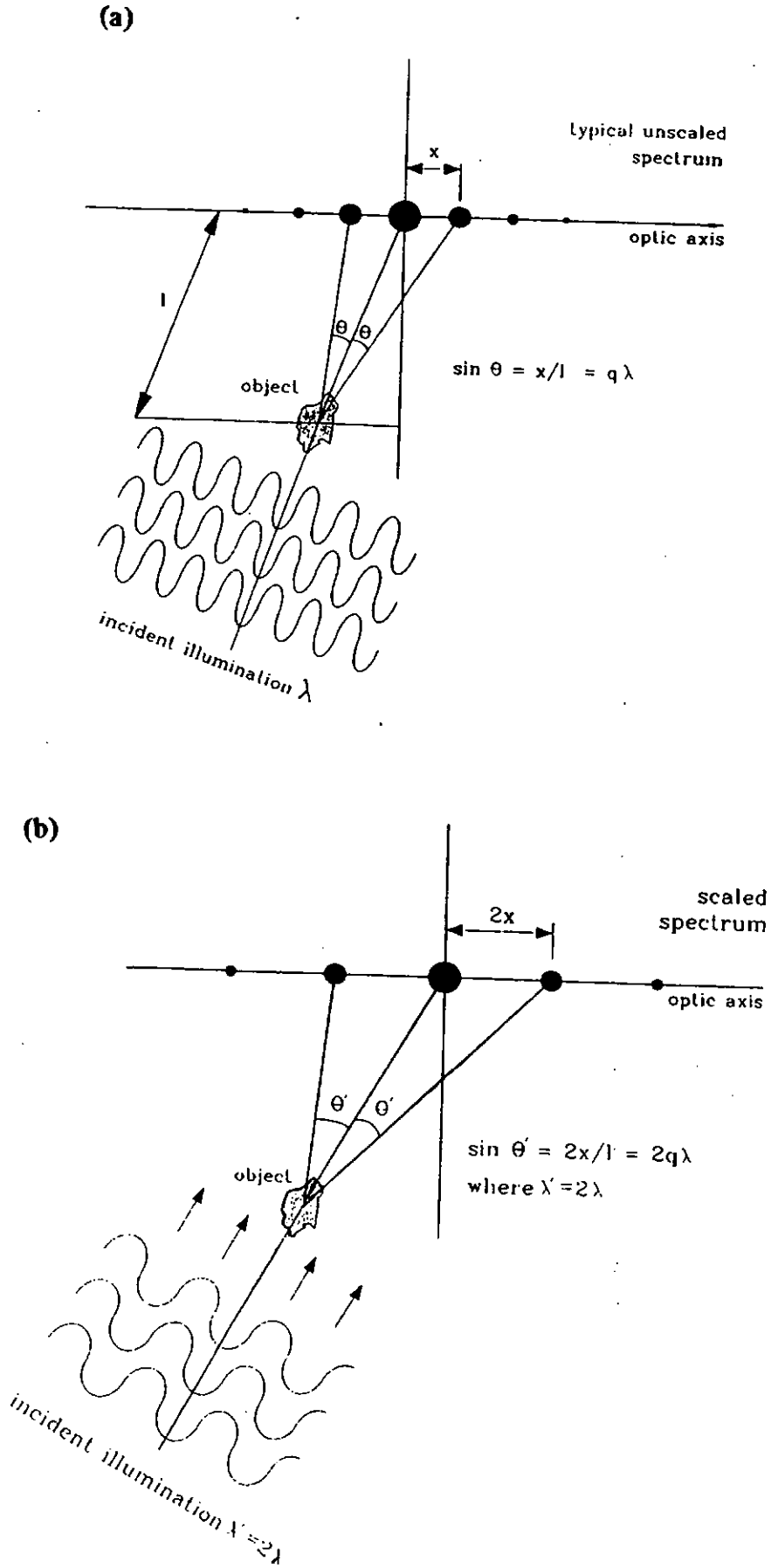

Figure 7.2: Altering the scale of the diffraction pattern through changing the wavelength of incident illumination; (a)- unscaled spectrum;(b)- scaled spectrum.

The significance of this is that in the engineering regime, a whole range of lasers with different wavelengths can be used to generate the corresponding diffraction pattern of the object. When the size of the asperities is comparable to a number of commercially available wavelengths, a number of reasonable diffraction patterns can be generated for the same object by merely utilising sources of different wavelengths. However, as would be expected, each diffraction pattern is differently spread, and represents details of the same object, only on a different scale and a different abundance of spectral components.

Apart from the fact that the most expanded spectrum is the one which is most amenable to phase extraction, to conceive a more reliable reconstruction of the object signal, it will be highly advantageous to utilise a number of scaled spectra to double check whether they converge to the same object signal. Changing the wavelength of illumination to bring on the necessary change in scale is another area of work which deserves further investigation.

REFERENCES

Ahn, A., and Yagle, A.E., 1994, 'Relaxation procedure for phase retrieval of non-negative signals', IEEE Trans. on signal processing, vol 42, no.11, p. 2997.

Allen, G.C., and Brown, I.T., Dec. 1989, 'Seeing with ions', CEGB Research, p. 3.

Babus'haq, R.F., Evans, R., O'callaghan, P.W., and Probert, S.D., 1992, 'Deformation of engineering surfaces under static load', Int. J. Mach. Tools Manufact., vol 32, no.1/2, p.39.

Baher, H., 1990, Analog and digital signal processing, Wiley.

Barrett, A.N., and Mackay, A.L., 1987, Spatial structure and the microcomputer, Camelot Press Ltd., p. 83.

Bates, R.H.T, 1982, 'Fourier phase problems are uniquely solvable in more than one dimension.I: underlying theory,' Optik 61, p. 247.

Bates, R.H.T., Oct. 1984, 'Phase restoration is successful in the optical as well as the computational laboratory', Indirect imaging, Cambridge University Press, p. 120.

Bates, R.H.T., and Fright, W.R., 1983, 'Composite two-dimensional phase restoration procedure', J. Opt. Soc. Am., vol. 73, p. 362.

Bates, R.H.T., and Fright, W.R., 1984, 'Reconstructing images from their Fourier intensities', Advances in computer vision and image processing, vol. 1, p. 227.

Bates, R.H.T., and Mnyama, D., 1986, 'The status of practical Fourier phase retrieval', Advances in electronics and electron physics, vol. 67, p.1.

Beckmann P. and Spizzichino A., 1963,' The scattering of electromagnetic waves from rough surfaces', Pergamon, New York, 1963, Chap.5.

Behar, J., Porat, M., Zeevi, Y.Y., 1988, ' The importance of localised phase in vision and image representation', Visual commu. image processing 88, SPIE Proc., vol 1001, p.61.

Bracewell, R.N., 1986, The Fourier transform and its applications, McGraw Hill International.

Brigham, E.O., 1988, The fast Fourier transform and its applications. Prentice Hall international Editions.

Broadmann, R., Gerstofer, O. Thurn, G., May /June 1985,' Optical roughness measuring instrument for fine machined surfaces', Optical engineering, vol. 24, no. 3, p.408.

REFERENCES

Broadmann, R., 1986, 'roughness form and waviness measurement by means of light scattering', Precision Eng., vol. 8, p.221.

Chalasinska-Macukow, K., and Arsenault, H.H., 1985, 'Fast iterative solution to exact equations for the two-dimensional phase retrieval problem', J. Opt. Soc. Am. A, vol. 2, no.1, p. 46.

Champeney, D.C., 1973, Fourier transforms and their physical applications, Academic press, chap. 4, p. 56.

Chandley, R.J., 1976, 'Surface roughness measurements from coherent light scattering', Optical and Quantum Electronics, vol. 8, p. 323.

Chetwynd, D.G. Liu, X., Smith, S.T., 1992, 'Signal fidelity and tracking force in stylus profilimetry' Int. J. Mach. Tool Manufact., vol 32, no. 1/2, p. 239.

Chien, R.T., and Snyder, W.E., 1975, 'Hardware for visual image processing', IEEE Trans. on Circuits and Systems, p. 541.

Church, E.L., Jenkinson, H.A., and Zavada, J.M., 1977, 'Measurement of the finish of diamond-turned metal surfaces by different light scattering', Optical Eng., vol. 16, p. 360.

Church, E.L., Jenkinson, H.A., and Zavada, J.M., 1979, 'Relationship between surface scattering and microtopographic features', Optical Eng., vol. 18, no. 2, p. 125.

Cizek, V., 1970, 'Discrete Hilbert transform', IEEE Trans. on Audio and Electroacoustics, vol. AU-18, no.4, p. 340.

Cochran, D., 1994, ' Phase and magnitude in normalized images', IEEE Trans. on Image Processing, vol. 3, no.6, p.858.

Creath, K., Wyatt, J., Sept. 1990, 'Absolute measurement of surface roughness', Applied optics, vol 29, no. 26, p.3823.

Crimmins, T.R., Fienup J.R. and Thelen, B.J., Jan. 1990, 'Improved bounds on the object support from autocorrelation support and application to phase retrieval', J. Opt. Soc. Am., vol. 7, no.1, p. 3.

REFERENCES

Dainty, J.C., Fienup J.R., 1987, 'phase retrieval and image reconstruction for astronomy', Image recovery: theory and application, H.Stark edition, Academic, New York, p. 231.

Dragoset, R. A, and Vorburger, T.V., 1987, 'Scanning tunnelling microscopy of a diamond turned surface and a grating replica', SPIE, Metrology figure and finish, vol. 749, p. 54.

Dudgeon, D., and Mersereau, R.M., 1984, 'Multi Dimensional digital signal processing', Prentice-hall.

Eastman, J., and Baumeister, P., 1974, 'The microstructure of polished optical surface', Optics Communications, vol. 12, no. 4, p. 418.

Elson, J.M., Bennett, H.E., and Bennett, J.M., 1979, 'Scattering from optical surfaces', in Applied Optics and Optical Engineering, Academic Press New York, vol. 7, chapter 7.

Elson, J.M., and Bennett, J.M., 1979, 'Relation between the angular dependence of scattering and the statistical properties of optical surfaces', J. Opt. Soc. Am., vol. 69, no. 1, p. 31.

Fienup, J.R., 1978, 'Reconstruction of an object from the modulus of its Fourier transform', Optics Letters, vol. 3, no. 1, p. 27.

Fienup, J.R., 1979, 'Space object imaging through the turbulent atmosphere', Opt. Eng., Vol 18, p. 529.

Fienup, J.R., 1982, 'Phase retrieval Algorithms: a comparison', Applied Optics, vol. 21, p. 2758.

Fienup, J.R., 1984, 'Experimental evidence of the uniqueness of phase retrieval from intensity data', Indirect imaging, J.A. Roberts ed., Proceedings of the Int. union of radio science, Cambridge university press, Cambridge, p.99.

Fienup, J.R., 1987, 'Reconstruction of a complex valued object from the modulus of its Fourier transform using a support constraint', J. Opt. Soc. Am. A, vol. 4, no. 1, p. 118.

Fienup, J.R. and A.M. Kowalczyk, March 1990, 'Phase retrieval for a complex valued object by using a low resolution image', J.Opt. Soc. Am., A/vol. 7, no.3, p. 450.

Garcia, R., July 1991, 'Scanning tunnelling microscopy in biology: changing the pace', Microscopy and analysis, issue 24, p. 27.

REFERENCES

Gerchberg, R.W., and Saxton, W.O., 1972, 'A practical algorithm for the determination of phase from image and diffraction plane pictures', Optik 35, p. 237.

Gerchberg , R.W, and Saxton, W.O, 1971, 'Phase determination from image and diffraction plane pictures in electron microscopy', Optik 34, p. 275.

Gold, B., Oppenheim, A.V., and Rader, C.M., 1970, 'Theory and implementation of the discrete Hilbert transform', Proc. Symp. Comput. Process Commun., p. 235.

Goodhew, P.J., and Humphreys, F.J., 1988, Electronmicroscopy and analysis, Taylor and Francis.

Guerra, J.M., 1993, ' Photon tunnelling microscopy of diamond turned surfaces', Applied optics, vol. 32, no.1, p.24.

Hayes, M.H., Lim, J.S., and Oppenheim, A.V., 1980, ' Signal reconstruction from phase or magnitude', IEEE Trans. Acoust. Speech Signal Process., ASSP 28, p 672.

Hayes, M.H., April 1982, 'The reconstruction of a multidimensional sequence from the phase or the magnitude of its Fourier transform', IEEE Trans. on Acoustics, Speech and Signal proc., vol. ASSP-30, p. 140.

Hayes, M.H. and Quatieri, T.F., 1983, 'Recursive phase retrieval using boundary conditions', J. Opt. Soc. Am. vol 73, p. 1427.

Holt, D.B., Napchan, E., and Russell, J.D., May 1991, 'Image processing for defect location in SEM inspection of VLSI circuits', Microscopy and Analysis, issue 23, p. 39.

Izraelevitz, I., and Lim, J.S., 1987, 'A new direct algorithm for image reconstruction from Fourier transform magnitude. IEEE Trans. on Acoust., Speech, and Signal Proc., vol. ASSP_35, no. 4, p. 511.

Jordan, D.L., Hollins, R.C., Jakeman, E. and Rewett, A., 1988, ' Visible and infrared scattering from well characterised surfaces' surface topography, vol. 1, p. 27.

Jungles, J. and Whitehouse, D.J., 1970,' An investigation of the shape and dimensions of some diamond styli', J.Phys Ed., vol. 3, p. 437.

REFERENCES

Jungles, J., 1992, 'High speed measurement of engineering surfaces', Int. J. Mach. Tools. Manufact., vol 32, no.1/2, p.27.

Kim, W. and Hayes M.H., March 1993, ' Phase retrieval using a window function', IEEE Trans. on Signal Process., vol 41, no.3, p. 1409.

King T.J. and Stout, K.J., 1977, 'Some topographic features of the wear process, theory and experiment', Ann. CIRP 25, p 351.

Kreis, T.M., 1987, 'Fourier transform evaluation of Holographic interference patterns', SPIE vol. 814, Photomechanics and speckle metrology, p. 365.

Kries, T.M. and Juptner, I.W., ' Digital processing of holographic interference patterns using Fourier transform methods',1988, Measurement, vol.6, no.1, p.37.

Lamourex, M.P., March 1993, ' The Poormans transform: Approximating the Fourier transform without multiplication', IEEE trans. on Signal Process., vol. 41, no.3, p. 1413.

Lee, J.J., Garinis, D., Frost D.L., Lee, J.H.S. and Knystautas, R., 1995,' Two- dimensional autocorrelation function analysis of smoked foil patterns', Shock Waves, vol. 5, p.169.

Leichte, H., March 1991, 'Holography in high resolution electron microscopy', Microscopy and analysis, issue 22, p. 13.

Lim, J.S., 1990, Two signal and image processing, Prentice Hall.

Lipson, S.G., and Lipson, H., 1981, Optical Physics, Cambridge University press.

Lorincz, E., Richter, P., and Engard, F., Aug. 1986, 'Interferometric statistical measurement of surface roughness', Applied optics, vol. 25, no. 16, p. 2278.

Marx, E., Leridon, B., Lettieri, T.R., Song, J.F. and Vorburger, T.V., 1993, 'Autocorrelation function from optical scattering for one-dimensionally rough surfaces', applied optics, vol.32, no.1, p. 67.

Mavardi, O.K., 1972, 'Amplitude-only and phase-only holograms', Acoustical Holography, G.Wade ed. Plenum, New York, vol. 4, p. 519.

McGregor, J.J., and Watt, A.H., 1983, Pascal for science and engineering, Pitman, p. 229.

REFERENCES

Millane, R.P., 1990, 'Phase retrieval in crystallography and optics', J. Opt. Soc. Am., A/vol 7, no.3, p.394.

Misell, D.L., 1978,' The phase problem in electron microscopy', Advances in optical and electron microscopy, V.E. Cosslett and R.Barer Ed., vol. 7, Academic press, New York. P. 185.

Nakajima, N., and Asakura, T., 1982, 'Study of zero location by means of an exponential filter in the phase retrieval problem, Optik 60, p. 289.

Nakajima, N., and Asakura, T., 1983, 'Extraction of the influence of zeros from the image intensity in the phase retrieval using the logarithmic Hilbert transform', Optick 63, no. 2, p. 99.

Nakajima, N., and Asakura, T., 1986, 'Two dimensional phase retrieval using the logarithmic Hilbert transform and the estimation technique of zero information', Applied Physics, vol. 19, p. 319.

Newton, R.E.I., 1990, Wave Physics, Edward Arnold.

Niblack, W., 1986, An introduction to digital image processing, Prentice Hall International.

Obray, C., 1983, 'Application of the scattering models to optical surface inspection', PhD thesis, Department of Systems Science, City University, London.

Oppenheim, A.V., and Schafer, R.W., 1975, Digital signal processing, Prentice Hall international editions, p. 337.

Oppenheim, A.V., and Lim, J.S., 1981, 'The importance of phase in signals', Proc. IEEE 69, p. 529.

Oppenheim, A.V., Lim, J.S., Kopec, G.E., Pohlig, S.C., 1979, 'phase in speech and pictures', IEEE Trans. Acoust. Speech Signal Process., ASSP 27, p. 632.

Outwater, C., and Hamersvald, V., 1974, A guide to practical Holography, Prentangle press, p. 1.

Pakhomov, A.A., Apr. 1996, ' Optimization of an image restoration algorithm from its Fourier spectrum phase', Opt. Eng., vol. 34, no.4, p 1044.

Perry, M., 1994, 'Using 2D FFTs for object recognition', The Int. Conf. on Signal Process. Appl. and Techn., vol 2, p. 1043.

Press, W.H., Flannery, B.P., Teukolsky, S.A., and Vetterling, W.T., 1986, Numerical Recipes: The Art of Scientific Computing, Cambridge University Press, Chapter 12.

REFERENCES

Proakis,J.G., Manolakis, D.G., 1988, 'Introduction to digital signal processing', Macmillan Publishing, NewYork.

Porter III, G.B., and Mundy, J.L., 1980, 'Visual inspection system design', Computer, vol. 13, no. 5, p. 40.

Powers, J., Landry, J., Wade, J., 1970, 'Computed reconstructions from phase-only and amplitude-only holograms', Acoustical Holography, A.F. Metherell and L. Larmore editions, Plenum, New York, vol.2, chap. 13, p. 185.

Raja, J., and Radhakrishnan, V., 1977, 'Analysis and synthesis of surface profiles using Fourier series', Int. J. Mach. Tool Design. Res., vol. 17, p. 245.

Ramachandran, G.N., and Srinivasan, R., 1970, Fourier methods in crystallography, New York, Wiley Interscience.

Ramirez, R.W., The FFT fundamentals and concepts, Prentice-Hall, 1985.

Saxton, W.O., 1978, Computer techniques for image processing in electron microscopy, New York, Academic.

Schmid, H.G., and Pflug, L., 1989, 'Automatic recognition of defects by parallel contour analysis using fast Fourier transformation', Surface Topography, vol. 2, p. 7.

Schudder, H.J., 1978, 'Introduction to computer aided tomography', Proc. IEEE, vol. 66, no.6, p. 628.

Scott, G., 1988, 'Gaussian laser beam propagation modelling', Aerospace Dynamics, issue 24, p. 2.

Sherrington, I., and Smith, E., 1987, 'Parameters for characterising the surface topography of engineering components', Proc. Inst. Mech. Eng., vol. 201, no. C4, p. 297.

Sherrington, I., and Smith, E.H., 1986, 'A quantitative study of the influence of stylus shape and load on the fidelity of data recorded by stylus instruments', Second national conference on production research, Napier College, Edinburgh, p. 762.

REFERENCES

Sherrington, I., and Smith, E.H., March 1988, 'Fourier models of the surface topography of engineering components', Surface topography, issue 1, vol. 1, p. 11.

Sotoudeh, N., Greatrix, G.R., and Goldspink, G.F., 1989, 'The modulus of the Fourier transform in image reconstruction', Third international conference on image processing, no. 307, IEE Warwick, p. 705.

Sotoudeh, N., Greatrix, G.R., Prasad, R., and Goldspink, G.F., 1991, 'The use of the modulus of the Fourier transform in modelling surface topography', Eighth international conference on mathematical and computer modelling, Washington D.C., Vol. 2, 1993, Section A, p.517.

Sotoudeh, N., Greatrix, G.R., Prasad, R., and Goldspink, G.F., 1992, 'Fourier domain compression techniques in resolving spatial characteristics of surfaces', Fourth international conference on image processing, no. 354, IEE Maastricht, p. 172.

Sotoudeh, N., Greatrix, G.R., and Goldspink, G.F., 1993, ' Fourier Domain rescaling and truncation for improving the 3D reconstruction of objects', Ninth international conference on mathematical and computer modelling, Berkely, California.

Sotoudeh, N., Greatrix, G.R., and Goldspink, G.F., 1993,'Fourier domain contrast enhancement of spectral coefficients to improve 3D reconstruction of objects', Ninth international conference on mathematical and computer modelling, Berkely, California.

Sotoudeh, N., Greatrix, G.R., and Goldspink, G.F., 1994, ' Improving the recovery of the microgeometry of object surfaces by Fourier scaling', ICSPAT 94, Dallas, Texas, Vol. II, P.1008.

Staufert, G., 1979, ' description of roughness profile by separating the random and periodic components', Wear, vol. 57, p. 185.

Steward, E.G., 1983, Fourier optics an introduction, Ellis Horwood Limited.

Stewart, J., 1988, 'From Vacuum Tubes to CCD Imagers', Aerospace Dynamics, Issue 24, p. 35.

Stout, K.J., Sept. 1981, 'Surface Roughness, measurement, interpretation and significance of data , Part I:Statistical parameters', Materials in engineering, vol. 2, p. 260.

REFERENCES

Stout, K.J., Sept. 1981, 'Surface Roughness, measurement, interpretation and significance of data, Part II: Experimental considerations and significance of data, Materials in engineering, vol. 2, 287.

Sullivan, P., Poroshin, V., Ooke, C., 1992, 'Application of a three dimensional surface analysis system to the prediction of asperity interaction in metallic surfaces', Int. J. Mach. Tools Manufact., vol 32, no.1/2, p. 157.

Sullivan, P.,1989, ' The demand for a 3-D surface finish standard', Surface topography, vol. 2, p.1.

Tanner, L.H., June 1976, 'The use of the laser light in the study of metal surfaces', Optics and laser technology, p. 113.

Tanner, L.H., 1979, 'Comparison between talysurf 10 and optical measurements of surface roughness and slope', International conference on metrology and properties of engineering surfaces, p. 80.

Teague, E.C., Vorburger, T.V., and Maystre, D., 1981, 'Light scattering from manufactured surfaces', CIRP annals, Manufacturing Technology, vol. 30, no. 2, p. 563.

Thomas, T.R., 1981, 'Characterisation of surface roughness', Prec. Eng., vol. 3, part 2, p. 97.

Thomas, T.R., March 1988, 'Surface roughness: the next ten years', Surface topography, issue 1, vol. 1, p. 3.

Thomas, T.R., and Charlton, G., 1981, 'Variation of roughness parameters on some typical manufactured surfaces', Prec. Eng., vol. 3, part 2, p. 91.

Thwaite, E.G., 1982, ' A quantitative comparison of the wavelength spectrum of a surface obtained by optical Fourier transformation with calculations from profile measurements', Wear, vol 83, p. 181.

Toyoshima, H., and Takahashi, S., 1992, 'Design of stable 2-D recursive digital all pass filters using Hilbert transform', IEE fourth international conference on image processing and applications, p. 559.

REFERENCES

Van Hove, P.L., Hayes, M.H., Lim, J.S., and Oppenheim, A.V., Oct. 1983, 'Signal reconstruction from signed Fourier transform magnitude', IEEE Trans. on Acoustics, speech and signal processing, vol. ASSP-31, no.5, p. 1286.

Vorburger, T.V., and Teague, E.C., 1981, 'Optical techniques for on line measurement of surface topography', Prec. Eng., vol. 3, p. 61.

Vorburger, T.V., Teague, E.C., Scire, F.E. and Rosberry, F.W., 1979, ' Measurement of stylus radii', Wear, 1979, vol. 57, p.39.

Welford, W.T., 1977, 'Optical estimation of statistics of surface roughness from light scattering measurements: a review', Opt. Quant. Elect., vol. 9, p. 269.

Wolf K.B., 1979, Integral transforms in science and engineering, Plenum press, p. 101.

Wyant, J.C. and Creath, K., 1992, 'interferometric optical profiling', Int.J. Mach. Tools Manufact., vol 32, no. 1/2, p.5.

Yang, G., Dong, B., Gu, B., Zhuang, J. and Ersoy, O., 1994, 'Gerchberg-Saxton and Yang-Gu algorithms for phase retrieval in a non-unitary transform system: a comparison', J. Opt. Soc. Am., vol. 33, no. 2, p. 209.

Younes, M.A., Croft, J.R., and Hill, W.J., 1984, 'Surface roughness measurement using the angular distribution field from a small laser spot', Proc. SPIE, vol. 473, p. 122.

APPENDIX A

listings of the Hilbert retrieved signal alongside the original signal for three different studies illustrated in:

(i)- graphs 6.6-6.8 and table 6.1 pages 198-200;

(ii)- graphs 6.14-6.18 and table 6.2a pages 231-245;

(iii)- graphs 6.20-6.22 and table 6.2b pages 247-249.

the sum of the total squared error for tables 6.1, 6.2a and 6.2b has been shown at the bottom of each listing.

APPENDIX A

sequence order	set 1 original sequence	set 1 reconstructed sequence	set 2 original sequence	set 2 reconstructed sequence	set 3 original sequence	set 3 reconstructed sequence
x(1)	5	5.002E+00	5	5.307E+00	5	5.411E+00
x(2)	0	3.163E-03	0	5.543E-01	0	7.818E-01
x(3)	0	2.147E-03	0	3.642E-01	0	4.770E-01
x(4)	1	1.001E+00	1	1.131E+00	1	1.084E+00
x(5)	1	1.000E+00	1	9.132E-01	1	7.045E-01
x(6)	1	9.990E-01	1	7.085E-01	1	3.538E-01
x(7)	1	9.982E-01	1	5.707E-01	1	1.302E-01
x(8)	1	9.977E-01	1	5.395E-01	1	8.865E-02
x(9)	1	9.977E-01	1	6.292E-01	1	2.613E-01
x(10)	1	9.981E-01	1	8.233E-01	1	6.184E-01
x(11)	1	9.990E-01	1	1.077E+00	1	1.098E+00
x(12)	0	-2.341E-04	0	2.655E-01	0	4.926E-01
x(13)	0	2.538E-04	0	3.334E-01	0	6.823E-01
x(14)	0	7.289E-04	0	3.152E-01	0	6.854E-01
x(15)	0	1.080E-03	0	2.089E-01	0	4.686E-01
x(16)	0	1.214E-03	1	1.098E+00	1	1.181E+00
x(17)	0	1.081E-03	1	1.012E+00	1	9.061E-01
x(18)	0	8.875E-04	1	9.145E-01	1	8.494E-01
x(19)	0	1.012E-04	1	8.303E-01	1	4.831E-01
x(20)	0	-5.607E-04	1	7.822E-01	1	4.520E-01
x(21)	0	-1.153E-03	1	7.848E-01	1	5.705E-01
x(22)	0	-1.534E-03	1	8.412E-01	1	8.129E-01
x(23)	0	-1.599E-03	1	9.417E-01	1	1.156E+00
x(24)	0	-1.305E-03	0	2.857E-03	0	4.251E-01
x(25)	0	-6.879E-04	0	7.188E-03	0	5.464E-01
x(26)	0	1.393E-04	0	1.117E-02	0	5.529E-01
x(27)	0	1.007E-03	0	1.298E-02	0	4.128E-01
x(28)	0	1.721E-03	0	1.172E-02	1	1.244E+00
x(29)	0	2.106E-03	0	9.146E-03	1	1.096E+00
x(30)	0	2.046E-03	0	7.516E-03	1	9.403E-01
x(31)	0	1.517E-03	0	8.453E-03	1	8.106E-01
x(32)	0	5.965E-04	0	1.095E-02	1	7.477E-01
x(33)	0	-5.389E-04	0	1.262E-02	1	7.472E-01
x(34)	0	-1.651E-03	0	1.186E-02	1	8.075E-01
x(35)	0	-2.485E-03	0	9.109E-03	1	9.311E-01
sum of squared errors		7.089E-04		1.732E+00		8.137E+00

sequence order	set 1 original uncompressed sequence	set 1 reconstructed sequence	set 2 original sequence compressed by a factor of 2	set 2 reconstructed sequence	set 3 original sequence compressed by a factor of 4	set 3 reconstructed sequence	set 4 original sequence compressed by a factor of 8	set 4 reconstructed sequence	set 5 original sequence compressed by a factor of 16	set 5 reconstructed sequence
x(1)	5	5.563E+00	5	5.412E+00	5	5.307E+00	5	4.999E+00	5	5.000E+00
x(2)	0	9.371E-01	0	8.183E-01	0	5.543E-01	0	-1.695E-03	0	-3.284E-08
x(3)	0	8.660E-01	0	7.172E-01	0	3.642E-01	0	1.989E-04	0	-9.039E-09
x(4)	1	1.800E+00	1	1.581E+00	1	1.131E+00	1	1.002E+00	1	1.000E+00
x(5)	1	1.704E+00	1	1.450E+00	1	9.132E-01	1	1.002E+00	1	1.000E+00
x(6)	1	1.506E+00	1	1.284E+00	1	7.085E-01	1	1.001E+00	0	-3.598E-08
x(7)	1	1.450E+00	1	1.130E+00	1	5.707E-01	1	9.996E-01	1	1.000E+00
x(8)	1	1.411E+00	1	1.014E+00	1	5.395E-01	0	-1.485E-03	1	1.000E+00
x(9)	1	1.446E+00	1	9.399E-01	1	6.292E-01	0	-1.508E-03	0	-1.816E-07
x(10)	1	1.509E+00	1	8.932E-01	1	8.233E-01	1	9.991E-01	0	-2.466E-08
x(11)	1	1.535E+00	1	8.514E-01	1	1.077E+00	1	1.000E+00	0	4.709E-08
x(12)	1	1.547E+00	1	7.991E-01	0	2.855E-01	1	1.001E+00	0	2.357E-08
x(13)	1	1.368E+00	1	7.240E-01	0	3.334E-01	1	1.001E+00	0	1.317E-07
x(14)	1	1.210E+00	1	8.387E-01	0	3.152E-01	0	7.680E-04	0	3.750E-08
x(15)	1	1.095E+00	1	5.598E-01	0	2.069E-01	0	-1.006E-06	0	1.019E-07
x(16)	1	1.012E+00	1	5.229E-01	1	1.096E+00	0	-8.816E-04	0	1.267E-07
x(17)	1	9.609E-01	1	5.381E-01	1	1.012E+00	0	-1.230E-03	0	-1.869E-08
x(18)	1	9.339E-01	1	6.301E-01	1	9.145E-01	0	-7.207E-04	0	-4.536E-08
x(19)	1	9.207E-01	1	7.904E-01	1	8.303E-01	0	3.966E-04	0	7.808E-08
x(20)	1	9.075E-01	0	-5.455E-02	1	7.822E-01	0	1.420E-03	0	3.443E-08
x(21)	1	9.007E-01	0	8.038E-02	1	7.848E-01	0	1.847E-03	0	-1.272E-07
x(22)	1	8.932E-01	0	2.373E-01	1	8.412E-01	0	8.692E-04	0	-1.674E-08
x(23)	1	8.823E-01	0	3.721E-01	1	9.417E-01	0	-4.544E-04	0	-3.023E-08
x(24)	1	8.674E-01	0	4.355E-01	0	2.857E-03	0	-1.463E-03	0	-2.332E-08
x(25)	1	8.513E-01	0	4.180E-01	0	7.188E-03	0	-1.467E-03	0	1.509E-07
x(26)	1	8.240E-01	0	3.117E-01	0	1.117E-02	0	-4.407E-04	0	5.250E-08
x(27)	1	7.745E-01	0	1.539E-01	0	1.298E-02	0	9.149E-04	0	7.760E-08
x(28)	1	7.211E-01	1	1.042E+00	0	1.172E-02	0	1.810E-03	0	7.821E-08
x(29)	1	5.837E-01	1	9.964E-01	0	9.148E-03	0	1.048E-03	0	-5.270E-08
x(30)	1	4.739E-01	1	9.500E-01	0	7.516E-03	0	-5.192E-04	0	-1.533E-07
x(31)	1	4.096E-01	1	9.137E-01	0	8.453E-03	0	-2.083E-03	0	-5.704E-08
x(32)	1	3.872E-01	1	8.854E-01	0	1.096E-02	0	-2.520E-03	0	-1.849E-07
x(33)	1	4.193E-01	1	8.677E-01	0	1.262E-02	0	-1.367E-03	0	-1.271E-07
x(34)	1	5.161E-01	1	8.448E-01	0	1.186E-02	0	7.991E-04	0	-4.428E-08
x(35)	1	6.784E-01	1	8.274E-01	0	9.109E-03	0	2.661E-03	0	7.686E-08
x(36)	0	-1.804E-01	1	7.929E-01	0	7.113E-03	0	3.006E-03	0	4.587E-07
x(37)	0	-7.365E-02	1	7.261E-01	0	6.321E-03	0	1.566E-03	0	4.650E-07
x(38)	0	8.948E-02	1	6.475E-01	0	6.069E-03	0	-7.369E-04	0	5.331E-07
x(39)	0	1.218E-01	1	5.835E-01	0	3.008E-03	0	-2.339E-03	0	3.536E-07
x(40)	0	1.471E-01	1	5.798E-01	0	-4.559E-03	0	-2.087E-03	0	-1.199E-07
x(41)	0	9.689E-02	1	6.404E-01	0	-1.503E-02	0	-7.745E-05	0	-5.830E-07

x(42)	0	-1.412E-02	1	7.920E-01	0	-2.434E-02	0	2.304E-03	0	-9.788E-07
x(43)	0	-1.593E-01	1	9.581E-01	0	-2.818E-02	0	3.249E-03	0	-1.139E-06
x(44)	0	-3.827E-01	0	8.959E-02	0	-2.695E-02	0	1.775E-03	0	-9.075E-07
x(45)	0	-3.194E-01	0	4.456E-02	0	-2.289E-02	0	-1.492E-03	0	-2.460E-07
x(46)	0	-3.684E-01	0	4.312E-02	0	-2.076E-02	0	-4.582E-03	0	8.159E-07
x(47)	0	5.192E-01	0	8.017E-02	0	-2.011E-02	0	-5.401E-03	0	1.737E-08
x(48)	0	4.378E-01	0	6.584E-02	0	-1.858E-02	0	-3.170E-03	0	2.331E-06
x(49)	0	2.819E-01	0	6.436E-02	0	-1.287E-02	0	9.341E-04	0	2.055E-06
x(50)	0	2.383E-01	0	5.314E-02	0	-2.379E-03	0	4.420E-03	0	1.158E-06
x(51)	0	1.157E-01	0	5.261E-02	0	5.868E-03	0	5.073E-03	0	-7.838E-07
x(52)	1	9.984E-01	0	8.148E-02	0	8.795E-03	0	2.510E-03	0	-3.043E-06
x(53)	1	9.372E-01	0	8.049E-02	0	4.208E-03	0	-1.441E-03	0	-4.717E-06
x(54)	1	8.742E-01	0	1.111E-01	0	-1.231E-03	0	-3.859E-03	0	-5.272E-06
x(55)	1	8.260E-01	0	1.518E-01	0	-5.298E-04	0	-2.711E-03	0	-3.844E-06
x(56)	1	7.962E-01	0	1.834E-01	0	9.872E-03	0	1.585E-03	0	-2.777E-07
x(57)	1	7.862E-01	0	2.025E-01	0	2.413E-02	0	8.218E-03	0	4.548E-06
x(58)	1	8.022E-01	0	1.742E-01	0	3.328E-02	0	7.898E-03	0	9.054E-06
x(59)	1	8.175E-01	0	1.568E-01	0	3.866E-02	0	4.239E-03	0	1.140E-05
x(60)	1	8.508E-01	0	9.628E-02	0	3.717E-02	0	-2.746E-03	0	1.009E-05
x(81)	1	8.158E-01	0	1.498E-01	0	3.969E-02	0	-9.318E-03	0	4.335E-06
x(82)	1	8.087E-01	0	1.388E-01	0	4.449E-02	0	-1.139E-02	0	-5.275E-06
x(83)	1	8.264E-01	0	8.666E-02	0	4.933E-02	0	-7.474E-03	0	-1.602E-05
x(64)	1	8.140E-01	0	5.053E-02	0	4.904E-02	0	-8.311E-03	0	-1.282E-05
x(65)	1	7.851E-01	0	9.922E-02	0	2.819E-02	0	-1.281E-02	0	3.578E-06
x(66)	1	7.462E-01	0	1.380E-01	0	8.368E-03	0	-1.177E-02	0	1.779E-05
x(67)	1	7.003E-01	0	1.055E-01	0	1.018E-02	0	8.069E-03	0	1.699E-05
x(68)	1	8.665E-01	0	4.507E-02	0	1.049E-02	0	2.336E-02	0	4.819E-06
x(69)	1	6.248E-01	0	5.530E-02	0	9.089E-04	0	2.323E-02	0	-5.098E-06
x(70)	1	5.717E-01	0	1.429E-01	0	-1.358E-02	0	8.291E-03	0	-1.089E-05
x(71)	1	8.130E-01	0	8.694E-02	0	-2.789E-02	0	-9.364E-03	0	-1.130E-05
x(72)	1	6.475E-01	0	3.601E-02	0	-2.770E-02	0	-1.673E-02	0	-6.825E-06
x(73)	1	6.603E-01	0	-3.638E-02	0	-1.928E-02	0	-1.095E-02	0	-1.455E-06
x(74)	1	8.467E-01	0	-7.467E-02	0	-8.922E-03	0	-5.088E-04	0	4.081E-07
x(75)	1	5.957E-01	0	-9.084E-02	0	-2.950E-03	0	8.413E-03	0	-8.500E-06
x(76)	1	5.339E-01	0	-8.820E-02	0	-7.385E-03	0	7.565E-03	0	-4.141E-07
x(77)	1	4.852E-01	0	-7.499E-02	0	-1.305E-02	0	4.893E-03	0	-4.333E-07
x(78)	1	4.620E-01	0	-8.531E-02	0	-1.589E-02	0	2.405E-03	0	-4.004E-07
x(79)	1	4.859E-01	0	-5.507E-02	0	-1.243E-02	0	1.821E-03	0	-2.690E-07
x(80)	1	4.878E-01	0	-6.597E-02	0	-1.072E-02	0	1.461E-03	0	-1.773E-09
x(81)	1	5.000E-01	0	-8.013E-02	0	-1.228E-02	0	3.469E-04	0	1.137E-07
x(82)	1	3.464E-01	0	-5.958E-02	0	-1.591E-02	0	-7.874E-04	0	2.445E-07
x(83)	1	2.386E-01	0	-2.298E-02	0	-1.793E-02	0	-1.284E-03	0	2.350E-07
sum of squared errors		1.388E+01		5.091E+00		1.732E+00		2.803E-03		1.857E-09

sequence order	set 1 original uncompressed sequence	set 1 reconstructed sequence	set 2 original sequence compressed by a factor of 2	set 2 reconstructed sequence	set 3 original sequence compressed by a factor of 4	set 3 reconstructed sequence	set 4 original sequence compressed by a factor of 8	set 4 reconstructed sequence
x(1)	4	3.943E+00	4	3.974E+00	4	4.033E+00	4	3.993E+00
x(2)	0	2.379E-03	0	-9.111E-03	0	8.961E-02	0	-7.244E-03
x(3)	0	4.921E-03	0	-1.392E-02	0	8.358E-02	0	-3.118E-03
x(4)	1	1.029E+00	1	9.957E-01	1	1.062E+00	1	1.001E+00
x(5)	1	1.072E+00	1	1.019E+00	1	1.083E+00	1	1.005E+00
x(6)	1	1.114E+00	1	1.048E+00	1	1.055E+00	1	1.006E+00
x(7)	1	1.027E+00	1	1.080E+00	1	1.041E+00	1	1.008E+00
x(8)	1	9.352E-01	1	1.114E+00	1	1.019E+00	1	1.003E+00
x(9)	1	8.385E-01	1	1.146E+00	1	9.947E-01	1	9.993E-01
x(10)	1	7.698E-01	1	1.174E+00	1	9.699E-01	1	9.954E-01
x(11)	1	7.301E-01	1	1.196E+00	1	9.482E-01	1	9.927E-01
x(12)	1	7.210E-01	1	1.208E+00	1	9.328E-01	0	-7.744E-03
x(13)	1	7.332E-01	1	1.204E+00	1	9.250E-01	0	-5.690E-03
x(14)	1	7.571E-01	1	1.180E+00	1	9.259E-01	0	-2.340E-03
x(15)	1	7.830E-01	1	1.135E+00	1	9.347E-01	0	1.490E-03
x(16)	1	8.048E-01	1	1.074E+00	1	9.498E-01	0	4.948E-03
x(17)	1	8.198E-01	1	1.005E+00	1	9.891E-01	0	7.309E-03
x(18)	1	8.290E-01	1	9.390E-01	1	9.905E-01	0	8.085E-03
x(19)	1	8.354E-01	1	8.875E-01	1	1.012E+00	0	7.125E-03
x(20)	1	8.424E-01	1	8.569E-01	0	2.110E-02	0	4.648E-03
x(21)	1	8.525E-01	1	8.480E-01	0	1.813E-02	0	1.186E-03
x(22)	1	8.863E-01	1	8.537E-01	0	1.288E-02	0	-2.522E-03
x(23)	1	8.830E-01	1	8.855E-01	0	6.447E-03	0	-5.687E-03
x(24)	1	9.006E-01	1	8.718E-01	0	1.930E-04	0	-7.835E-03
x(25)	1	9.173E-01	1	8.724E-01	0	-4.718E-03	0	-7.948E-03
x(26)	1	9.320E-01	1	8.841E-01	0	-7.731E-03	0	-6.552E-03
x(27)	1	9.454E-01	1	8.619E-01	0	-9.027E-03	0	-3.736E-03
x(28)	1	9.588E-01	1	8.816E-01	0	-9.377E-03	0	-8.883E-05
x(29)	1	9.745E-01	1	8.800E-01	0	-9.751E-03	0	3.815E-03
x(30)	1	9.940E-01	1	8.803E-01	0	-1.083E-02	0	8.582E-03
x(31)	1	1.017E+00	1	8.659E-01	0	-1.261E-02	0	8.164E-03
x(32)	1	1.043E+00	1	8.794E-01	0	-1.433E-02	0	7.998E-03
x(33)	1	1.068E+00	1	9.023E-01	0	-1.474E-02	0	6.090E-03

x(34)	1	1.089E+00	1	9.340E-01	0	-1.263E-02	0	2.819E-03
x(35)	1	1.102E+00	1	9.723E-01	0	-7.424E-03	0	-1.134E-03
x(36)	1	1.109E+00	0	6.292E-03	0	4.235E-04	0	-4.924E-03
x(37)	1	1.110E+00	0	3.176E-02	0	9.627E-03	0	-7.725E-03
x(38)	1	1.111E+00	0	5.262E-02	0	1.826E-02	0	-8.902E-03
x(39)	1	1.117E+00	0	6.637E-02	0	2.456E-02	0	-8.155E-03
x(40)	1	1.131E+00	0	7.182E-02	0	2.718E-02	0	-5.593E-03
x(41)	1	1.157E+00	0	6.937E-02	0	2.534E-02	0	-1.722E-03
x(42)	1	1.191E+00	0	6.093E-02	0	1.925E-02	0	2.649E-03
x(43)	1	1.226E+00	0	4.954E-02	0	1.010E-02	0	6.575E-03
x(44)	1	1.253E+00	0	3.879E-02	0	-8.335E-05	0	9.174E-03
x(45)	1	1.265E+00	0	3.190E-02	0	-9.047E-03	0	9.822E-03
x(46)	1	1.255E+00	0	3.087E-02	0	-1.498E-02	0	8.304E-03
x(47)	1	1.225E+00	0	3.579E-02	0	-1.708E-02	0	4.877E-03
x(48)	1	1.185E+00	0	4.470E-02	0	-1.600E-02	0	2.329E-04
x(49)	1	1.146E+00	0	5.371E-02	0	-1.346E-02	0	-4.642E-03
x(50)	1	1.124E+00	0	5.796E-02	0	-1.151E-02	0	-8.672E-03
x(51)	1	1.130E+00	0	5.271E-02	0	-1.171E-02	0	-1.093E-02
x(52)	1	1.164E+00	0	3.544E-02	0	-1.389E-02	0	-1.082E-02
x(53)	1	1.219E+00	0	6.748E-03	0	-1.666E-02	0	-8.282E-03
x(54)	1	1.268E+00	0	-2.709E-02	0	-1.703E-02	0	-3.752E-03
x(55)	1	1.287E+00	0	-5.788E-02	0	-1.336E-02	0	1.644E-03
x(56)	1	1.241E+00	0	-7.136E-02	0	-4.482E-03	0	7.293E-03
x(57)	1	1.122E+00	0	-6.872E-02	0	7.383E-03	0	1.134E-02
x(58)	1	9.123E-01	0	-3.284E-02	0	2.014E-02	0	1.300E-02
x(59)	1	6.756E-01	0	-1.127E-02	0	3.191E-02	0	1.177E-02
x(60)	1	3.834E-01	0	1.913E-02	0	4.030E-02	0	7.799E-03
x(61)	1	2.632E-01	0	-4.586E-02	0	4.295E-02	0	1.861E-03
x(62)	1	7.080E-02	0	-8.094E-02	0	3.630E-02	0	-4.798E-03
x(63)	1	8.283E-01	0	-6.477E-02	0	2.626E-02	0	-1.072E-02
x(64)	1	5.535E-01	0	-1.276E-01	0	5.496E-02	0	1.749E-02
sum of squared errors		6.766E+00		1.336E+00		1.532E-01		3.595E-02

APPENDIX B

Publications by the author

1. The modulus of the Fourier transform in image reconstruction;

2. The use of the modulus of the Fourier transform in modelling surface topography;

3. Fourier domain compression techniques in resolving spatial characteristics of surfaces;

4. Fourier domain contrast enhancement of spectral coefficients to improve 3D reconstruction of objects;

5. Fourier domain re-scaling and truncation for improving the 3D reconstruction of objects;

6. Improving the recovery of the micro-geometry of object surface by Fourier scaling.

THE MODULUS OF THE FOURIER TRANSFORM IN IMAGE RECONSTRUCTION

N. Sotoudeh*, G.R. Greatrix+, C.F. Coldspink*

* Middlesex Polytechnic, + Teesside Polytechnic, UK

INTRODUCTION

Reconstructing a three-dimensional surface profile from only the modulus of the Fourier transform of its reflectance function is usually regarded as impossible. However, there are several important applications where such reconstruction would be extremely useful. These include X-ray crystallography, electron microscopy and optical image processing where the Fourier Transform domain is extensively invoked.

The essential difficulty is that optical sensors cannot yet respond to phase and amplitude variations above the terahertz band. Sensors respond to the time-averaged intensity of the optical field. The optical field from a surface of uniform reflectance can be written as

$$\Psi(t,x,y,z) = A \sin[\omega t + \varphi(x,y,z)]$$

while the sensor responds to $\langle \Psi^2(t,x,y,z) \rangle$

$$= \langle A^2 \sin^2[\omega t + \varphi(x,y,z)] \rangle$$

$$= \langle A^2 [1 - \cos\{2\omega t + 2\varphi(x,y,z)\}]/2 \rangle$$

$$= A^2/2$$

so that the phase information is totally lost. The phase component characterises the field at the sensor in terms of the spatial co-ordinates of the reflectance element from which the field emanated. The loss of the phase information implies that it is impossible to identify the precise co-ordinates of the reflecting element. This difficulty arises in both the image domain and in the Fourier transform domain. Even in the case of a two-dimensional surface with a reflectance function $R(x,y)$, it is impossible to reconstruct that reflection function uniquely from only the modulus of its Fourier transform.

For example, a Ronchi grating and a triangular grating of the same fundamental spatial frequency are only two of a whole set of gratings that yield identical Fourier transform magnitude distributions irrespective of their relative (x,y) co-ordinates.

Consequently, in the complete absence of any knowledge of phase in the Fourier transform domain, we cannot uniquely reconstruct either the reflectance profile or the surface profile of an object. Provided that some prior information is available regarding either the object or the phase distribution in the Fourier transform domain, this will restrict the set of surface and reflectance profiles that yield the same Fourier Transform magnitude distribution.

In some applications, it may not be necessary to reconstruct the image uniquely because the common characteristics of a limited set of profiles may be all that is required. The limitation of the set is brought about by known constraints regarding the spatial frequency, amplitude and phase variations in the profile. The characterisation of machined surfaces is just such an application.

This paper introduces an aspect of a research programme based at Middlesex Polytechnic in which selected classes of surfaces are being characterised using only the modulus of their optical Fourier transforms.

CHARACTERISING THE PROFILE OF MACHINED SURFACES

Turned and shaped machined surfaces are produced by a single point cutting tool. The ratio of pitch to depth varies considerably. During the cutting process chips are detached by the tool and a drag occurs just behind the cutting edge which compresses the fragmented metal into a layer of amorphous or smear metal. The heat and pressure of the operation destroys the true crystalline structure of the metal producing a layer of low strength and weak load bearing capacity. If the tool is perfectly guided and the chips uniformly produced, the mean level of the grooves should be on a geometrical surface having the perfect form designated by the drawing. If the guiding is not perfect or the cutting not uniform, the grooves themselves will be on an undulating surface. The complete texture of the surface may be very complex with errors resulting from the feed of the tool, the cutting action, vibration and anisotropy in the crystalline structure of the metal.

In order to produce reasonably well defined diffraction patterns, the area of surface sampled by the laser beam needs to possess features that are comparable in size with the wavelength of light. A range of size from 1 to 500 microns is suitable. Additionally, the area sampled should be larger in diameter than the size of the largest feature of interest.

The commonest parameter used for characterising machined surfaces is that of the roughness average or Ra. Figure 1 shows a typical surface profile. X-X is a line representing the average height of the profile and L is the sampled length. Then

$$Ra = (\text{Sum of areas a} + \text{Sum of areas b}) / L$$

where Ra is expressed in microns.

Clearly, the value of Ra provides no information regarding the detailed shape of the profile nor of the pitch of its repetitive or cyclic features. The Ra value refers to a cross-section of the profile along a line. In practice, the Ra will be a function of the coordinates of the line sample and of its orientation. Such measures are obviously inadequate where the surface quality specification is stringent.

The surface profile is generally assessed by instruments based upon the stylus probe. The stylus, having a radius of about 2 microns is drawn across the surface at right angles to the lay. Continuous contact is ensured by a static force not exceeding 35mN which is not great enough to cause damage to the profile. In this research, a Talysurf is being used to check the surface profile against the characterisation parameters available from the Fourier transform magnitude distribution. Various standard surfaces, prepared by Rubert & Co Ltd to BS 1134, have been examined and reasonably informative diffraction patterns are produced by machined, lapped or ground surfaces with Ra values up to 0.2 microns. This implies that the depth of cut should be less than one wavelength of light in order that the scattering should be reasonably coherent. Such surfaces accord with Lord Rayleigh's definition of a smooth surface in terms of small phase differences between rays reflected from two points separated by a height parameter h. When the phase differences exceed the wavelength of light for the same height parameter, the surface is regarded as rough or diffuse.

THE MEDIUM SPATIAL FREQUENCY BAND

In this band, the surface structures are significantly larger than the wavelength of light and are therefore 'rough' surfaces.

In the case of random surface structure, a computational expression for the modulus of the normalised scattering coefficient, defined as the ratio of the scattered field to that of its specular component, has been formulated as

$$|p|_{norm} = \left[\frac{2F^2 \cos\vartheta_i}{(\cos\vartheta_i + \cos\vartheta_s)} \cdot \exp\left(\frac{V_x^2 \cot(\beta_o)}{V_z^2} \right) \right]^{-1/2}$$

where F is the surface obliquity factor, ϑ_i is the angle of specular reflection, ϑ_s is the scattering angle, $\tan(\beta_o)$ is the r.m.s. slope of the surface irregularities, and V_x and V_z are respectively the summation of the variations of phase among waves scattered parallel to and perpendicular to the surface.

Figure 2 shows the scattering geometry appropriate to this model. Figures 3 and 4 show the comparison between the computed and the measured scattering envelope for directions parallel to the lay and across the lay respectively for a ground surface of Ra = 0.2 microns.

Such envelopes will statistically characterise the randomly distributed features of the surface in terms of the mean optical slope and its standard deviation, σ, through the factor $\tan(\beta_o) = 2\sigma$ /(optical correlation length).

THE HIGH SPATIAL FREQUENCY BAND

In this band, structural sizes are comparable with the wavelength of light. So far, periodic structures have been considered because they possess well defined Fourier transforms and are therefore easier to detect against any incoherent scattering.

Figure 5 shows the envelope for a face-turned surface in a direction parallel with the lay. The macroscopic features across the lay give rise to a gaussian envelope as predicted by the computational expression above. However, there is some modulation of this gaussian curve resulting from the regular pitch of the machined grooves. The base of these grooves has been subject to microscopic tool chatter with a spatial period of 0.12 mm yielding a well defined structure in the Fourier transform magnitude domain. The two-dimensional inverse Fourier transform of this structure will yield information regarding the statistical parameters of the distribution of random features together with a reconstruction of any cyclic features as well as their orientation.

When this face-turned surface was rotated, so that the laser sampled area remained at a constant radial position, the speckle and other random localised noise was eliminated thus enhancing the structure in the Fourier transform domain.

The reconstruction of the surface profile from only the modulus of the optical field in the Fourier transform domain will not truly represent the actual surface since all cyclic features will be reconstructed with a common alignment if zero phase is assumed for all points on the surface. The individual profile of the features cannot be uniquely reconstructed without support from prior knowledge of the type of surface being considered.

Dudgeon and Mersereau (1) have reviewed various proposals for the correct recovery of a signal from only the magnitude of its Fourier transform. Hayes (2) has analysed the recovery problem in detail and concluded that a suitable algorithm had not yet been devised. Gerchberg and Saxton propose an iterative algorithm for recovery of a complex signal from only its magnitude and the magnitude of its Fourier transform.

CONCLUSIONS

Machined surfaces are a special class of profiles where correct recovery is less important than the establishment of quantitative descriptive parameters. Initially, this research programme will investigate the establishment of suitable parameters through only the magnitude of the Fourier transform. Later study will address the possibility of true profile recovery through the application of phase variations to the digitised data. Additionally, a database will be created of known digitised Fourier transform magnitude distributions and their surface profile equivalents.

One particular advantage of working in the Fourier transform domain rather than in the image domain is that movement of the machined surface enhances the Fourier transform structure by eliminating speckle and localised surface noise.

REFERENCES

1. Dudgeon, D and Mersereau, R.M., 1984, "Multidimensional digital signal processing", Prentice-Hall.

2. Hayes, M.H., 1982, "The reconstruction of a multi-dimensional sequence from the phase or magnitude of its Fourier Transform", IEEE Transactions on Acoustics, Speech and Signal Processing, 2, April.

3. Gerchberg, R.H. and Saxton, W.O., 1972, "A practical algorithm for the determination of phase from image and diffraction pictures", Optic, 35, 237-246.

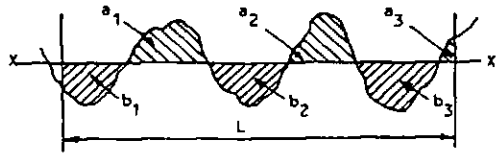

Figure 1 Characterising a surface profile by specifying the roughness average, Ra microns

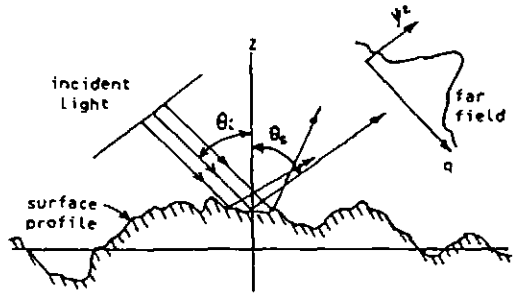

Figure 2 Scattering geometry for a random surface

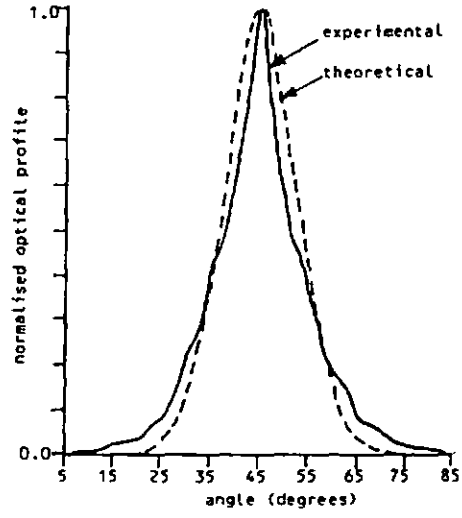

Figure 4 Experimental and theoretical optical profile in a direction across the lay for a surface-ground Rubert specimen Ra = 0.2 micron

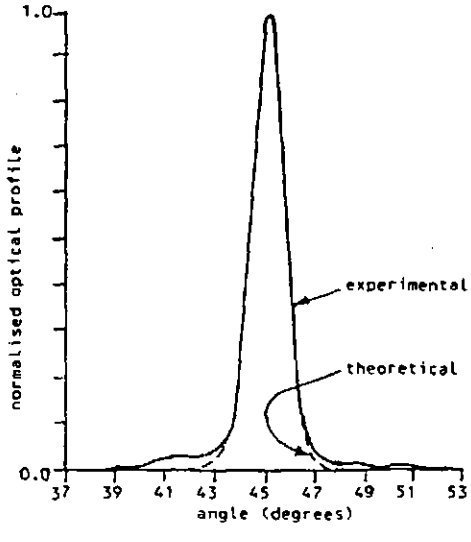

Figure 3 Experimental and theoretical optical profile in a direction parallel to the lay for a surface-ground Rubert specimen Ra = 0.2 micron

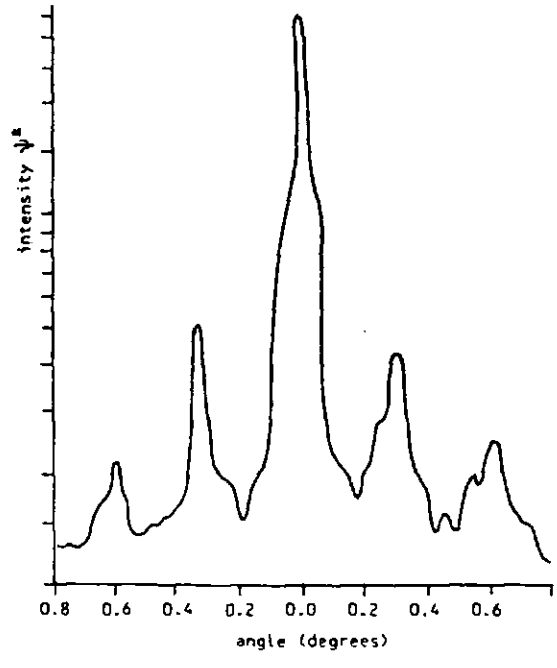

Figure 5 Reflectance envelope across laser beam axis and parallel to the lay for face-turned surface

THE USE OF THE MODULUS OF THE FOURIER TRANSFORM IN MODELLING SURFACE TOPOGRAPHY

N. Sotoudeh*, G.R. Greatrix+, R. Prasad*, G.F. Goldspink*

* Middlesex Polytechnic, School of Electronic Engineering
Bounds Green Rd., London, N 11 2NQ
+ Teesside Polytechnic, Division of Instrumentation and Control Engineering
Physics Section, Middlesbrough, Cleveland, TS1 3BA

ABSTRACT

The use of the modulus of the Fourier transform is demonstrated as a method for the reconstruction of the surface topographical features without access to the phase information. Computer generated pseudo-images of a machined surface have been obtained which reveal the various spatial components by making use of the auto-correlation function. The existence of the recovered spatial features has been verified by scanning electron microscopy results and also traditional contact profiling measurements. This techniqne can be applied to surfaces possessing cyclic or patterned structures and can form the basis of a non-contact, non-destructive surface characterisation technique for use in industry.

KEYWORDS

Fourier modulus; phase; surface characterisation; optical spectrum; non-contact profiling.

INTRODUCTION

When coherent light illuminates surface features whose dimensions are comparable with the wavelength of light, the far-field diffraction pattern is a Fourier transform of those features. The true surface profile as well as the position in space of individual surface features can only be determined uniquely if the phase of the scattered light is also recorded. All currently available detectors sense the light intensity in the diffraction pattern and their outpnt is therefore independent of the phase of the amplitude components. Hence the modulus of the scattered field is the only quantity that can he measured in the optical wavelength region and consequently the phase information is totally lost.

The fundamental difficulty is that optical sensors cannot yet respond to the phase and amplitude variations above the terahertz band. Sensors respond to the time averaged intensity of the optical field. When the incident radiation illuminates the object, it is changed or modulated according to the physical characteristics and dimensions of the object. The incident radiation is deviated or diffracted in a way which is unique to that particular object and is encoded with information about the object. The light which reaches the detector after being reflected by the object now deviates in intensity and phase from its original values. Consider the incident radiation impinging on an object with reflection coefficient R and surface height variations h(z), (Sotoudeh *et al.*, 1989):

$$\mathcal{E}(t,x,y,z) = A\sin[\omega t + \phi(x,y,z)] \tag{1}$$

The reflected radiation would be a function of R and h(z):

$$\mathcal{E}'(t,x,y,z) = f(\mathcal{E}, R, h(z)) \tag{2}$$

$$\mathcal{E}'(t,x,y,z) = A'\sin[\omega t + \phi'(x,y,z)] \tag{3}$$

while the sensor responds to: $< \mathcal{E}'^2(t,x,y,z)] >$

$$=< A'^2\sin^2[\omega t + \phi'(x,y,z)] > \tag{4}$$

$$=< A'^2\sin^2[\omega t + \phi'(x,y,z)] > \tag{5}$$

$$=< A'^2[1 - \cos(2\omega t + 2\phi'(x,y,z))]/2 > \tag{6}$$

$$= A'^2/2 \tag{7}$$

So that the phase information is totally lost.

Various attempts have been made to reconstruct objects from the magnitude of the Fourier transform. There has been iterative algorithms (Fienup, 1982; Bates *et al.*, 1983) and non-iterative methods (Gonsalves, 1987; Nakajima, 1986) for the recovery of the phase from the modulus of the Fourier transformed data. It has been shown (Nakajima and Asakura,1986; Walker, 1981) that the exact reconstruction of the object is not possible without the use of further moduli at the Fourier transform plane. However there are certain classes of surfaces where the exact recovery is less important than the establishment of quantitative descriptive parameters, such as the dimensional range of the spatial features. Many surfaces contain cyclic and patterned features which yield well-defined diffraction patterns. Machined surfaces fall into this category. Authors (Sherrington and Smith, 1989) have reported the use of the Fourier data as a means of representing surface characteristics. Their analysis is based on generating Fourier models of surfaces by obtaining 1-D line scan data by the conventional surface profiling instruments and have reported that the Fourier transformation is a concise data bank for representing surfaces. Previously the use of the Modulus of Fourier transform for characterizing surfaces has been discussed in (Sotoudeh *et al.*, 1989). This work mainly reported on the feasibility of the use of Fourier techniques provided the surface exhibited some degree of periodicity. In this paper we demonstrate the characterisation of a machined specimen by using the Fourier transform data obtained experimentally.

Theoretical Formulation

Consider a surface height variation where $h(z) = f(x,y)$; then in terms of the object domain f(x,y) and the Fourier domain $f(u,v)$ the following pair of relationships exists:

$$f(x,y) = \int_{-\infty}^{\infty}\int_{-\infty}^{\infty} f(u,v)e^{2\pi iux}e^{2\pi ivy}\,du\,dv \tag{8}$$

$$f(u,v) = \int_{-\infty}^{\infty}\int_{-\infty}^{\infty} f(x,y)e^{-2\pi ixu}e^{-2\pi iyv}\,dx\,dy \tag{9}$$

$$f(u,v) \propto \mathcal{E}'(t,x,y,z) \tag{10}$$

where $\mathcal{E}'$ is the diffracted field by the object

$$f(u,v) = |f(u,v)|e^{i\phi(u,v)} \tag{11}$$

where $f(u,v)$ and $\phi(u,v)$ are the modulus and the phase respectively. The observed intensity is $|f(u,v)|^2$ which by inverse Fourier transformation yields the auto-correlation function of the object signal.

Surface Spatial Characteristics

The turned machined specimen was produced by a single point cutting tool. The cutting process produced well defined grooves in addition to microscopic components as a result of the tool- chatter during the cutting process. The combination of the above spatial structures, provided a well defined and structured Fourier transform pattern for characterising the surface. The existence of the above components has been verified by both contact-profiling measurement results and scanning electron microscopy results. Figure 1 shows a pictorial view of the grooves together with the tool-chatter which lies at the bottom of the grooves at right angles to the direction of the groove lay.

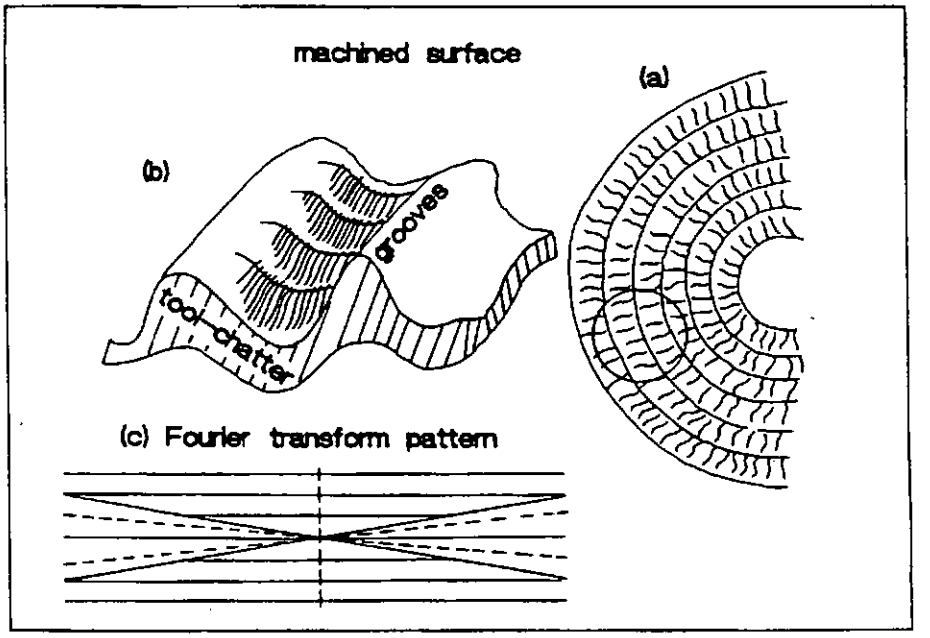

Fig. 1. Pictorial view of the machined specimen. (a) area illuminated by the laser beam. (b) spatial structures present in the illuminated area.

Recording The Optical Data

A He-Ne laser ($\lambda \simeq 6328$ nm) was used to illuminate the surface inclined at a small angle to the optical axis. Optical data was recorded via a vidicon camera and digitised on to a 256x256 sampling grid. By rotating the specimen, surface localised noise was virtually eliminated. The digitising software also provided low pass filtering by recording an average of the subsequent frames. Figure 2 shows the setnp and Figure 3 shows the resulting diffraction pattern.

COMMENTS AND DISCUSSION OF RESULTS

Figure 4 shows the inverse Fourier transformation of the optical data with zero phase. In the case of the machined specimen the resultant diffraction pattern is due to the contribution of two different spatial components: the reflection from the gross features plus the diffraction from the small features. Gross features have dimensions much larger than the wavelength of light and if they produce any diffraction it is negligible as compared to any diffraction from the smaller

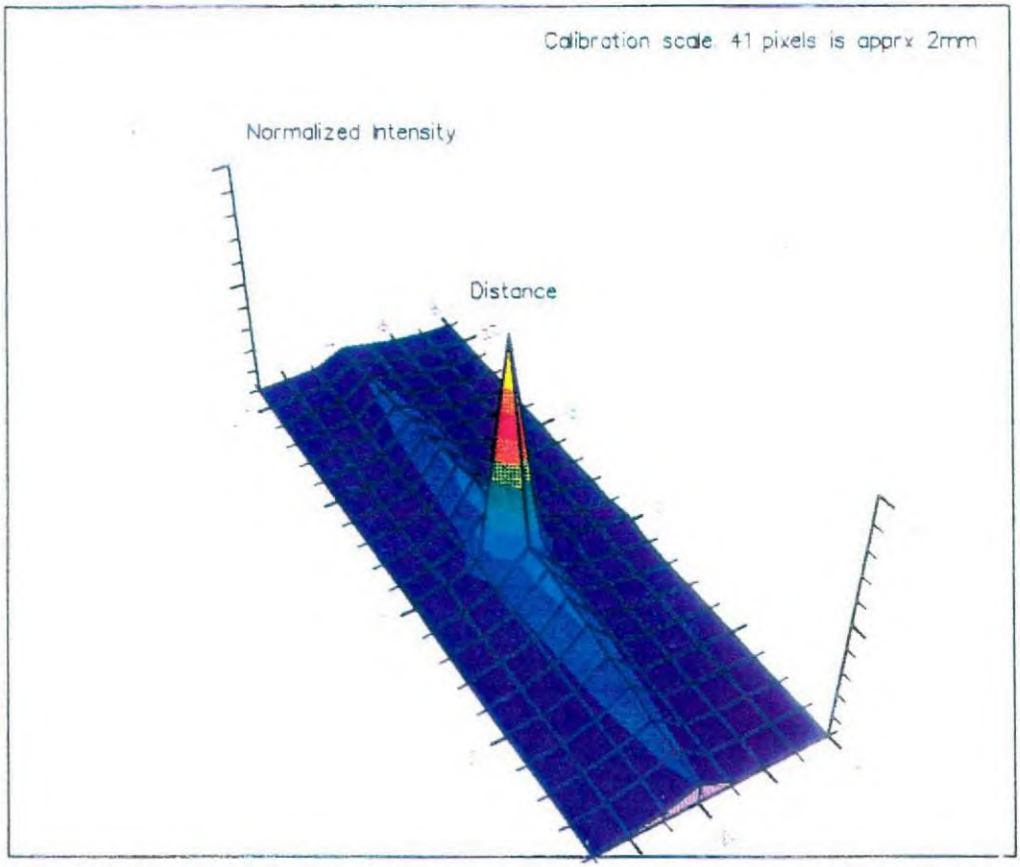

Fig. 4. Inverse Fourier transform of the optically recorded diffraction pattern. (Laser beam profile is super-imposed on the machined surface reflectance profile.)

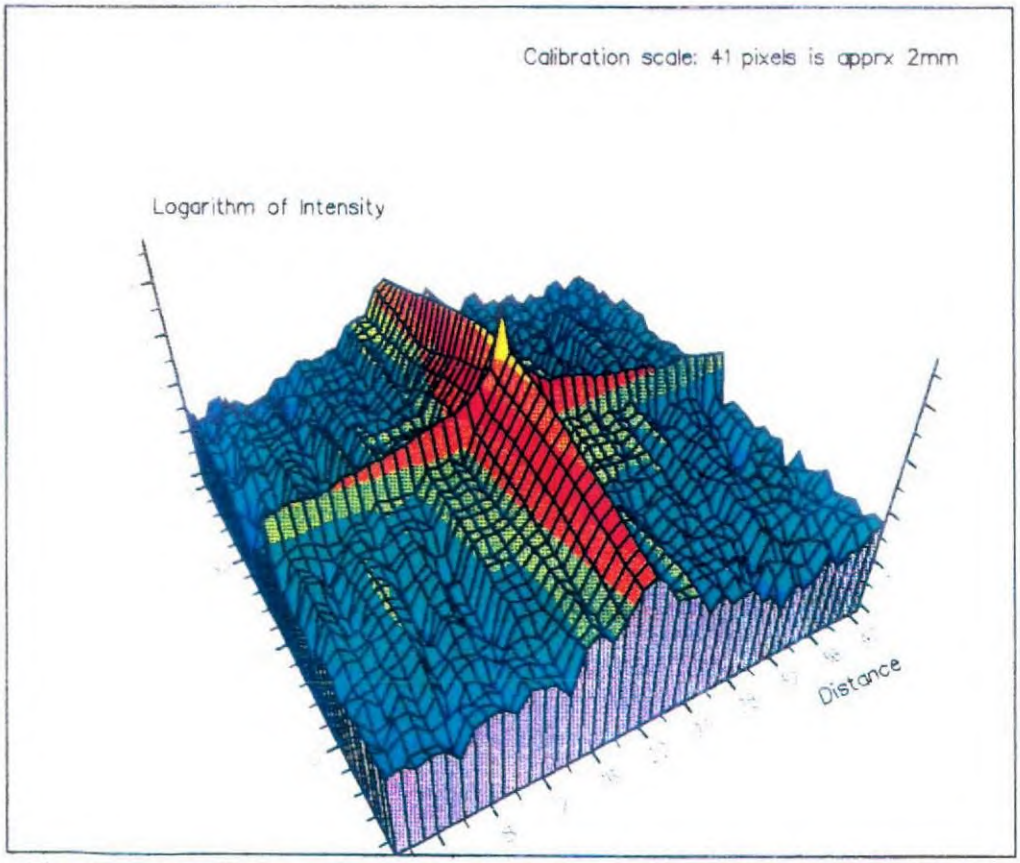

Fig. 5. Logarithmic enhancement of the inverse Fourier transformed diffraction pattern. (Spatial structures of similar periodicity to that of the grooves have been recovered.)

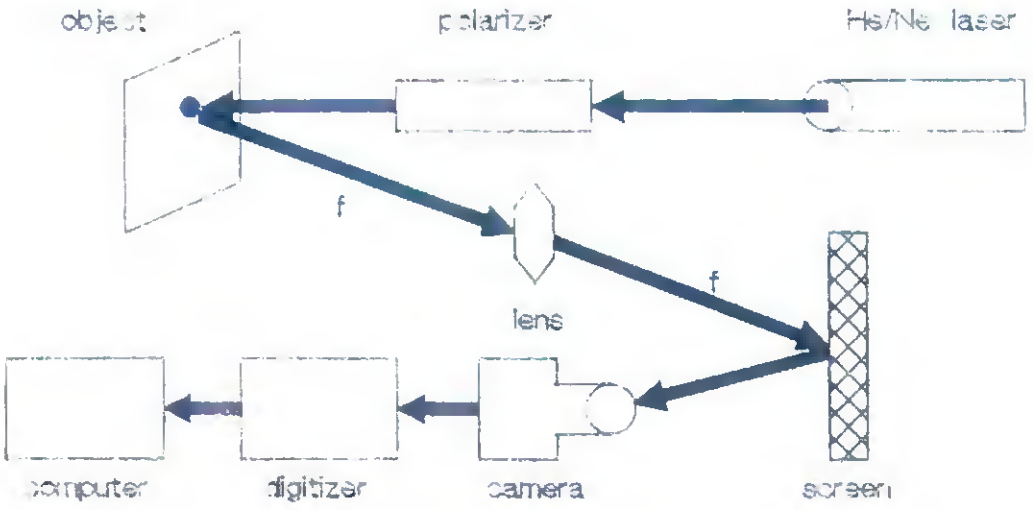

Fig. 2. Experimental setup for recording the far-field pattern.

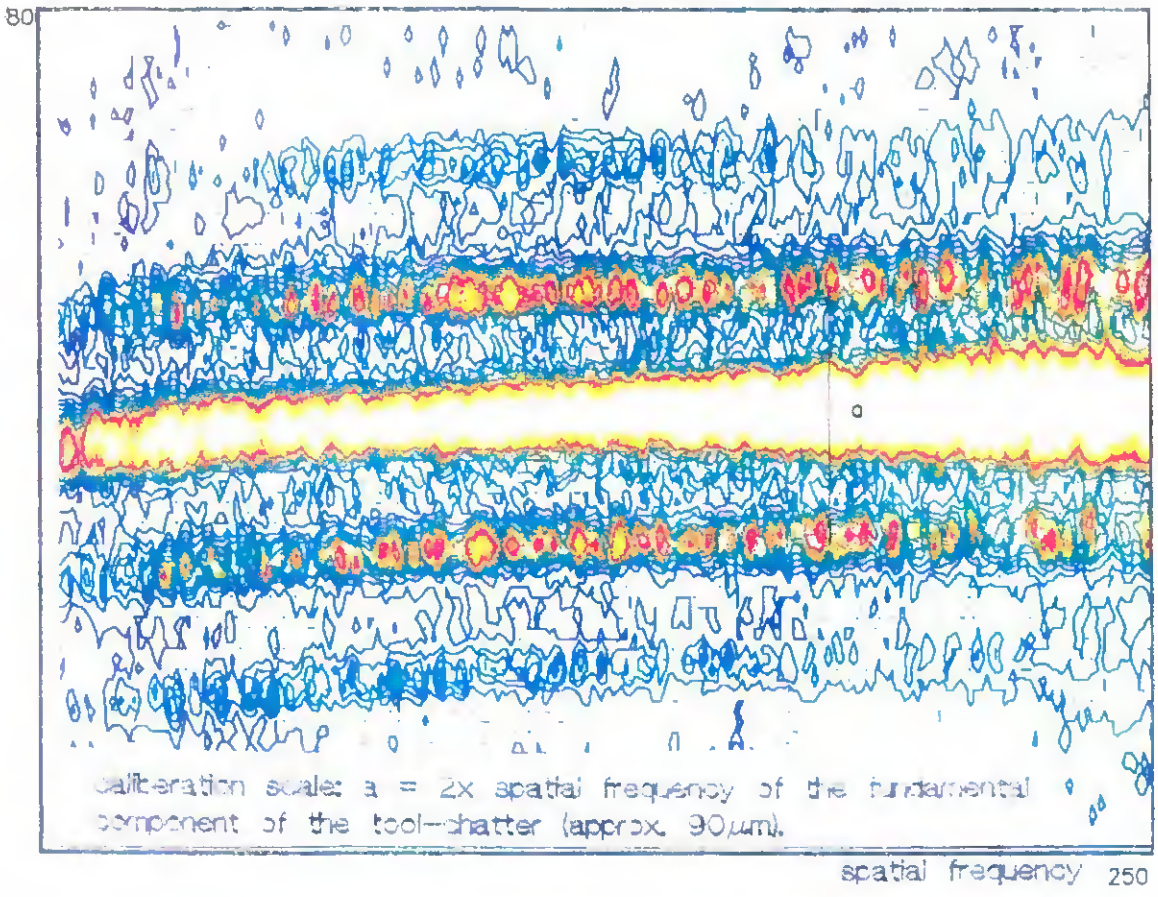

Fig. 3. 3D optical Fourier transform for the machined surface. The central region indicates spectral lines due to the grooves; the extra pair of spectral lines on either side of the central region are due to the tool-chatter and its harmonics.

features. The gross features are the grooves which have approximately a spatial spacing of 200μm and the small features are the tool chatter components which have a spatial spacing of 100-5μm respectively. When the laser beam illuminates the surface, the gaussian intensity distribution of the laser beam is multiplied by the surface reflectance profile. The intensity data recorded by the detector is the convolution of the Fourier transform of the laser beam with the Fourier transform of the surface reflectance profile hence, upon inverse Fourier transformation, one gets back the product. The distorted shape of the laser beam is due to the non planar surface of the machined specimen i.e. reflection from the grooves distorts the expected circular shape of the recovered laser beam upon inverse Fourier transformation.

Figure 5 shows the logarithmic enhancement of Figure 4. As there is a large dynamic range the logarithmic display will enhance the smaller amplitude features. As can be seen, there is a pronounced evidence of periodic components whose dimensions are found to be approximately the same as those of the grooves. To measure the physical dimensions of the recovered features the approximate diameter of the laser beam was set eqnal to the distance for which the intensity has dropped to 1% of its maximum value. In the diagram a transition of 5-3 on the logarithmic scale accounts for a 100-fold drop in intensity. As near the edge of the laser beam the intensity drops off very significantly this distance is a good approximation for the calculation of the edge of the laser beam.

CONCLUSION

Machined surfaces with pronounced structures can be characterised by the inverse Fourier transformation of their corresponding diffraction patterns. If the surface possesses periodic components, inverse Fourier transformation will reveal their presence with all the recovered structures having a common alignment. However if the surface contains coarse periodicity, inverse Fourier transformation will yield components due to the fundamental spatial period together with the higher harmonics of this spatial period which are needed to synthesize the coarse structure. In our case features with a spatial period similar to that of the grooves has been recovered. Subsequent magnification of these recovered features resolves higher frequency spatial structures which is the subject of a forthcoming paper.

REFERENCES

Bates, R.H., W.R. Fright (1983). Composite two-dimensional phase restoration procedure. *Opt. Soc. Am.*, 73, 358-365.

Fienup, J.R. (1982). Phase Retrieval algorithms: a comparison. *Applied Optics*, 21, 2758-2769.

Gonsalves, R. A. (1987). Phase retrieval by differential intensity measurements. *J. Opt. Soc. Am*, A4, 166-170.

Nakajima, N. and T. Asakura (1986). Two dimensional phase retrieval using logarithmic Hilbert transform and estimation technique of zero information. *J. Phys.*, D19, 319-331.

Nakajima, N. (1986). Improvement in evalnating the logarithmic Hilbert transform in phase retrieval. *Optics Letters*, 1, 600-602.

Sherrington, I. and E.H. Smith (1988). Fourier models of the surface topography of engineering components. *Surface Topography*, 1, 11-25.

Sotoudeh, N., G.R. Greatrix and G.F. Goldspink (1989). The modulus of the Fourier transform in image reconstruction. *Third Inter. Conference on Image Processing.*

Walker, J.G. (1981).The phase retrieval problem: A solution based on zero location by exponential apodization. *Optica Acta*, 28, 735-738.

FOURIER DOMAIN COMPRESSION TECHNIQUES IN RESOLVING SPATIAL CHARACTERISTICS OF SURFACES

N Sotoudeh*, G R Greatrix+, R Prasad*, G F Goldspink*

* Middlesex Polytechnic, UK
+ Teesside Polytechnic, UK

INTRODUCTION

It is often desirable to zoom-in on a particular region of the image of a surface. The techniques of replication and interpolation are well known for magnifying images in the spatial domain. However if the information is in the spatial frequency domain such as the optical Fourier transform of a surface reflectance profile, frequency compression techniques could be used to resolve the spatial characteristics of a surface on a magnified scale.

The Fourier transform of a surface reflectance function is the signature of various spatial features which are present in the surface. It maps spatial structures into the spatial frequency domain and their physical dimensions are encoded into this space via reciprocal relationships. If the object exhibits large periodic structures as well as small, the Fourier domain will map such structures into its low frequency and high frequency regions respectively. It is the high spatial frequency regions which contain the fine surface details and to resolve such structures demands very fine sampling intervals in the frequency domain.

Characterising Machined Surfaces

Earlier work by Sotoudeh et al (1) had reported on the feasibility of the use of the modulus of the Fourier data in characterising surfaces possessing structured and semi-patterned features. It was shown that because such surfaces possess well-defined Fourier transforms, it is possible to characterise them without the use of the phase information. Further work by Sotoudeh et al (2) has applied the above argument to the study of the spatial characteristics of a machined surface. This surface exhibited a range of spatial structures from coarse periodic components to very fine details resulting from the cutting process, as shown in Figure 1. The combination of coarse and very fine periodicity gave rise to the high frequency as well as the low frequency spectral characteristics in the Fourier domain. This work has shown that low frequency structures with similar characteristics to those present on the surface can be recovered without any recourse to phase.

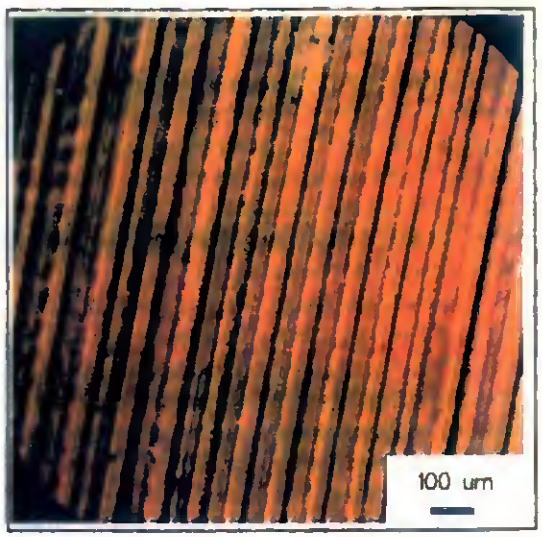

Figure 1: Photo micrograph of the machined surface showing various spatial structures.

The present paper describes a technique which can recover fine structural details whose existence is mapped into the diffraction pattern but their physical presence cannot be established without *modification* of the available frequency spectrum.

The Magnification Principle

To resolve the finer structural details whose presence is so prominent in the diffraction pattern, requires frequency domain compression of the optical data. This can be achieved both in

hardware and software by making the Fourier spectrum a much smaller part of a larger data array.

The power of the principle then lies in the inverse dimensional property which operates between the Fourier domain and the object domain in that large spatial structures are coded into small spatial frequencies very near the central region and small spatial structures are coded into large spatial frequencies which are distant from the central region of the frequency spectrum. Hence for an object to appear large in the spatial domain its captured frequency spectrum should appear compressed. This can be achieved through zero-padding the recorded optical spectrum and then applying the *scaling* property of the Fourier domain to enlarge the reconstructions through inverse Fourier transformation.

For a surface function of h(x,y) in the spatial domain, its Fourier transform ($\mathcal{F}\{h(x,y)\}$) can be expressed as :

$$H(f_x,f_y) = \sum_{m=0}^{m-1}\sum_{n=0}^{n-1} h(x,y)\cdot e^{-2\pi j(f_x x + f_y y)} \quad (1)$$

If the surface function of h(x,y) in the spatial domain is magnified by a factor M in both the x and the y directions, i.e. h[M(x,y)] the following property exists:

$$\sum_{m=0}^{m-1}\sum_{n=0}^{n-1} h[M(x,y)]\cdot e^{-2\pi j(f_x x + f_y y)} \quad (2)$$

$$\frac{1}{M^2}\, H\left(\frac{f_x}{M},\frac{f_y}{M}\right)$$

therefore

$$\frac{1}{M^2} H\left(\frac{f_x}{M},\frac{f_y}{M}\right) \Leftrightarrow h[M(x,y)] \quad (3)$$

This *modified* spectrum with the new frequency intervals compressed by a factor of 1/M requires processing large arrays with an excessive amount of computational time. However it is known that not all the coefficients in the Fourier domain are needed to reconstruct a surface satisfactorily, Raja and Radhakrishnan (3), and surfaces can be represented by using a fraction of the detail in the Fourier spectrum, Sherrington and Smith (4). This fact has also been employed in image coding techniques whereby a small fraction of Fourier coefficients is found to result in acceptable reconstructions as shown by Lim (5).

Application and Conclusions

By combining the two effects of *Fourier domain compression* and *Fourier coefficient removal*, optically recorded Fourier transform for the machined surface was compressed in the frequency domain which upon inverse Fourier transformation, resulted in an expansion in the spatial domain. The far-field diffraction pattern was obtained via illuminating the machined surface with a 0.632 μm He-Ne laser beam, fuller details of which can be found in reference (2). All the reconstructions have the laser beam profile superimposed on the recovered surface reflectance profiles. Figures 2 and 3 show the reconstruction before employing the compression technique. Figures 4 and 5 show the compressed spectrum and the recovery of the finer spatial details after applying the compression technique respectively.

Due to the absence of phase, the recovered zero-phase characteristics could either be due to the higher harmonics needed to synthesize a coarse structure or they could actually represent physically realisable detail. In either case this novel technique of combining frequency compression and reduction of Fourier domain coefficients is capable of resolving such details. It has also been shown that there is a limit for further magnification set by:

i) the number of spectral coefficients that can be

ignored when compressing the data, and ii) the extent to which the zero-padding of the consequent data array can be performed without introducing aliasing.

REFERENCES

1. Sotoudeh, N., G.R. Greatrix and G.F. Goldspink, 1989." The Modulus of the Fourier Transform in Image Reconstruction". Third International Conference on Image Processing IEE, Warwick.

2. Sotoudeh, N., G.R. Greatrix, R. Prasad and G.F. Goldspink, 1991. "The use of the Modulus of the Fourier transform in modelling surface topography". Eighth International Conference on Mathematical and Computer Modelling, Washington USA.

3. Raja, J. and V. Radhakrishnan, 1977. International Journal Mach. Tool Des. Res. M17, 245-251.

4. Sherrington, I. and E.H. Smith, 1988. "Fourier models of the surface topography of engineering components". Surface Topography, 1, 11-25.

5. Lim, J.S. 1990, "Two dimensional signal and image processing", Prentice Hall.

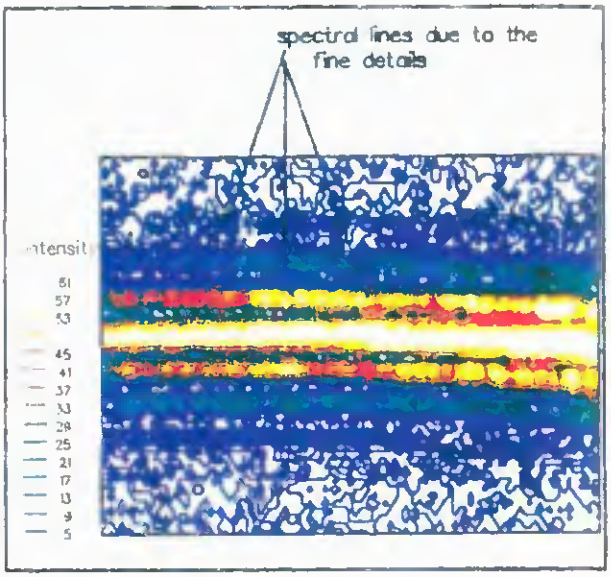

Figure 2: Optical Fourier transform of the machined surface.

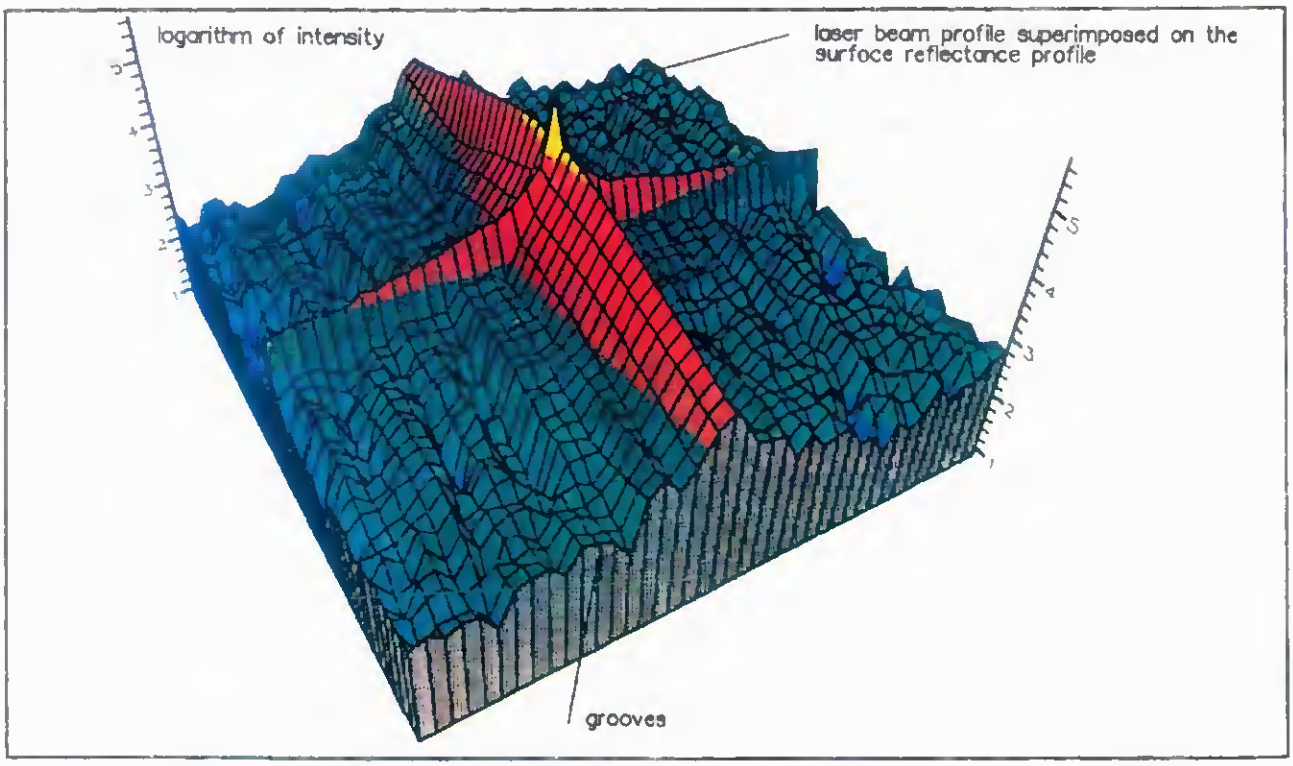

Figure 3: Inverse Fourier transform of the optical spectrum.

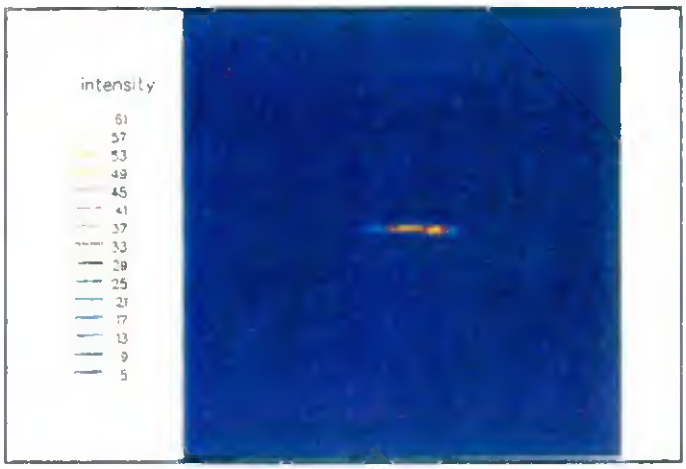

Figure 4: Compressed optical spectrum of Figure 2 with reduction of Fourier coefficients by 50% (Note that the background is extended by a factor of 4).

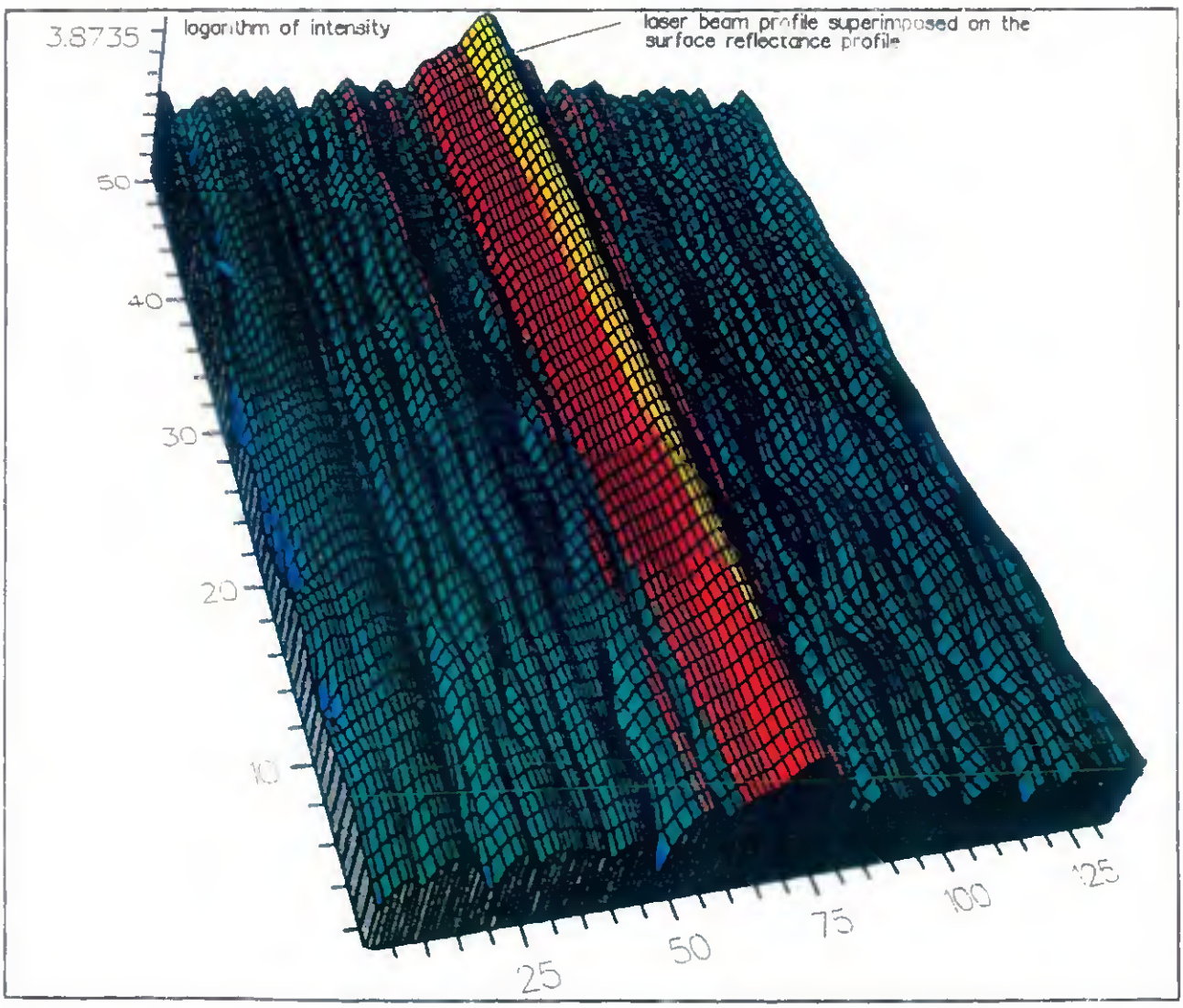

Figure 5: Reconstructed reflectance profile of the machined surface by using the compressed spectrum.

FOURIER DOMAIN CONTRAST ENHANCEMENT OF SPECTRAL COEFFICIENTS TO IMPROVE 3D RECONSTRUCTION OF OBJECTS

* + *

N.Sotoudeh, G.R.Greatrix & G.F.Goldspink

* Middlesex University, School of Electronic Engineering, Bounds Green Rd., London N11 2NQ, UK.
+ University of Teesside, School of Science & Technology, Middlesbrough, Cleveland, TS1 3BA, UK.

ABSTRACT

This work is concerned with the retrieval of the three-dimensional reconstruction of the microstructure of object surfaces from the recorded Fourier modulus spectrum associated with such objects. In order to recover a faithful reconstruction of the object in the spatial domain, the Fourier modulus data employed in the logarithmic Hilbert transform algorithm has to be modified prior to being subjected to phase recovery calculations.

It has been shown that this modification has to accentuate the amplitude level of the higher order Fourier coefficients with respect to that of the zero-order component. Object surfaces generally yield a zero-order term with a magnitude level which both saturates the recording and overwhelmingly dominates all other frequency components. This reduces the accuracy of the Hilbert Algorithm in retrieving phase. In particular, object surfaces with sharp edges give rise to many discontinuities in their Fourier spectrum. Preservation of contrast in an adequate number of higher order lobes is required to maintain fidelity in the reconstruction of such objects.

Contrast enhancement can be achieved through spatial filtering of the central region of the Fourier spectrum by experimental and computational means. In this paper computer simulated reconstructions of a real object, based on different levels of the visibility of the higher order coefficients are provided. It has been shown that without such contrast enhancement, the actual intensity profile is not recoverable. The recovery of an object's accurate intensity profile is a necessary precursor to the recovery of the correct surface depth profile.

KEYWORDS

Fourier Contrast enhancement, object recovery, phase retrieval, reflectance profile, depth from shading, 3D reconstructions

INTRODUCTION

For object images in the spatial domain, it is always possible to tailor a level of contrast so that the object is well distinguished from its surround whilst preserving its very salient features (Oppenheim, 1975). However, when the only source of the object retrieval is the optical Fourier modulus spectrum, it is the diffracted intensity information which has to be

modified to bring out such contrast between the object and its background. Any phase retrieval technique (Feinup, 1984), (Gerchberg & Saxton, 1972), (Nakajima, 1986) based on the modulus of the Fourier spectrum, has to rely on the Fourier map in preserving much of the intelligibility of the object characteristics. Whether the object has any distinct prominent features, or no dominant spatial information, its intelligibility is retained in the fraction of spatial frequency components diffracted by the object as opposed to any surrounding background contribution. In addition, this intelligible fraction of the Fourier map, i.e the object related part of the frequency spectrum, has to possess a good span of frequency harmonics both in terms of amplitude levels and sampling intervals (Bates & Fright, 1983) if phase variations are to be restored faithfully from the modulus data.

Often, object surfaces such as very smooth reflectance objects, have Fourier spectra well dominated by a very bright zero-order term which obliterates all other frequency terms present in the Fourier map. Under such circumstances, the diffracted intensity information seems to be confined to the very near centre of the frequency map, with the higher order frequency terms almost invisible to the recording device. Real object surfaces possess many regions of discontinuity which map as many isolated lobes, or lobes separated by minima, into the Fourier plane. Although, not all Fourier coefficients are needed to synthesize the object's reflectance profile, (Sotoudeh *et al.*, 1992), a reasonable proportion of this information has to contribute towards the synthesis of the object.

If the fraction of the captured frequency terms is registered accurately by the camera and digitiser, then the reconstructed reflectance profile would only be degraded through the exclusion of the higher spatial frequency terms . However, for high levels of background interference, this information is either lost through saturation, or it would be recorded mainly as one entity which has enclosed a number of higher order lobes. This would lead to certain complications and ambiguities regarding the true nature of the object characteristics.

The origin of these ambiguities depends very much on how the weaker higher frequency information has been perceived by the recording device. Integration of a number of isolated lobes into a single entity would create a low frequency plateau, and would falsify the true spatial period of the object. Any slight variations, associated with the outer contours of these lobes which are still preserved within this plateau would cast an intensity variation in the form of a shadow upon the surface of the retrieved object with a uniform reflectance profile. It is extremely important that such shading variations in the reflectance profile are object related and are not artifacts introduced by low frequency variations which are not signal based.

In addition, any *true* shading variations in the reflectance profile of the object, would appear as fine undulations in the intensity of the Fourier components whose information has to be preserved. Such shading variations in the reflectance profile, signify the presence of the structural components in the object such as an edge. Hence the retrieval of the micro-geometry of very smooth reflective objects, necessitates some form of spatial filtering applied to the frequency spectrum prior to resorting to any form of phase retrieval.

DEPTH PERCEIVED AS DIFFERENCE IN SHADING

The three-dimensional reconstruction of object surfaces from the diffracted intensity information in the Fourier map, would only be feasible if object depth is coded as a difference in shading in the recovered reflectance profile. For instance, a flat object surface, with uniform reflectance, should have a flat reflectance profile recovered if the source of illumination has sampled the object normally, as in case 1 of Fig.1. As can be seen, an object structure with a spatial structure which incorporates depth, would be perceived as flat. This is due to the fact that the only information which codes the structural characteristics of the object is its reflectance profile. Under normal illumination, all structural aspects of a surface material i.e. flat regions as well as the edges, contribute in a similar manner towards

this raflectance profile. Hance, there would be uniform reflectance irrespectivs of the change in the atructure brought about by its depth.

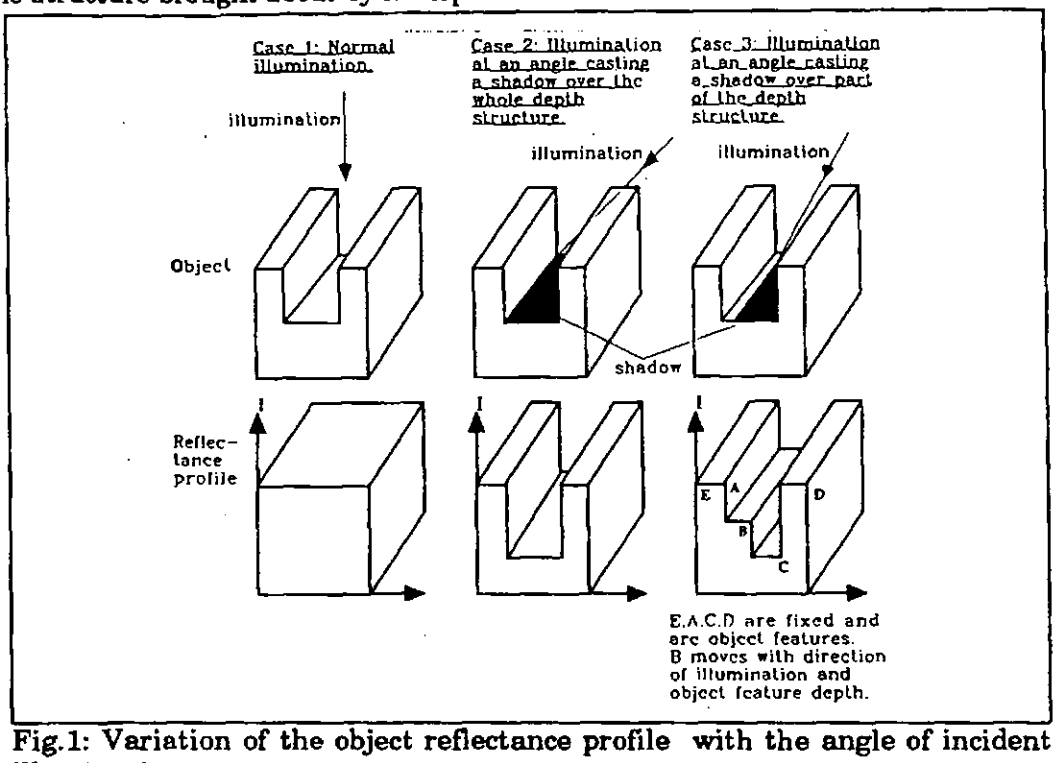

Fig.1: Variation of the object reflectance profile with the angle of incident illumination.

However, with a change in the angle of illumination, the reflectance profile varies across the edges of the object casting a ahadow over part or whole of the depth feature as can be seen in case 2 of fig.1. This ahadow varies with the angle of illumination or with the tilt of the object plane. At the particular angle of illumination for case 2, the reflectance at the edges ia much brighter than that of the depth feature, i.e the bottom aurface, and this particular reflectance profile has coded the true object structural characteristica. With a further change in the angle of illumination, as in case 3, part of the deepest feature, haa a ahadow cast over it and the graduations in amplitude level of the shadow, would give riae to a aimilar graduation in the reflectance profile of the object. As can be aeen, this reflectance profile now differs considerably from the depth profile of the actual object.

However, it is possible to isolate the *true structural* characteristics of the object which appear *stationary* in a series of such reflectance profiles from the *shading artifacts* which *move* with the shadow cast on the surface. This can be seen in case 3 of fig. 1, where the true structural features, edges E and D are common in all the reflectance profiles, followed by the reoccurrence of edges, A and C in the laat 2. Hence, the *stationary* features which are the edge features, do not change, but the *moveable* feature B, which is the edge of a shadow, spans the width of the depth object, with a change in the angle of incident illumination.

These considerations, indicate that if the object's true atructural characteristics are to be realised, the reflectance profile for any particular angle of incidence ahould be recovered accurately. This would enable one to deduce the true atructural configuration and hence the depth characteristics from a series of auch reflectance mapa. However, frequency characteristics are usually degraded by the limited quantisation intervals of the digitiser, the available sample points and the finite aperture of the recording device. Any background contribution in the object domain would further degrade the perception of such information, *particularly when an undesired low frequency information, which is not signal related, contributes towards the object synthesis.*

SPATIAL FILTERING OF REFLECTIVE OBJECTS

For a faithful recovery of object surfaces which give rise to frequency domain characteristics with an abnormally high DC term, the amplitude of light distribution in the diffracted orders has to be made comparable in magnitude with respect to the D.C. term. This can be achieved through spatial filtering of the Fourier map. The D.C. term can be attenuated to a value such that the intensity of the diffracted orders can yield the information content of the object. The DC level cannot be blocked completely because this would result in frequency doubling (Lipson & Lipson, 1981).

The procedure for modifying the frequency spectrum via spatial filtering depends on the original characteristics of the object and how the shape of its immediate surrounding aperture contributes towards the overall spatial frequency information. Studies by (Bates & Fright, 1983) concerning object contrast, were based on the recovery of astrophysical objects which mainly consist of a faint detail on a bright background saturating the finer information. The bright surrounding background acting as a large aperture, has control over the low spatial frequency region mainly the central lobe, and the smaller astrophysical features merely manifest themselves in the higher order lobes. Hence there is a need to alter the intensity level of the very central lobe. This has been referred to as a defogging process whereby the fainter object characteristics are made to shine through the fog as their higher frequency information is selectively strengthened. Such modification of the frequency spectrum has been brought about by having access to both the object image in the spatial domain and its corresponding Fourier pattern.

Our recovery scheme however, is from the diffracted intensity information alone, without any information regarding the object spatial configuration other than that it is a reflective surface. The object surfaces consist mainly of chromium regions of different geometrical shape with a dimensional range of 100-20 μm residing on a glass background. Although, the higher reflectivity of chromium provides good contrast with respect to the glass, the back reflection from the glass, reinforces the strength of the D.C. term. Hence, a spatial filter which mainly attenuates the central point is required to alleviate the recording of this diffraction.

Furthermore, as we are confronted with a signal contribution mainly towards the zero-order term, a mere attenuation of the D.C. term would suffice. This would also protect the fine undulations of the intensity of the Fourier components, from a filtering mask which extends into the low frequency region. Such fine undulations in the Fourier map, emerge from the shading variations of the object's reflectance profile with a change in the angle of illumination. As already mentioned, shading variations of an object's reflectance profile, are a precursor to the realisation of the object depth.

In practice, it is not possible to generate a spatial mask with an infinitely small diameter, which would only attenuate the zero-order term, hence the finite aperture width of such a filter extends into the near central region. Nor would it be possible to introduce a computer generated continuum of infinite width that would give rise to a single delta function in the Fourier domain to allow the use of a filter mask that just attenuates this point.

Hence, the closest analogy to the experimental situation that can be realised through computer simulations, would be the study of the distortion introduced by a highly reflective background restricted by a finite square data aperture. This study is valuable in terms of identifying how a very low frequency component, whose reflectance level reaches that of the object of interest, affects the recovery of the object's reflectance profile.

COMPUTER SIMULATIONS AND DISCUSSION OF RESULTS

In order to illustrate the aforementioned effects, computer simulated studies for two object profiles have been performed. The first object is a square with uniform reflectance profile for which the background contribution has been raised almost to the reflectance level of the object. The reflectance profile of this object is then recovered from its computer generated Fourier spectrum and the phase retrieved from the modulus of this spectrum by using the convolution integral of the logarithmic Hilbert transform (2) below:

For an object with reflectance profile f(x,y), its two dimensional Fourier spectrum is (1):

$$f(x,y) \sim |F(u,v)|\, e^{i\phi(u,v)} \tag{1}$$

$$\phi(u,mc) = \frac{-1}{\pi} P\int_{-\infty}^{\infty} \frac{F(u',mc)}{(u-u')}\, du' + C_0 \tag{2}$$

whereby the two dimensional phases $\phi(u,v)$ plus an additive constant phase C_0 are calculated as an independent series of one dimensional phases $\phi(u,mc)$. To generate a coherent pattern of two dimensional phases, the phases along an orthogonal direction through the centre of the frequency spectrum are also evaluated, namely $\phi(0,v)$ (Nakajima & Asakura, 1986) and are added to the phases of the individual strips $\phi(u,mc)$. The recovered phases, are than inverse Fourier transformed with the filtered and unfiltered Fourier data to show the effect on the object recovery. To satisfy the continuity of the logarithm of the modulus data, a constant value was added to all the frequency data in the Fourier domain. Such a continuum results in the addition of an impulse or a delta function to the object which, dependent upon the level of this delta, it can always be distinguished from the rest of the object characteristics (Sotoudeh, *et al.*, 1993).

Prior to exploring the distortion in the object characteristics brought on by high level background interference, the object's Fourier spectrum has been enhanced in terms of sampling points. This is to ensure, that any degradation in the object's reflectance profile, stems from the effects of such high background as opposed to the distortions introduced by the very low amplitude of the higher frequency terms. Phase inaccuracies are inevitable in the vicinity of any enclosed frequency minima for structured objects. The enhancement in the sample points is introduced effectively, by the expansion of the frequency spectrum brought about by a reduction in size of the object (Sotoudeh, *et. al*,1993).

The first reconstruction is for one of our square features of 16x16 pixels as part of a 256x256 data matrix, with high contrast with respect to its surround , Fig. 2.1. The Fourier spectrum Fig. 2.2, of this object, has optimally preserved all the intelligibility of the object and the reconstructed reflectance profile can be seen in Fig. 2.3 as a very faithful recovery of the original object.

Figure 2.4, is the Fourier spectrum of the same object but with a high level of background interference, namely the reflectance level has been raised by 87%. The Fourier spectrum of the square feature which has a slightly higher reflectance than its surround, is a Sinc frequency distribution with the zero cross over point at 1/L in the Fourier space.Where L is the object extent in the spatial domain i.e 16 pixels across in both the x and the y directions.

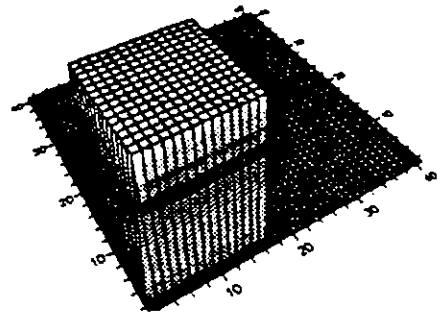

Fig. 2.1:Original reflectance object.

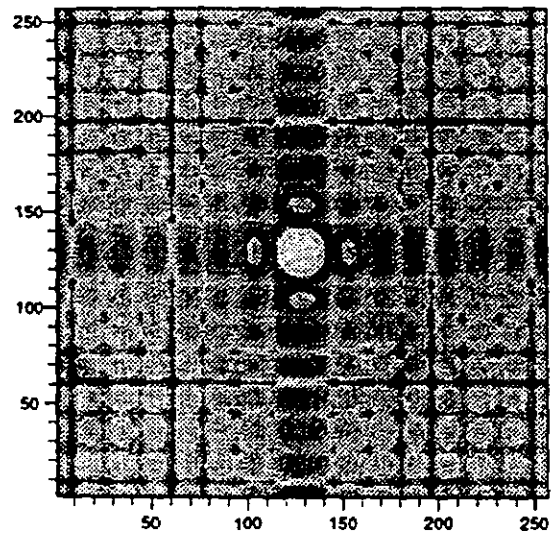

Fig. 2.2: Fourier spectrum of the reflectance object without background contribution.

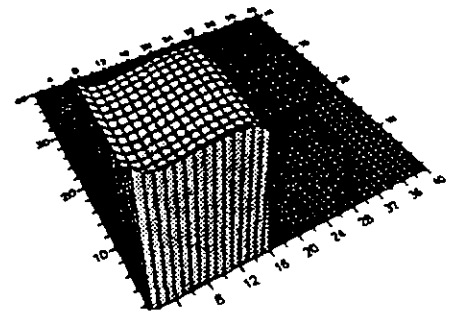

Fig.2.3: Reconstructed reflectance profile from the Fourier modulus spectrum of Fig.2.2.

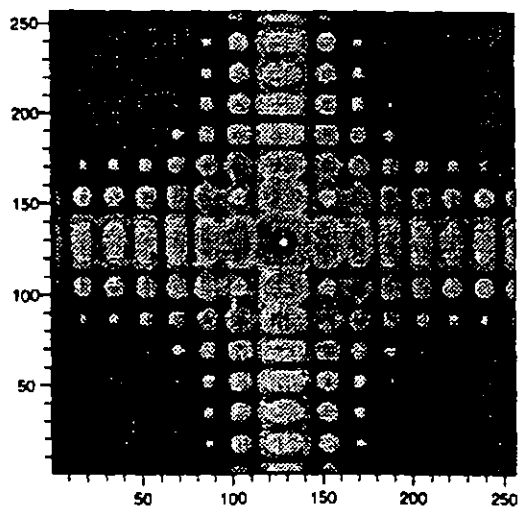

Fig.2.4: Fourier Spectrum of the reflectance object with a high level of background interference.

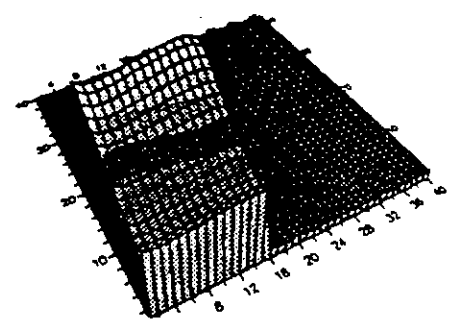

Fig.2.5: Recovered reflectance profile from the Fourier modulus spectrum of Fig. 2.4.

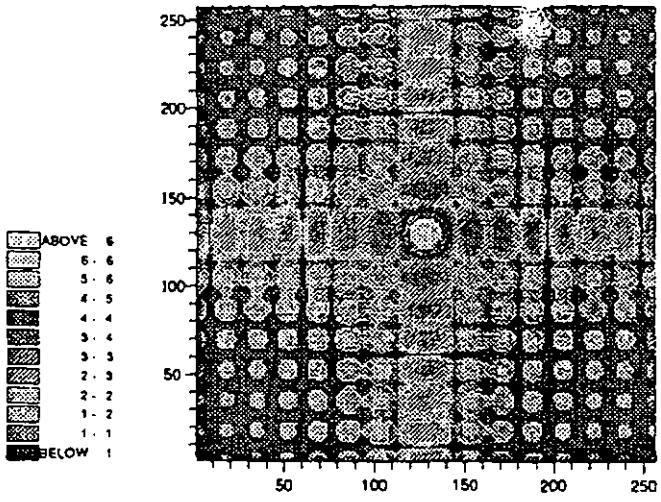

Fig.2.6: Fourier modulus spectrum of Fig.2.4 after spatial filtering.

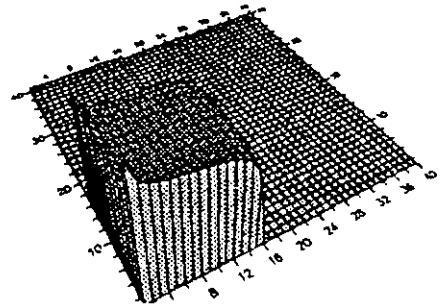

Fig.2.7: Recovered reflectance profile of the object from the filterd spectrum of Fig.2.6.

A background signal such as a continuum in the object domain, dnes not give rise to a single impulse in the frequency domain, but would generate another Sinc distribution with zero cross over points of 1/16L apart. Hence, the first half lobe of our small object feature would be enclosing 15.5 lobes of the larger surrounding background in the Fourier space. When the background signal strength is increased, the central point is increased in amplitude by several orders of magnitude as compared with the next immediate frequency term. However, the strength of the rest of the points associated with this large background, is also increased, affecting the very low frequency region in amplitude variations. Hence, the merged spatial frequency information of both the background and the object would include slight variations in the very first lobe where the most of the signal strength resides. As a result, the recovered characteristics seen in Fig. 2.5, would retrieve the object spatial extent, i.e the same square but with a non-uniform reflectance profile. i.e there are shading variations cast on the surface.

As can be seen this is a low frequency signal superimposed on the recovered reflectance profile which confirms the fact that the distortion has mainly resulted from the low frequency regime of the frequency map. Figure 2.7 is the recovered object characteristics, with the application of a spatial filter in the very central region of the fourier map of Fig.2.4 to attenuate the central point. The attenuation is such that the amplitude of this point is kept slightly higher than the next immediate frequency point, the modified spectrum can be seen in Fig.2.6. This is to ensure that the signal has an average reflected component, i.e D.C. point to maintain the correct spatial extent of the object.

The immediate improvement in the recovered characteristics can be seen, the recovered signal is obviously lower in amplitude as compared with the original signal, but this is to be expected when the overall energy is attenuated. This can be alleviated by using a filter which simultaneously attenuates the very central region and increases the relative strength of the higher frequency information (Oppenheim, 1975). For our purposes, the current amplitude of the recovered reflectance profile sufficiently identifies it from the rest of the surrounding background. More importantly, the spatial filtering has restored the uniformity of the object's reflectance profile.

In general, any larger aperture information other than the object of interest would contribute towards the low frequency end of the apectrum. Depending upon the spread of the frequency characteristics in this region, it would distort the recovered object reflectance profile by a low frequency shadow. As has been emphasised, any shadow cast on the surface of the object brought about by a change in tha angle of incidence , is an *indication* of variation in structural characteristics of an object, i.e encountering a feature edge. Hence, it is increasingly important to eliminate any low frequency contributions whose origins are not signal related. This would prevent the misinterpretation of shadows as depth features.

Figure 3.1 is a computer generated dapth object whose depth can be realised from the shading contrast of the bottom surface as compared with the edges. The addition of a very low frequency signal in the form of background reflection, would again distort the object characteristics, particularly when the amplitude level of the shaded region is the same level as background interference. Figure 3.2 is the Fourier spectrum of object, illustrating the well distributed Fourier components recognisable in magnitude. Figure 3.3 is the recovered object characteristics using the Hilbert integral of (2). With the addition of a high constant background, the D.C. point of the new spectrum of Fig.3.4 is again raised reducing the relative the amplitude level of the other Fourier components. This results in the lower amplitude of the depth feature, to be almost indistinguishable from the surround, Fig.3.5. With the application of a spatial filter to the Fourier modulus spectrum of Fig. 3.4, resulting in the new spectrum of Fig.3.6, the depth feature is recognisable in the reconstructed profile as can be seen in Fig.3.7.

As shading variations across the edges could assume any amplitude level, depending upon the angle of incidence, low amplitude shades are in grave danger of being masked by the central intensity. Hence structural depth realised from shading maps has to have this information well protected by means of spatial filtering in the presence of an undesired background interference, which is reminiscent of very smooth, reflective micro-structures.

CONCLUSIONS

Object surfaces have to map the Fourier domain with signal related frequency components as opposed to any background information which is not signal based. Such background interference manifests itself as a low frequency component which deprives much of the intelligibility of the desired object signal and introduces low frequency artifacts alongside the reconstructed object. Spatial filtering of the low frequency region is a pre-requisite for recording the optical diffraction pattern of surfaces with an abnormally intense zero-frequency point. It is also a necessity for eliminating any shading variations upon the surface of the object with has not originated from the structural depth variations.

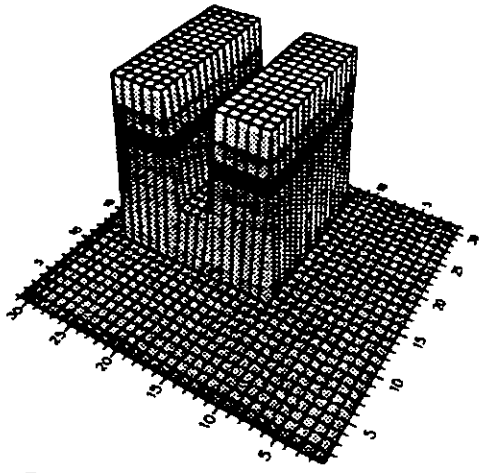

Fig.3.1: Original depth object.

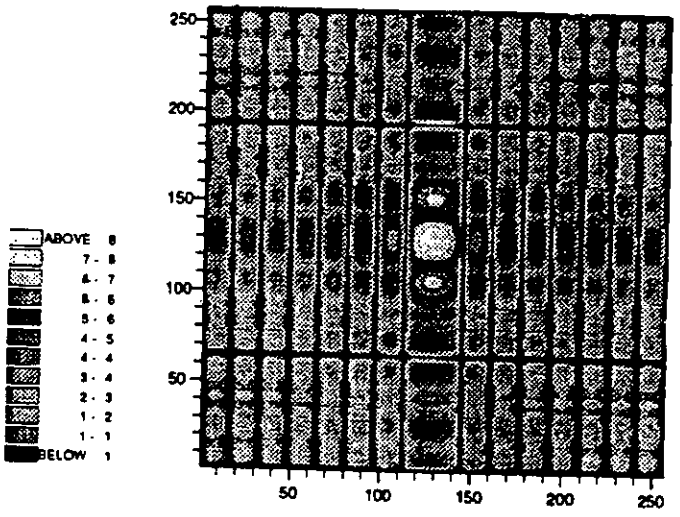

Fig.3.2: Fourier modulus spectrum of the depth object without background interference.

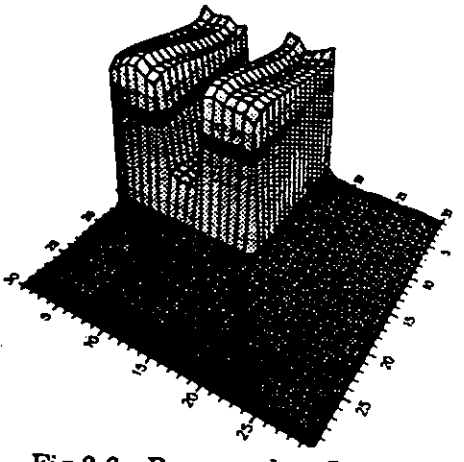

Fig.3.3: Recovered reflectance profile of the depth object from the modulus spectrum of Fig. 3.2.

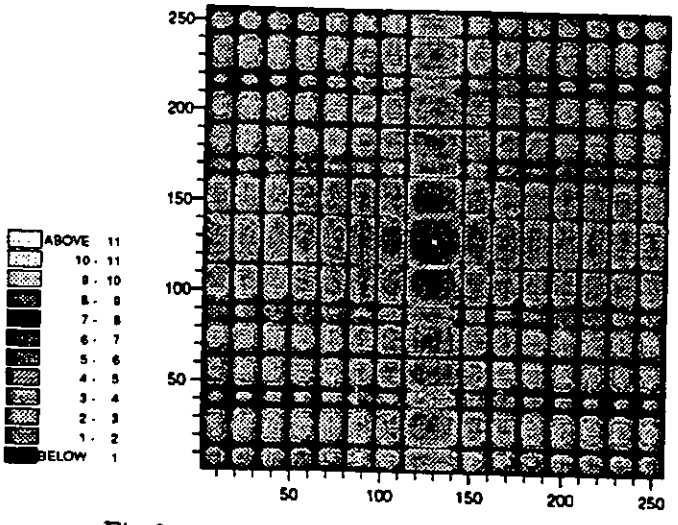

Fig.3.4: Fourier modulus spectrum of the depth object with background interference.

depth feature
not recognisable

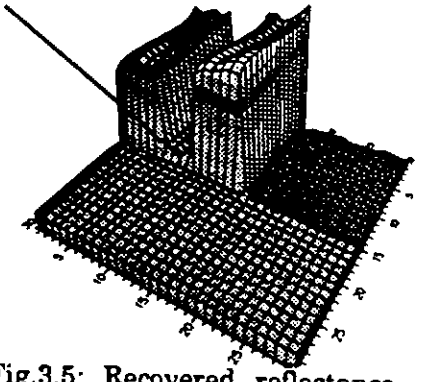

Fig.3.5: Recovered reflectance profile of the depth object from the modulus spectrum of Fig.3.4.

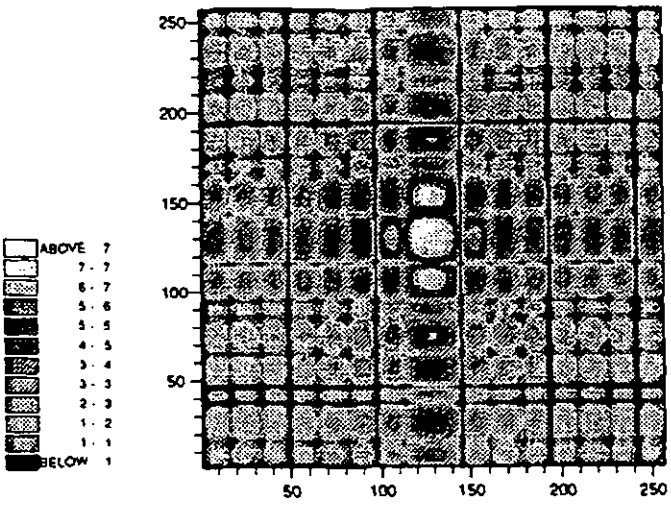

Fig.3.6: Fourier modulus Spectrum of Fig. 3.4 after spatial filtering.

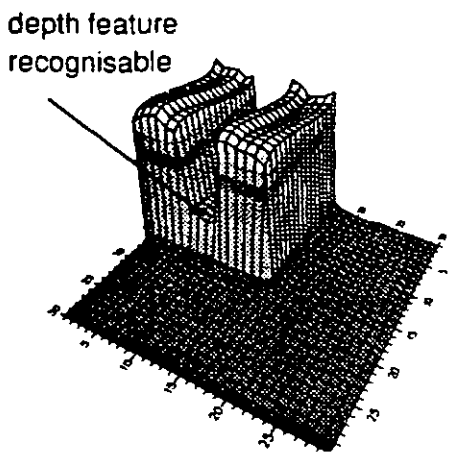

Fig.3.7: Recovered reflectance profile of the depth object from the filtered spectrum of Fig.3.6.

REFERENCES

1. Gerchberg R.W. & W.O.Saxton,(1972). A practical algorithm for the determination of phase from image and diffraction pattern pictures. *Optik* 35, 237-246.
2. Feinup J.R., (1984). Experimental evidence of the uniqueness of phase retrieval from intensity data. *Proc. of URSI/IAU Symposium* on *Indirect Imaging*, J.A. Roberts ed. Cambridge Press, 99-109
3. Nakajima, N. & T.Asakura,(1986). Two dimensional Phase retrieval using the logarithmic Hilbert transform and the estimation technique of zero information *Appl. Phys.* 19, 319-331
4. Lipson S.G. & H.Lipson (1981). *Opticol Physics*. Cambridge university press.
5. Bates, R.H. & W.R.Fright (1983). Composite two dimensional phase restoration procedure' *J.Opt. Sco. Am.*, 73, 358-365.
6. Sotoudeh, N. ,G.R. Greatrix, R.Prasad & G.F.Goldspink (1992), Fourier domain compression techniques in resolving spatial characteristics of surfaces. *4th int. Conf. on Image Processing IEE Mastricht*,354, 172-175.
7. Sotoudeh, N., G.R. Greatrix & G.F.Goldspink (1993). Fourier domain re-scaling and truncation in improving the 3D reconstruction of objects.*9th Int. Conf. On Math. & Compt. Modelling, Berkeley, California*.
8. Oppenheim A.V., R.W.Schaffer (1975). *Digital Signal Processing*, Prentice Hall International editions.

FOURIER DOMAIN RE-SCALING AND TRUNCATION FOR IMPROVING THE 3D RECONSTRUCTION OF OBJECTS

* + *

N.SOTOUDEH, G.R.GREATRIX & G.F.GOLDSPINK

* Middlesex University, School of Electronic Engineering, Bounds Green Rd., London N11 2NQ, UK.
+ University of Teesside, School of Science & Technology, Middlesbrough, Cleveland TS1 3BA, UK.

ABSTRACT

This paper utilises the scale change property of the Fourier domain as a novel means of controlling the quality of the 3D reconstruction of an object profile from its modular Fourier spectrum. Computer simulation studies of phase retrieval from the intensity of the Fourier spectrum have identified two distinct techniques which facilitate a reasonable reconstruction of an object profile. Firstly there must be adequate maintenance of the contrast between the higher order coefficients with respect to the zero-order term. Secondly, there should be a re-scaling of the Fourier spectrum followed by truncation of the number of Fourier coefficients.

Real object surfaces map many discontinuities into the Fourier domain. The addition of a delta function in the object domain, raises the level of any such discontinuity to a minimum and restores the continuity of the modular spectra for evaluation through the logarithmic Hilbert transform integral. However, phase computations from modular spectra include many errors in the vicinity of any such minima, leading to distortion in the object characteristics. This is reminiscent of the structured and repetitive profile which populate the Fourier space with many regions of minima and maxima. Computer simulated reconstructions of a real object, based on re-scaling and truncation of the Fourier modulus spectrum, are presented in this paper and demonstrate the profound improvements that can be achieved in the recovery of the correct intensity profile of such objects.

KEYWORDS

Fourier scaling, phase retrieval, spectrum expansion, object reconstruction, non-contact recovery

INTRODUCTION

In many areas such as X-ray crystallography, Electron microscopy and optical surface characterisation, the intensity of the diffracted information is measured and not the phase. In order to arrive at the correct object profile, it is necessary to have access to phase as well as the modulus of the diffracted intensity. An object function f(x,y), could then be restored from its Fourier modulus spectrum | F(u,v) | via inverse Fourier transformation of the

Fourier modulus spectrum and the estimated phase ϕ (u,v)

$$f(x,y) = \mathcal{F}^{-1} \; | F(u,v) | \; e^{i\phi(u,v)} \qquad (1)$$

There are basically two methods to arrive at an estimate of the object phase starting from the Fourier modulus information. There are iterative techniques, initiated by (Gerchberg & Saxton, 1972) whereby some knowledge of the object and its support are required in advance. An acceptable solution, or set of solutions, is eventually arrived at by iterating back and forth between tha object domain and Fourier domain and imposing the known constraints in each transition. The problem with iterative techniques, ia tha large number of computations performed without any guarantee of success, if the initial phases are chosen on a totally random basis. Any prior phase knowledge would be extremely valuable to aid the convergence of these iterations and successful reconstructions are usually commenced with the so called seeded iterations, embedding the prior phase knowledge.

The logarithmic Hilbert transform on the other hand is a non iterative technique that can be applied to object functions classed as entire functions. Two basic requirements place the object function in that category. Firstly, the object is to be of finita extent, and secondly a transform relationship should exist for the object function (Nakajima & Asakura, 1986). Both of these requirements can be satisfied under the usual experimental conditions.

The Hilbert phases ϕ (u,mc), for any arbitrary atrip of the two dimensional Fourier data are then extracted from the modulus of tha Fouriar spectrum using the convolution integral below (Cizek,1970). This would yield the phases, plus an additive constant C_0 without the effect of any contributions from the zeros of the complex field. The Hilbert phases would be the required phases if there are no zeros in tha complex upper half plane which is the frequency range for the evaluation of this integral . However, this cannot be guaranteed before hand and many object functions have a varying distribution of these zeros in the complex plane. This by no means reduces the credibility of using the Hilbert transform to extract initial phase estimates as opposed to no phase information. In addition, the extracted phases would be valuable to any iterativa phase retrieval technique.

$$\phi(u,mc) = \frac{-1}{\pi} P\int_{-\infty}^{\infty} \frac{Ln\,|F(u',mc)|}{(u-u')} du' + C_0 \qquad (2)$$

Furthermore, many object functions can be adequately restored through the extracted Hilbert phases alone, if a region of the frequency spacs is chosen which excludes such zeros. Even so tolerable reconstructions of multi-dimensional objects have been achieved with a small number of isolated zeros (Nakajima & Asakura, 1985). However, with an increasing number of zeros, object functions need to hava this effect accounted for in their Hilbert phases or have them reduced in number to restora tha correct object profile. The difficulty arises when object characteristics give rise to a large number of such zero distributions since that requires a very sensitive scheme for their scan in the complex plane. In addition, there would always be some uncertainty in locating and identifying an exact zero in the complex plane as compared with its immediate minima. As a result, the real and imaginary part of each harmonic generated from the phase and modulus data in this region would suffer some inaccuracy.

Many object structures, such as square and rectangular geometries, give rise to lines of discontinuity or cuts in the Fourier plane. In particular any repetition or regularity in a collection of similar patterns gives rise to many cuts with an increasing number of zeros. Depending upon the level of background contribution in both the object domain and the Fourier domain, such discontinuities would never be intercepted as such by the camera and the recording device. More so, the limited quantisation intervals of the digitiser would not capture the amplitude variations with the same fidelity as can be realised for purely computer simulated frequency spectra.

As a result, any structural configuration which gives rise to a frequency domain behaviour dominated by many contours of repetitive maxima and minima, or zeros intercepted as minima, would suffer from inaccuracy for a large number of enclosed minima. Hence one should direct every effort to maintain the object's structural characteristics with the least effect introduced by such minima. Our aim is to restore the object's structural configuration by having control over the *spread* of its Fourier spectrum. This can be done in the most elegant manner by utilising the Fourier scale change property which relates the *spread* of the frequency behaviour to the *scale* of the object in the spatial domain.

Before embarking on the principles by which such change in scale can be brought about, we digress on to the continuity requirements for the logarithm of the modulus of the Fourier data, to allow the use of integral equation (2). The use of the logarithmic Hilbert transform of equation (2) is appropriate for continuous modulus data and object structural characteristics giving rise to isolated discontinuities. Multi-dimensional objects with well defined edges and some form of repetition, give rise to connected discontinuities which violate the aforementioned requirements. In order to use the Hilbert integral for phase recovery of such objects, any discontinuities in the Fourier modulus spectrum can be altered by adding a delta function to the object in the spatial domain or by raising the level of the Fourier modulus spectrum by a constant amount in the frequency domain. The addition of a delta or impulse in the object domain, is equivalent to adding a continuum to the complex Fourier spectrum and would raise the level of any zeros of the spectrum.

FOURIER DOMAIN SCALE CHANGE OPERATION

Not all the Fourier coefficients are needed to restore the object's structural characteristics (Sotoudeh, *et al.*,1992). Hence, it is always possible to select a fraction of the frequency space, truncated and limited to a fewer number of Fourier coefficients thereby utilising a smaller number of such terms in the object synthesis. However, it is also possible to re-accommodate much of this lost higher frequency information into the lower frequency region and at the same time have this region *spread out* in terms of sample points. In fact, such spreading out of the spectrum can be realised when an object function experiences a reduction in size in the spatial domain.

The underlying reason for such a readjustment in scale, rests with the uncertainty principle. According to this principle (Baher, 1990), the narrower the duration of the signal, the wider would be its frequency spectrum. The Fourier scale change property operates such that this relationship is always maintained between the two domains when a change in the scale of the object is involved. Hence, when an object f(x), of spatial dimensions x, is compressed in size by a factor p, it's previous frequency spectrum f(u) would be expanded by the same factor. The frequency domain behaviour of the original object and its compressed version can be realised from (3) and (4):

$$f(x) \leftrightarrow F(u) \tag{3}$$

and the compressed object f(px), would have the new spectrum of F(u/p), i.e:

$$f(px) \leftrightarrow \frac{1}{|p|} F(\frac{u}{p}) \tag{4}$$

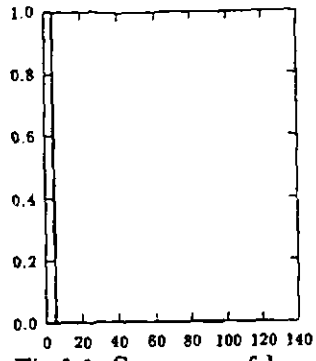

Fig.1.1: Sequence of length 4 pixels.

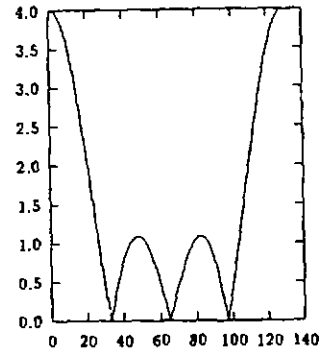

Fig.1.2:Fourier modulus spectrum of 1.1.

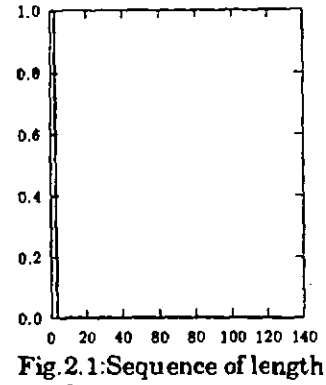

Fig.2.1:Sequence of length 2 pixels.

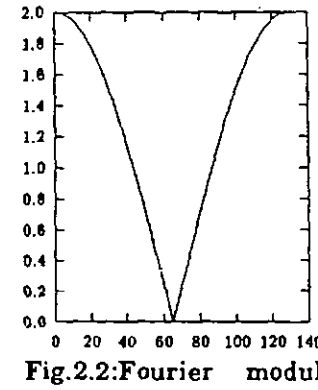

Fig.2.2:Fourier modulus spectrum of 2.1.

Such effect can be seen for a sequence of length 4 and 2 pixels as part of a data window of duration 128 pixels. As can be seen, with a reduction in the scale of the object, Figs 1.1 and 2.1, the Fourier modulus spectrum expands accordingly Figs 1.2 and 2.2. Experimentally, the re-scaling of the spectrum can be brought about by firstly truncating the frequency characteristics to a fewer number of higher order lobes and secondly interpolating the lower frequency region to spread out the frequency characteristics in a manner similar to Fig 2.2.

The advantages of such a manoeuvre are as follows: firstly, the increase in the number of sample points within the low frequency lobes as a result of the expansion of the frequency spectrum would provide a more accurate trace of phase variations. Though it is possible to increase the number of sample points by keeping the size of the object constant and zero padding the object in the spatial domain, this would preserve the full spectral characteristics of the object and would still include all the coefficients in the reconstruction process. This would not only demand very large data arrays for processing the two dimensional Fourier data, but by including a larger proportion of Fourier coefficients, phase calculations are strained in accuracy by the greater number of preserved minima in the enclosed region.

Secondly, since compression of object scale retains all of the lower and higher frequency information, in an expanded spectrum, the structural characteristics of the object are preserved. This implies that if a similar modification of the spectrum is introduced to the experimental data, it would be possible to restore the structural characteristics of such objects from the interpolated version of the lower frequency information alone. In fact, many iterative algorithms rely on a well interpolated frequency spectrum to give the most realistic region of support of the object in the spatial domain (Bates and Mnyama, 1987). The most probable region of support of the object has been identified as the one being the most compact in size. The solution phase is then regarded as the one which fulfils such criterion; i.e the phase which gives rise to the most compact support for the object is likely to be the most faithful amongst all the possible phases.

Thirdly, the scaling property can act as an alternative means of restoring the object reflectance profile, where its regularity and sharp structural characteristics dominate the Fourier space with many regions of maxima and minima. This is particularly reminiscent of the geometry of integrated circuits. Fourthly, such re-scaling of the spectrum can be conveniently achieved experimentally, by capturing a magnified version of the Fourier modulus data. This can be done by varying the distance of the camera from the diffraction plane or through the digitising software, providing an interpolated version of the captured spectrum.

RECOVERY OF THE OBJECT REFLECTANCE PROFILE

The object specimens used for reconstruction were an array of reflectance objects consisting of chromium features deposited on to a glass background. The dimensions of the square features were 100x100 μm with a 50 μm spacing as shown in the photomicrograph of Fig. 3. Computer generated images of these features from their digitised photomicrograph, obtained via a travelling optical microscope was then used to generate their two dimensional Fourier modulus spectrum.

In order to achieve optimum contrast for the object, the background contribution for the square array in the spatial domain has been set to zero. The computer generated Fourier spectrum, has many discontinuities appearing as cuts in the Fourier plane. As mentioned earlier, any isolated discontinuity would appear as a singularity to the logarithm of the modulus and any connected regions of discontinuities appearing as cuts, cannot be handled by the Hilbert integral. In order to restore the continuity of the logarithm of modulus data a constant level has been added to the modulus data.

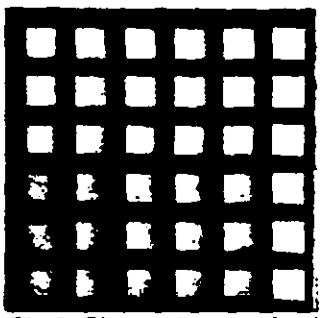

Fig.3: Photomicrograph of the reflectance array. Square features are 100x100 μm with 50 μm spacing.

The logarithmic Hilbert transform integral of equation (2) is then applied to each strip of the Fourier modulus spectrum $|F(u,mc)|$ for the array to evaluate the phases along each line. In order to convert these one dimensional phases $\phi(u,mc)$, into a coherent pattern of two dimensional phases $\phi(u,v)$, the phases along an orthogonal direction through the origin $\phi(0,mc)$ are evaluated and added to the phases of the horizontal strip passing through the corresponding vertical point. The two dimensional phases are then inverse Fourier transformed with the available moduli to arrive back at the object's reflectance profile.

Figure 4.1 shows the digitised image of this array of overall size 256x256 pixels, prior to being compressed, and Fig.4.2 is the corresponding Fourier spectrum. The spectrum contains many regions of discontinuity whose level can be raised by the addition of a constant background in the Fourier space. As mentioned, a continuum in the frequency space would be transformed to a delta in the object space. However, this is the case for an infinite continuum and a continuum which is limited by the data window aperture would result in a very near impulsive Sinc distribution in the object domain. Hence, this Sinc distribution would be added to the recovered reflectance profile of the square lattice. The envelope of such variation can be seen superimposed on the recovered object characteristics in Fig.4.3. The object profile itself would be distorted due to the many errors arising from tracing the phase variations for a spectrum which has many minima. In particular, when the intensity lobes have very rapid variations sampled by few pixels across, inaccuracies in the phase values are imminent.

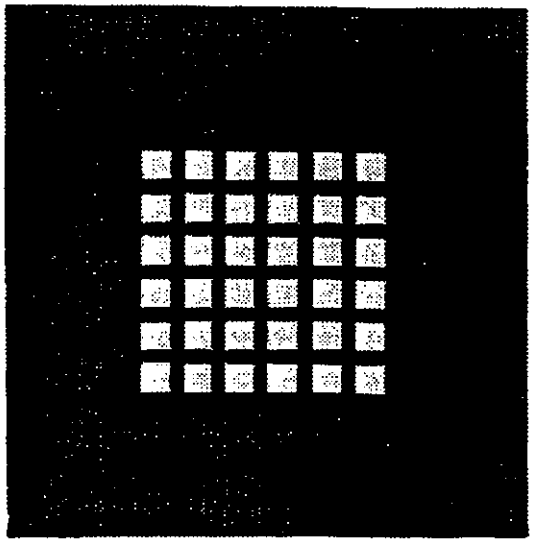

Fig.4.1: Digitised image of the square array without any compression in scale.

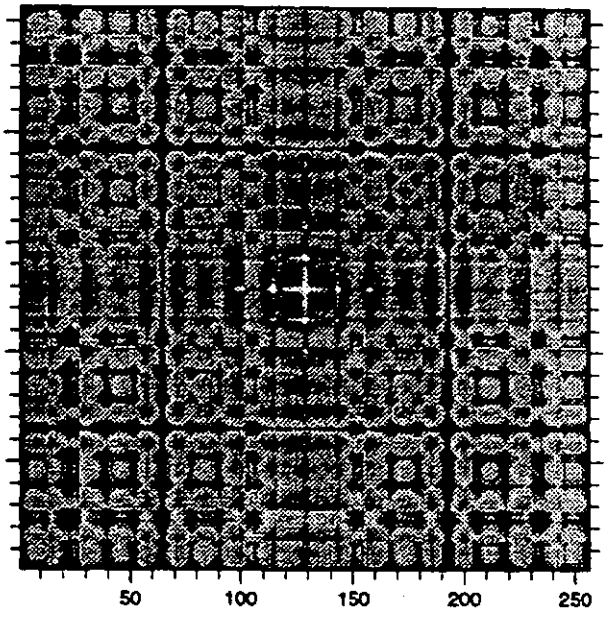

Fig.4.2: Fourier spectrum of the uncompressed array.

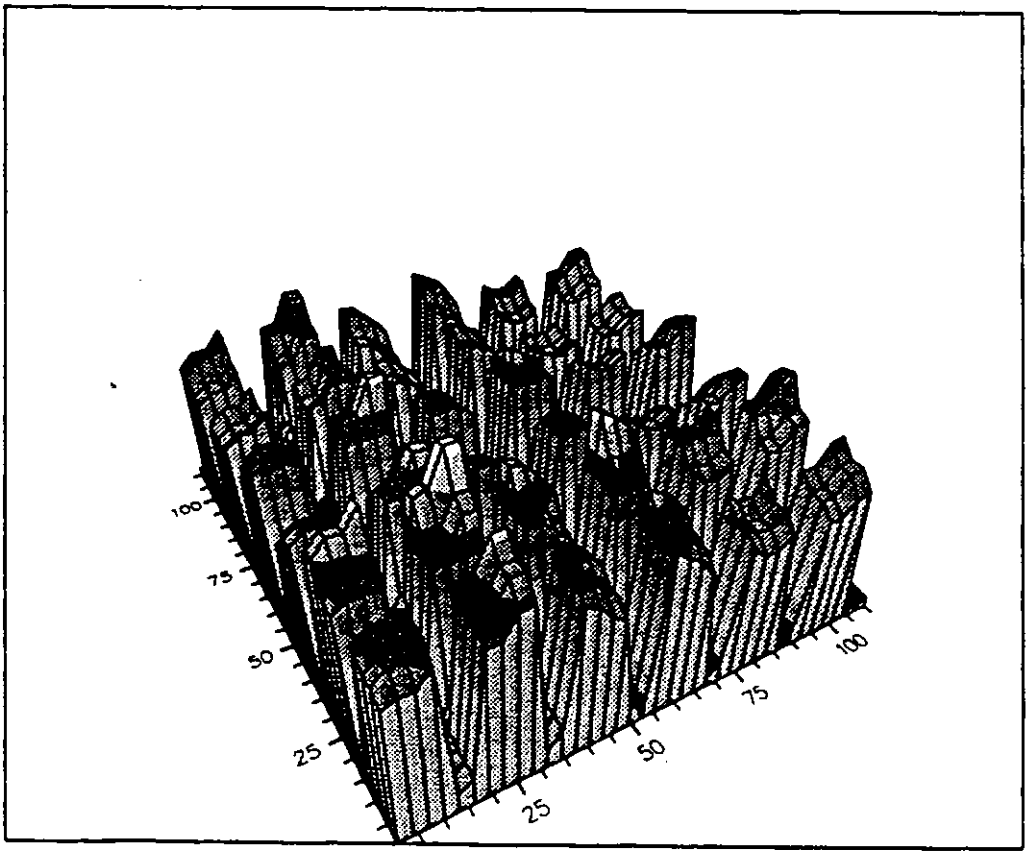

Fig.4.3: Recovered reflectance profile of the square array.

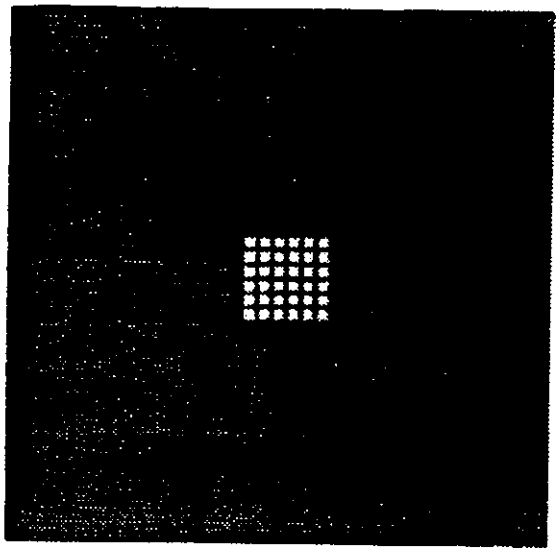

Fig.5.1: Digitised image of the square array, compressed in scale by a factor of 3.

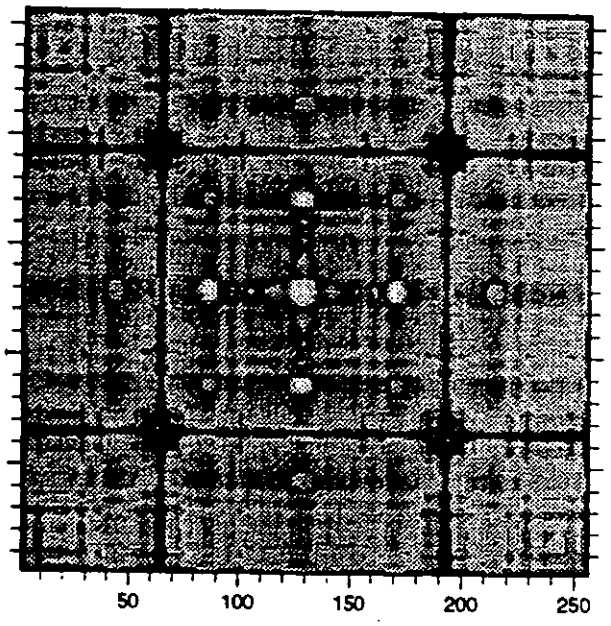

Fig.5.2: Fourier spectrum of the compressed array of Fig.5.1.

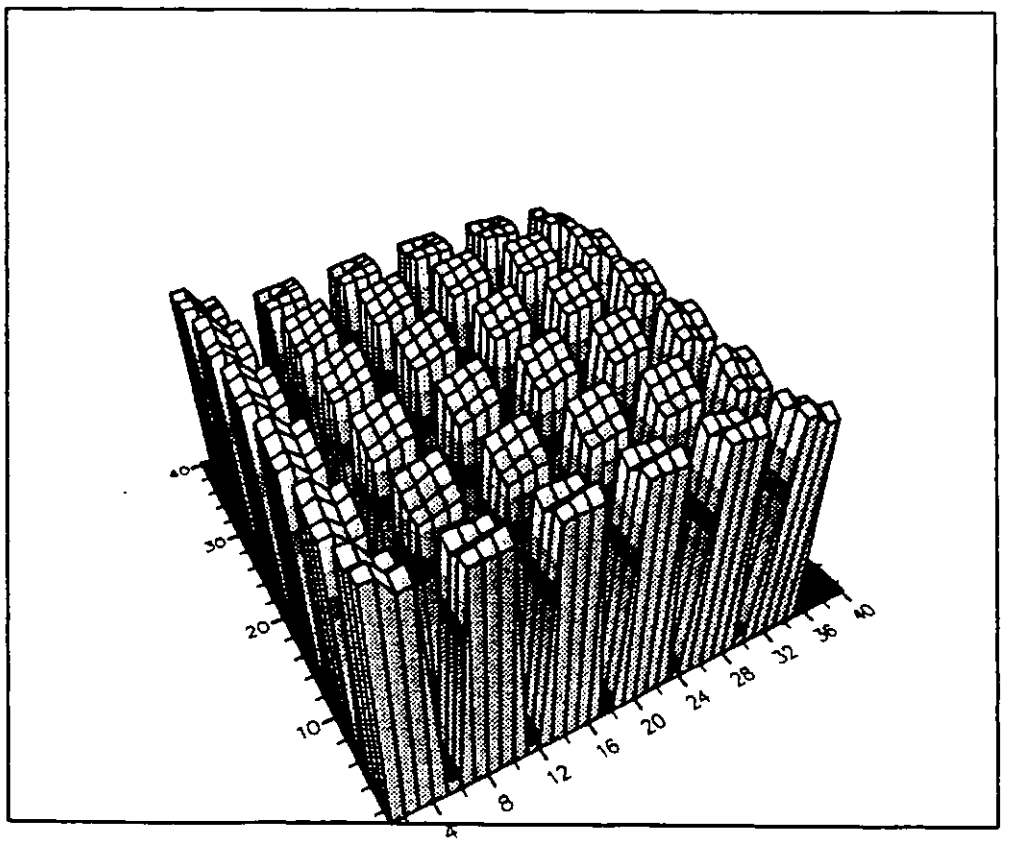

Fig.5.3: Recovered reflectance profile of the compressed square array.

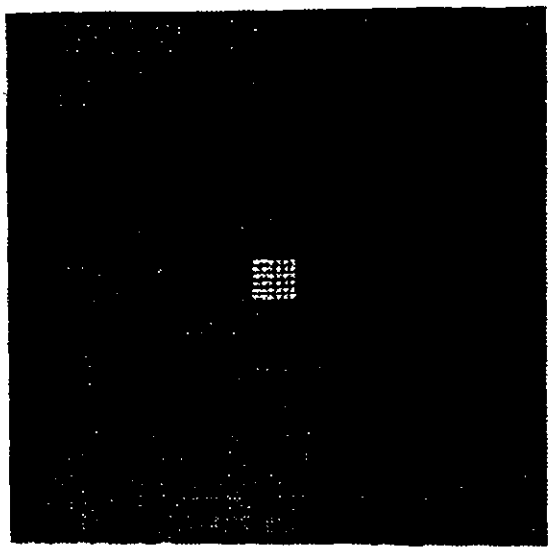

Fig.6.1: Digitised image of the square array, compressed in scale by a factor of 6.

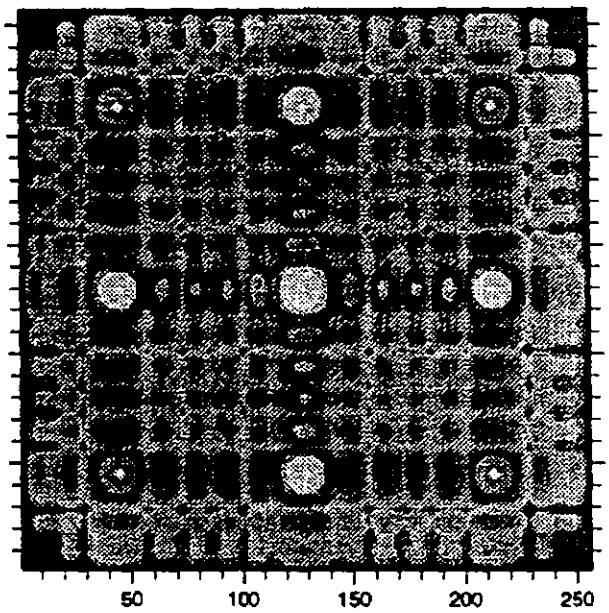

Fig.6.2: Fourier spectrum of the compressed array of Fig.6.1.

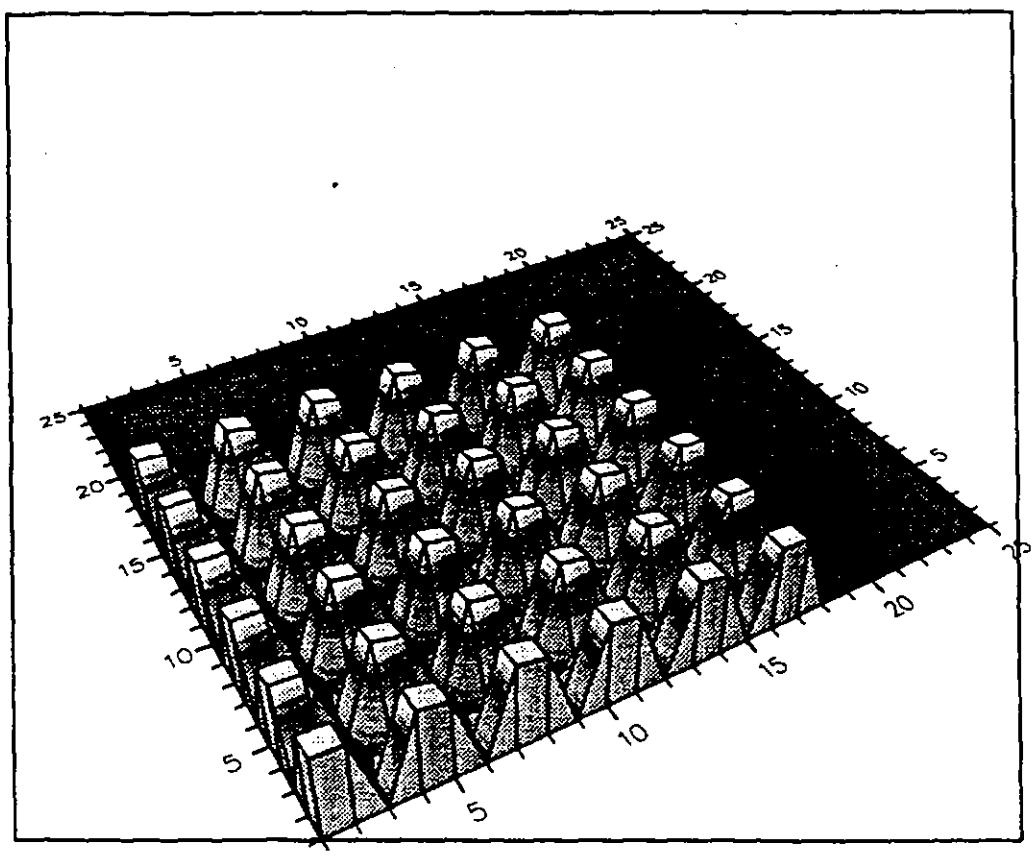

Fig.6.3: Recovered reflectance profile of the compressed square array.

Figure 5.1 is the same array of reflectance objects compressed by a factor of 3 in the overall size but retained as part of a data matrix of overall size 256x256 pixels. The immediate expansion of the new Fourier spectrum can be seen in Fig 5.2. A comparison of this expanded spectrum Fig 5.2, with the previous unexpanded spectrum Fig 4.2, reveals the very manner by which the new frequency characteriatics is focused within the central region. As can be seen , this new spectrum not only incorporates a lesser proportion of the previous frequency map but it has also been spread out in terms of sample points within the focused low frequency region. This not only provides a better trace of phase variations but it also limits the number of any minima which it has to intercept. The recovered object characteristics can be seen in Fig. 5.3. The profound improvement in the reflectance profile of the square array is apparent. The recovered characteristics still suffer from the effect of the superimposed data window as mentioned earlier.

A further compression of the object scale, would still result in a yet more expanded spectrum and a more faithful reconstruction as seen in figures 6.1-6.3. However, by reducing the overall size of the object the pixel resolution in the spatial domain would be degraded. This implies that one cannot enhance resolution optimally in both domains (R.Ramirez, 1985). Much enhanced resolution in the frequency domain is accompanied by a loss of resolution in the spatial domain in terms of the available pixels. Therefore, object compression can only be afforded up to a point whereby a reasonable fraction of object characteristics are still preserved when subjected to an overall scale change. For the type of the specimens being studied, such a degree of compression was exercised with the assumption that the chromium regions were free of any fine structural characteristics, such as a flaw or scratch whose structural detail would not survive through severe compression of the object scale.

CONCLUSIONS

This paper has addressed the use of the Fourier scaling property as an effective means of restoring the reflectance profile of object surfaces with many repetitive and structural characteristics. Such surfaces populate the Fourier space with many regions of maxima and minima. By utilising the re-scaling principle, it has been shown that the structural characteristics of such surfaces can be realised from an expanded spectrum. Such spectrum not only maintains fewer minima but also enhances phase evaluations when the envelope of the spectral components is spread out. This would restrict any degradation in the object characteristics due to phase inaccuracies which would otherwise arise if the frequency envelope maintains a large population of such minima.

REFERENCES

Sotoudeh, N., G.R.Greatrix, R.Prasad & G.F.Goldspink (1992). Fourier domain compression techniques in resolving spatial characteristics of surfaces,*4th Int. Conf. on image processing IEE Mastricht*,354, 172-175.

Gerchberg, G.R. & W.O.Saxton (1972). A practical algorithm for the determination of phase from image and diffraction plane pictures. *Optik* 35, 237-246.

Baher, H. (1990). *Analog & Digital Signal Processing.* John Wiley & Sons, Great Britain.

Bates, R.H. & D.Mnyama (1987). *Advances in Electronic and Electron Physics.Vol* 67, 1-64.

Nakajima, N. & T.Asakura (1986). Two dimensional Phase retreival using the Logarithmic Hilbert transform and the estimation technique of zero information. *Applied Physics*,19, 319-331.

Ramirez, R.W. (1985). The FFT Fundamentals and Concepts, *Prentice Hall.*

Cizek, V. (1970). Discrete Hilbert Transform, *IEEE Trans. on Audio Electroacoustics,* AU-18, No.4, 340-343.

IMPROVING THE RECOVERY OF THE MICRO-GEOMETRY OF OBJECT SURFACES BY FOURIER SCALING

N.SOTOUDEH*, G.R.GREATRIX+ & G.F.GOLDSPINK*

* Middlesex University, School of Electronic Engineering, Bounds Green Rd., London N11 2NQ, UK.
+ University of Teesside, School of Science & Technology, Middlesbrough, Cleveland TS1 3BA, UK.

INTRODUCTION

When coherent light illuminates object surfaces whose dimensions are comparable to the wavelength of light, the far-field diffraction pattern is the Fourier transform of the surface reflectance profile. The true reflectance profile can only be obtained if the phase of the Fourier spectrum is available alongside the frequency moduli.

However, optical sensors cannot yet respond to phase and amplitude variations above the terahertz band. Sensors respond to the time-averaged intensity of the optical field which results in a loss of phase, leaving only the modulus of the Fourier components at one's disposal. Consequently, in order to restore the true reflectance profile, phase data has to be extracted from the Fourier modulus spectrum. The object's reflectance profile $f(x,y)$ can thus be obtained via inverse Fourier transformation of the Fourier modulus $|F(u,v)|$ and the recovered phases $\phi(u,v)$ where u and v are the spatial frequency variables from (1) :

$$f(x,y) = \mathcal{F}^{-1} \; |F(u,v)| \cdot e^{i\phi(u,v)} \qquad (1)$$

Phase extraction from the modulus of the Fourier spectrum can only be obtained with reasonable accuracy if the diffracted information is well distinguished from the average reflected information and also the captured frequency spectrum has a reasonable span of spectral components both in amplitude and range. Such span is often degraded in the required precision and range by the limited quantisation intervals of the digitiser as well as the truncating aperture of the device. In particular, amplitude excursions in the proximity of spectrum minima suffer the most inaccuracy.

Real object surfaces with well-defined structural characteristics map many discontinuities and minima into the Fourier space. Background contribution together with the limited sensitivity of the recording device often lead to real discontinuities being intercepted as false minima. Phase computations from the Fourier modulus spectra are strained in accuracy in the vicinity of any minima leading to distortion in the recovered object characteristics. In particular, such distortion is unacceptably high for repetitive profiles which populate the Fourier space with numerous maxima and minima.

Our aim is to recover the object's structural characteristics with the least effect introduced by any minima. This can be achieved by using the Fourier scale change property which relates the spread of the frequency spectrum to the scale of the object in the spatial domain. As opposed to truncation which eliminates the higher frequency information , spectrum modification based on the scaling principle would retain all the objects's higher and lower spectral components.

If the object size were to reduce in scale so that it ultimately diminished to a delta function, its associated Fourier spectrum would tend towards a continuum.

This implies that with a gradual reduction in the scale of the object in the spatial domain, the many individual lobes in the frequency spectrum would be disposed of in favour of redistributing the new spectral information amongst fewer lobes. Both the enhanced continuity of the spectral components as well as the reduction in the number of the higher frequency lobes facilitate a more faithful means of tracing phase variations.

Based on this principle, the digitised image of an array of reflectance objects was compressed in scale and the resultant Fourier spectrum was subjected to phase extraction on each occasion. Computer simulated reconstructions of the recovered reflectance profile exhibit profound improvements in the retrieved micro-geometry with each subsequent reduction in the overall size of the object.

Prior to the application of the scaling principle to the two dimensional array of the reflectance objects under study, we digress on to the study of the frequency domain characteristics of structured and repetitive profiles. Comparison of the Fourier modulus spectrum of a single object with a repeated version of itself would unveil the manner in which the frequency envelope of a repetitive object is modulated in shape as compared to that of a single object. The extent of such modulation can be seen to be dependant upon: i) the spatial width of a single object, ii) the spatial period of an object in repetitive form and iii) the number of repetitive objects.

It was felt that such comparison would then enable the reader to appreciate how severely the frequency envelope can be modulated by a change in any of the aforementioned parameters. In particular, for an object specimen with fixed width and periodicity, an increase in the number of the features would lead to an impulsive frequency envelope with highly rapid excursions in the amplitude of maxima and minima. Unless such rapid excursions are intercepted at high enough sampling rate, the frequency spectrum lacks intelligence to restore the full geometrical configuration of the object.

It is the intent of this paper to introduce scaling principle as a novel way to compensate for such lack of intelligence. In what remains to be seen, a more intelligible version of frequency components can be generated when frequency data are re-scaled. Such re-scaling not only limits the amplitude excursions in number, but it also expands the overall frequency envelope thereby smoothing out the highly impulsive behaviour associated with repetitive profiles.

Frequency Domain Characteristics of Repetitive Profiles

It is known that in general the phase of the object signal often captures much of the intelligibility of the signal as compared with the modulus of its transform (Hayes, 1982), (Lim, 1990), (Bates & Fright, 1984). Studies by the above authors has revealed that the inverse Fourier transformation of phase data with arbitrary amplitude arrives at a more intelligible version of the object characteristics as compared to the inverse Fourier transformation of the modulus spectrum with arbitrary phase.

However, for repetitive and structured profiles, it can be said that their Fourier modulus spectrum maintains adequate intelligence to restore certain object attributes such as its periodicity. If adequate intelligence is considered as information regarding the cyclic pitch of the features, irrespective of their geometrical shape, this information is always coded reciprocally into the Fourier domain. Hence, it can be argued that this aspect of the object i.e its periodicity, is well preserved in the modulus spectrum and is always retrievable for an inverse transformation of the modulus spectrum with zero-phase (Sotoudeh, et.al. 1993).

Whilst the spectrum of repetitive objects contains enough intelligence to restore the correct periodicity of the features, ironically, it often lacks intelligence to yield the true nature of the object characteristics i.e its periodicity as well as its exact geometrical configuration. This is due to the fact that repetition in object characteristics gives an impulsive

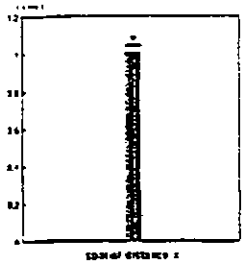

Figure 1a: A single object

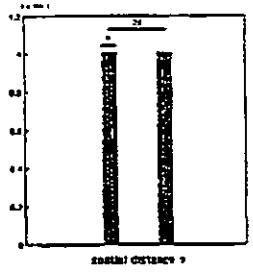

Figure 2a: Two objects with a spatial period of 2d.

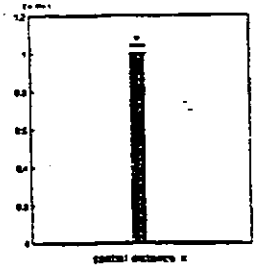

Figure 2b:Object of Fig.1a.

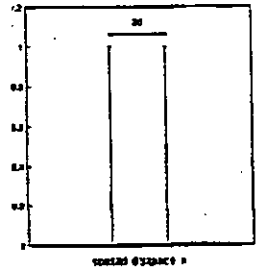

Figure 2c:A set of delta functions distanced 2d apart.

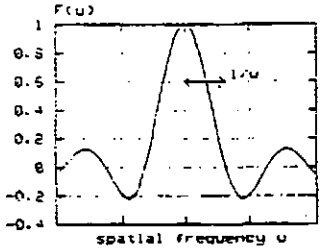

Figure 1b:Amplitude spectrum of the single object.

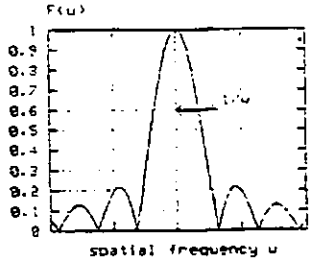

Figure 1c:Modulus spectrum of the single object.

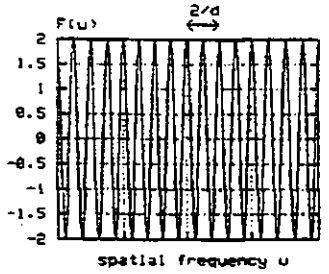

Figure 2d: Amplitude spectrum of the two delta functions.

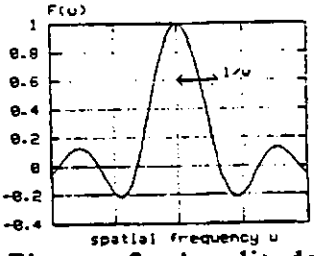

Figure 2e:Amplitude spectrum of the single object.

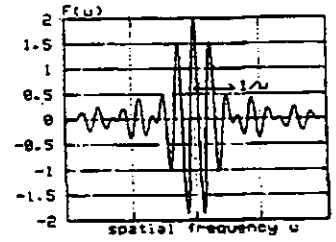

Figure 2f:Product of Fig.2e and Fig.2d.

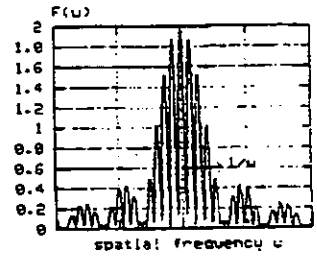

Figure 2g: Modulus spectrum of the two objects.

appearance to the frequency envelope. For fixed sampling intervals this implies that the object related information residing in the neighbourhood of impulses is often sacrificed and missed. In addition, intelligence of the spectrum is further lowered by the infidelity in the amplitude levels of the large colony of minima and zeros associated with repetitive profiles.

To show the effect that object repetition has on the Fourier modulus spectrum, the modulus spectrum of a single object has been compared with that of a repeated version in Figures 1-2. The original object denoted by the top hat function of Fig.1a can be seen to have a Sinc amplitude spectrum in Fig.1b followed by its Fourier modulus spectrum in Fig.1c. A repeated version of original object with a spatial period of 2d as in Fig.2a, can be brought on by the convolution of a single object with a set of delta functions distanced 2d apart.

The Fourier amplitude spectrum of the repeated object is equivalent to the product of the Fourier amplitude spectrum of the deltas which is the cosinusoid seen in Fig. 2d with the Fourier amplitude spectrum of the single top hat function i.e

Fig.2e. The product of the multiplication of Figures 2d and 2e can be seen in Fig.2f whereby the original Sinc frequency distribution is now modulated or scaled by a cosinusoidal variation. Comparison of the Fourier modulus spectrum of the repeated object Fig.2g with the modulus spectrum of the single object Fig.1c reveals the general traits of such modulation as : i) increase in the number of maxima and minima; ii) less sample points across each lobe of the modulated spectrum ; iii) early signs of an impulsive behaviour seen as narrowing of the lobes as well as their sharper slopes.

With the aid of Figures 1-2, it is now possible to identify how each individual aspect of a repetitive object i.e periodicity, feature size and the number of repeated features contribute towards such modulation. It would also be possible to identify which of those aspects are at our disposal to limit the severity of such modulation.

i) The periodicity of the repeats (distance d): this controls the frequency of the cosinusoid which modulates the Fourier map of a single feature as seen in Fig.2d. Large feature separation leads to a very high frequency cosine and severe modulation of the Fourier map.

ii) The size of the individual features (width w): this controls the spread of the frequency information whereby the word spread has been used to denote the width of the individual lobes. Small objects give rise to spectra with large spread and a more continuous stream of frequency information.

iii) The number of repetitive features (the number of required deltas): this controls the complexity of the shape of the cosinusoid that modulates the Fourier envelope of a single object. For instance, two delta functions give rise to a simple cosinusoid whereas four deltas at equal spacing result in a more complex curve which is the addition of a cosine and its higher harmonic.

With the number of repetitive features fixed for an object specimen, any modifications to the frequency spectrum has to be brought on by the two remaining factors i.e : individual feature size and its periodicity interval. Both smaller feature size and smaller periodicity interval are in favour of a more continuous trend of frequency data. This implies that the most faithful reconstruction of an object would be the one which has been recovered on a reduced scale.The overall size of the recovered object can be indirectly adjusted by the scale of its frequency spectrum. Such scaling effect can be realised in the following section.

Fourier Scaling Principle

When the object undergoes a reduction in scale, its overall frequency spectrum would be expanded. Expansion of the spectrum is associated with the enhanced continuity of the spectral components and reduction in the number of higher order lobes. This effect can be seen in Figures 3a-3d from the comparison of the modulus spectrum of the two object sequences of width 4 pixels and 2 pixels.

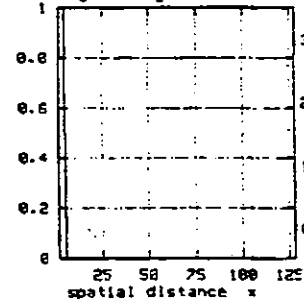

Figure 3a: Sequence of width 4 pixels.

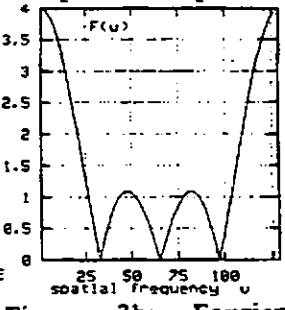

Figure 3b: Fourier modulus spectrum of 3a.

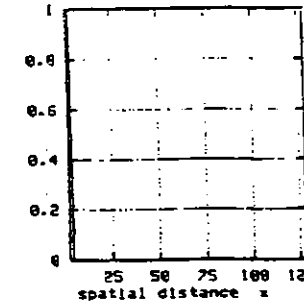

Figure 3c: Sequence of width 2 pixels.

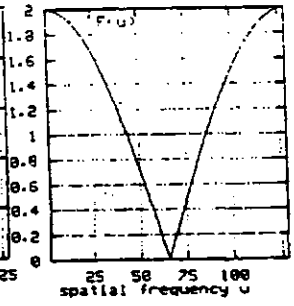

Figure 3d: Fourier modulus spectrum of 3c.

What also emerges out of such comparison, is the reduction in the number of regions where the modulus spectrum runs into a zero as can be seen for the spectrum of the smaller length sequence Fig.3d. Even more significant, is the manner in which all the higher and lower spatial frequencies of the object have been preserved under one lobe so that the object's structural characteristics are unaltered apart from a mere reduction in scale.

Phase Extraction From The Fourier Modulus Spectrum

Phase data was extracted from the Fourier modulus spectrum, using the non-iterative technique of the logarithmic Hilbert transform (Nakajima & Asakura, 1986) in which the integral relationship of (2) has been implemented digitally:

$$\phi(u,mc) = \frac{-1}{\pi} \int_{-\infty}^{\infty} \frac{Ln\ |F(u',mc)|}{u-u'}\, du' + C_0 \quad (2)$$

where the two-dimensional phases $\phi(u,v)$ are obtained as a series of independent one-dimensional phases $\phi(u,mc)$ along m arbitrary lines c, of the two-dimensional frequency spectrum and the term C_0 denotes the constant phase at the origin. To generate a coherent pattern of two-dimensional phases, the phases along an orthogonal direction through the centre of the frequency spectrum are also evaluated namely $\phi(0,mc)$. These phases are then added to the phases of individual strips $\phi(u,mc)$.

Since phase data is extracted from the logarithm of the modulus i.e $Ln|F(o,v)|$ any zeros of the modulus spectrum would appear as singularities of the logarithm which would make the $Ln\ |F(u,v)|$ term infinite. In order to satisfy the continuity of the logarithm, the level of any zeros of the modulus spectrum can be raised by lifting the background in the Fourier domain by a minimum level. A constant level was added to the computer generated frequency data of the array thereby creating similar conditions to those which exist in an optical laboratory, where the true zero levels are either lifted by a background contribution or are unavoidably recorded as minima.

The object specimen used in the reconstruction study was an array of chromium features deposited on to a glass background the photomicrograph of which can be seen in Fig.4. The size of the individual square features within the array was 100 μm x 100 μm with a 50 μm spacing. The digitised image of the array was captured via a travelling optical microscope fitted with a camera and digitiser. The digitised image data was then adjusted to reveal optimum contrast between the chromium features and its glass background. Using this well contrasted image data, a series of Fourier spectra was then generated for the object array and its compressed version. the Fourier spectrum associated with the object for each different scale was then subjected to phase extraction using integral equation (2). The extracted phases were then inverse Fourier transformed alongside their corresponding moduli, to arrive at the reconstruction of the object array.

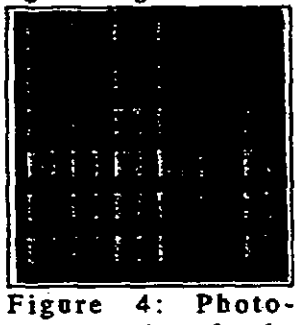

Figure 4: Photo-micrograph of the object.Sqaure features are 100μm x 100μm with a 50μm spacing.

Fig. 5a shows the 256x256 digitised data for the square array, prior to compression in size followed by its Fourier modulus spectrum of Fig.5b and the resultant reconstruction in Fig.5c. As seen the reconstructed object is severely distorted. This distortion stems from: i) the rapid swings in the envelope of the frequency data which is only monitored by a limited number of frequency samples, and ii) the very large number of enclosed minima leading to many phase errors.

Figure 6a is the compressed version of the object array with the overall size being reduced by a factor of 3. Figure 6b is the Fourier modulus spectrum seen as an expanded version although the size of the available frequency samples is kept

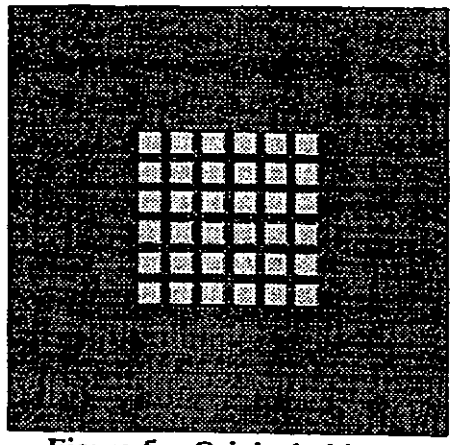

Figure 5a: Original object

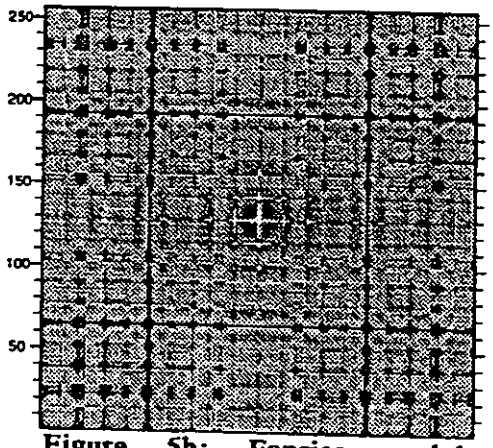

Figure 5b: Fourier modulus spectrum of the original object.

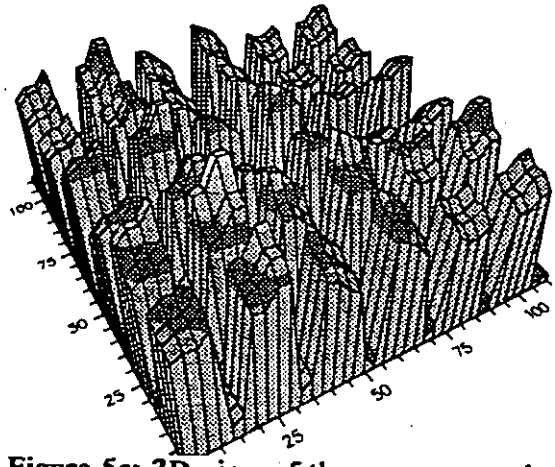

Figure 5c: 3D view of the reconstructed object from spectrum of Figure 5b.

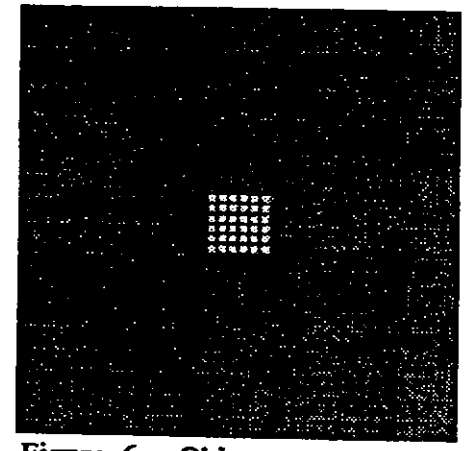

Figure 6a: Object compressed in size by a factor of 3.

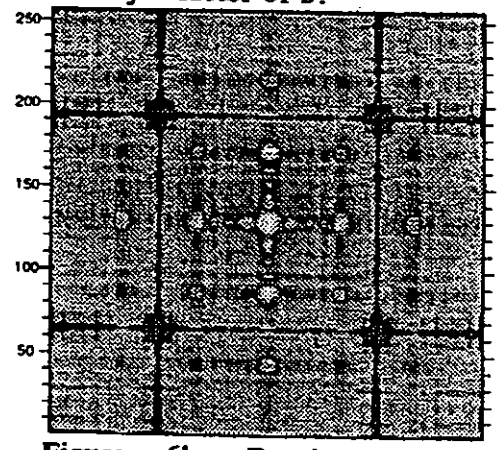

Figure 6b: Fourier modulus spectrum of the compressed object.

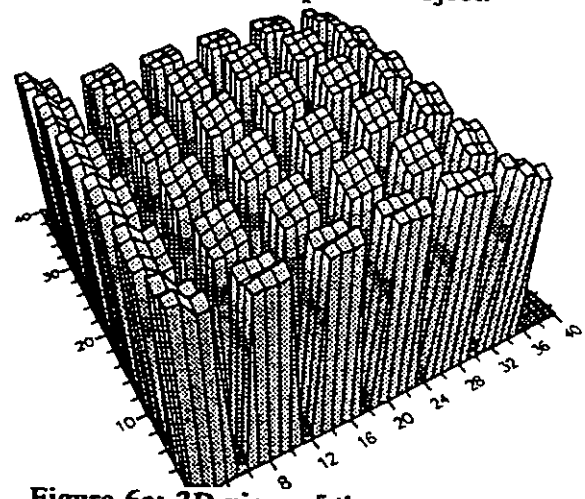

Figure 6c: 3D view of the reconstructed object from the spectrum of Figure 6b.

constant at 256x256 pixels, there would be more samples across the expanded lobes, and also a much smaller colony of minima enclosed by this spectrum. Both such factors lead to an improvement in phase evaluations and thus an improvement in the reconstructed object as seen in Fig.6c.

A further compression in the overall size of the object by a factor of 6 would lead to a yet expanded spectrum and a more improved version of the reconstructed object Figures 7a-7c. However, in compressing the overall scale of the object, one loses resolution in the object domain due to the reduction in the number of available pixels across the object. It is thus apparent that much enhanced resolution in the frequency domain, seen as the more samples across the expanded lobe of the frequency spectrum is associated with a loss of resolution in the object domain. Therefore, object compression can only be exercised up to a point whereby a reasonable fraction of object characteristics are still preserved when subjected to an overall scale change.

CONCLUSIONS

This paper has addressed the use of the Fourier scaling property as an effective means of restoring object geometries containing repetitive and structural characteristics. Such objects populate the Fourier space with numerous regions of maxima and minima. By utilising the scaling principle it has been shown that an improvement in the recovered structural characteristics can be made by using an expanded spectrum. Such expanded spectrum enhances phase evaluations through maintaining fewer minima as well as improving the continuity between frequency components.

References

Hayes, M.H.(1982). *IEEE Trans. on Acoustics Speech & Signal Processing.* Vol ASSP-30, 511-519.

Lim, J.S (1990). Two dimensional signal and image processing. *Prentice Hall.*

Bates, R.H.T & W.R.Fright(1984). *Advances in computer vision and image processing,* Vol 13, No.5, 227-264.

Sotoudeh, N., G.R. Greatrix, G.F.Goldspink & R.Prasad(1993). *Mathematical Modelling & Scientific Computing,* Vol 2, Section A 517-52

Nakajima, N. & T.Asakura(1986). *Applied Physics,* 19, 319-331.

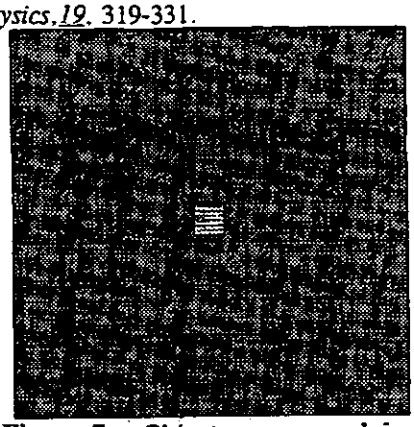

Figure 7a: Object compressed in size by a factor of 6.

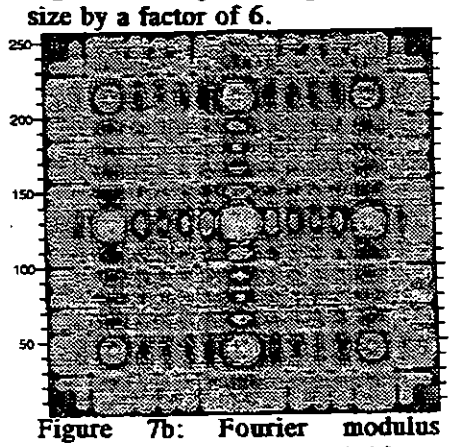

Figure 7b: Fourier modulus spectrum of the compressed object.

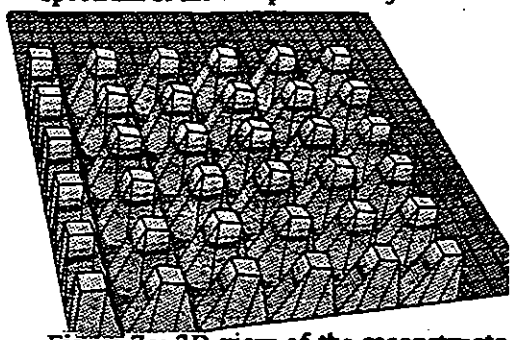

Figure 7c: 3D view of the reconstructe object from the spectrum of Figure 7b.

APPENDIX C

Approximate bounds of zero-phase characteristics

The calculations on page 158 leading to an approximate size for the dimensions of the grooves were based on the assumption that the zero-phase characteristics of the machined surface were bound to a region which is approximately equal to the diameter of the laser beam that illuminated the surface. To validate this approach, the approximate bounds of the zero-phase characteristics of another object specimen when shone with a laser beam of known diameter was obtained in a separate set of measurements.

12
11
10
9
8
7

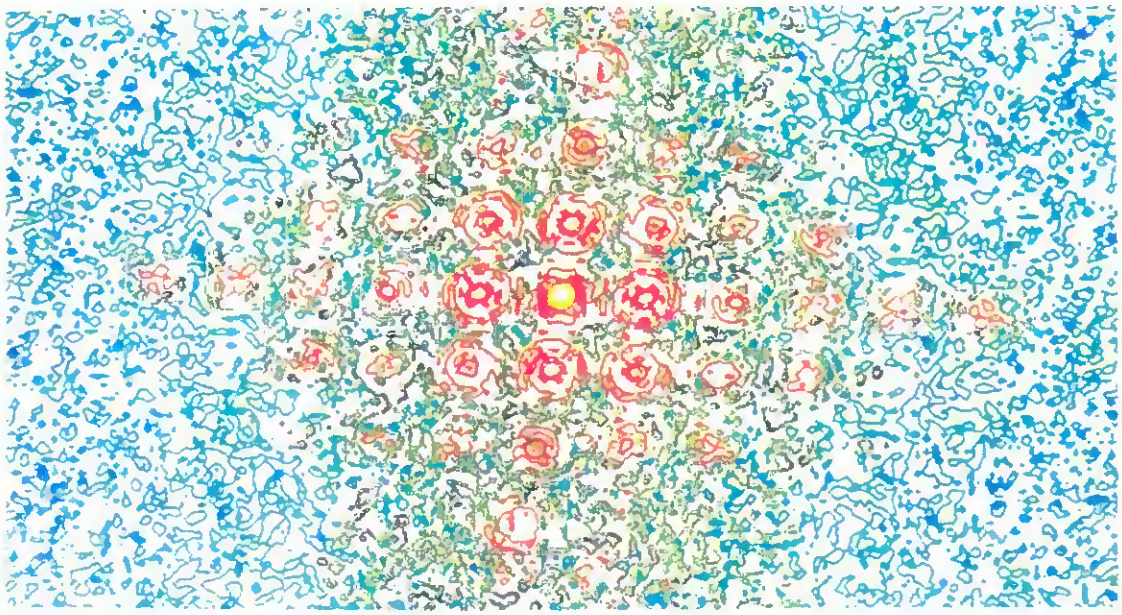

Figure c1: Displayed zero-phase characteristics for the lattice of circular apertures obtained from the inverse Fourier transformation of the optically recorded diffraction pattern of the features.

Figure c1, shows the zero-phase inverse Fourier transformation of the lattice of circular apertures seen on page 110 of this thesis. This is a 513x260 display of the recovered zero-phase characteristics showing the number of repetitive features within the displayed region. The spatial period of repetitive features is approximately 92um and the features were illuminated with a laser beam of 1mm diameter. Counting the number of repeated features horizontally, it can be seen the displayed characteristics are limited to within a region which is approximately equal to the diameter of the illuminating laser beam.